

Phytolith analysed to Compare Changes in Vegetation Structure of Koobi Fora and Olorgesailie Basins through the Mid- Pleistocene-Holocene Periods.

By

KINYANJUI, Rahab N.

Student number: 712138

Submitted on 28th February, 2017

Submitted the revised version on 22nd February, 2018

Declaration

A thesis submitted to the Faculty of Science in fulfilment of the requirements for PhD degree.

At School of Geosciences, Evolutionary Studies Institute (ESI)

University of Witwatersrand, Johannesburg

South Africa.

I declare that this is my own unaided work and has not been submitted elsewhere for degree purposes

A handwritten signature in black ink, appearing to read 'Rahab N. Kinyanjui', with a stylized flourish above the name.

KINYANJUI, Rahab N.

Student No. 712138

Abstract

Phytolith analyses to compare changes in vegetation structure of Koobi Fora and Olorgesailie Basins through Mid-Pleistocene-Holocene Periods.

By

Rahab N Kinyanjui (Student No: 712138)

Doctor of Philosophy in Palaeontology

University of Witwatersrand, South Africa

School of Geological Sciences, Evolutionary Science Institute (GEOS/ESI)

Supervisor: Prof Marion Bamford.

The Koobi Fora and Olorgesailie Basins are renowned Hominin sites in the Rift Valley of northern and central Kenya, respectively with fluvial, lacustrine and tuffaceous sediments spanning the Pleistocene and Holocene. Much research has been done on the fossil fauna, hominins and flora with the aim of trying to understand when and how the hominins evolved, and how the environment impacted on their behaviour, land-use and distribution over time. One of the most important factors in trying to understand the hominin-environment relationship is firstly to reconstruct the environment.

Important environmental factors are the climate, rate or degree of climate change, vegetation structure and resources, floral and faunal resources. Vegetation structure/composition is a key component of the environments and, it has been hypothesized the openness and/or closeness of vegetation structure played a key role in shaping the evolutionary history not only of man but also other mammals. Various proxies have been studied to determine and reconstruct vegetation history. They include: fossil pollen, stable isotopes, fossilised wood and phytoliths.

This study applied phytolith analyses to reconstruct the vegetation history of the Koobi Fora and Olorgesailie Basins during the Pleistocene to Holocene periods respectively. Firstly, modern phytolith analogues from plants and surface soils were used to interpret the past vegetation from fossil phytolith assemblages. Four vegetation structures were clearly recognisable: grasslands, wetlands/riparian, woodlands/forests and mixture of woody and herbaceous dicotyledons.

Although the proposed goal of this study was to compare temporal changes in phytolith assemblage, hence vegetation structure for the two basins, this was not achieved due difference in the sampling strategies available for the two basins. A continuous sediment core was drilled from the Olorgesailie

Basin representing ~970kyr to ~77kyr, while in Koobi Fora sampling was done from well dated archaeological and geological exposures representing the early Pleistocene period (2.525-2.51Ma) and the Holocene period (9.6kyr to 0.93kyr), lacking mid-late Pleistocene deposits. Determining the vegetation structure from both basins was possible. Two approaches were applied, a general approach for vegetation reconstruction (phytolith abundance) and phytolith indices (aridity and tree cover indices). Phytolith assemblages from paleosols deposited between 1.525Ma and 1.52Ma suggest a general vegetation cover dominated by woodlands which shifted to woody mixed grasslands that resemble present savanna habitats and a moister grassland habitat is also reflected. From ~970kyr to ~77kyr the vegetation structure comprised open grasslands, wooded grasslands, woodland/forest, and wetland/riparian/riverine habitats. These habitats fluctuated and the environments were unstable. The rate of fluctuations changed from high to low throughout the Olorgesailie sequence. From the Koobi Fora samples the Early Holocene (~9.6kyr to ~4.2kyr) was to the Early Pleistocene with woodlands remaining dominant, mixed grassland always present and a mosaic vegetation. A clear vegetation shift is noted during the late Holocene period (~1.34kyr to 0.93kyr), where woodlands declined while Chloridoideae grasses increased significantly indicating arid habitats similar to present-day savanna grasslands.

For future research directions it will be a valuable opportunity to have a long sediment core drilled from either the current Lake Turkana basin or a paleolake basin from which phytolith data can be analysed and studied to give a continuous vegetation reconstruction history.

Key words: Phytoliths, Pleistocene, Holocene, Paleoenvironments, Koobi Fora, Olorgesailie

Dedication

This work is
dedicated to my adorable children
Gathoni-, Ngima- and Wahome Ndegwa
for being my inspiration.

Acknowledgements

First and foremost, I thank the Almighty God for not only granting me the opportunity to study but also for the courage and resilience to walk this journey to completion. Secondly, this research would not have been accomplished without the financial and logistical support received from various institutions and people. Hopefully I will be able to acknowledge each one of them but in case I forget, I sincerely apologise.

The research was funded financially by the following institutions:

1. Palaeontological Scientific Trust (PAST) and Centre of Excellence in Palaeosciences (CoE-Pal) both based at the Evolutionary Studies Institute (ESI), University of Witwatersrand, paid all costs related to learning and living expenses while in South Africa and analyses costs for the Koobi Fora samples, through Student Bursary funds.
2. Olorgesailie Drilling Project (ODP) supported field work, sampling and analyses of the Olorgesailie samples.
3. The Koobi Fora Field School (KFFS) supported field work and sampling logistics for all the Koobi Fora samples.
4. The National Museums of Kenya for granting me study leave and also offered infrastructural and logistical support in the Palynology and Palaeobotany lab, Earth Sciences department.
5. Lastly but not least, the East African Association for Palaeoanthropology and Palaeontology (EAAPP) society for granting me the opportunity to attend and present my work, for it is in this forum when Prof Jack Harris introduced me to Prof. Marion Bamford who later became my supervisor-greatly indebted to the 2011 EAAPP conference organising committee- to you I say a big thank you!

Numerous people have contributed greatly to the success of this study:

- First of all I am sincerely grateful to my supervisor Prof. Marion Bamford who believed in my potential to undertake this project and who has worked with me patiently and tirelessly, and supported me throughout the process. Her kindness and understanding made this journey bearable especially during those “down moments”-you are the best mentor-thank you!
- My sincere gratitude goes to Prof. Rick Potts, who has walked with me throughout my entire postgraduate studies; it is through his kind support during my MSc Program that I qualified to get to this level, he did not stop it there but considered me to be part of the ODP team and work on the phytolith component - in my research world you always be star!
- I would like to thank the KFFS directors- Prof. Jack Harris, Dr. Purity Kiura, Ass. Prof. David Braun and Dr. Emmanuel Ndiema for the support they have accorded me during all the summer field work in Koobi Fora. Special thanks goes to Dr. Purity Kiura for offering me the

opportunity to participate in the KFFS expeditions as trainer which was a great opportunity to learn more about the basin and interact with renowned paleoanthropologists, archaeologists, palaeoecologists and geologists who added value in the understanding of my research.

- I would like to thank Dr. Idle Farah and Dr. Mzalendo Kibunja, former and current Director General respectively, for the moral support they have accorded me especially in ensuring that I could access all the equipment I needed during laboratory and microscopic analyses of all the samples in this study. I also do appreciate the moral support accorded to me by the entire Earth sciences colleagues, especially palynology and palaeobotany family, Dr. Stephen Rucina and Ms. Rebecca Muthoni.
- Special thanks go to Dr. Kay Behrensmeyer who spent her valuable time and expertise to ensure I have the correct geological information reported in this study, for both basins. Drs Amelia Villasenor and Andrew Du for drawing the Koobi Fora geological sections sampled for this work.
- Last but not least, to my family for support and more so, for the perseverance during my frequent absence while away either in the field or in school. To both my mums, I salute you for your love and support you accorded me and my children during some of the challenging times in the journey. Although this thesis is dedicated to my daughters and son, I sincerely appreciate them for they have been a source of great inspiration, they never complained but they have always regarded me as their role model and best mum in the whole world, to all of you I say—I adore you!
- Allow me to thank the three anonymous reviewers who took their time to read and suggested valuable revisions which have greatly improved this final thesis.

Table of contents

Declaration.....	ii
Abstract.....	iii
Dedication.....	v
Acknowledgements.....	vi
Table of contents	viii
List of figures.....	xiii
List of Tables	xvi
CHAPTER ONE: BACKGROUND INFORMATION.....	17
1.1. Highlights of major climatic events, vegetation cover and human impact in East Africa	22
1.1.1. The Pleistocene period	22
1.1.2. The Holocene period.....	23
CHAPTER TWO: PHYTOLITH STUDIES.....	26
2.1. Benchmark for phytolith data analytical approach	26
2.1.1. What are phytoliths?	26
2.1.2. Phytolith formation in plants.....	27
2.1.3. Plant silica functionality	27
2.1.4. Phytolith preservation and taphonomy.....	27
2.2 Phytoliths classification.....	28
2.2.1. Diagnostic morphotypes	28
2.2.2. Non Diagnostic morphotypes	35
2.3 Background of Phytolith studies	38
2.3.1 Opportunities and limitations of phytolith data	41
2.4. Goals and Objectives.....	42
2.4.1. Justification	42
2.4.2. Research questions	42
2.4.3. Specific goals and objectives.....	43
2.4.4. Research Hypothesis.....	43
CHAPTER THREE: STUDY SITES.....	44
3.1. Introduction	44
3.1.1 Contemporary climates in East Africa.....	44
3.1.2. Contemporary vegetation in East Africa.....	46
3.2. Olorgesailie basin.....	46

3.2.1. Climate	47
3.2.2. . Vegetation cover	47
3.2.3. . Geo-archaeology and core lithology	48
3.3. Koobi Fora basin.....	50
3.3.1. Climate	50
3.3.2. Vegetation cover	51
3.3.3. General geology and drainage system.....	51
3.3.4.. Geo-archaeology	52
CHAPTER FOUR: MATERIALS AND METHODS.....	55
4.1. MATERIAL.....	55
4.1.1. Modern soil samples.....	55
4.1.2. Fossil samples.....	55
4.2. METHODS.....	70
4.2.1. Laboratory work.....	70
4.2.2. Counting and identification	72
4.2.3. Basic Analytical Approach	72
4.2.4. Data analyses	80
CHAPTER FIVE: MODERN PHYTOLITH REFERENCE COLLECTION	83
5.1. Introduction	83
5.2. Description of the morphotypes selected to reconstruct Early Pleistocene-Holocene vegetation cover.	83
5.2.1. Analyses of woody dicots, herbaceous and GSSCs morphotypes.....	83
5.2.2. Analyses of GSSCs morphotypes-Poaceae	85
5.2.3. Summarised results of GSSCs analyses	87
5.2.4. Analyses of non-GSSCs morphotypes	89
5.2.5. Summarised results of non-grass analyses	92
5.2.6. Testing the significance of the modern reference data as a benchmark to interpret fossil assemblage in this study	92
CHAPTER SIX: OLOGESAILIE PHYTOLITH ASSEMBLAGE	94
6.1. Introduction	94
6.2. ODP phytolith spectra: Individual key morphotypes	94
6.2.1. Zone ODP I (975-675kyr).....	95
6.2.2. Zone ODP II (675-325kyr).....	95

6.2.3. Zone ODP III (325-77kyr).....	95
6.3. Phytolith Indices-ODP	96
6.3.1. D: P index	96
6.3.2. Iph index.....	98
6.3.3. Dynamism in both Iph and D/P indices.....	110
5.3.2. ODP Phytolith assemblages, $\delta^{18}O$ and eccentricity	110
CHAPTER SEVEN: KOOBI FORA PHYTOLITH ASSEMBLAGES	112
7.1. Introduction	112
7.2. Phytolith Assemblages: Site-based results	112
7.2.1. Early-Pleistocene assemblages	112
7.2.2. Early Holocene assemblages	114
7.2.3. Early-mid-Holocene phytolith assemblages.....	114
7.2.4 Mid-late-Holocene phytolith assemblages	115
7.2.5. Modern phytolith surface samples	116
7.3. Temporal changes in phytolith assemblage of the Koobi Fora sequence	117
7.3.1. Early Pleistocene	117
7.3.2. Early Holocene	117
7.3.3. Early-Mid transition	118
7.3.4. Mid-Holocene.....	118
7.3.5. Late Holocene	118
7.4 Phytolith Indices-KOOBI FORA	120
7.4.1. The D:P index	120
7.4.2. Iph index.....	121
7.4.3. Dynamism in both Iph and D:P indices	123
CHAPTER EIGHT: VEGETATION HISTORY AND ENVIRONMENTAL CHANGES IN THE OLOGESAILIE BASIN AND THE SURROUNDING ENVIRONS.	125
8.1. INTEPRETATION	125
8.1.1. Understanding the last 1Ma of vegetation structure using the general approach	125
8.1.2. Application of indices: D:P and Iph	128
8.2. DISCUSSION.....	129
8.2.1. Significance of vegetation structure and the Palaeoenvironments of the Ologesailie basin	129
8.2.2. Phytolith data, $\delta^{18}O$ and eccentricity	131

8.3. Significance of the ODP phytolith data in relation to other proxies studied from the Ologresailie Formation and surrounding regions	133
8.3.1. ~500kyr to ~350kyr period.....	133
8.3. 2. ~350kyr to 300kyr period.....	134
8.3.3. 225ky to 200kyr period	134
8.3.4. 200kyr to 100kyr period.....	134
8.4. Role of Ologresailie vegetation cover on the Hominin landscapes	135
CHAPTER NINE: EARLY-PLEISTOCENE AND HOLOCENE VEGETATION DYNAMICS IN KOOBI FORA BASIN.....	136
9.1. INTERPRETATION	136
9.1.1. Early Pleistocene vegetation structure	136
9.1.2. Holocene vegetation change and palaeoenvironments	137
9.1.3. Phytolith Indices.....	138
9.2. DISCUSSION.....	139
9.2.1. Significance of vegetation structure and the Palaeoenvironments of the Koobi Fora basin	139
9.3. Significance of the phytolith data in relation to other studies in Koobi Fora region.....	140
CHAPTER TEN: VEGETATION STRUCTURE OF THE OLOGRESAILIE AND KOOBI FORA BASIN AND HOW IT CHANGED THROUGH PLEISTOCENE –HOLOCENE PERIODS	142
10.1. Introduction	142
10.2. Significance of the vegetation changes in the Ologresailie Basin during the Pleistocene Period to Human evolution History.....	142
10.3. Significance of the vegetation changes in the Koobi Fora Basin during Early-Pleistocene and Holocene Periods to Human evolution History	142
10.3.1. Early Pleistocene (FwJi14E).....	143
10.3.2. Holocene	143
10.4. How similar/different is the vegetation structure in Koobi Fora and Ologresailie basins? ...	144
CHAPTER ELEVEN: CONCLUSIONS AND FUTURE RESEARCH DIRECTIONS	145
11.1 CONCLUSIONS.....	145
10.2. FUTURE RESEARCH DIRECTION	145
REFERENCES	146
APPENDICES	172
Appendix I. Age versus depth of the ODP core; the model assigns depth age on a cm-by-cm scale (Deino et al., <i>in progress</i>).....	172
Appendix II: List of plants species analysed for modern phytolith reference data	182

Appendix III. Raw phytolith data counted in ODP core samples	205
Appendix IV: Raw phytolith assemblage count for Koobi Fora Basin	220

List of figures

Figure 1. Shows the plots of plant wax biomarkers and δ^{13} variation in relation to the Hominin Evolutionary tree (<i>After</i> , Feakins et al., 2005).....	20
Figure 2. Grass phytolith in modern and fossil assemblages; a-h) bilobates, i) cross j) polylobate, k-m saddles, n-q) towers/rondels, r) trapezoid, s-t) bulliforms, u) scutiform in-situ, r) long-cell; elongate type, v). saddle long, w) Hair cell. Scale bar=10 μ m.....	29
Figure 3. Shows grass phylogenetic tree based on combined molecular results (GPWG, 2001, after Stromberg, 2003)	33
Figure 4. Non-grass phytoliths in the fossil assemblages; a) Tracheid, b) elongate facetate, c) scutiform, d) papillae/hat-shaped e) achene, f) globular psilate, g-i) globular echinate, palm type, j-l) globular decorated /granulate(k-top left) Scale bar=10 μ m	36
Figure 5. Non-grass phytoliths; a-d) globular verrucate, e-g) sponge spicules and diatoms, h) parallelepiped, i) sponge spicules, j-k) parallelepiped variants. Scale bar=10 μ m	37
Figure 6. Shows location of the study sites: Koobi Fora basin in north and Olorgesailie Basin in south	44
Figure 7. General patterns of precipitation, trade winds, pressure and convergence over Africa during a) northeast monsoon and b) southeast monsoon, CAB patterns based on Nicholson, 1996.	46
Figure 8. Map showing the location of the Olorgesailie outcrops in north and the ODP drilling sites in the Koora plains ~20km, south of Mt. Olorgesailie y (after Behrensmeier, 2002).....	47
Figure 9. Showing the preliminary lithological and geochronological data and levels of sampling for phytolith, diatoms, CaCO ₃ mud and zeolite analyses.....	49
Figure 10. Map showing Lake Turkana, Koobi Fora Basin and sampling localities (modified from Forman et al., 2014)	50
Figure 11. Map of Turkana basin showing the three “Omo-Group” Formations; Shungurra, Nachukui and Koobi Fora and their respective Members (Brown & Feibel, 1991; 1986; Cerling et al., 2015)...	54
Figure 12. Map showing the drill location of the ODP sediment core. Note the proximity to the Olorgesailie Basin. Source: (http://humanorigins.si.edu/sites/default/files/styles/home_slider_phablet/public/Lake%20Koora%20map.jpg?itok=dhIGtI7C&timestamp=1481139547).....	56
Figure 13. Showing the image of a short section of the ODP sediment core with different lithologies and cm-scale ruler	57
Figure 14. Explanation of a part of core section and lithological symbols by Behrensmeier et al., unpublished report.	59
Figure 15. The key used to identify sedimentary structures and clasts.....	60
Figure 16. ODP age- model showing a smooth progression toward older ages with increasing core depth. 1.07Ma date is obtained from trachytic basement rock.	61

Figure 17. Map showing some of the Holocene sites sampled for this study (Red stars this study, grey circles (Ndiema, 2011)).....	62
Figure 18. A geo-section drawn by Amelia Villaseñor and Kay Behrensmeyer, showing some of the palaeosol sampled and their relationship to the Ileret Tuffs.	64
Figure 19. Photograph showing one of the geo-section sampled for Early Pleistocene samples	65
Figure 20. A scatter plot of Correspondence Analyses (CA) showing the relationship between the identified morphotypes and their parent species. Three clusters according to plants form and habits are identified.	84
Figure 21. A scatter plot of Correspondence Analyses (CA) showing the relationship between GSSCs morphotypes and grass species. Four clusters are defined which corresponds to the four grass sub-families analysed.....	86
Figure 22. Relative abundance of phytoliths observed in grass sub-families.	88
Figure 23.	90
Figure 24.	91
Figure 25. Relative abundance of phytolith assemblages observed in Cyperaceae	92
Figure 26. Relative abundance of single morphotypes that identified vegetation habitats (top) versus age (left) of the ODP sediment core. Phytolith assemblage zones identified by CONISS in TILIA....	99
Figure 27. Relative abundance of key identified vegetation types /habitat versus age (left). Zones identified by CONISS in TILIA	100
Figure 28. A graph showing rapid and gradual shifts in aridity (Iph, in red) and tree cover density (D/P, in blue) indices of the ODP core. The arrows shows the levels with wide range of vertical change.	110
Figure 29. Showing woody cover (positive values) versus grasses (negative values). Phytolith data indicate more persistent woody signature at the top of the core and grassland expansion ~275kyr to 300kyr (at ~110m, depth).....	111
Figure 26. Preliminary results indicate vegetation structure fluctuations a) correspond with a) orbital eccentricity cycle b) grasslands expansion correspond are in phase with $\delta^{18}O$ record (Tyler et al., in <i>progress</i>).	Error! Bookmark not defined.
Figure 31. Percentage diagram of major habitats identified by phytolith assemblages in site FxJj-14E, Area 1A (the top ten samples) and Area 8A (the bottom two samples)- Early-Pleistocene paleosols.	113
Figure 32. Percentage diagram of major habitats identified by phytolith assemblages in site FxJj108, an early Holocene site.....	114
Figure 33. Percentage diagram of major habitats identified by phytolith assemblages in site FxJj27, an early-mid-Holocene transition site.....	115

Figure 34. Percentage diagram of major habitats identified by phytolith assemblages in mid-late-Holocene sites.	116
Figure 35. Percentage diagram of major habitats identified by phytolith assemblages in modern surface samples.....	117
Figure 36. Relative abundance of key phytolith types, main vegetation habitats versus sample # and estimated age (right) of the Koobi Fora samples	119
Figure 37. Shows a graph of both Iph and D:P indices and their variation between Early-Pleistocene to late-Holocene samples.	124
Figure 38. Preliminary results indicate vegetation structure fluctuations a) correspond with a) orbital eccentricity cycle b) grasslands expansion correspond are in phase with $\delta^{18}O$ record (Tyler et al., in <i>progress</i>).	132

List of Tables

Table 1. <i>showing the four vegetation habitats, where modern soil samples were collected.</i>	55
Table 2. <i>Lithostratigraphic details of Early Pleistocene samples collected from Ileret area and their relative ages depending on their collection point in relation to the Ileret Complex Tuff.</i>	66
Table 3. <i>Lithostratigraphic section for FxJj 108 (After Ashley et al., 2011).</i>	67
Table 4. <i>Lithostratigraphic section for FxJj 27 (after Ashley et al., 2011).</i>	68
Table 5. <i>Lithostratigraphic section for GaJj4 (after Ashley et al., 2011).</i>	68
Table 6. <i>Lithostratigraphic section for FwJj25 (after, Ashley et al., 2011).</i>	69
Table 7. <i>Lithostratigraphic section for FwJj5 (after, Ashley et al., 2011).</i>	70
Table 8. <i>Morphotype categories identified from the modern phytolith reference collections and are used in this study.</i>	73
Table 9. <i>Table showing three main plants' categories and their corresponding statistical attributes.</i> 93	
Table 10. <i>Showing identified morphotypes from the ODP core assemblages of 48,638 categorised into four broad abundance classes (% of the total assemblage) 'abundant' (>10%), 'common'(>1-10%), 'Uncommon' (0.1-1.0%) and 'rare' (<0.1%).</i>	94
Table 11. <i>Showing aridity (Iph) and tree cover density (D:P) of the ODP core calculated from the selected GSSCs and globular granulate (modified from Bremond et al., 2008). Shading follows the D:P indices, not the aridity indices from the grasses. Note that the two do not correlate.</i>	101

Part 1: General introduction

CHAPTER ONE: BACKGROUND INFORMATION

East Africa is famous for numerous early hominin sites that have provided quality archives of human evolutionary history data that address not only human evolution questions but also evolution of other faunal species dating back to the Miocene period. The region is also very rich in archaeological sites, from which various levels of toolkits have been discovered, technology transitions, for example, transition from Acheulean to Middle Stone Age (MSA) to Late Stone Age (LSA), have been preserved, human cultural interactions and their response to variable climatic events through time (Potts et al., 1999; Basell, 2008; Tryon et al., 2010; Potts and Faith, 2015).

Generally, East Africa experiences tropical climates, controlled by intersection and interactions of the following factors: the Intertropical Convergence Zones (ITCZ), the Congo Air Boundary (CAB), the El Nino-Southern oscillation (ENSO), the East African Monsoon (both SE and NE) and the Indian Ocean Sea Surface Temperature (SST) (Nicholson, 1996; 2000). In addition, a complex, regional topography ranging from mountain ranges, rift valleys and large lakes create diverse regional-local ecological niches (Nicholson, 1996; Mutai and Ward, 2000). Consequently, these interactions lead to dynamic cultural practices and dynamic land-use patterns.

In the past, the global Quaternary Palaeoclimates shifted orbitally between glacial (cold) and interglacial (warm) phases in response to precessional insolation changes (Milankovic cycles). In the African tropics, the Palaeoclimates were predicted to be dry with low lake levels during the glacial periods and wet with high lake-water levels during the interglacial phase (Trauth et al., 2001; 2003; Bergner et al., 2009).

However, recent multi-proxy and multidisciplinary studies of deep lake cores in Africa shown varied local conditions in the tropics contrary to what was initially predicted with greater variance than expected (Cohen et al, 2007; Scholz et al, 2007; Trauth et al., 2007; Bergner et al., 2009). Other than the influence of the Orbital scale precession insolation, factors such as sea-surface temperatures (SST), the irregular shifts in position of the Intertropical Convergence Zone (ITCZ) and the strength in Monsoon currents (Nicholson, 1996; 2000) affect local hydrologic cycles, hence local climates (Clark et al., 1999; Clement et al., 2004; Maslin and Christensen, 2007; Scholz et al., 2007; Bergner et al., 2007). For example, during the last interglacial period (135ka-127ka, 110ka-85ka and 78ka-74ka) Palaeoclimates around Lake Malawi and Lake Tanganyika experienced extreme aridity, causing Lake Malawi to become a shallow saline lake surrounded by semi-deserts (Scholz et al., 2007; Bergner et al., 2007). On the other hand, around similar time periods a series of high-lake stands were recorded in

Lake Naivasha (146ka-120ka, 139-133ka, 113ka-108ka and ~ 90ka), in Turkana-Suguta and Magadi-Natron basins around 135ka-130ka (Trauth et al., 2001; 2003; Bergner et al., 2009).

Recent studies suggest that tropical responses to climate changed during the 70ka, following closely the temperature fluctuations in the northern hemisphere on millennial and centennial scales observed in the Greenland records (Heinrich Events 1, 4-6, and some Dansgaard-Oeschger events). These climatic phases are expressed as sharp peaks and moisture in the tropics (Stager et al., 2005; Verschuren et al., 2009a, b).

The geological processes such volcanism resulted in the formation of the rift valley systems, new lake basins, while drying of others, provided an ideal scenario for abrupt sedimentation/ burial which was critical for good preservation of faunal and floral remains. Periodic volcanic eruptions deposited geological markers, in between fossil bearing sediments, that consist of uniquely identified chemical signatures that can be accurately dated using varied techniques. Subsequent rifting and volcanism exposed geological markers and sedimentary sequences in which fossils are preserved. Such sites are numerous especially within the rift valley system, distributed from north (Ethiopia) to south (Tanzania). Geological, paleontological and archaeological data from these sites justify why the Eastern Africa region has played a crucial role in evolutionary history, especially mammalian and human since Cretaceous-Tertiary (KT) boundary ~65Ma through the emergence of the modern man, *Homo sapiens* ~300ka to present.

Among these sites, Koobi Fora and Olorgesailie basins have contributed greatly to scientific data that have addressed various research questions not only in human evolutionary history but also other life forms, and palaeoenvironmental and palaeoclimatic reconstructions both temporally and spatially.

Unique and important research findings have been published since late 70's. Millions of paleontological, anthropological and archaeological collections from these sites have been analysed leading to thousands of publications not only in highly regarded peer reviewed journals but also in both main stream and social media (e.g. Behrensmeyer, 1970; Leakey, 1970; 1995; Isaac, 1971; Isaac et al., 1971; Behrensmeyer et al., 1997; Potts et al., 2004; Bennet et al., 2009, among others). Consequently, making Kenya earn her glory of cradle of mankind.

Both basins are located within the Kenyan rift system; Olorgesailie in the Southern rift while Koobi Fora northern rift, approximately 900 km apart. However, despite the distance separating them both basins share some similarities in that they are located within semi-arid to arid regions and that they represent paleolake basins with lithostratigraphic sequences that span from Pleistocene and earlier, to Holocene periods and which are well correlated spatially across the landscapes (Baker and Mitchel, 1976; Isaac 1978; Brown and Feibel, 1986; Harris et al., 1988; Deino and Potts, 1990).

In addition a common hominin species, *Homo erectus*, and the associated archaeological artefacts, have been preserved well in both basins (Brown et al., 1985; Potts et al., 2004). In contrast, while in the Olorgesailie basin there is only a single hominin species found (*Homo erectus*), in the Koobi Fora basin several species have been found (*Australopithecus/ Paranthropus* sp and *Homo habilis*) in addition to various specimens of *Homo erectus*. This could be partially due to the size of the basin; Koobi Fora is relatively larger than the Olorgesailie basin.

Remarkable pilot studies in evolutionary history have been undertaken in the region, for example; testing the three major hypotheses to explain the events that led to human evolution from one clade to another; Savanna hypothesis (deMenocal, 1995; Cerling et al., 1992; 1997a), turnover-pulse hypothesis (Bobe et al., 2002; Bobe and Behrensmeyer, 2004) and the environmental variability hypothesis (Potts, 1996; 1998). These studies so far have laid the foundation of the role of paleoclimates and palaeoenvironments in evolution history, particularly during Pliocene, Plio-Pleistocene and Pleistocene periods in East Africa (Wynn, 2004; Feakins et al., 2005; Behrensmeyer, 2006; Cerling et al., 2011).

A model has been developed using various multiproxy datasets to illustrate the role of changing climates and consequential impact on the vegetation cover to shape the evolution trajectory of the Homo species (Figure 1). Carbon isotope ratio from terrestrial and lacustrine sediments indicated close correlation between the emergence of *Paranthropus* Genus with expansion of C₄ grasslands around 3Ma while C₃ vegetation declined rapidly. More expansion of grasslands is noted around 2Ma corresponding with the period when *Homo erectus* appeared and migrated out of Africa (Lahr and Foley, 1998; Feakins et al., 2005; McDougall et al., 2005).

More so, faunal analyses are consistent with the above mentioned studies (deMenocal, 1995; Potts, 1996; Bobe and Behrensmeyer, 2004), emphasizes that vegetation cover remains critical to understand past ecological interactions. Late Pleistocene period, the relationship between the distribution and concentration of the Middle Stone Age (MSA) sites in East Africa clearly suggested that vegetation cover and climatic events played a great role in early human occupation choices and technological development (Basell, 2008).

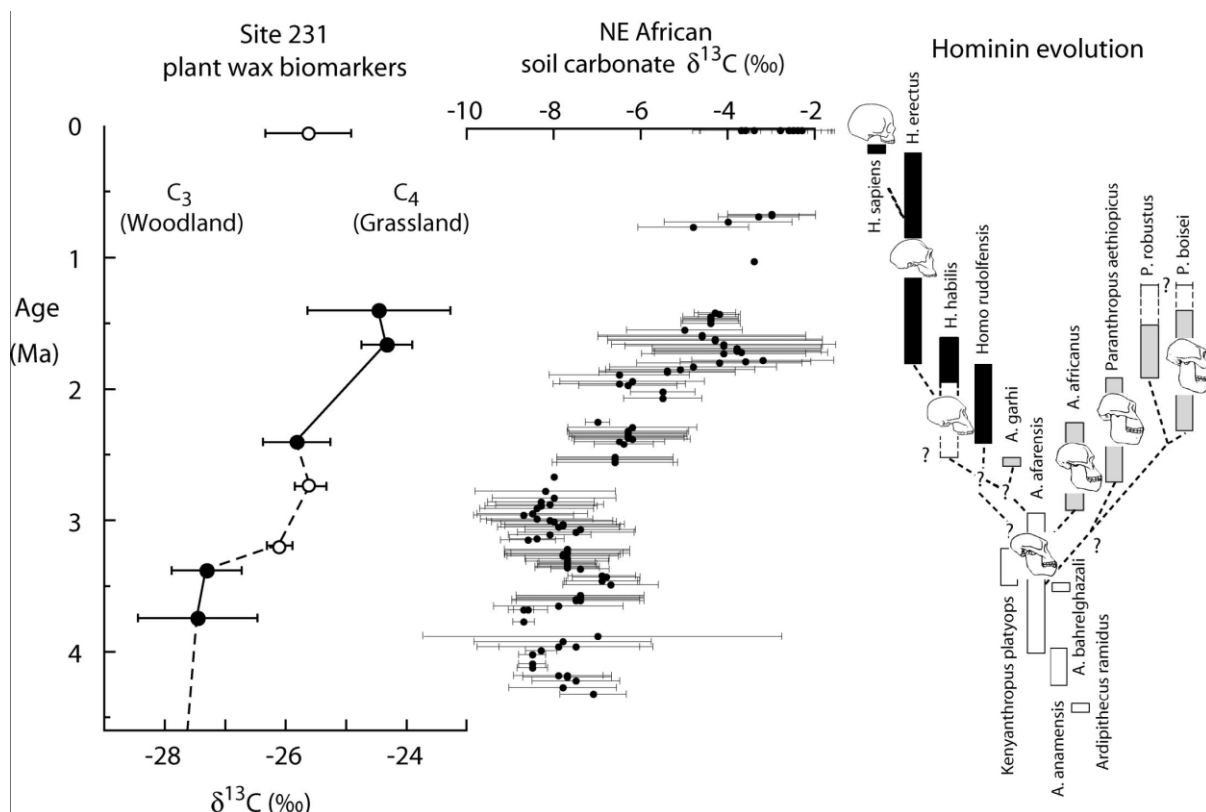


Figure 1. Shows the plots of plant wax biomarkers and $\delta^{13}\text{C}$ variation in relation to the Hominin Evolutionary tree (After, Feakins et al., 2005).

Pollen analyses and stable isotopes were the main proxies analysed to address such questions (Owen et al., 1992; Bonnefille et al., 1986; Cerling et al., 1988; Levin et al., 2011). However, these proxies could not explicitly differentiate habitats with tall versus short grasses and lowland C_4 versus highland C_3 grasslands, which are critical in understanding the palaeoenvironments. Recently, phytoliths, microscopic silica bodies deposited within and/or between plants cells, preserved in the sediments after parent plant decomposes (Piperno, 1988; 2006; Pearsall, 1989; Rapp and Mulholland, 1992a), have proved valuable in identifying and classifying grasses to their ecological significance beyond family level enabling researchers to reconstruct past vegetation cover especially those that surrounded early humans (Alexandre et al., 1997; Barboni et al., 1999; Albert et al., 2006, 2007).

It is a general understanding that Pleistocene period is a critical period not only when the modern human (*Homo sapiens*) emerged but also when major global climatic events occurred (Lahr and Foley, 1998; McDougall et al., 2005; Tyron et al., 2010; Stewart and Jones 2016) that are associated with series of severe population reductions and subsequent rapid expansions (Lahr and Foley, 1994; Rogers and Jorde, 1995, Basell, 2008). During such global events, it is suggested climates were extreme in the northern hemisphere, whereas equatorial and tropical Africa offered refugia and it is thought hominin species could have been maintained here (Basell, 2008). The earliest fossil evidence of *Homo sapiens* has been

found in the East African region (~ 195ka-130ka): Singa in South Sudan (Grun and Stringer, 1991; McDermott et al., 1996), Herto and Omo in Ethiopia (Brauer, 1984; Clark, 1988; McBrearty and Brooks, 2000; Clark et al., 2003; White et al., 2003; Haile Selassie et al., 2004; McDougall et al., 2005) and Mumba in Tanzania (Mehlman, 1987; 1991; Mabulla, 1996).

As mentioned earlier, Pleistocene global climatic variabilities recorded contrasting effects to those recorded in the Northern hemisphere compared to the African continent, and even more unique effects are registered in different regions within the continent (see, Jones and Stewart, 2016). Considering that the earliest fossil evidence of anatomically modern man is found in East Africa (~195ka), (McDougall et al., 2005; Brown et al., 2012) and the probable source of human populations dispersal during the late Pleistocene (~70ka) out of Africa as indicated by genetic evidence (Soares et al., 2012; 2016), strongly suggest that Pleistocene climate variabilities played a great role in human evolutionary history (Lahr and Foley, 2016). More so., it is during this period when MSA technology is recorded at various archaeological sites across the continent (e.g. McBrearty and Brooks, 2000; McBrearty, 2007; Basell, 2008). Nevertheless, the question on how the changes in climates influenced the direction of human evolution and consequent dispersal remains not fully resolved and is the main current debate among researchers in different field of specialities. Stewart and Jones (2016) have synthesized evidence derived from different regions in the African continent between Marine Isotope stages 6 and 2 (~191ka and 14ka) and it stands out that the following challenges need to be addressed to conclusively address the question:-

- 1) Discontinuity and /or lack of chronologies from various sites hindering evidence comparisons both spatially and temporally,
- 2) Local responses to climate variabilities differed greatly, hence leading to some sites being favourable refugia, thus some sites having rich evidence while others lack of evidence (e.g. Basell, 2008)
- 3) The nature of the African vegetation cover which was quite varied and largely controlled by local topography, the responses and resilience of these vegetation structures varied greatly across the continent (Stewart and Jones, 2016).

One of the crucial step that has been undertaken in the past and needs to continue, is the multidisciplinary and multiproxy data analyses from a site/ core and which can be comparable from inter-and intra-basin scale to a regional scale.

The research work presented here compares vegetation data inferred from a similar proxy, phytolith assemblage of two important prehistoric basins, the Olorgesailie basin in the southern Kenyan rift and the Koobi Fora basin north of the Kenyan rift. This research is unique in that, it presents the first

phytolith data from Koobi Fora basin and first long, continuous high resolution data from the Ologesailie basin. In addition, the Ologesailie data will be compared with other paleoenvironmental proxies analysed from the same levels to determine and interpret long-term environmental dynamics and the possible role these changes played in modifying the paleolandscapes. Although data from Koobi Fora basin is not continuous, it provides well dated sequence covering the early Pleistocene and Holocene period which is missing from the Ologesailie core. However, since this project is directed mainly by the overall objectives of the Ologesailie Drilling Project (ODP) which only focused on sampling the Pleistocene sediments, the data of Holocene period is therefore not reported here.

On the other hand, the Koobi Fora analysis is advantaged because it includes data for the Holocene period from a site that has published dates and can be compared to already within-site published palaeoenvironmental data (Ashley et al., 2011). However, it suffers the setback of discontinued chronology since sampling was done from geological sections that were believed to expose paleosol layers that are chronologically placed within the Pleistocene period and the dates used are taken from the dated tuffs bracketing these paleosol layers. In addition, the existence of a disconformity occurring during Late Pleistocene made it difficult to compare phytolith datasets between the basins.

Nevertheless, vegetation dynamics reflected by the phytoliths data from each basin are discussed and interpreted on basin-scale and the surrounding environments and inter-basin comparisons for the period ~1Ma. In addition, the role played by the vegetation cover of the Pleistocene environments to influence human-environmental interaction is discussed for each basin and consequently compared.

1.1. Highlights of major climatic events, vegetation cover and human impact in East Africa

1.1.1. The Pleistocene period

Detailed palaeoenvironmental and paleoclimate studies indicate that African climates were highly variable since early Pliocene to Holocene periods. The climates oscillated from warm-humid to cool-dry episodes in response to the global orbital precession insolation (Milakovic) cycles (Trauth et al., 2007) and vegetation cover was highly variable. Multiproxy climatic and palaeoenvironmental data from East Africa sites show that the region experienced significant episodes of climate change during the Pleistocene and Holocene epochs (Verschuren et al., 2000; 2009). Lacustrine rift basins have been identified as excellent archives of various proxies studied to reconstruct the past environments and climates, such as diatoms, pollen, lake sediments and minerals, stable isotopes, water chemistry and other faunal and floral remains preserved in these basins (Marchant and Taylor, 1998; Lamb and Verschuren, 2003; Rucina et al., 2010; Ashley et al., 2011).

Previous studies have demonstrated that African climates at during this period oscillated from warm and humid to cool and dry episodes (deMenocal, 1995; deMenocal and Bloemendal, 1995). This resulted in habitats varying between wooded vegetation to open savannah grasslands. It has been hypothesised that this variability in habitats was an important driving factor for evolution and speciation of mammals (Environmental Forcing Hypothesis; Bobe *et al.*, 2002). Kingston *et al.* (1994) found the palaeoenvironmental setting of the Kenyan rift was best described as "...a heterogeneous environment with a mix of C₃ and C₄ plants that persisted for the last 15.5 Ma". Other hypotheses based on palaeoenvironmental changes, and associated with major fossil discoveries linked to human evolution and their interactions with environmental context are discussed and summarised in Table 3.1 by Potts (1998). Recent debate on the possible vegetation context in which *Ardipithecus ramidus* (Aramis ~4.4 Ma) interacted with the surrounding environments in Ethiopia (WoldeGabriel *et al.*, 2009; Cerling *et al.*, 2010; White *et al.*, 2010) is a perfect example that demonstrates the need for paleovegetation data from African hominin sites.

Plio-Pleistocene and Pleistocene (4.2-0.6Ma) environments of the Koobi Fora basin were more mesic than present day. Varied palaeoenvironments were indicated from each Member of the Koobi Fora Formation which was controlled dominantly by the changes occurring in the paleo-Omo river channel and Lake Turkana basin. Vegetation structure consisted of gallery forest along the ancient Omo river channel and seasonal grasslands on its flood plain (Feibel, 1988).

1.1.2. The Holocene period

Palaeoenvironmental proxies studied from different archives indicate that Africa in general and East African region in particular experienced significant climatic variability during the Holocene period (Owen *et al.*, 1982; Stager *et al.*, 2003; Ashley *et al.*, 2004; Driese *et al.*, 2004; Verschuren, 2004; Russel and Johnson, 2005; Olago *et al.*, 2009; Verschuren *et al.*, 2009).

Rift valley lake basins have archived excellent data that have provided non-conflicting insights on past regional climatic changes during the Holocene period. This coupled with archaeological and paleobotanical data dated to Early-late Holocene; helps understand the impact of climate variability on palaeoenvironments and human socioeconomic strategies (e.g. Ndiema, 2011).

Climate during early to mid-Holocene (10,000-7,000yrs BP) was warmer and wetter than the subsequent periods with expanding grasslands and decreased forests and woody species (deMenocal *et al.*, 2000). High lake stands within the rift valley were evidenced, for instance Lake Turkana level rose to 80m above the current (1976) level ~365m a. s. l (Butzer, 1980; Harvey and Grove, 1982; Olago and Odada, 2000; Umer *et al.*, 2004). This humid period is also referred to as the African Humid Period, and was as a result of orbitally-induced weakening of monsoon strength (Wright, 2017).

Available proxies indicate the mean climate regime during the late Holocene (~5000yrs BP) was significantly wetter than the mid Holocene (7000-5000yrs BP) at the equator. This has been attributed to the intensification of the north-eastern monsoon causing enhanced southern hemisphere summer insolation (e.g. Russell and Johnson, 2005; Verschuren et al., 2009; Wright, 2017).

Climate variability continued to be experienced in the last 2500 years in the African tropics (Verschuren, 2004; Verschuren and Charman, 2008). The East African lakes and wetlands provide evidence of several decadal-to- century scale drought events (Verschuren et al., 2000; Stager et al., 2003; Ashley et al., 2004; Driese et al., 2004; Russell and Johnson, 2005; 2007).

The last 2500yrs BP was marked with more climate variability across East Africa with four dry events experienced during ~50BC-200AD, ~900-1250AD, ~1780-1830AD and ~1920-1960AD. These drought events were interrupted by two cool and moist events (Little African Ice-age (LIA)); early LIA between ~1250-1550AD and main LIA occurring between ~ 1550-1825AD (Verschuren et al., 2000; Stager et al., 2003; Ssemmanda et al., 2005). Pollen records from lake sediments further suggest vegetation changed in response to climatic variation during the late Holocene (e.g. Lamb 2001, Lamb et al., 2003, Rucina et al., 2010).

Transition from warm and humid to cool and dry climates is associated with ecological conditions that were favourable for the emerging complex social systems not only in Africa but also in South western Asia where new agricultural practices emerged such as irrigation, new subsistence resources and extended resource exchange among different communities, which in some regions were managed by hierarchical leaders (Ndiema, 2011; Wright, 2017).

Archaeological studies on how early humans interacted with the surrounding environments in response to the said climatic variability show great dynamism in social- economic and cultural adaptations to changing landscapes and resource availabilities (Robertshaw and Taylor, 2000, Taylor et al., 2000; Robertshaw et al., 2004; Ndiema, et al., 2011). In Lake Turkana region, for instance, humans switched social, economic and cultural practices and subsistence acquisition from hunters and gatherers to fishing to pastoralism between early-mid-late Holocene respectively (Ndiema, 2011).

There are more extensive temporal paleo-vegetation studies based on pollen analyses for late Pleistocene to Holocene period than Early to Mid-Pleistocene periods. This is because of reliable lake sediment cores recovered from various lakes in East Africa. Some of these researches have analysed and discussed the possible impact the palaeoenvironments and paleoclimates had on early humans. However, there is a serious existing gap brought about by the inaccuracy of grass pollen grains to taxonomically identify grasses below family level (Twiss, 1992). We are aware from previous paleoenvironmental studies that expansions of C₄ grasslands, especially in African arid and semi-arid

regions, have shaped evolutionary history of species since the Miocene period (Cerling and Hay, 1988; Cerling, 1992; Cerling et al., 1997, Bobe and Behrensmeyer, 2004; DeMenocal, 2004; Bobe, 2006; Levin et al., 2011).

The critical role played by African grasslands is well explained in various paleontological and paleo-environmental studies on African Late Quaternary Extinctions (LQE) suggesting that Late Pleistocene (126,000-12,000yrs ago) climates influenced the emergence of *Homo sapiens* between 200,000-100,000yrs ago, landscape cover changes and eventual extinctions of various faunal species (Klein, 1980; 1984; Bobe and Behrensmeyer, 2004; Bobe, 2006; Codron et al., 2008; Faith, et al., 2012, 2013). These studies observed that the most species extinctions were attributed to declining grasslands toward the end of Last Glacial Maximum (Klein, 1980; 1984, Brink and Lee-Thorp, 1992; Faith et al., 2012; 2013). Other key factors highlighted include increased niche specialization (Codron et al., 2008) and Late Stone Age (LSA) human impacts due to the improved hunting tools, particularly during Pleistocene-Holocene transitions (12,000-9,500yrs ago) (Klein 1980, 1984).

Considering that grasslands are a key component in the African ecosystems both for the high and low altitude vegetation cover (Potts, 1998; DeMenocal, 2004; Plummer et al, 2009; Faith et al., 2012), it is therefore important to understand dynamics in the past ecosystems to more accurately reconstruct the past vegetation changes and discuss the implication of this over the palaeolandscapes. Fortunately grass phytoliths, especially the silica short cells (GSSC) have been used not only to identify grasses beyond family level but also between wild and domesticated grasses such as cereals (Piperno and Pearsall, 1998; Piperno, 2006).

It is on the basis of this strength that this study applies phytolith analyses to reconstruct vegetation changes since the Pleistocene period. More so, phytoliths preserve well in a variety of depositional regimes including alkaline conditions as opposed to pollen grains, and hence are strong proxies to be studied in paleo-lakes such as Koobi Fora and Olorgesailie basins.

CHAPTER TWO: PHYTOLITH STUDIES

2.1. Benchmark for phytolith data analytical approach

This section reviews the existing published literature and modern phytolith data as a palaeoecological tool in reconstructing the past vegetation structure considered in this work. In addition, limitations and opportunities of using phytolith data are highlighted and their significance in this study is presented.

Phytolith research is a field that has developed over time with a major milestone being a concerted attempt to standardize the classification system; International Code of Phytolith Nomenclature (Madella, 2005). Unfortunately not all specialists use this classification system, and a few only use it for certain morphotypes. This setback is partly due to variation of vegetation habitats across the globe, and partly because of different lab protocols used to extract and analyse phytoliths (10th International Meeting for Phytolith Research-IMPR).

However, despite this setback, phytolith analyses have been used to determine domesticated versus wild crops in archaeological settings (Bozarth, 1996; Pearsall, 2000; Piperno and Pearsall, 1993), to determine and reconstruct vegetation structure (Alexandre, et al., 1997; 1999; Bremond et al., 2008) and define the prevailing climates in the past (Fredlund and Tieszen, 1997; Alexandre, 1999; Baker et al., 2000). Phytolith data is therefore a potential tool to investigate the vegetation dynamics of the Pleistocene-Holocene environments of the prehistoric basins reported here.

2.1.1. What are phytoliths?

Phytoliths are opaline silica deposits that form within and between plant cells (Piperno, 1988; 2006). They form when plants absorb soluble silica $[\text{Si}(\text{OH})_4]$ from ground water and then precipitate in and around plant cells at different locations through polymerisation processes (Piperno, 1988, 2006; Pearsall, 1989; Rapp and Mulholland, 1992a). On decay and decomposition of the plant, the silica “casts” are deposited in the soils preserving their original cells shapes and forms, as phytoliths. They therefore qualify as botanical micro-fossils and can provide significant paleobotanical and paleoenvironmental information (Rovner, 1988; Rapp and Mulholland, 1992a, Piperno, 2006).

Phytoliths, like pollen are potential plants index microfossils, hence useful in reconstruction of vegetation history (Rovner, 1971; Piperno, 1988; 2006). Unlike pollen, phytoliths being inorganic are resistant to oxidation, hence, preserve well in a variety of sediments where pollen is poorly preserved (Brown, 1984; Piperno, 2006). More important, is the potential of phytoliths to distinguish grasses into subfamilies, tribes or genera (Twiss, 1992; Twiss et al., 1969, Brown, 1984; Mulholland and Rapp, 1992; Piperno and Pearsall, 1998), making phytoliths the most preferred proxy to determine and

investigate East Africa's vegetation dynamics, both temporally and spatially, which constitute largely of grasslands component (White, 1983; Timberlake et al., 2010).

2.1.2. Phytolith formation in plants

Phytoliths are present in angiosperms, gymnosperms and pteridophytes (Piperno, 1988). However, different plants species deposit silica variably depending on various factors; most monocotyledons are better phytolith producers than dicotyledonous plants (Bozarth 1992; Piperno, 1989; 2006). Plant families known to be consistent accumulators of identifiable phytoliths include the following: Poaceae, Cyperaceae, Cucurbitaceae, Asteraceae and Leguminosae. Nevertheless, production of phytolith is not exclusive only in the above listed families, other plants produce little or non-identifiable types. Some plants produce calcium phytoliths, for example Cactaceae family produce Calcium oxalate crystals formed in the wood, while Calcium carbonate crystals (cytoliths) have been found in Urticaceae, Moraceae, Acanthaceae and Cannabinaceae ((see Rapp and Mulholland, 1992 and references therein).

2.1.3. Plant silica functionality

Available evidence suggests that silica uptake is both an active and passive process and, both genetic and environmental factors play an important role (Cooke and Leishman, 2011). It has been found that active silica uptake has some benefits to some plant species; they provide structural support (Kaufman et al., 1985, Piperno, 1988) and protection from herbivores (McNaughton et al., 1985; Massey and Hartley, 2009; Massey et al., 2007; Reynolds et al., 2009). Recent studies have attributed silica deposition in some domesticated plants/crops such as *Zea mays* (maize) and *Oryza sativa* (rice) to be an adaptation mechanism against drought and leaf diseases (Chang et al., 2002; Ahmed et al., 2011b; Malhotra et al., 2016).

2.1.4. Phytolith preservation and taphonomy

Phytoliths are mainly inorganic and are resistant to a variety of chemical conditions that affect other types of plant remains. They are therefore well preserved in a variety of depositional regimes devoid of other plants' macro-and micro-fossils especially in terrestrial environments.

Taphonomic issues are also crucial for accurate interpretation of fossil phytolith assemblage. Differential dispersal associated with each morphotype or each size class affect their distribution in the sediments (Mulholland and Rapp, 1992; Cabanes et al., 2012; Cabanes and Shahack-Gross, 2015). Phytoliths are produced within many parts of the plants and are deposited directly in the humus layer of the soil during plants' decomposition, hence give signal of the local vegetation cover. In other instances, strong erosional process (fluvial, Aeolian) and fires lead to long-distance dispersal by water and wind. Phytoliths in the soils and sediments are affected by various active physical and chemical

processes. In particular, opaline silica dissolve easily under strong alkaline conditions (Mulholland and Rapp, 1992; Piperno, 2006).

2.2 Phytoliths classification

Classification system used in this work is guided by a combination of previous research depending on the diversity of morphotypes in the fossil assemblage. This is referenced accordingly. Modern phytolith reference based at the National Museums of Kenya is also consulted. Two broad classification categories is considered following Stromberg, (2004): 1) diagnostic and 2). Non-diagnostic morphotypes.

2.2.1. Diagnostic morphotypes

These are silica with distinctive shapes and sizes and are known to occur in high abundance in specific vegetation taxa. Examples of such phytoliths have been identified mostly in grasses, sedges and palms (Twiss et al., 1969; Twiss, 1992; Ollendorf, 1992; Albert et al.2006; 2015).

The presence of diagnostic morphotypes in the fossil assemblage plays an important role in accurately defining past plant community structure and estimate potential climates. Since diagnostic morphotypes vary in size (2-800µm), it is therefore important to extract and analyse phytoliths of all size fractions in a given soil/sediment samples for accurate representation (Stromberg, 2002; 2004).

The presence or abundance of morphotypes of taxa often associated with specific habitats and have an ecological preference such as wetlands, springs and/or a high water table, have been considered as habitat-diagnostic morphotypes, implying such habitats existed on the palaeolandscapes. Such morphotypes include GSSCs that are not specific to particular sub-family but are known to indicate grasslands, morphotypes derived from woody dicots but are not specific to particular species, here generalised as forest indicators (FI) and those generally derived from herbaceous taxa.

These morphotypes have accurately defined Plio-Pleistocene, Pleistocene and Holocene vegetation habitats, (Barboni et al., 1999; Albert et al., 2006; Bamford et al., 2006; Ashley et al., 2010). However, their ecological application beyond the Plio-Pleistocene period has been questionable (see Stromberg, 2002, Tertiary studies). Diagnostic category includes morphotypes derived from palms and sedges; globular echinate and papillae/hat-shaped respectively (non-grass category) and Arundinoideae, Panicoideae, Chloridoideae (GSSCs category) (see figure 2).

The following is a detailed description of the diagnostic morphotypes:

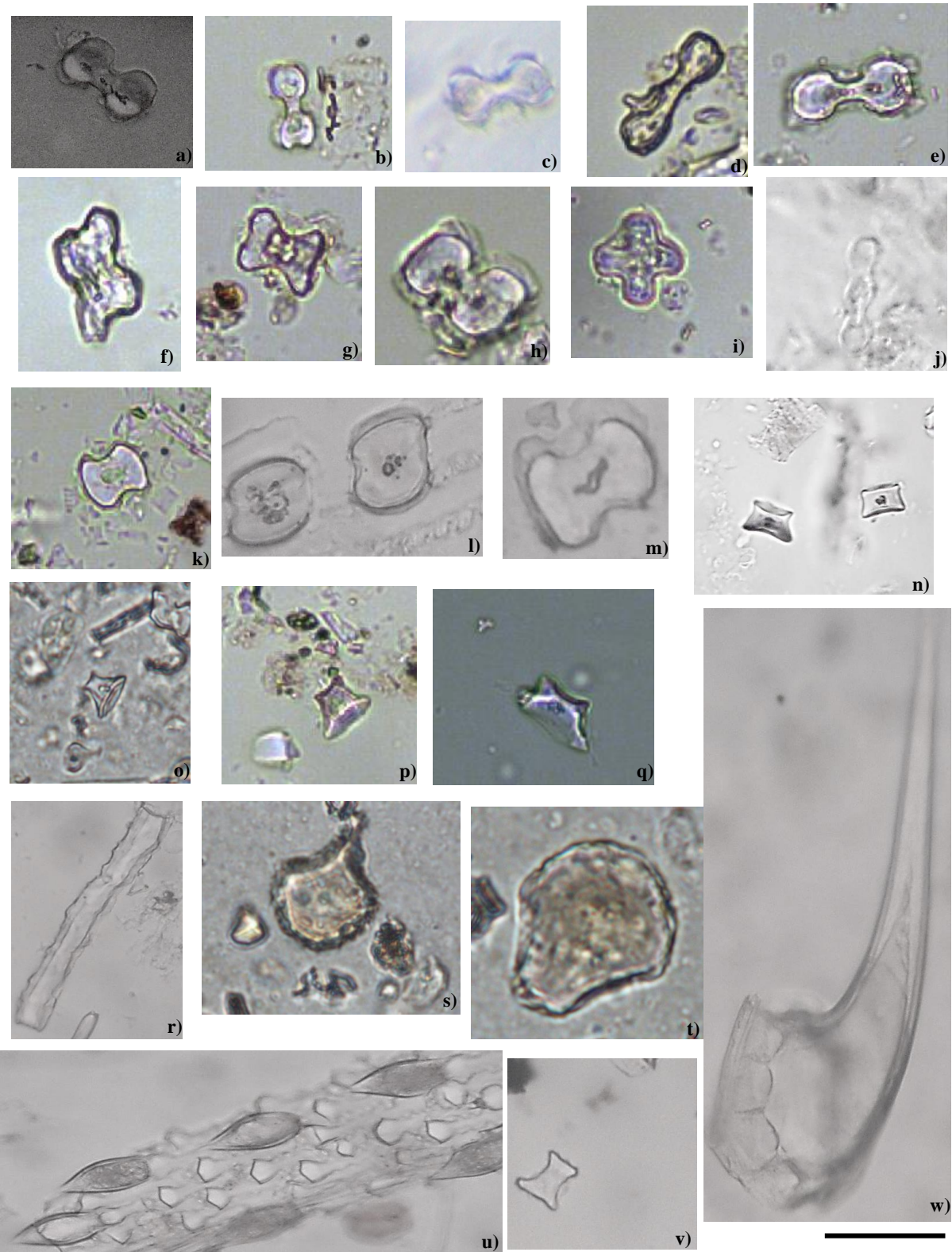


Figure 2. Grass phytolith in modern and fossil assemblages; a-h) bilobates, i) cross j) polylobate, k-m saddles, n-q) towers/rondels, r) trapezoid, s-t) bulliforms, u) scutiform in-situ, r) long-cell; elongate type, v). saddle long, w) Hair cell. Scale bar=10µm

a) Palms

Palm trees are key component of Tropical Savanna vegetation cover. They produce diagnostic morphotypes known as ‘globular echinate’ or spheroid echinate and are often included in the forest indicator category (Piperno, 1988; 2006; Barboni et al., 1999; 2007; Stromberg, 2004) and are considered as prolific phytolith accumulators (Albert et al., 2006; Bamford et al., 2006). However, most palms have specific ecological preferences and have been found in low frequencies in modern soil phytolith assemblage from dense forest (< 5%, Alexandre et al., 1997; Albert et al., 2015). Coconut and oil palms are cultivated, hence associated with human disturbance, forest clearing and open habitats (Boyd et al., 1998). Based on current ecological distributions palms are mainly associated primarily with warm and humid habitats (Stromberg, 2003) especially in the West African region and gallery forests in association with springs, seeps and/ or high water tables within the East African savanna ecosystems (Albert et al., 2006; Bamford et al., 2006; WoldeGabriel et al., 2009; Ashley et al., 2010; Barboni et al., 2010; Albert and Bamford, 2012). Accordingly, palm phytoliths are indicators of riparian/gallery forests with high water table, and are associated with warm and humid environments, especially in East African region.

b). Grasses

Grasslands have been a key component of various habitats in Africa throughout Pliocene Period. The evolution of grass-dominated ecosystems has been hypothesized to play a major role in the evolution history of humans and other mammals in Africa (Vrba, 1995; Bobe and Behrensmeyer, 2004).

Molecular studies by the Grass Phylogeny Working Group (GPWG I) initially revised the evolutionary grass clade GPWG, (2001); Kellogg, (2001) and classified grasses into two main evolutionary clades according to their ability to tolerate drought and thrive in open, dry habitats. These clades are as follows: 1) Pooideae (Festucoideae), which include Asian cereals, high elevation grasses of tropical latitudes and most northern temperate grasses and, 2) PACCAD, Panicoideae (tall grasses of tropical origin e.g. maize and sorghum), Arundinoideae (wetlands grasses such as reeds and *Phragmites*), Centothecoideae (forest grasses e.g. *Zeugites*), Chloridoideae (drought-adapted short grasses of prairies and savannas), Aristidoideae (short grasses found in disturbed shallow soils mainly roadsides and footpaths) and Danthonioideae (found mainly in the southern hemisphere, in both open and closed habitats) (GPWG, 2001; Kellogg, 2001).

A more recent phylogeny (GPWG II) has more advanced classification, which include more grasses. The two main clades according to their photosynthetic pathways: 1) BEP (Bambusoideae, Ehrhartoideae and Pooideae) all of which are C₃ cool grasses and, 2) PACMAD (Panicoideae, Arundinoideae, Chloridoideae, Micrairoideae, Aristidoideae and Danthonioideae) tropical grasses (GPWG, 2012). See figure 3.

The identified grass subfamilies are adapted to either C₃ or C₄ photosynthetic pathways depending on their ecological preference. In tropical Africa, the C₃ grasses are mainly found in high elevation, and are associated with cool and wet climates although in South Africa they are found in low elevation regions unlike in the tropics. C₄ grasses on the other hand are more commonly associated with warm climates but they spread along moisture gradients, with Panicoideae thriving best in warm but moist climates while Chloridoideae thrive in warm and dry climates (Twiss et al., 1969; Tieszen et al., 1979; Twiss, 1992; Rossouw, 2009).

Grasses not only accumulate substantial amount of silica, they produce diagnostic morphotypes that can discriminate between sub-families (Twiss et al., 1969; Twiss, 1992, Stromberg, 2003; Piperno, 2006). This is possible because grasses with different photosynthetic pathways (C₃ or/and C₄), have their epidermal cells arranged differently and with differing sizes. Silica is either deposited on the cells' outline or within the cell, the replicas/ casts retains the cell shape when deposited in the cell after the plant decompose (Twiss, 1992; Piperno, 2006).

As mentioned earlier, grasslands have been an important vegetation component in Africa's history, therefore understanding the evolution of grasslands and their role in evolutionary history is of importance. The fact that grasses accumulate substantial amounts of silica within and around the epidermal cells that form identifiable phytolith morphotypes that preserve well in sediments long after the grasses decompose, present a great opportunity to reconstruct the vegetation structure of the region.

Despite the existing overlap, where some GSSC morphologies are produced across grasses with dissimilar ecological preference and of different subfamilies (Rovner, 1983), previous studies have been able to identify specific morphotypes that discriminate the subfamilies (Twiss et al., 1969; Twiss 1992; Piperno, 2006). The following is a selection of grass phytoliths that have been generally considered to discriminate grass subfamilies (Twiss et al., 1969; Mulholland, 1989; Twiss 1992; Madella et al., 2005):

- a) Pooideae C₃: Rondels (pyramidal rodel (PY), conical rondel (CO) & keeled rondels (KR) types
- b) Panicoideae: Symmetrical & asymmetrical bilobates (dumbbells) figure 4a &h, cross-shaped figure (4i) and polylobate (4j)
- c) Chloridoideae: Saddle shaped figure (2k-m).

Recent studies further described the above categories into more diverse morphotypes that permit further identification of the subfamilies. For instance, bilobates are further described using the form of the lobes (whether convex or concave) and the length of the mid-Shank (long or short) (see Fredlund and Tieszen, 1994; Stromberg, 2003; Rossouw, 2009; Mercader et al., 2010). This has made it possible to discriminate Aristidoideae grasses as described in Piperno (2006) figures 4 (d-e).

In contrast, taxonomic attribution of some grass silica short cells is not always an obvious situation, it depends on the region they are found. For instance, rondels morphotype in temperate region are associated with Pooideae C₃ grasses, however in tropical Africa they are only attributed to Pooideae only in high elevations while in low elevations, rondels have been found to be associated with C₄ grasses, especially Chloridoideae C₄ short grasslands (Barboni and Bremond, 2007).

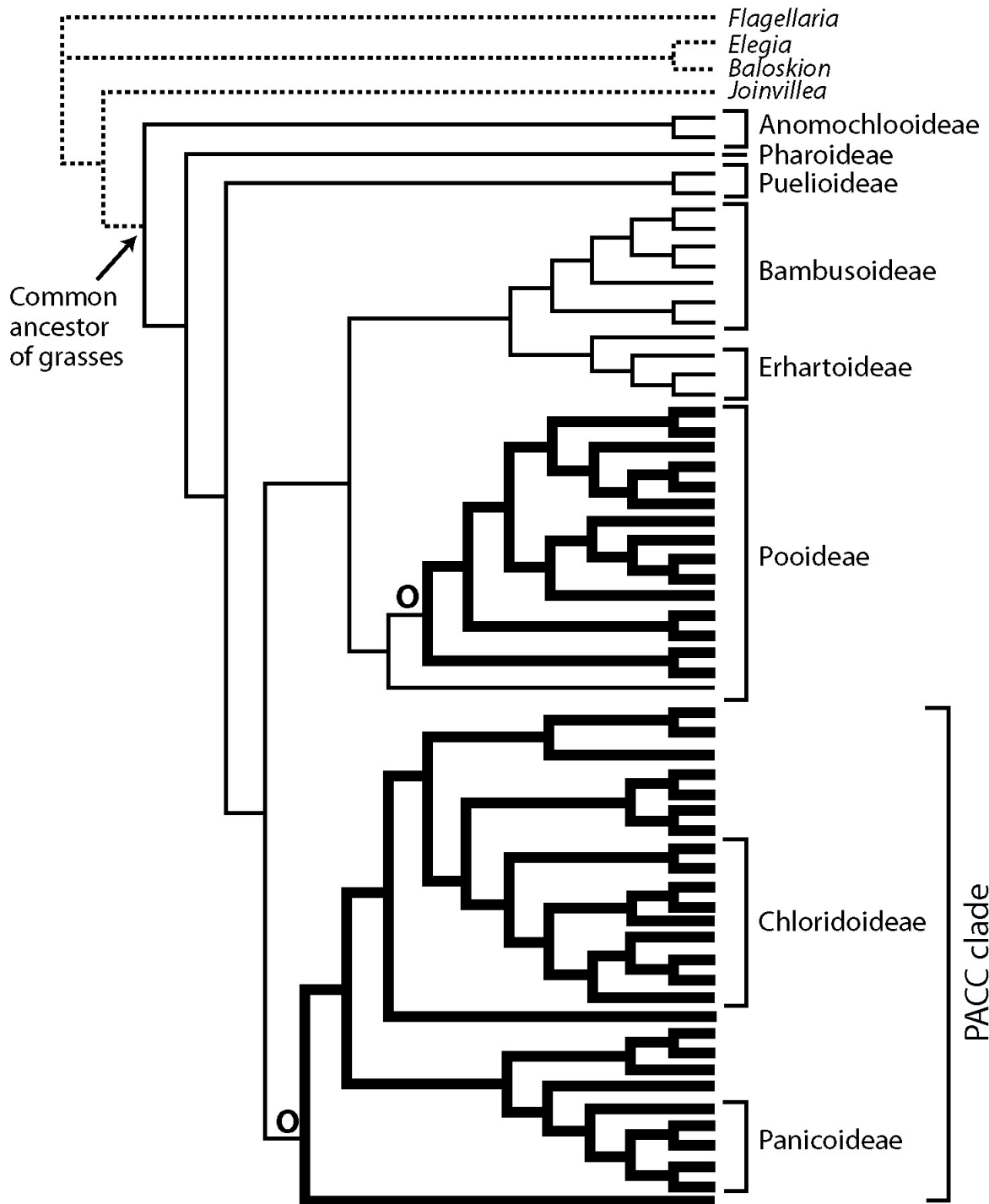


Figure 3. Shows grass phylogenetic tree based on combined molecular results (GPWG, 2001, after Stromberg, 2003)

c). Sedges (*Cyperaceae*)

Sedges are associated mainly with wetlands and swampy habitats. In palaeoecological records, they indicate proximity to water sources and swampy habitats (Stromberg, 2003) while in the archaeological

record they are mainly associated with human disturbance as they tend to form an important component of secondary vegetation (Piperno, 1988). Sedges produce unique conical shaped phytoliths that are distinguishable from other similar shapes produced in other plants. They have pointed apices and smooth surfaces which occur in achene bracts of sedges (Ollendorf, 1992; Piperno, 2006). These morphotypes are classified as achenes and papillae/hat-shaped (Honaine et al., 2009; Mercader et al., 2013). These morphotypes are rare in modern soils and in sediments because they usually do not preserve well, Therefore, their presence in the fossil assemblage is an absolute indication of sedges on the paleolandscapes. Detailed description of morphotypes is given in Table 1.

d). General forest indicators

These are morphotypes that are produced by woody dicotyledons. They are associated with closed habitats and indicators of moist climates (Piperno, 2006). However, phytoliths derived from woody dicots suffer major setbacks; they have very little taxonomic significance and morphotypes are mostly redundant across taxa. Studies have also shown that dicots are poor silica accumulators; hence occur in low abundance in soil phytolith assemblages (Albert et al., 1999; Hodson et al., 2005; Piperno, 2006; Mercader, 2009).

Key morphotypes often used to infer forest/woody habitats include: globular granulate (Runge, 1999; Neumann et al., 1999; Piperno, 2006; Mercader et al., 2009; 2013) figure (9j-1), treachery elements of xylem and sclerenchyma tissue (tracheid & sclereid) (Albert et al., 1999; Piperno, 2006; Mercader et al., 2009, 2013), decorated blocky type (Mercader et al., 2009, 2013), globular psilate (Mercader et al., 2009, 2013) figure (9f) and stomatal cells, trichome & hair bases (Mercader et al., 2010) figures (5c & 4w).

Presence and frequencies of the above mentioned morphotypes in the fossil assemblages are used to interpret the presence of woody components in the past vegetation structure (Albert et al., 2006; Mercader et al., 2009, 2013) and also help demonstrate the vegetation transition between open grasslands versus closed wooded habitats and the associated climates (Alexandre et al., 1997; Bremond et al., 2005; Barboni et al., 2007; Mercader et al., 2010; Novello et al., 2012).

e). Herbaceous indicators

Here we refer to non-woody plants except for grasses and sedges. Just as in woody dicots, herbaceous taxa are poor silica accumulators with phytoliths mostly restricted to fruits and seeds (Piperno, 2006). Most phytoliths derived from herbaceous taxa are similar morphologically to those produced in woody dicots, hence it is difficult to single out herbaceous taxa from woody dicots. Nevertheless, they are included in analyses and discussed within the woody and herbaceous taxa category (Figures 2, 4). These included spheroid/globular psilate, ellipsoid variants, epidermal assemblages among others.

2.2.2. Non Diagnostic morphotypes

Also present in phytolith assemblages are morphotypes that have no taxonomic value and are classified as non-diagnostic/ variable (Albert et al., 1999). They are not used to reconstruct the vegetation history because their occurrence seems to be largely controlled by the environmental parameters under which the parent plants developed (Piperno, 1988). Such morphotypes include wavy and smooth elongated trichome and bulliforms. Trichome/ prickles for instance have been assigned to angiosperms in general (Evert, 2006), while most researchers assign bulliforms to grasses (Piperno, 2006). They can also be associated with graminoids.

In this study, they have been included in the analyses because they give insights on environmental parameters and different habitats. For example, since bulliforms have a positive correlation with moisture availability, their abundance in an assemblage not only reflect expansive grasslands (together with other GSSCs) but also indicate high moisture (Rovner, 1983).

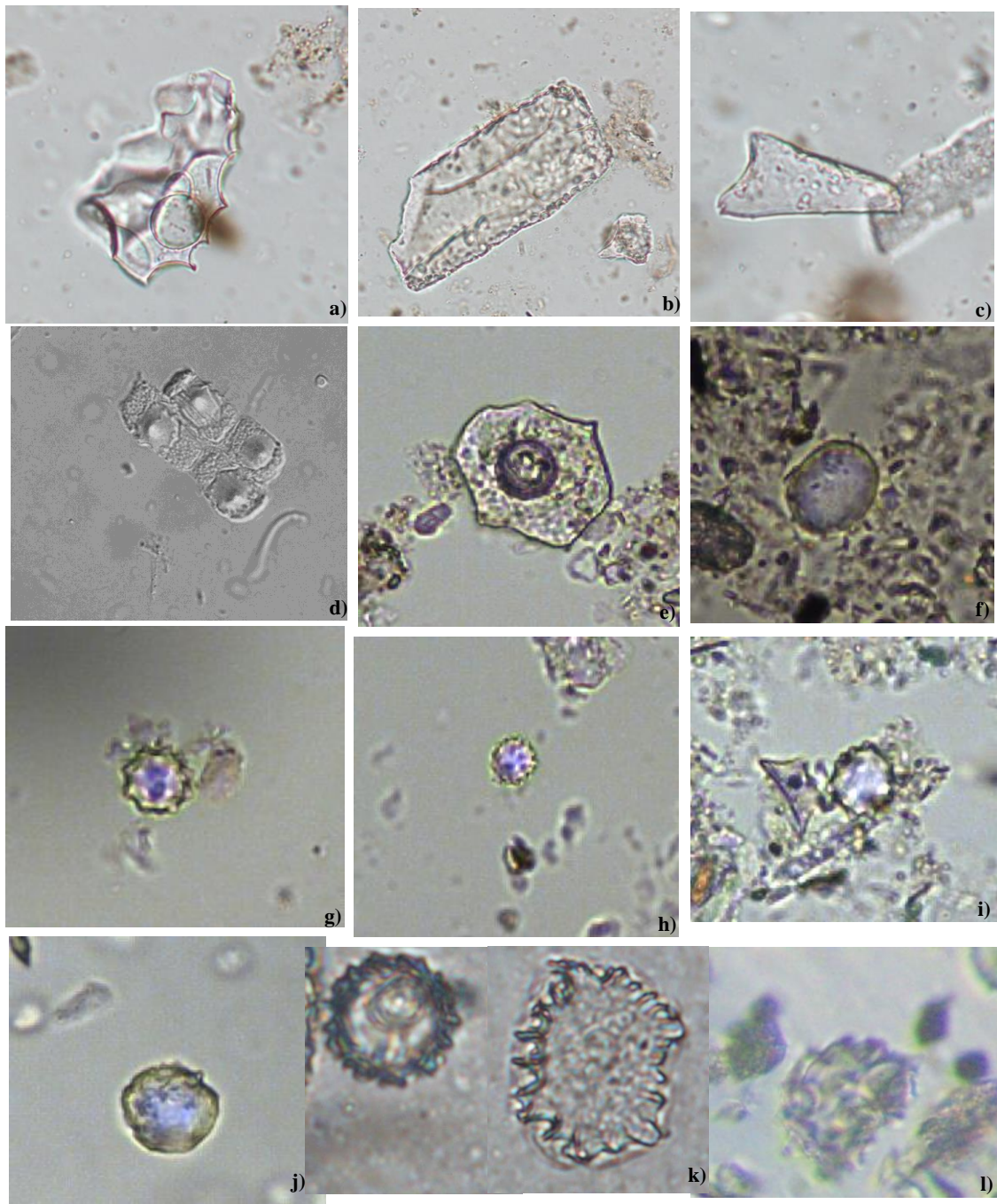


Figure 4. Non-grass phytoliths in the fossil assemblages; a) Tracheid, b) elongate facetate, c) scutiform, d) papillae/hat-shaped e) achene, f) globular psilate, g-i) globular echinate, palm type, j-l) globular decorated /granulate(k-top left) Scale bar=10µm

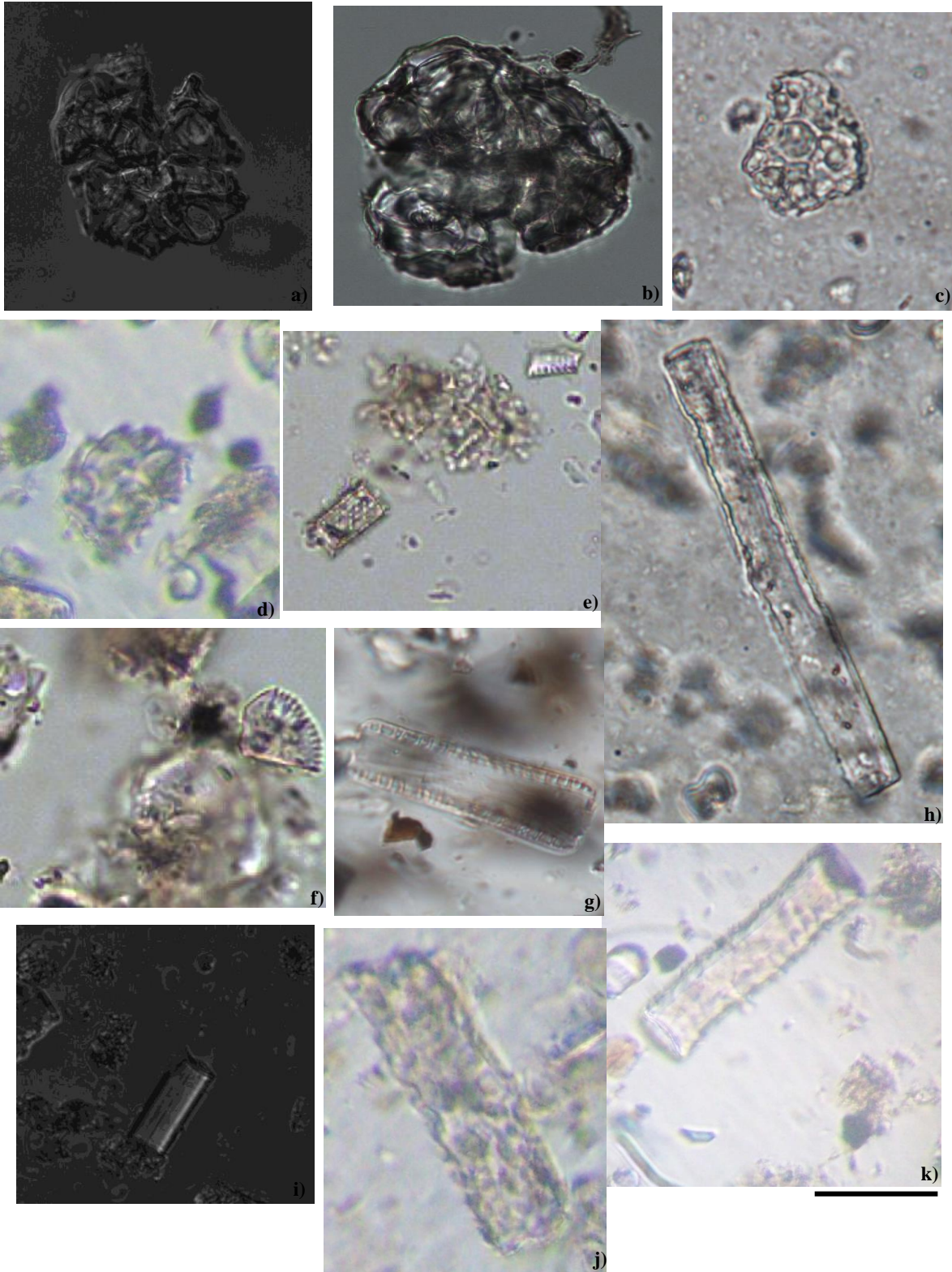


Figure 5. Non-grass phytoliths; a-d) globular verrucate, e-g) sponge spicules and diatoms, h) parallelepiped, i) sponge spicules, j-k) parallelepiped variants. Scale bar=10 μ m

2.3 Background of Phytolith studies

Phytoliths were first recognised in 1675, described and classified by Ehrenberg in 1836 (Rapp and Mulholland, 1992). Application of phytolith studies have increasingly gained popularity in the following categories: - 1) Actualistic studies (plant systematics), 2) past human-plants interactions (archeobotany) and 3) paleoecology (past environmental reconstructions) (Piperno, 1988; Mulholland and Rapp, 1992; Piperno and Pearsall, 1998) as summarised below.

Phytoliths systematics has played a great role in the rapid development of phytolith research, (Twiss et al., 1969; 1992; Madella et al., 2005; Stromberg, 2007; Alexandre and Bremond, 2008), it suffers a great challenge because of insufficient data standardisation in both identification and quantification which hinders broader connectivity in interpreting phytolith data between sites and across regions (Zurro et al., 2009; Shillito, 2012). The only baseline that exists so far that guides on phytolith morphological description, the International Code for Phytolith Nomenclature (ICPN) was published by Madella et al., (2005) which is not always used by researchers (Shillito, 2012). In addition, taphonomic biases and insufficient count size make it difficult to relate and interpret fossil phytolith data/assemblages for different sites especially for palaeoecological significance (Stromberg, 2009; Shillito, 2012).

Phytolith analyses have been used in archaeological studies since the 1970's and came of age in Old and New worlds (Rovner, 1971; Piperno, 2006). On 1980's application of phytolith was mainly focused on reconstruction of prehistoric agricultural systems (Piperno, 1988, Piperno and Pearsall, 1998; Piperno, 2009; Piperno et al., 2009) and archaeobotanical studies on various plants uses (Piperno, 1991). In Asia, investigating the agricultural development of rice, wheat and barley (e.g. Rosen 1992; Pearsall et al., 1995) and other historical non-food plant uses (Madella et al., 2002; Rosen, 2005; Albert et al., 2000; 2008; 2010).

In summary, these studies demonstrated that phytoliths can address the following archaeobotanical and agricultural questions which are critical in understanding the past human-plants interactions; 1) origins and dispersals of crop domestication and development of agricultural practices, 2) availability and socio-economic wild plants, 3) chronology of plant use and subsequent domestication, 4) functions of pottery and stone tools, 5) vegetation cover associated with archaeological sites and human-environment interactions and 6) the relation between existing technology and socio-economic organization (Piperno 2006: pg. 139). This is achieved especially when samples are collected within archaeological sites and from identified features such as hearths, grain threshing areas, storage areas and refuse/dustbin areas.

In addition, phytolith data derived from archaeological settings also provide information on the local vegetation cover and the environments with which early humans interacted with. More so, human influences on land-use patterns across the palaeolandscapes are understood.

In paleoecology, phytoliths are useful in quantitative indices of paleoclimates. This is especially so, because grass phytoliths distinguish C₄ grasses from C₃ grasses and computing their occurrence ratios, researchers have been able to infer past climates such moisture/rainfall and temperature gradients (e.g. Alexandre et al., 1997; Bremond et al., 2008). Phytolith assemblages identified from one fossil record provide interpretable data on past plant communities and vegetation structure e.g. forests vs grasslands (Stromberg, 2003; Rossouw, 2009).

A detailed chronology of application of phytolith studies in various disciplines in Africa (e.g. Alexandre et al., 1997; Barboni et al., 1999; 2007) has been provided in Rossouw (2009). However, I will mention a few examples for each category; as palaeovegetation and paleoclimates proxies (Fredlund and Tieszen, 1997; Bremond et al., 2012; Aleman et al., 2012), in archaeological records to infer early human-environment interactions (Rossouw and Scott, 2011; Barboni et al 2010; Mercader et al., 2000); to investigate early plant uses, particularly both domesticated and wild cereals/grasses (Mercader et al., 2009; Albert et al., 2008; Cabanes et al., 2010). In addition, other studies that document various phytolith morphologies and systematics as modern references to assist in identification and interpretation of fossil assemblage include (Bremond et al., 2005; Neumann et al., 2009; Novello et al., 2012 and Novello and Barboni, 2015).

Recent phytolith studies from various parts of Africa include work from Mozambique, quantitative and qualitative phytolith data to explore further on taxonomical strength of various morphotypes extracted from both grass and non-grass taxa (Mercader et al., 2009; 2010) and the taphonomic significance of phytoliths from modern top soils versus the Miombo woodlands in Mozambique (Mercader et al., 2011).

In Central and West Africa, Neumann et al., (2009) studied phytolith assemblages and indices to reconstruct local environments of Ounjougou (Mali) during Pleistocene and Holocene periods. In Chad central Africa, past fluvial habitats were reconstructed using phytolith analyses by distinguishing morphotypes based on modern analogue for aquatic vegetation studied in the region (Novello et al., 2012). Recent studies from East African region shows the significance of phytolith analysis on palaeocological reconstructions from renowned archaeological sites (Albert et al., 2009; Kinyanjui, 2012).

Although application of phytolith analyses is increasingly being utilised, challenges such as the taphonomic issues regarding differential phytolith reproduction by different plants, mode of deposition

and their depositional regimes and, local/ regional preservation status need to be considered as well as the sample size to be analysed for a data interpretation (Strömberg 2009; Shillito, 2011), consultation of modern phytolith analogue remains critical (Rossouw, 2009; Kinyanjui, 2012).

In addition, series of phytolith researches undertaken in West African tropical forest (e.g. Alexandre et al., 1997; Barboni et al., 1999) showed that fossil phytolith data can be reliably analysed to interpret changes in Holocene vegetation patterns and plant communities. The analytical approach applied here included extracting ~2-10µm volume of residue and using the ratio of selected morphotypes representing woody dicotyledons and Poaceae (dicot: Poaceae or D: P) respectively to interpret open and closed canopy vegetation structure.

The popularly used dicot morphotypes include rugose spheres/globular granulate, while for Poaceae they include: bilobate short cell, cross, saddle, rondel, polylobate and trapeziform morphotypes and their ratios have been effectively used to determine tree cover index (Bremond et al., 2008). Modern soil phytolith assemblages collected from known vegetation cover suggest a D:P value greater than 1 represents closed canopy such as tropical rain forest, while open environments are represented by D:P values close to 1 (savanna) and a value less than 1 represents open grasslands (Alexandre, et al., 1997). Although this may not be quite reliable for other parts of the world (e.g. North America) where plant communities may differ greatly from those in tropical Africa (Stromberg, 2003) the analytical approach has been successfully applied to reconstruct the African vegetation habitats (e.g. Neumann et al., 2009; Novello et al., 2012) whose phytolith assemblages match those of known soils derived from known habitats (Alexandre et al., 1997; Bremond et al., 2008).

In addition, the presence of indicator morphotypes which identify certain habitat-specific species such as palms, sedges and grasses within the fossil assemblage, contribute highly in interpreting primarily closed versus open vegetation habitats as well as specific ecological niches (Barboni et al., 1999; 2007; Bamford et al., 2006; Ashley et al., 2010a, Olduvai Gorge).

The data obtained in this study addresses the main objective of the research, to determine and understand the temporal vegetation dynamics of two localities and then climatic inferences are estimated. Similar phytolith studies related to hominin sites have successfully reconstructed the paleoenvironment and the vegetation cover in East Africa ; west side Awash, Ethiopia (Barboni et al., 1999); Olduvai Gorge (Albert et al., 2006; Bamford, 2006; Ashley et al., 2010 (a &b), Barboni et al., 2010 and Ologresailie basin (Kinyanjui, 2013).

Biases brought about by the differences in how various morphotypes are dispersed, transported and preserved (taphonomy; Piperno, 2006), are considered to have minimal influence on the assemblages identified and counted. This is because this study is based on assumption that the phytolith assemblages

analysed in both basins are representative of both local and extra-local plants and, geologically some of the sediments analysed are either paleosols (local terrestrial) or lacustrine (local aquatic & extra local terrestrial). For paleosol assemblages, there is a high likelihood that phytoliths are local with minimal extra-local brought in by Aeolian deposits, especially in open habitats. For the lacustrine settings, on the other hand, phytoliths are largely regional and brought in by wind and fluvial deposits with minimal local contributions from wetland associated plants such as palms and sedges (Stromberg et al., 2004). More so, temporal variation in vegetation structure is based on interpretation of the phytolith assemblage averaged through time/sampling profile.

Previous studies suggested that grasses accumulate and produce more phytolith as opposed to woody dicotyledons and argued this would affect phytolith data in that, most assemblages will be over-represented by grasses (see discussion in Piperno, 1988). However, later studies undertaken from tropical ecosystems of 5 continents showed that phytolith assemblages identified in tropical primary or secondary rainforest were mostly derived from dicotyledonous trees and shrubs (over 90% of the total assemblage) while those identified from soils underneath open grasses were dominated by up to 90% of grass silica short cells (GSSC) (Piperno, 1993; Kealhofer and Piperno, 1994; Piperno and Becker, 1996; Alexandre et al., 1997; 1999; Barboni et al., 1999; Runge, 1999; 2001; Mercader et al., 2000; Bremond et al., 2007). Two morphotypes considered as most important forest indicators are: 1) Rugose and smooth spheres found in leaves and wood of arboreal taxa, and 2) sclereids (silicified sclerenchyma cells) found in leaves of many tropical woody taxa (Piperno, 1988; Runge, 1996; 2001; Alexandre et al., 1997).

Determining the fraction of key forest- versus grassland- indicators present in the overall assemblage, can reliably record how closed or open a given vegetation ecosystem could have been, especially so in tropical regions.

2.3.1 Opportunities and limitations of phytolith data

Application of phytolith studies in various disciplines dealing with either fossil or modern or both assemblages have developed over time to accurately identify their parent plant species. However, the production of similar morphotypes by plants of different species-redundancy on one hand, and the production of different morphotypes by a single plants species-multiplicity on the other hand, have not been fully addressed (Rovner, 1971, Piperno, 1988; 2006).

Considering the broader application of phytolith studies to address various research questions and rate of research developments versus the challenges recently highlighted in Shillito (2012) and Zurro et al., (2009), it is clear that phytolith data have a great potential in determining introduction of various

domesticated crops and plants uses in archaeological context, plant diets from dental remains and reconstructing the vegetation history and dynamics in palaeoecological context (Alexandre et al., 1997; Barboni et al., 1999; Runge, 1999; Mercader et al., 2000; Stromberg 2003; Bremond et al., 2005; Rossouw, 2009; Ashley et al., 2010b).

As more phytolith studies are undertaken across space and through time, improved and more standardised methods to bridge the gap between the advantages and disadvantage will be achieved. The more datasets from different regions/localities presented, the closer we get to standardized methods and interpretation (see also Zurro et al., 2015).

It is on this basis that this research has been feasible. Koobi Fora and the Olorgesailie sites are paleolake basins and are located in semi-arid regions of the Kenyan rift systems. Plants microfossils are rare to absent in these basins due to poor preservation of organic materials. Fortunately, phytoliths, being inorganic in nature preserve well. Previous studies have demonstrated application of phytolith studies to address different questions in African.

2.4. Goals and Objectives

The main goal of this study is to investigate the palaeoenvironments of two major hominin sites in Kenya through mid-Pleistocene to Holocene periods. The study will compare the past vegetation cover between Olorgesailie and Koobi Fora Basins during a sequential geological time frame.

2.4.1. Justification

Phytolith analyses have been successfully applied to reconstruct the vegetation context of the Olorgesailie basin, south rift valley during the mid-late Pleistocene period (Kinyanjui, 2012). This work will therefore provide more data regarding the vegetation component of the basin with provision of a more continuous chronology, from a core obtained by the Olorgesailie drilling project 2012 which spans through mid-Pleistocene to Holocene periods. Similar analyses will be undertaken from Koobi Fora basin covering the same time frame, to compare and contrast the vegetation cover of these palaeolandscapes. This will contribute crucial information on the palaeoenvironments with which *Homo erectus* and other faunal populations interacted with, and the possible prevailing climates.

2.4.2. Research questions

1. What was the vegetation structure of Olorgesailie and Koobi Fora basin and how it has changed through the mid-Pleistocene-Holocene period?
2. How different or similar is the vegetation structure represented in the both basins?
3. Based on archaeological data, how did vegetation structure influence the faunal communities recorded from both basins?

2.4.3. Specific goals and objectives

To achieve this, the above mentioned goal, the following specific objectives/goals are addressed:-

- 1) Analyse and compare phytolith morphologies derived from palaeosols dated between mid-Pleistocene and Holocene periods from both basins,
- 2) Determine and compare the preservation status of fossil phytoliths from basins,
- 3) Interpret the temporal changes of vegetation structure as represented by fossil phytolith assemblages from both basins, and
- 4) Explain how the vegetation structure may have influenced faunal-environment interactions and adaptation strategies, including the hominins.

2.4.4. Research Hypothesis

Both the Koobi Fora and Olororgesailie basins have similar depositional regimes which include, alluvial, lacustrine and fluvial sediments and, they have varied habitats across the palaeolandscapes controlled by local topography and drainage systems (Brown and Feibel, 1986; Behrensmeyer et al., 2002). However, they differ greatly in the number of hominin species and faunal species preserved in the two basins as well as the concentration of archaeological artefacts associated with early hominins. In Olororgesailie, a single hominin fossil has been found in association with high density of Acheulean hand axes (Potts et al., 2004) while in Koobi Fora multiple hominin fossils have been found in association with a variety of archaeological artefacts (Brown et al., 1985; Braun et al., 2010). Moreover, Pollen analyses from the Olororgesailie basin showed poor pollen preservation due to oxidation (Mworia, 1999-*unpublished*) while in Koobi Fora although sparse, palynology data has contributed to the understanding of part of the basin's palaeoenvironments (Bonnefille, 1995; Mohammed et al., 1995). The hypothesis developed from this, is that, although both basins have unique prehistoric evidence, it is possible the preservation of fossils is controlled largely by local environments that most likely differ from one basin to the other. If a common proxy is used to determine the palaeoenvironments within a similar time frame, the disparities noted could be well explained.

CHAPTER THREE: STUDY SITES

3.1. Introduction

The Rift valley system runs from Red Sea in far north to Malawi in south (Frostick, 1997). It is marked by a series of lake basins and volcanoes/ craters which are bordered on the two sides by high relief escarpments and plateaus that run parallel (Frostick, 1997; Olago et al., 2009). This rift systems influences local climates, hydrology and surface drainage system resulting in the formation of many closed hydrological basins (Garcin et al., 2009; Olago et al., 2009). The Turkana and Olorgesailie basins are located within the East African rift system. Lake Turkana is located at 36°E, 3°N while Olorgesailie basin is located at 34°E 1°S (Figure 6).

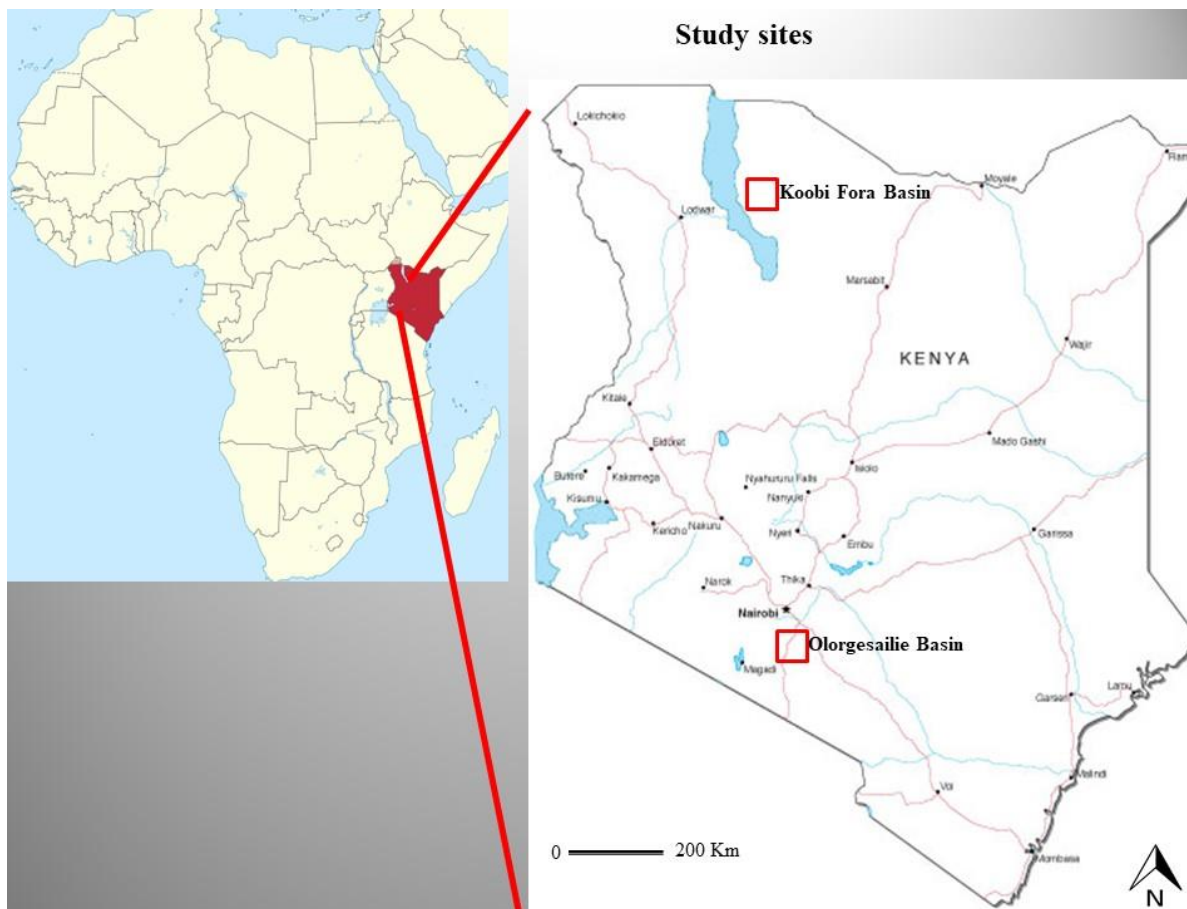


Figure 6. Shows location of the study sites: Koobi Fora basin in north and Olorgesailie Basin in south

3.1.1 Contemporary climates in East Africa

The current climate variability of the East African region is largely determined by the strong regional fluctuations in rainfall regime (Nicholson, 1996) and temporal variation in surface air temperature (King'uyu et al., 2000). The four main factors that are responsible for these climatic phenomena include 1) the inter-tropical convergence zone (ITCZ), 2) the Congo Air Boundary (CAB), 3) the El Niño-

southern Oscillation (ENSO) and 4) the East African Monsoon (Southeast (SE) and Northeast (NE) monsoons see figure 7.

This is further enhanced by complex interactions between extra-regional atmospheric circulation processes, maritime influences such as Indian Ocean's Sea Surface Temperatures (SST) and regional topography of mountain ranges, rift valley and large lake basins and general land-atmosphere feedbacks (Nicholson, 1996; 2000; Mutai and Ward, 2000).

The annual migration of the ITCZ and CAB across the equator from south to north and vice versa, is responsible for the general bimodal rainfall regime in the region; with long rains occurring between March and May while short rains occur between September/October and (Nicholson 1996; 2000 Mutai and Ward, 2000). However, local topography and Monsoonal wind systems (westerlies and easterlies) largely interfere with temporal rainfall distribution and intensity (Conway, 2002).

The strong relationship between monthly and seasonal rainfall patterns and phases of the ENSO enhances inter-annual rainfall variation where warm events of ENSO leads to above average rainfall (El-Niño years) and the cold events lead to below average rainfall (La-Niña) during the short rainy season (Nicholson, 1996; Nicholson and Kim, 1997; Mutai and Ward, 2000). Generally, mean annual rainfall varies from $\sim 200\text{-}400\text{mm yr}^{-1}$ in the most arid region e.g. North-eastern Kenya, and exceeds 1200mm yr^{-1} in the most humid region e.g. Mt Elgon. Seasonal rainfall patterns may vary greatly within a very short distance (10s of km) depending on local topography (Nicholson, 1996). The mean annual temperature varies from $21\text{-}26^{\circ}\text{C}$ (T_{max}) to $10\text{-}15^{\circ}\text{C}$ (T_{min}) (King'uyu et al., 2000).

In between the two strong rainfall seasons, there are two pronounced dry seasons that are notable in their extreme year-to-year draughts occurring especially in the semi-arid and arid regions (Mutai and Ward, 2000). The climatic anomalies associated with El-Niño and La-Niña events result in extreme flooding and droughts respectively, which have varied local impacts on environmental and socioeconomic aspects in the region (Maruo, 2002). Arid and semi-arid lands with scarce vegetation cover and, where the main socioeconomic activity is pastoralism, suffer greatly during such events. The Ologesailie and Koobi Fora basins are within the semi-arid regions within the East rift system, in south and north respectively.

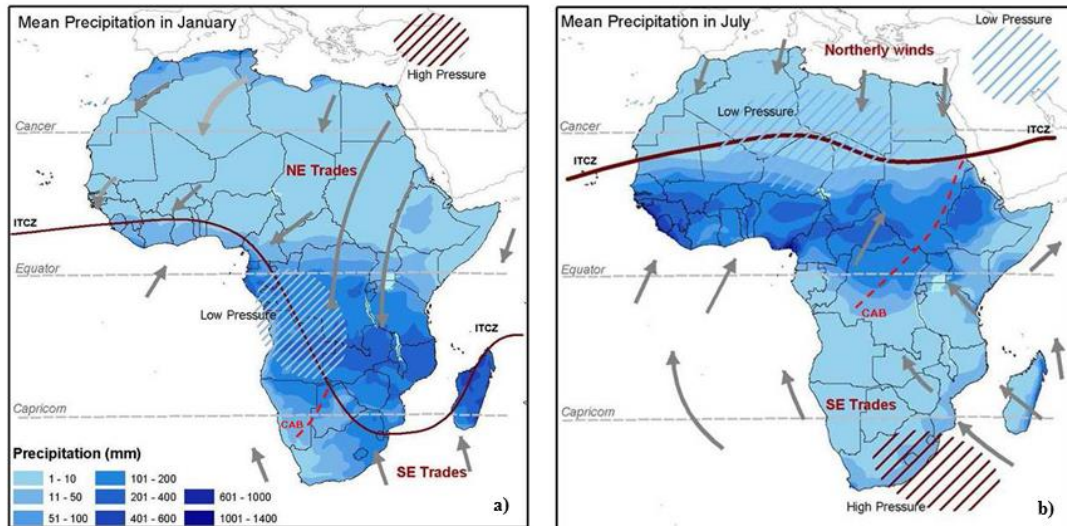


Figure 7. General patterns of precipitation, trade winds, pressure and convergence over Africa during a) northeast monsoon and b) southeast monsoon, CAB patterns based on Nicholson, 1996.

3.1.2. Contemporary vegetation in East Africa

Vegetation cover in East African region varies from highland montane forest in the high altitudes (mountains), to lowland woodlands to grasslands savanna. They are characterised into Afro alpine, Alpine, montane forests, Guineo-Congolian, Zambebian, Sudanian and Somali Masai (White 1983).

3.2. Olorgesailie basin

The Olorgesailie basin is located at 36° 26'E, 1° 34'S, in southern part of Kenyan rift valley system, about 110km south west of Nairobi city, Kenya. Fossil bearing sediments cover approximately 150km² area and lies between 940-1040m above sea level. The drilling sites are located within the Koora plains, approximately 20km south of Mt. Olorgesailie (Figure 8).

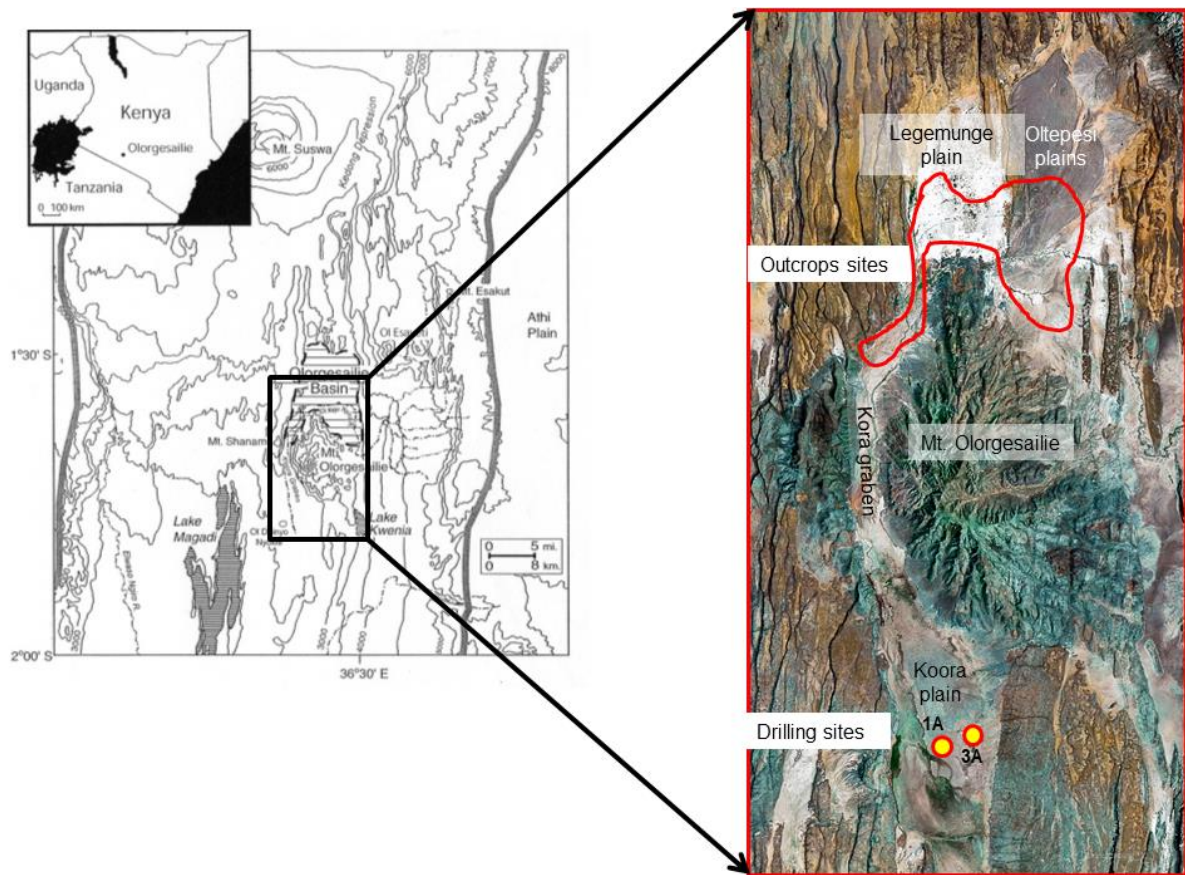


Figure 8. Map showing the location of the Olorgesailie outcrops in north and the ODP drilling sites in the Koora plains ~20km, south of Mt. Olorgesailie (after Behrensmeyer, 2002).

3.2.1. Climate

The climate of Olorgesailie basin and the immediate environs is characterised as semi-arid, with an average annual rainfall of 500mm and extremely high evapotranspiration rate of more than 2400mm per annum (Damnat and Taieb, 1995) see figure 1. This is as result of rainfall patterns altered by the topography within the central rift valley basin from normal bimodal rainfall pattern influenced by the seasonal ITCZ migration, to irregular rainfall pattern received in the basin in one season (Kenworthy, 1966; Nicholson, 1996; Mutai and Ward, 2000).

3.2.2. . Vegetation cover

The current vegetation cover is characterised as *Commiphora-Acacia* bushland (White, 1983) also known as Northern *Acacia-Commiphora* bushland (WWF Eco-regions). The dominant woody species include; *Acacia tortilis* (Forssk.) Hayne, *A. senegal* (L.) Willd., *A. mellifera*, *Balanites* spp. *Grewia bicolour* Juss. *G. villosa* Willd; *Boscia coriacea* Pax., *Salvadora persica* L., *Commiphora africana* (A. Rich.) Engl., *C. campestris/scheffleri* Engl. and *Terminalia* sp. (after Mworio et al., 1988).

The shrub components include *Sericocomopsis* sp, *Barleria* sp. *Aerva* sp, and *Indigofera* sp. The grasslands are dominated with C₄ grasses such as; *Chloris roxburghiana* Schult., *Dactyloctenium bogdanii* S.M. Phillips, *Eragrostis cilianensis* (All.) F.T. Hubb., *Tetrapogon cenchriformis* (A. Rich.) W.D. Clayton and *Sporobolus jacquemontii* Kunth (after Mworia 1988). A few riverine species are found along the dry river channels (“lugga”s), such as *Syzygium* sp. *Terminalia* sp and *Delonix elata* (L.) Gamble as well as wetland components like *Brachyachne* spp., *Kyllinga alba* Nees. and *K. welwitschii* Rindley (Mworia et al., 1988).

3.2.3. . Geo-archaeology and core lithology

The geo-archaeology of the basin is well studied and spans to Plio-Pleistocene period (Baker and Mitchel, 1976; Isaac, 1977; Potts, 1989; Deino and Potts, 1990; Potts et al., 1999; Brooks et al., 2007). The drainage system is controlled by the gradual North-South sloping of the rift valley floor over millennial scale (Behrensmeyer et al., 2002). The sediments are mainly diatomite, diatomaceous silts, clayey silts, volcanoclastic sands and gravels deposited in lacustrine, wetlands, fluvial and colluvial regimes which are well marked laterally across the basin (Deino and Potts, 1990). Primary core lithology described by Behrensmeyer et al., *in progress* is shown in the figure 9.

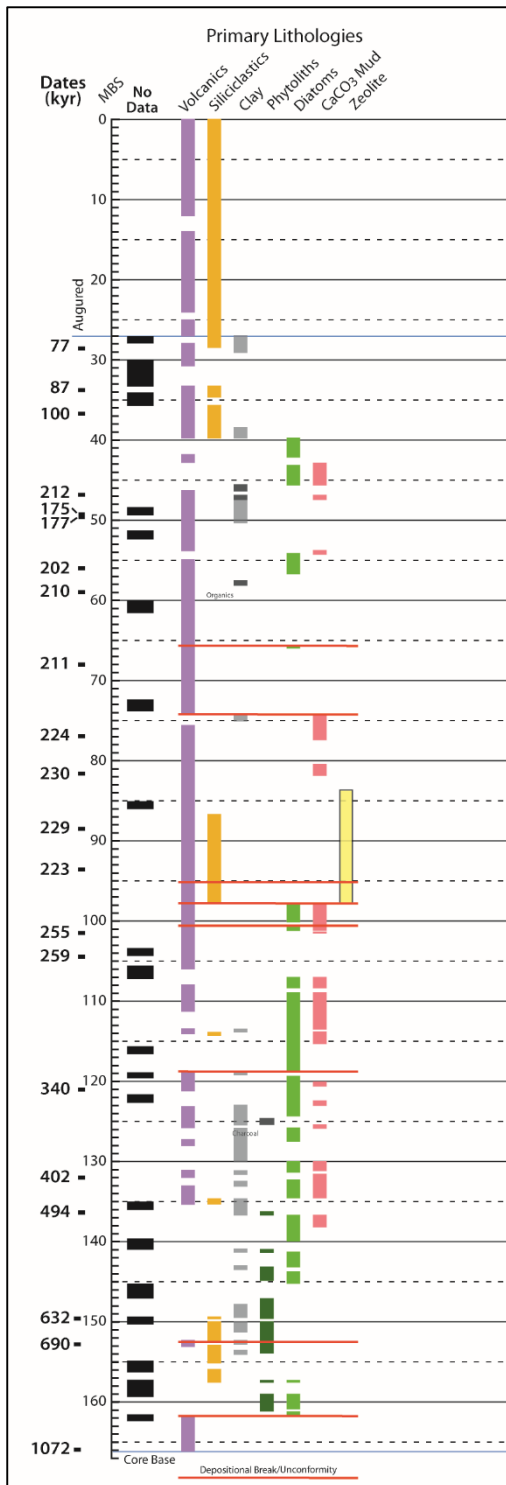


Figure 9. Showing the preliminary lithological and geochronological data and levels of sampling for phytolith, diatoms, CaCO₃ mud and zeolite analyses

The geological dates are obtained using a single crystal Ar⁴⁰/Ar³⁹ dating technique spanning from approximately 1.1Ma to 0.077Ma (Deino et al., *in progress*).

3.3. Koobi Fora basin

Koobi Fora basin is located in the Northern part of the Kenyan rift valley system approximately 800km north of Nairobi city. It is part of the larger Plio-Pleistocene sedimentary sequence and is discontinuously exposed approximately 1200km² along the eastern shore of Lake Turkana. It extends from Kenya-Ethiopia in north (Ileret) to Allia Bay in the south (Figure 10). It extends approximately 30-40km eastwards from the modern lakeshore up to Surgei and Gombe, Miocene and Pliocene plateaus (Brown and Feibel 1986; Feibel, 1988). Much of the area lies within the Sibiloi National Park which was gazetted in the early 1970s to protect the region's arid biodiversity and numerous, diverse, unique and well preserved faunal and floral fossils and archaeological artefacts that date back between Miocene and Holocene periods (Robertshaw, 1995; Willoughby, 2007). It was named as a UNESCO World Heritage site in 1997. The basin lies between ~360-560m a. s .l.

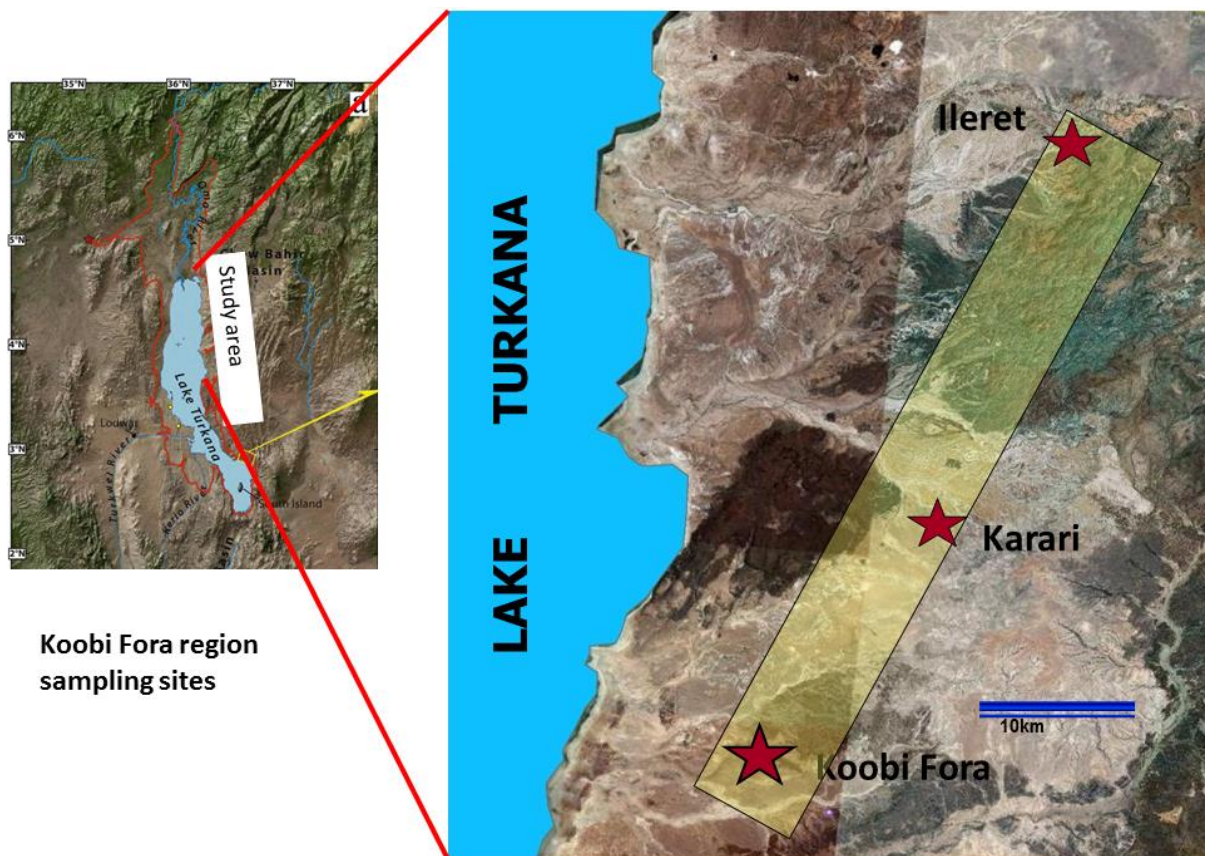


Figure 10. Map showing Lake Turkana, Koobi Fora Basin and sampling localities (modified from Forman et al., 2014)

3.3.1. Climate

The general climate of the basin is categorised as arid to semi-arid with mean annual rainfall of ~130-~150mm, estimated evaporation at ~2850mm per year and mean annual temperatures of 32°C (Yuretich & Cerling 1983). The Koobi Fora region is considered as one of the 1% hottest land area on Earth

(Hijmans et al., 2005), with mean maximum temperature at $\sim 37^{\circ}\text{C}$, mean minimum temperature at $\sim 27^{\circ}\text{C}$ and soil temperatures (25cm –depth) at 37°C . Strong south-easterly winds are prevalent in the region (Feibel, 1988). The rainfall pattern in the region is bimodal and is controlled by monsoon currents long rains between March and May, while short rains between September and November. The highest rainfall peaks in April and November for each season (See, Olago et al., 2009; Mbaluka and Brown, 2016). In recent times, just like other parts of Kenya, the region has experienced drastic changes in the rainfall pattern, both in season duration and intensity which have reduced greatly leading to devastating droughts that have caused deaths of both the wild and domesticated animals due to lack of pastures and drinking water.

3.3.2. Vegetation cover

The current vegetation cover for the general Lake Turkana basin is described as *Acacia-Commiphora* grassland and shrub lands (White 1983) and consists of woody riverine forest and semi-desert scrub, mainly *Acacia*, herbaceous vegetation and semi-desert grasslands with annual and perennial scrubs/bushes (Barthelme 1985; Butzer. 1982). Recent vegetation mapping from the Koobi Fora region shows the region has distinct flora heterogeneity that is highly controlled by the soil/rock type, topography and the drainage system (Mbaluka and Brown, 2016).

Dwarf shrub lands/grasslands cover the largest area $\sim 83\%$ and are dominated with *Indigofera spinosa*, *Dusperma longcalyx*, *Barleria spp.*, *Sporobolus spicatus* (perennial grasslands along the lake shore) and *Aristida mutabilis* (annual grasslands). Shrublands are mainly found on alluvium and outcrop exposures, dominated with *Commiphora sp.* *Euphorbia cuneata*, *Acacia recifiens*, *Cadaba rotundifolia* and *Salvadora persica* and are more prominent in the north, especially at Ileret. Woodlands and riparian vegetation cover are mainly associated with seasonal ponds and ephemeral stream channels (“lugga”s), are dominated with *Hyphaene compressa*, *Acacia elatior*, *Ziziphus mauritiaum*, *Cordia sinensis*, *Lawsonia inermis*, *Terminalia spinosa*, *Acacia tortilis* and *Grewia sp.* These species constitute the riverine gallery forests along the river channels which grades rapidly into shrubs and grasslands. The herbaceous component constitutes predominantly with *Barleria spp*, *Aloe sp*, *Sansveria sp.* and C_4 grasslands (see Mbaluka and Brown, 2016 for more details).

3.3.3. General geology and drainage system

The entire Lake Turkana based is characterised by Tertiary to Pleistocene basalts, trachytes, phonolites and rhyolites that extend from the Ethiopian highlands in the north and outcrops of granitic volcanoes in the lower region towards the south and is largely covered by alluvium deposits brought in by the Omo River. The South and South Western part of the lake consist of extensive outcrops of Precambrian quartzite, amphibolite schists, biotite gneisses, hornblende gneisses, migmatites and plagioclase

amphibolites of the Upper Proterozoic Turbo-Kitale Group (Pallister, 1971; Halfman et al., 1989). On the Eastern edge, it is bordered by the volcanic plateau, Surgei-Assile (Ferguson and Harbolt, 1982).

These rocks are overlain by a mixture of fluvial, fluvial-lacustrine and littoral lacustrine sediments that have been subjected to a series of erosional and deposition processes and range from Pliocene-Pleistocene to Holocene periods which have preserved critical information on biological, behavioural and cultural evolution of living organisms including humans (e.g. de Heinzelin, 1983; Owen and Renault, 1983; 1986; Harris et al., 1988; Brown and Feibel, 1986; Olago et al., 2009).

Sediments in the Koobi Fora basin are mainly conglomerates, sands, silt and clays deposited in lacustrine, deltaic and fluvial settings with distinct lateral variation (McDoughall and Brown, 2006). These sediments span the Pliocene through Pleistocene to Holocene periods and are found in the southeast, northeast and east of Lake Turkana basin. These sediments overlay Miocene volcanic rocks and they archive a long record of the landscapes changes with transition from forests into open arid grasslands vegetation cover.

The current drainage system of the region flows in an E-W direction, draining into the Lake. Ephemeral streams, known as “lugga” cuts through the volcanic rocks, sedimentary outcrops and parts of alluvial surfaces and carry surface water only briefly, 1-2 days after the rains. Some larger streams carry below-surface water ~1-3m depth, for longer periods, 6 to 12 months.

Lake Turkana is a closed basin whose average alkalinity is about pH~9.2 and derives its waters from the Omo River which drains from the Ethiopian highlands in the north, the quasi perennial Turkwel and Kerio rivers in the west and the ephemeral streams/rivers that drain the surface flow to the lake only a few days to hours after a heavy downpour in East and West (Walsh and Dodson, 1969; Frostick and Reid, 1990; Olago and Odada 2000). The salinity increases from north to south.

3.3.4.. Geo-archaeology

The basin is part of the larger fossil bearing locality of the Turkana basin which constitute three main geological sequences; the Shungura, Mursi, and Usno Formations (Lower Omo valley) in the north (de Heinzelin, 1983); the Nachukui Formation in the west (Harris et al., 1988) and the Koobi Fora Formation on the northeast of present Lake Turkana (Brown and Feibel, 1986) all of which belong to the Omo Group (de Heinzelin, 1983). These sediments have a paleontological record that stretches back to the Pliocene period and archaeological record that dates back to 2.4 million years (Brown and Feibel, 1986). The Koobi Fora region is further sub-divided into three main geographical sub-regions; Ileret sub-region in north, Koobi Fora in the central and Allia bay sub-region in south (Feibel, 1988).

The Koobi Fora Formation has an aggregate thickness of 560m, dated from 4.3 to 0.6 Ma (Brown and Feibel, 1986). It constitutes eight members, the older five are Pliocene (Lonyumun, Moiti, Lokochot, Tul Bor and Burgi) while younger three are Pleistocene (KBS, Okote and Chari). These Members are distinguished using volcanic ash horizons (tephra) which have a unique chemical composition (Figure 11). Two significant unconformities occur within the Koobi Fora Formation; one within the Burgi Member, dividing this Member into two informal Members (lower and upper Burgi) and the second one occurs within the Chari Member. The Formation overlies “disconformably or unconformably on, or are in fault contact with Miocene and Pliocene volcanic rocks and /or associated sediments, and are disconformably overlain by the Holocene Galana Boi beds” (*see detailed geological description of the Formations*; Brown and Feibel 1986; Gathogo and Brown, 2006).

The Holocene Galana Boi Formation overlay the Chari Member of the Koobi Fora Formation during a high lake stand (approximately 80m above the current lake level) of Lake Turkana during the Holocene Period (McDougall and Brown, 2006). There is a 40-10ka hiatus between the Pleistocene sediments, the Chari Member and the Holocene sediments, the Galana Boi Formation (Butzer et al., 1972; Owen and Renaut 1983; 1986; Olago et al., 2009).

At Koobi Fora, the Galana Boi Formation constitutes lacustrine and shoreline deposits characterised by diatomaceous siltstones, sand and molluscs and fish remains (Owen and Renaut, 1986). Although the research history for both the Koobi Fora and Galana Boi Formations go back to the 1960's, a lot more have been documented/published from the Koobi Fora Formation compared to the Galana Boi. Already the existing published paleoanthropological and archaeological research show more research have been done from the Koobi Fora Formation (e.g. Harris, 1978; Brown and Feibel, 1986; Feibel, 1988; Walker and Leakey, 1988; Rogers, 1997; Leakey et al., 2001; Braun, 2006) as opposed to research undertaken from the Galana Boi Formation (Owen et al., 1982; Barthelme 1985; Ndiema, 2011; Ndiema et al., 2011). In addition, research from the Koobi Fora Formation has a longer history while in Galana Boi, it only started recently in 1980's. , In terms of paeloobotanical works very little is known from both Formations especially on plants micro-fossils analyses. The palaeoenvironmental significance of the Galana Boi Formation in particular offers a great opportunity of investigating the past vegetation cover across the Holocene palaeolandscape of the Koobi Fora basin (Ashley et al., 2011).

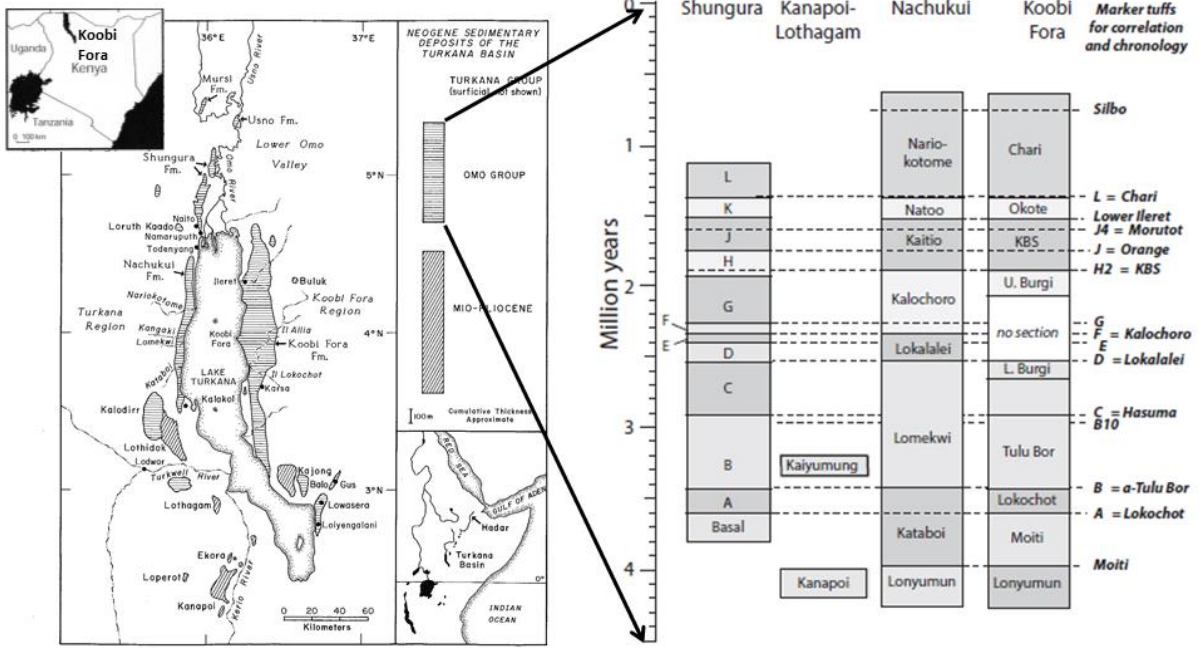


Figure 11. Map of Turkana basin showing the three “Omo-Group” Formations; Shungurra, Nachukui and Koobi Fora and their respective Members (Brown & Feibel, 1991; 1986; Cerling et al., 2015).

CHAPTER FOUR: MATERIALS AND METHODS

4.1. MATERIAL

To apply phytolith analysis as a tool for reconstructing the vegetation history of the Ologesailie and Koobi For a paleo-sites, three sets of samples were collected and analysed for phytoliths. These included: 1) modern reference collection (from modern plants and soils), 2) Ologesailie paleolake drill core (ODP core) and 3), Koobi Fora sediment samples (collected from geo-trench and archaeological excavation). Sampling differed between sites as reported in the following below sections:-

4.1.1. Modern soil samples

Four modern surface samples were collected from different vegetation cover as shown in Table 1

Table 1. showing the four vegetation habitats, where modern soil samples were collected.

Sample no.	Vegetation description	Habitat	Soil Types
SS1	<i>Acacia-Commiphora</i> shrublands	Short woodlands	Shallow soils on rocky substrates
SS2	<i>Acacia-Syzygium-Sanseveria</i> woodlands	Riverine gallery woodland	Sandy-silty fluvial clays along the “lugga”s
SS3	<i>Barleria</i> sp. dominated scrubland	Open scrubland	Silty-sandy soils
SS4	Open grasslands	Grasslands	Silty-sandy soils

4.1.2. Fossil samples

Different sampling approaches were used for each basin depending on the available resources. From the Koobi Fora basin, sampling was undertaken from sediment outcrops. Freshly dug geo-sections were measured and lithology described, samples were taken from all the paleosol layers. From the Ologesailie Basin, a core was drilled from the paleo-lake basin under the Ologesailie Drilling Project (ODP) in 2012. This is a multi-disciplinary and multi proxy project, whose sampling is targeted in all lithostratigraphic levels. However, while comparing the datasets from the both basins, only the paleosol layers that match similar time frames will be considered for this analysis.

4.1.2.1. Ologesailie samples

Two sediment cores were obtained from two locations in the Koora plain, approx. 10-20km south of the Ologesailie basin (figure 12). The cores were drilled where the basin’s depocenter occurred periodically over the past 500ka, based on the seismic survey data (Potts et al., *in progress*). The core

was recovered in segments ranging between 1m and 3m long. Sampling was done in all sediments types reflecting lacustrine, volcanic and terrestrial regimes/phases (see figure 13). A total of 272 (3cc) samples were collected from approximately 166m (below surface) sediment core at 48cm sampling interval.

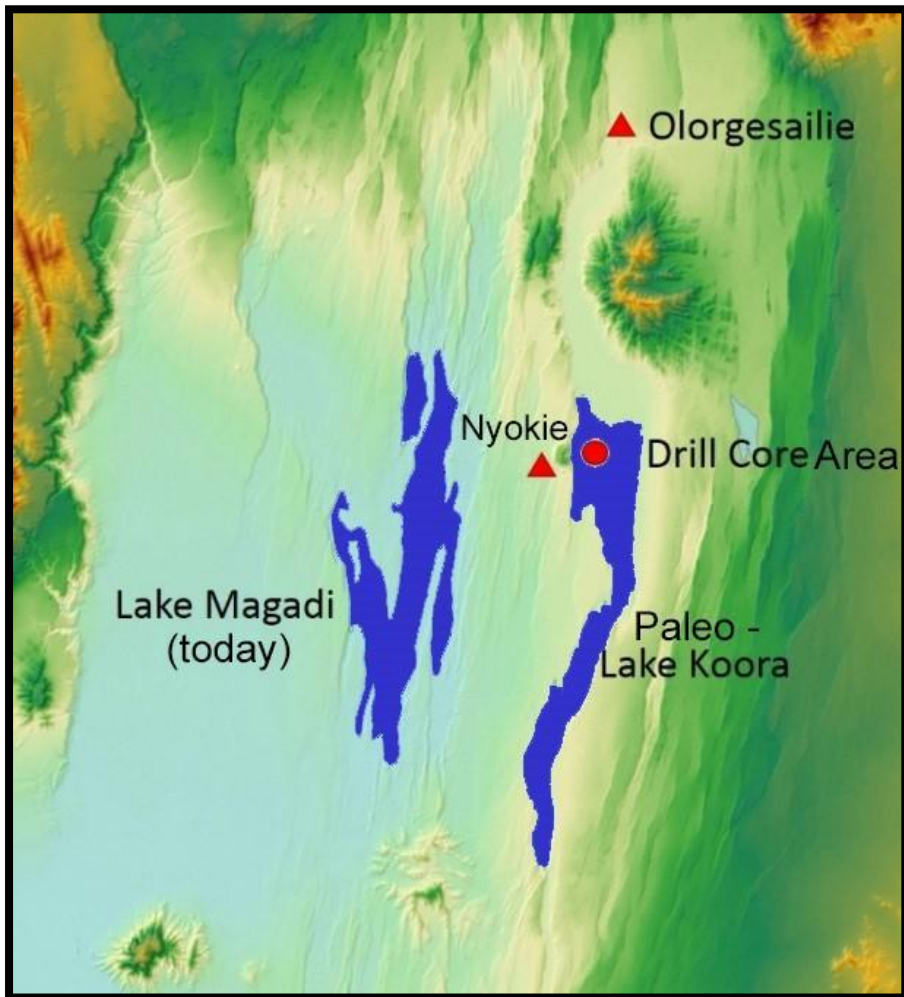


Figure 12. Map showing the drill location of the ODP sediment core. Note the proximity to the Olorgesailie Basin. Source: (http://humanorigins.si.edu/sites/default/files/styles/home_slider_phablet/public/Lake%20Kooraa%20map.jpg?itok=dhIGtI7C×tamp=1481139547)

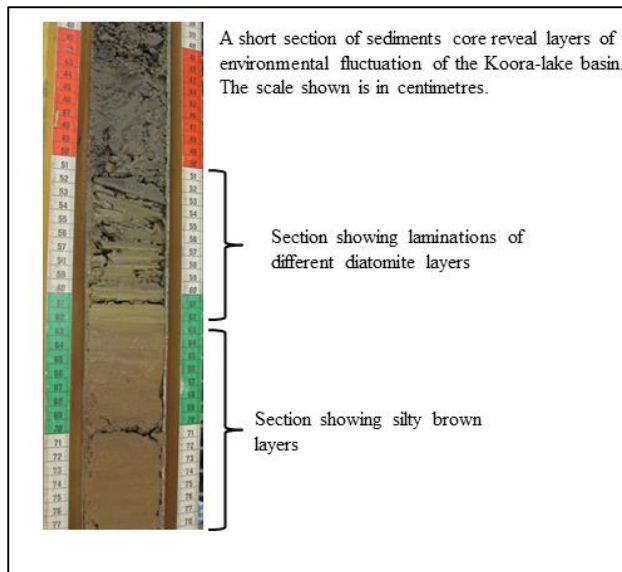


Figure 13. Showing the image of a short section of the ODP sediment core with different lithologies and cm-scale ruler

The overall goal of the ODP project is to build a detailed and continuous environmental record in the Olorgesailie basin during the last 1Ma. Detailed geological, anthropological and archaeological data have been recorded from the Olorgesailie outcrop that spans to 1.2Ma. However, crucial data for the last 500 ka-300ka, an interval corresponding to the oldest known evidence of a key shift in hominin behaviour and technological transitions is missing from the outcrops due to an erosional, non-deposition phase (Deino and Potts, 1990; 1992; Behrensmeyer et al., 2002). In the Olorgesailie basin, such evidence would have included the transition from Acheulean to Middle Stone Age (MSA) coupled with the extensive mammal turnover recorded from the nearby outcrops excavations (Potts et al., 1999; Brooks et al., 2007).

Phytolith data reported here is one of the proxies analysed aimed to characterize changes in vegetation structure and environmental dynamics in relation to the overall ODP goal climate variability on a seasonal to orbital scale and the possible impact on human evolution in the region will be discussed.

4.1.2.1.1. Geochronology, stratigraphy and Age modelling

The age model used here is obtained from $^{40}\text{Ar}/^{39}\text{Ar}$ dating technique on numerous tephra sampled from the sediment core as well as correlations to chronology available from the nearby archaeological and faunal sites. The preliminary age provisions span from ~1072kyr at the base of the core and ~77kyr at 27m below surface (Deino et al., *in progress*). Preliminary lithologies show volcanic, siliciclastic and lacustrine deposition; formation of zeolite suggests alkaline lake phases (Behrensmeyer et al., *in progress*, see figure 14).

a). Sample chronology

As mentioned earlier, the ODP project is a multi-disciplinary and multi-proxy project therefore has a common bench mark on which all the datasets can be compared and contrasted. The most critical aspect is the chronostratigraphic data which will be the main guideline on all other data acquisition, analyses and interpretation. The 272 samples were collected based on the available stratigraphic data analysed from 242 smear slides (Behrensmeyer et al., *in progress*) and chronological data obtained through $^{40}\text{Ar}/^{39}\text{Ar}$ dating technique of 140 tephra samples (Deino et al., *in progress*).

The core was drilled in phases and had to be matched according to depth to create an accurate vertical base sections. The different core sections have a varying degree of expansion depending on the lithological characteristics and mineral composition which varies from one section to another. Consequently, the initial core measurements taken using scales do not represent accurate down-core distance. Therefore, the down-core distance measured during the drilling are the “gold standard” for all resulting data and lithological data has to match these numbers (Behrensmeyer et al., 2013).

The lithological description is based on sedimentological including grain size and micro-fossils data analysed from smear slides. The core log lithological data is transferred from the core sheets noting the measured down-distance for core sections tops and bottoms. This permitted to note the missing sections based on down-core distance measurements provided in the excel spread sheet.

The sketched logs are adjusted such that lithological boundaries fit within the given measurements for core tops and bottoms (marked in red) e.g. a core section measuring 150cm in the lab and a base of 35cm had expanded by 20cm after it was pulled up, thus the lithological section needed to be compressed into this distance (1.3m). See figures 14 & 15 for more details.

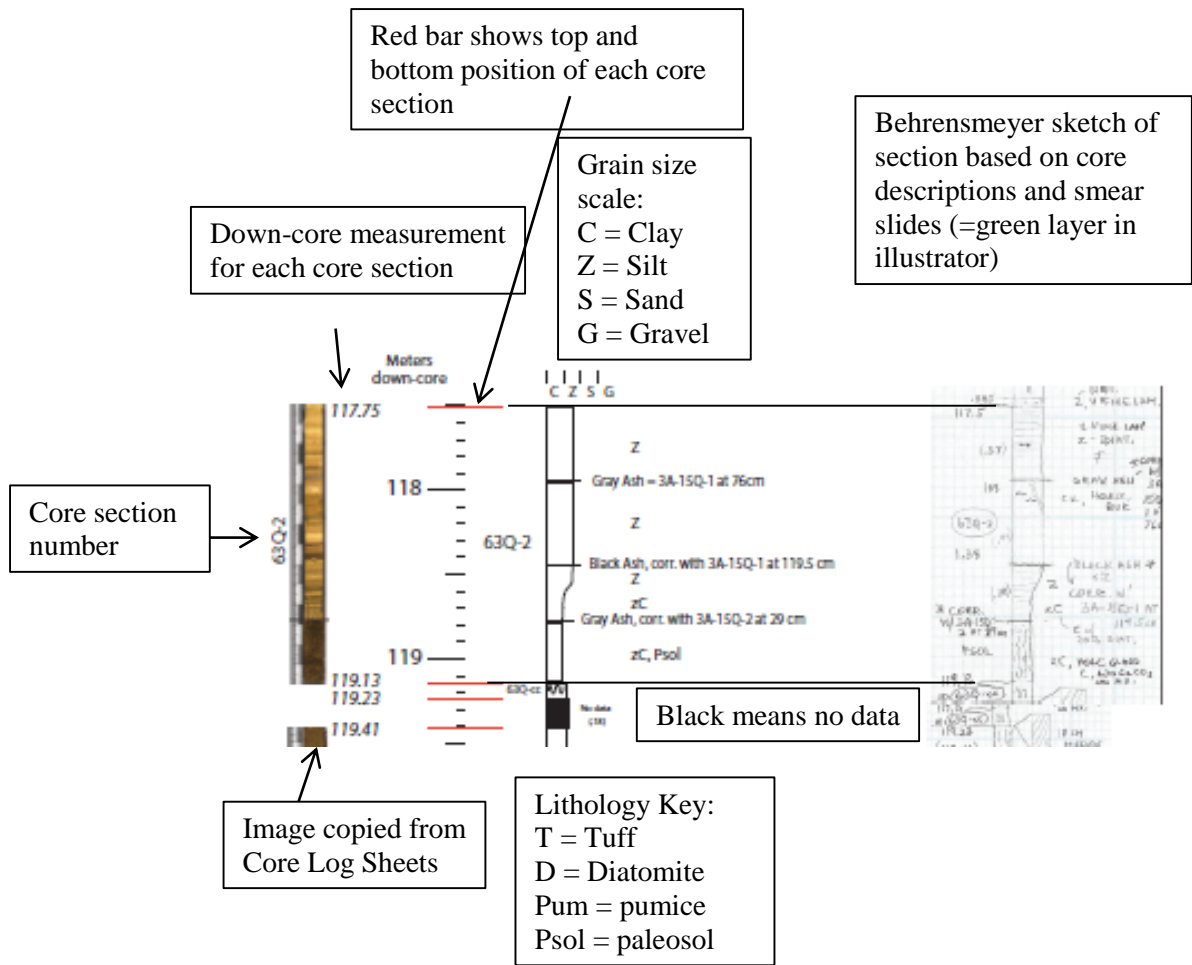


Figure 14. Explanation of a part of core section and lithological symbols by Behrensmeier et al., unpublished report.

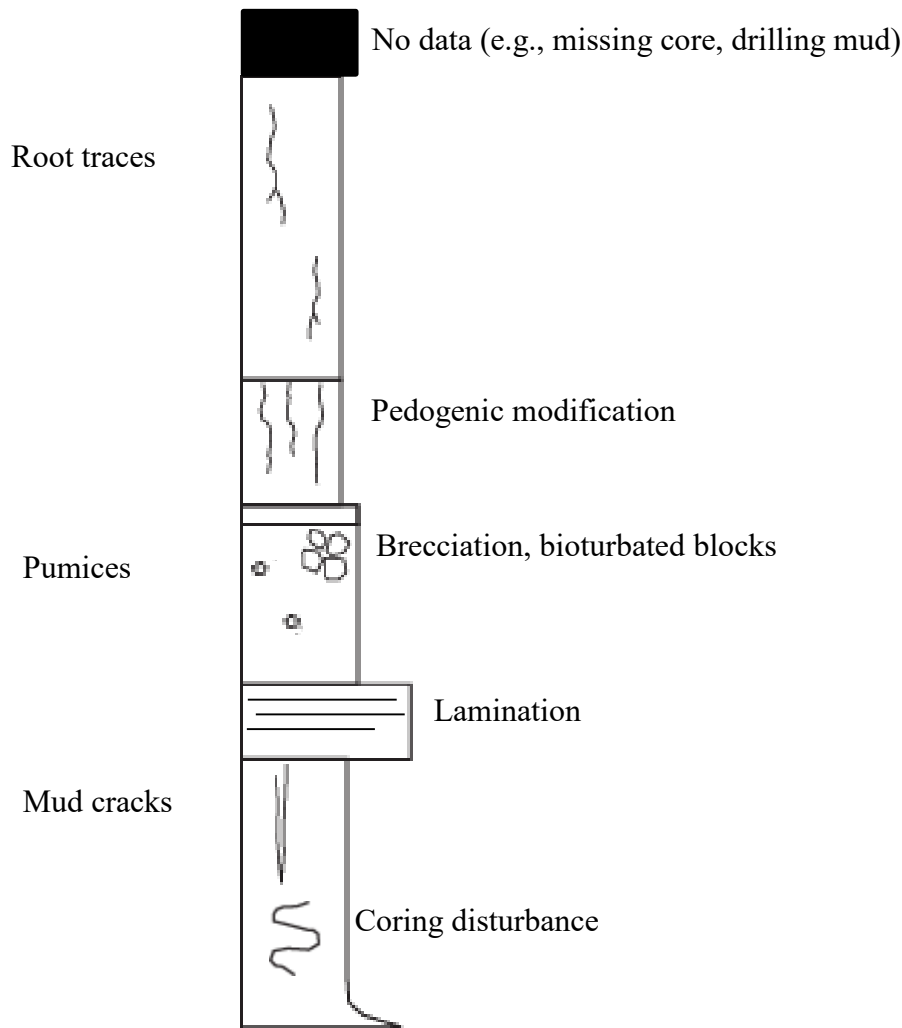


Figure 15. The key used to identify sedimentary structures and clasts

The following criteria are considered (in order of priority) in order to develop the chronology of the core (Behrensmeyer et al., *unpublished*): 1) presence/absence of bedding especially continuous sequences of lamination. For instance fine lamination indicates slow, fairly regular deposition; such deposition was labelled “NO COMPRESSION” for the age model, 2) grain size analyses where fine grained reflect slow deposition while coarse grains (sand and grit) reflect rapid deposition. Pumices were not included in the analyses as they could either be part of slow or fast deposition depending on how they were emplaced, airborne, fluvial deposits or settling out after deposition, 3) sediment composition-the percentage proportion of vitric glass/tephra suggest the rate of sediment accumulation. More than 60% to 75% tephra presence indicates 70% compression; between 75% and 90% indicate 90% compression. 40% non-tephra (e.g. quartz/feldspars) indicates influx and mixing with other sources thus slow accumulation.

Initial geochronological analyses on approximately 140 samples of tephra and the trachytic basement dated using $^{40}\text{Ar}/^{39}\text{Ar}$ dating technique suggest that the sequence extends from ~70ka at the top to ~1.07Ma at the basement lava floor underlying the sedimentary sequence (Deino et al., *unpublished*).

Although the dating work is still in progress, a reliable age model that has been derived from more than twenty $^{40}\text{Ar}/^{39}\text{Ar}$ dates shown in figure 16, below is being used for all the multi-proxy analyses undertaken from the ODP core.

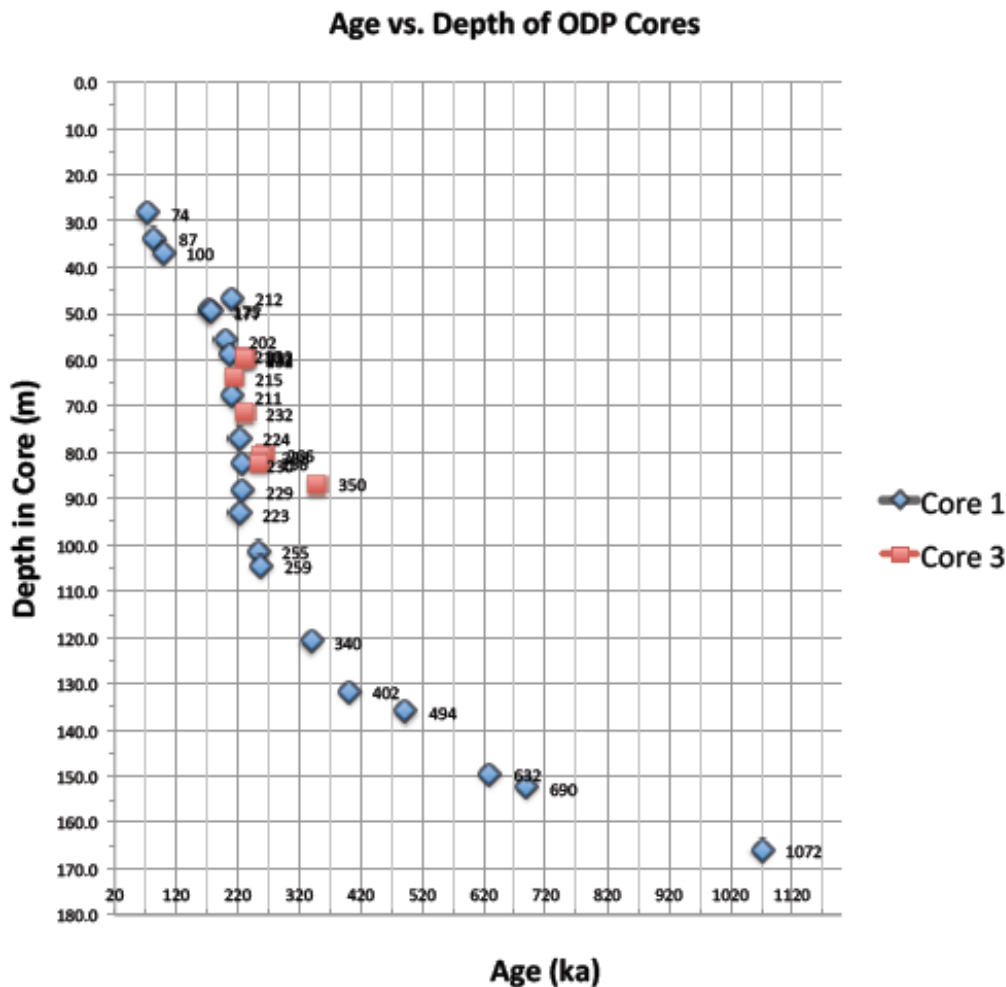


Figure 16. ODP age- model showing a smooth progression toward older ages with increasing core depth. 1.07Ma date is obtained from trachytic basement rock.

The protocols followed accounted for tephra events and other rapid depositional episodes, an approach that compresses these rapid events in time relative to other types of sedimentation. The approach also ensured that new depth model referred to Z-prime that assigns interpolated ages (most probable ages) on a cm- by cm- scale throughout the core as shown in appendix I

4.1.2.2. Koobi Fora samples

From the Koobi Fora basin, sampling was undertaken from selected geo-sections which are located in two localities, the Ileret area and Koobi Fora area. The locations were marked using a handheld GPS device. Although we had initially proposed to sample only the paleosols layers, this was not feasible in all the localities we sampled. We therefore, considered the availability of sediments dated to Pleistocene and Holocene periods as the primary criteria for our sampling. However, multiple samples were collected from thick (> 20cm) paleosols. A total of 36 samples were collected. We targeted mainly the paleosols layers exposed from various freshly dug geo-sections in different localities. See map in figure 17.

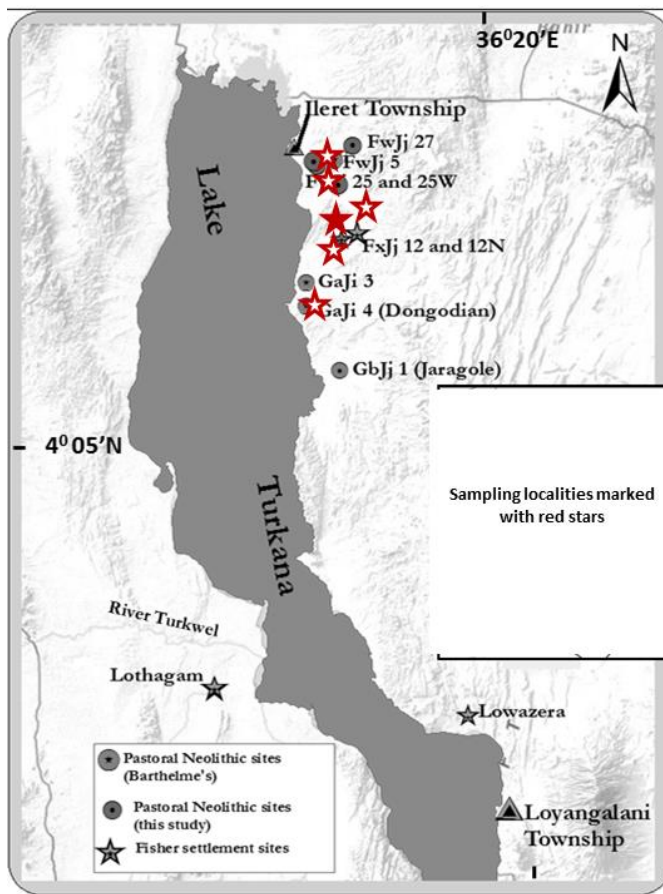


Figure 17. Map showing some of the Holocene sites sampled for this study (Red stars this study, grey circles (Ndiema, 2011))

4.1.2.2.1. Sample distribution

At Ileret, a total of thirty three samples were collected from Early Pleistocene sediments in two localities; 1A and 8 where either/or both the Okote Member (~1.56-1.36Ma) or the Ileret Complex [Lower Ileret Tuff (1.525 Ma), Ileret Tuff (1.52 Ma) and Northern Ileret Tuff (1.51 Ma)] Members were exposed. The ages of the samples therefore range between 1.53 Ma and < 1.36 Ma.

From locality 1A, a total of twenty one samples were collected from four geo-sections as follows; four samples from 6-11/1, five samples from 1A-DU-ET-11-01, seven samples from 1A-DU-ET-11-02 and five samples from AV-ET-11-1. A total of twelve samples was collected from a series of short geo-sections in locality 8 namely 14A-8A-GS2-9. Of these samples, based on chronological correlation, twelve samples were selected for the analyses as will be described in the following sections of this chapter.

A total of twenty samples was collected from the Holocene deposits (Galana Boi), from five archaeological sites, six samples from FxJj108 (early-Holocene), three samples from FxJj27 (early-mid-Holocene), five samples from GaJ4 (mid-Holocene), three samples from FwJj25 (mid-Holocene) and three samples from FwJj5 (late-Holocene). The samples are estimated to date between ~9.6kyr to ~0.93kyr.

4.1.2.2.2. Geochronology, lithostratigraphy and depositional environments

Unlike the Ologesailie samples, the chronology of the Koobi Fora samples is more complex. Sampling strategy and sequence are discontinuous but representative of Pleistocene and Holocene environments. The key driving factor for the sampling criteria is the availability of well dated sequence/sites. Pleistocene samples were collected from paleosol layers while Holocene samples were collected from highly silted and/or diatomaceous sandy layers, which are the main constituents of the Galana Boi Formation.

Early Pleistocene samples have their age estimated based on the dates of the Ileret tuff complex (1.53Ma and 1.51Ma) embedded in the Okote Member of the Koobi Fora Formation (1.64Ma) (Cohen and Gibbard, 2016), while for the Holocene samples I used the existing site-based published dates spanning between ~9.6kyr and ~0.93kyr (see Ashley et al., 2011; Ndiema 2011). It is important to note the existence of a huge chronological gap between the -Pleistocene and the Holocene samples, partly because of the a major disconformity immediately after the Chari Member; the youngest of the Koobi Fora Formation (1.39Ma) and partly, because this member is extremely localised and therefore was missing from the geo-sections sampled for this study, and instead the samples are most likely from the Okote Member (~1.56 -1.36Ma). The geochronology of Plio-Pleistocene deposits was acquired using $^{40}\text{Ar}/^{39}\text{Ar}$ dating technique (Brown and Feibel, 1991; Brown and McDougall, 2011).

For clear understanding of the phytolith assemblages of various samples, below is a description of various geological characteristics of each site:

a). Early-Pleistocene samples

The samples were collected from the Plio- Pleistocene sediments of the Koobi Fora Formation in the Ileret area. The deposits are lithologically distinct from the overlying Holocene Galana Boi deposits.

They are composed of “brown and olive mudstones, calcite cemented sandstones, and undulated fine pebble conglomerates while Galana Boi deposits are characteristically whitish to olive grey loose siltstones and diatomaceous claystone” (Gathogo et al., 2006). Samples were collected from two designated localities, area 1A (FwJi14E-footprint site) and area 8A. (See table 3 for more details). The estimated age of the samples lies between 1.525 and 1.51, bracketed within the Ileret complex tuffs found in the Okote Member of the Koobi Fora Formation (see, figure 18, one of the geo-section sampled from area 1A). Figure 19 shows a photograph of one of the sections sample.

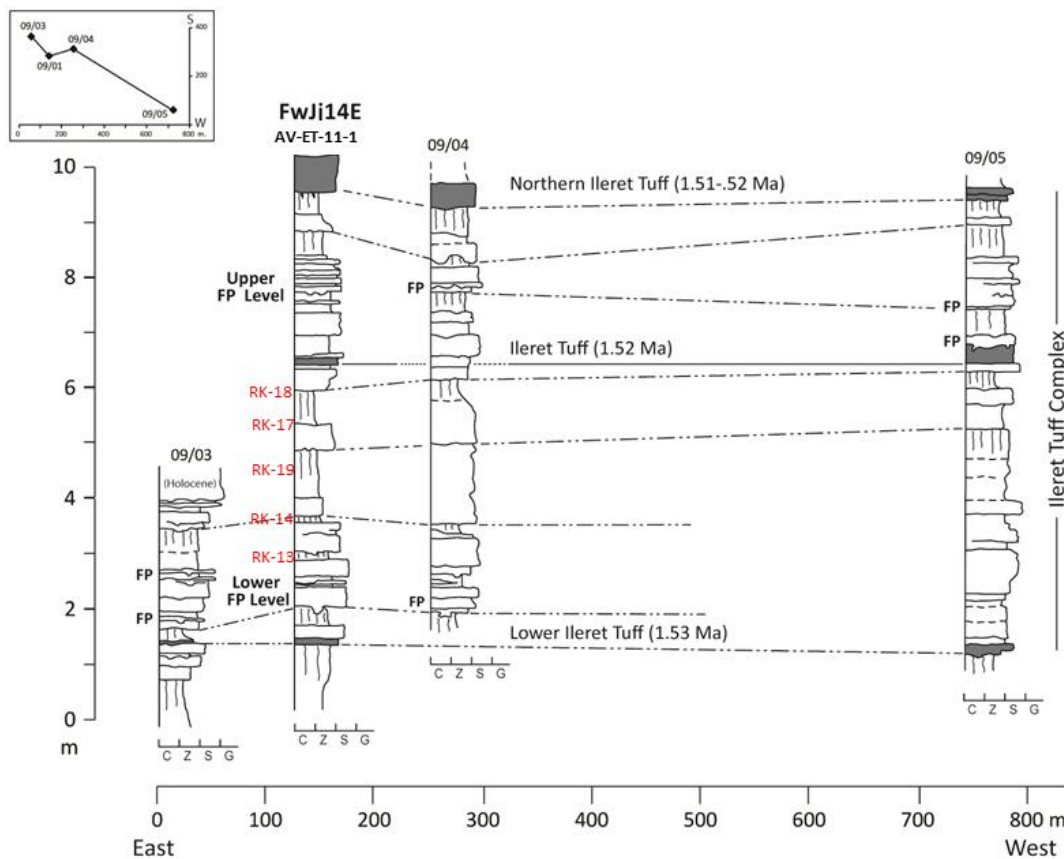


Figure 18. A geo-section drawn by Amelia Villaseñor and Kay Behrensmeier, showing some of the palaeosol sampled and their relationship to the Ileret Tuffs.

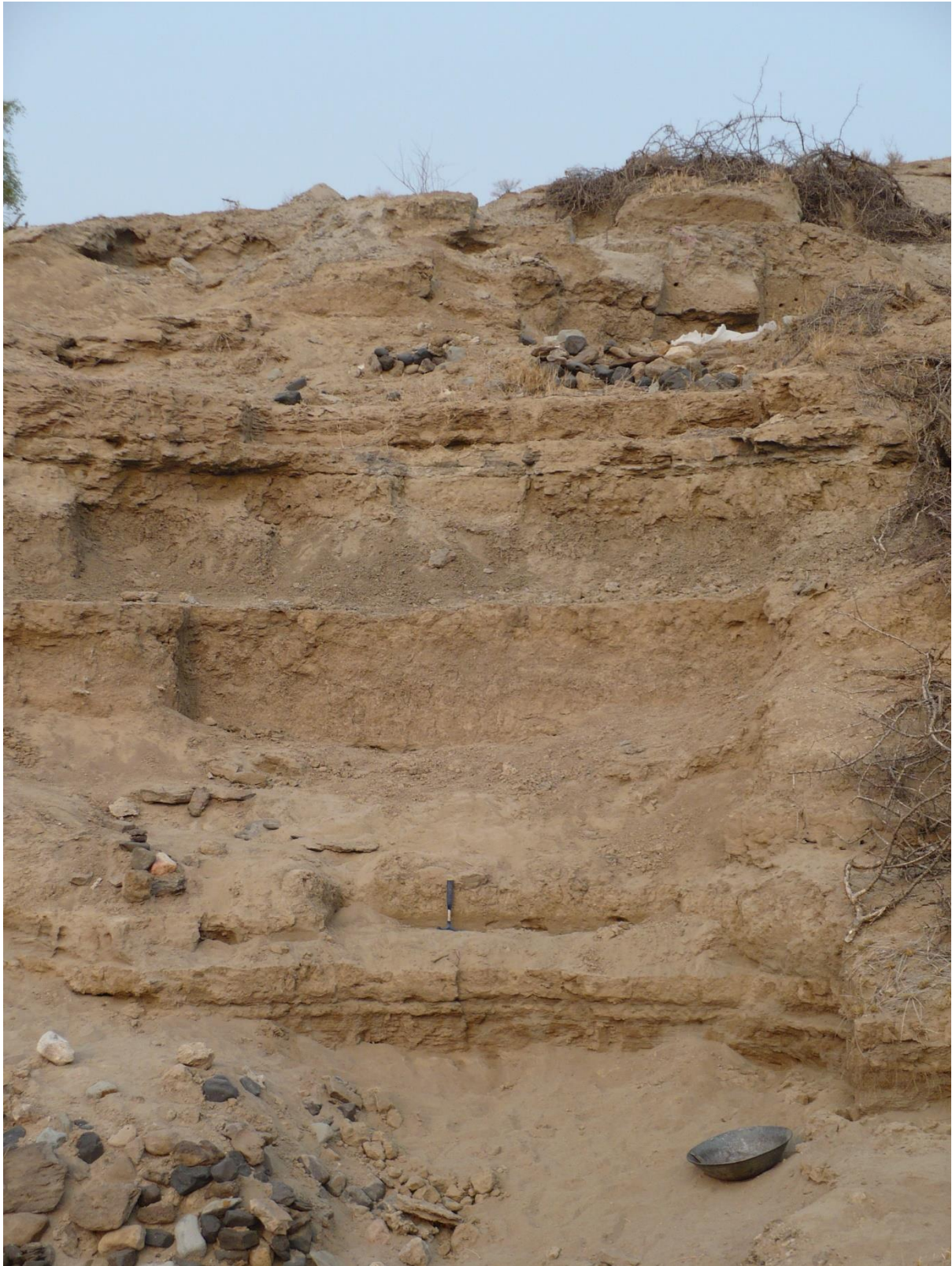


Figure 19. Photograph showing one of the geo-section sampled for Early Pleistocene samples

Table 2. Lithostratigraphic details of Early Pleistocene samples collected from Ileret area and their relative ages depending on their collection point in relation to the Ileret Complex Tuff.

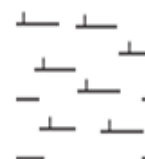
Geosection	Sample #	Lithology	GPS co-ordinates/Elevation	Loc in relation to Ileret complex
1A-DU-ET-11-02, Area 1A	RK-15	Silty sandy paleosol with CaCO ₃	37N 0197263, E0477283 Z-402m	Above Ileret tuff (1.52 Ma), Samples<1.52)
AV-ET-11-1, Area 1A	RK-21	Paleosol wt hard CaCO ₃ , roots	37N 0196763, E0477156	Below Ileret tuff (1.52 Ma) Samples>1.52)
AV-ET-11-1, Area 1A	RK-18	Distinctive paleosol	37N 0196763, E0477156	
AV-ET-11-1, Area 1A	RK-17	paleosol wt CaCO ₃	37N 0196763, E0477156	
AV-ET-11-1, Area 1A	RK-20	Paleosol wt CaCO ₃ , roots	37N 0196763, E0477156	
AV-ET-11-1, Area 1A	RK-19	Paleosol wt CaCO ₃ , roots	37N 0196763, E0477156	
1A-DU-ET-11-02, Area 1A	RK-14	Silty paleosols with CaCO ₃	37N 0197263, E0477283 Z-402m	Above Lower Ileret tuff (1.525Ma) Samples<1.525Ma
1A-DU-ET-11-02, Area 1A	RK-13	silty Paleosol, pink in colour wt CaCO ₃	37N 0197263, E0477283 Z-402m	
1A-DU-ET-11-02, Area 1A	RK-12	Sandy Paleosol, roots casts	37N 0197263, E0477283 Z-402m	
1A-DU-ET-11-02, Area 1A	RK-11	Sandy silty paleosols, with CaCO ₃	37N 0197263, E0477283 Z-402m	~5cm Below Lower Ileret tuff, Samples>1.525Ma
14A-8A-GS-2	RK-1	Brown silty sand Paleosol,with CaCO ₃ nodules	37N 0197644, E0471003, Z-440m	10 cm below lower Ileret tuff. 50-60 cm from the top of the paleosol
14A-8A-GS-5	RK-4	Silty sandy paleosol with CaCO ₃	37N 0197836, E0471488, Z-431m	3.6m below lower Ileret tuff, samples >1.525 1.9m below the base of the Okote Member, 50-70 cm from the top of contact

b). FxJj108 (N4°.101911N, E°36.339443, Z-456m a. s. l.)

The site is also within the Galana Boi Holocene deposits located in area 117, in Karari. Little is known from this site; however, recent archaeological findings and geological studies identify the site to be early Holocene site, with a high lake-level stand (80m above the current lake level). At least two occupation horizons has been so far been identified. So far, no available dates have been carried out from the site, but based on the available data, correlated with other sites with similar lithostratigraphic sequence and archaeological records; it is assumed to date between ~9.6kyr to ~6kyr.

Six samples were collected from sediment profile as illustrated in table 3.

Table 3. Lithostratigraphic section for FxJj 108 (After Ashley et al., 2011).

Sample no.	Lithology	Description	Colour	
FxJj108-RK-6		Loose sands with pebbles	Yellowish brown	Top  Bottom
FxJj108-RK-5		Compact tuffaceous	Light grey	
FxJj108-RK-4		Sandy layer	Dark grey	
FxJj108-RK-3		Angular tuffaceous with CaCO ₃	Dark grey	
FxJj108-RK-2		Tuffaceous level	Light grey	
FxJj108-RK-1		Paleosol layer	Brown in colour	

c). FxJj27 (N4°.291200, E36°.307083, Z-445m a. s. l)

The site is found within the Galana Boi Holocene deposits located in area 10, Ileret. It has been dated between ~9.3 and ~4.2kyr, and it records cultural transition from early- to mid-Holocene period. Archaeological and geological findings show at least two distinct occupation; fisher-gathers during high-lake-stand and a later Pastoral-Neolithic occupation. Three phytolith samples were collected from the excavation profile as illustrated in table 4.

Table 4. Lithostratigraphic section for FxJj 27 (after Ashley et al., 2011).

Sample no.	Lithology	Description	Colour	
FxJj27-RK-3		Fine silt sands	Yellowish brown	 Top Bottom
FxJj27-RK-2		Medium-coarse sands	Brown	
FxJj27-RK-1		Loose coarse sand	Brownish yellow	

d). Dongodien (GaJj4) (N4°.31513, E36°.29741, Z-1829m a. s. l.)

The site is located in the Holocene deposit known as Galana Boi overlying un-conformably on the Plio-Pleistocene sediments of the Koobi Fora Formation. It is located in area 102 along the Koobi Fora ridge, East Turkana. It is well dated mid-Holocene using both OSL and radiometric Carbon to ~ 4.2kyr (Ashley et al., 2011; Ndiema et al., 2011). Five phytolith samples were collected from the five distinct stratigraphic units with medium to fine grains, moderately sorted, pale yellow-brownish yellow in colour. Ashley et al., (2011) found the mineralogical contents included quartz, magnetite and garnet traces (see table 5).

The archaeological record and sedimentary process suggest Lake Turkana stood at 55m higher than today, but had dropped from 80m, the high lake stand recorded in mid-Holocene, indicating the inception of an increased aridity period (Barthelme, 1981; Ndiema, 2011).

Table 5. Lithostratigraphic section for GaJj4 (after Ashley et al., 2011).

Sample no.	Lithology	Description	Colour	
GajJ4-RK-5		Medium fine sand	Yellowish brown	
GajJ4-RK-4		Very fine sand	Pale yellow	
GajJ4-RK-3		Medium-fine sand	Yellowish brown	
GajJ4-RK-2		Silt	Pale yellow	
GajJ4-RK-1		silt	Light yellow	

e). FwJj25 (N4°.74314, E 37°.0199546, Z-442m a. s. l.) and FwJj5 (N4°.74387, E37°.0200212, Z-442m a. s. l.)

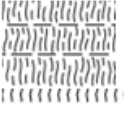
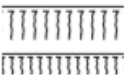
FwJj25 and FwJj5 sites are located in area 10 (Koobi Fora designated palaeontological collection areas) (Figure 16). They are found within the Galana Boi deposits overlying an erosional contact with Plio-Pleistocene deposits of the Koobi Fora Formation. FwJj25 was dated using OSL technique to ~4.2kyr (archaeological horizons) overlain by sterile layer dated ~1.34kyr (Ashley et al., 2011). The sediments grade upward from the most coarse-grained pebbles to medium-grained sands to fine-grained sands. This depositional trend is interpreted to represent a receding lake level which created a beach environment. Ashley et al., (2011), research showed a series of lake level changes i.e. rising, then fluctuating and falling of the lake level producing a coarse beach deposit which is overlain by Aeolian dune sediments. The archaeological site is located on sediments indicative of a sand dune environment (Ashley et al., 2011). Three samples were collected from the site as illustrated in table 6.

Table 6. Lithostratigraphic section for FwJj25 (after, Ashley et al., 2011).

Sample no.	lithology	Description	colour	Environment	Top
FwJj25-RK-3		Fine silts with scattered shells	brownish yellow	beach	
FwJj25-RK-2		Fine silty sands with CaCO ₃ cement	brownish yellow	beach	
FwJj25-RK-1		Coarse sands	yellow	coarse beach	

FwJj5 is OSL dated to ~0.93kyr and is composed of inter-bedded and highly variable sandy and silty sediments and two weakly developed paleosols. Carbonate nodules and Carbonate cemented sand (tufa) sand occurs throughout the sequence. The site represents a lake margin and fluvial environments. The presence of tufa is interpreted to indicate spring water resource (Ashley et al., 2011; Ndiema 2011). Three samples were collected from the weakly developed paleosol layers and the dated archaeological horizon as illustrated in table 7.

Table 7. Lithostratigraphic section for FwJj5 (after, Ashley et al., 2011).

Sample	lithology	Description	colour	Environment	Top
FwJj5-RK-3		Medium-coarse sand, granules, modern roots, minor shell fragments	yellow	Fluvial	
FwJj5-RK-2		Carbonate cement, modern roots, calcium deposits, scattered shells, possible paleosol	grey-brown	Terrestrial	
FwJj5-RK-1		Bioturbated poorly sorted fine sand, silty clay. Vertical trace fossil indicating paleosol	grey	Terrestrial	

4.2. METHODS

To reconstruct the vegetation history from the fossil assemblages, two analytical approaches were adopted: 1). general approach, where vertical changes in relative abundance of various morphotypes described, and 2) two phytolith indices were calculated for both modern and fossil sediments samples. Modern phytolith assemblages extracted from modern plants were used to attribute fossil morphotypes to their respective vegetation types.

4.2.1. Laboratory work

4.2.1.1. Modern reference collection

A modern phytolith database for plants observed and identified in the study sites is considered crucial to help in identification and classification of the morphotypes in the fossil assemblage to determine the past vegetation cover more accurately.

The extraction of phytoliths from plant specimens (specific parts or whole plant, see appendix II for more details) followed a modified Albert and Weiner protocol (after Mercader et al., 2009) which included both quantitative and qualitative analyses. Plant specimens were soaked in 5% Calgon solution overnight while placed on an automatic shaker to loosen alien materials adhering to the specimens. They were then washed with distilled water through a 1mm sieve after which they were sonicated for

30min using a Fisher Scientific FS 60 sonicator. The specimens were then dried overnight at 100°C, weighed and ashed in the muffle furnace at 500°C for 12 hrs; some woody specimens were ashed for up to 36hrs to achieve complete combustion.

The weight of the cooled dry ash was then recorded for each specimen to determine the proportion of combustible carbon. The ash was transferred into test tubes where 10ml of equivolume solution of hydrochloric acid (HCl) and nitric acid (HNO₃) was added (at 3N). This was heated to boiling until the residue formed a paste. The samples were washed three times with distilled water (dH₂O) each time centrifuging at 3000rpm for 5min. 10ml of hydrogen peroxide (H₂O₂) was added to each sample which was then transferred into Petri dishes, placed on the hot plate at 70°C until the reaction ceased. The samples were transferred back to the test tubes, washed with dH₂O three times at 3000rpm for 5min before drying in the oven at >100°C. The resulting residue was weighed and stored in vials ready for mounting and microscopic analyses. 1 mg of each residue was finally mounted on the slide, mixing thoroughly with the mounting medium, "Entellan New".

4.2.1.2. Fossil assemblages

There are various published phytolith extraction protocols that have been increasingly refined through time. The variation occurs in step-wise procedures and choice of treatment acids and heavy liquids. Different factors dictate on the best technique to be applied in various projects (Stromberg, 2003). Important factors determining the most appropriate lab techniques include: 1) research questions to be addressed in a particular study and the data needed to answer the questions, 2) what phytolith size fraction to be analysed (e.g. Alexandre et al., 1997), 3) whether pollen and other palynomorphs are to be extracted along with phytoliths (Lentfer and Boyd, 2000), 4) sediment type and clay content (Piperno 1988, Lentfer and Boyd, 1998; Zhao and Pearsall, 1998) and 5) chronology (Stromberg, 2003).

The factors that have contributed to the continued modification of the existing protocols are: efficiency, safety and cost effectiveness but ensuring research questions are adequately addressed by the data obtained (Lentfer and Boyd, 1998; Zhao and Pearsall, 1998; Albert et al., 1999; Parr, 2002, Katz et al., 2010). Preliminary results in this study showed the processing protocol outlined in Katz et al., (2010) provided optimal results for samples selected randomly according to their lithological properties. In addition, the method is not complicated and saves more time.

The extraction technique involved disaggregating phytoliths from the sediments, removal of organic materials and carbonates. Gravitational cleaning was carried out for the clay-rich samples. The procedure is as described in the following paragraphs.

Sediments weighing between 30-50mg was put into a 10ml vial. 50µl of hydrochloric acid, 37% was added to dissolve carbonates, and 50µl hydrogen peroxide (H₂O₂) to oxidise/remove organic matter.

The supernatant was poured off and decant washed twice, centrifuging at 3000rpm for 3minutes to remove any remaining acids. 10ml of 2.4g/ml Sodium Polytungstate solution was then added for heavy liquid floatation process. The samples were thoroughly mixed and centrifuged at 3000rpm for 4 minutes, the floating fraction was then transferred to another set of 10ml-centrifuge plastic tubes, and water washed till we got rid of all the salts. For those samples rich in clay minerals, Calgon detergent solution (5% Sodium Phosphate) was added to dislodge phytoliths from the clay particles. The samples were thoroughly shaken and left to decant/rest for at least 30 minutes before pouring off the supernatant and lastly the residue was oven dried. This process cleaned the samples for clarity during microscopy analyses.

4.2.2. Counting and identification

Approximately 1 mg aliquot was mounted on a 25.4mm X 76.2mm slide using “Entellan New” as the mounting media, thoroughly mixed, then a 11mm X 11mm coverslip was carefully placed ensuring no bubbles were trapped and the sample spread evenly on the slide. Phytolith identification and counting was carried out on freshly mounted slides to ensure that the sample was not dry and could be manipulated in three dimensions to optimise identification. This ensured that ecologically and taxonomic diagnostic morphotypes are accounted for (Rossouw, 2009; Stromberg, 2003).

The counting was done along vertical transect across slide, identifying and counting all phytoliths encountered. However for phytolith-rich slides, tallying were done along random transects. This was carried out under an Olympus BX52 microscope at X400 magnification. For each sample/level, a total of 300 grass silica short cells (GSSC) was counted except for those samples/levels that were completely “barren” or had insufficient count size even after preparing a second slide.

Phytolith images were captured using image processing software; Image-Pro plus 5.1 and Infinity Capture software 2. Images were stored in the computer as TIFF/JPEG files from which some of the images were selected and presented in this work.

4.2.3. Basic Analytical Approach

Based on previous phytolith studies and the existing modern analogues, the following are the key factors considered to help define more accurately the Pleistocene vegetation structure as recorded in the phytolith assemblage extracted:

- a) The relative abundance of forest indicators relative to grasses to determine how closed or/and open vegetation structure was,
- b) Presence/abundance of key indicator taxa to determine specific ecosystems such as wetlands, and riverine forests,

- c) Include all identified phytoliths irrespective of classes, taxonomic- and ecological- significance through time to understand temporal changes of the vegetation structure.

4.2.3.1. Morphological classification

Morphological description and classification scheme used in this work is based mainly on the International Code of Phytolith Nomenclature (ICPN, Madella et al., 2005), Albert, (1999) and Albert et al., (2009) unless otherwise stated. Modern reference collections were consulted in identifying plant-specific morphotypes as well as previously published reference data (Fredlund and Tieszen, 1999; Rossouw, 2009; Mercader et al., 2009, 2010), standardised literature (Twiss et al., 1969, 1992; Piperno, 1988, 2006; Mulholland and Rapp, 1992) and local modern reference collection (Kinyanjui, 2012, *work in progress*). Studies focused in East-Central African plants and extant vegetation reconstruction are considered (Bamford et al., 2006; Barboni and Bremond, 2009; Barboni et al., 2007; Neumann et al., 2009; Novello et al., 2012; Novello and Barboni, 2015).

Emphasis is placed in the identification of the grass family since they are the most dominant component of vegetation cover in the East African region. Moreover, geographical distribution of various subfamilies is highly controlled by climatic factors such as precipitation, temperature and altitudinal gradient, hence very informative of past climatic and ecological regimes (Twiss et al., 1969, Mulholland and Rapp, 1992; Ollendorf, 1992; Twiss, 1992; Alexandre *et al.*, 1997; Thorn, 2004; Barboni *et al.*, 2007; Bremond *et al.*, 2008). The subfamilies identified in this work include, Panicoideae, Chloridoideae, Arundinoideae and Aristidoideae, all of which belong to the C₄ category.

In addition, phytoliths produced by sedges and palm trees are also identified as a single category each, for their ecological significance (Piperno, 1988; 2009). Other general categories are the woody and herbaceous taxa, and all classified together to represent dicotyledons category as shown in Table 8.

Table 8. Morphotype categories identified from the modern phytolith reference collections and are used in this study.

Categories-	Morphological description.	Figure no	References
1. Bilobate (also known as dumbbells) Descriptions based on the outline of the lobes and length of the connecting shank)	Grass silica short cells with two distinct lobes connected with a shank. (Twiss <i>et al.</i> , 1969; Mulholland, 1989).		Twiss et al., 1969; Twiss, 1992; Madella <i>et al.</i> , 2005; Stromberg, 2003; Rossouw, 2009; Mercader <i>et al.</i> , 2010.

a) Bilobate convex outer margin short shank (BCXSS) c.f. BI-7	Bilobate with rounded lobes connected with a short shank. <20µm.	Fig.1 &h	Piperno and Pearsall, 1998; Stromberg, 2003; Fahmy, 2008; Mercader <i>et al.</i> , 2010.
b) Bilobate convex outer margin long shank (BCXLS) c.f.BI-5	Bilobate with rounded outer lobes connected with long shank >20µm.	Fig.1d	Stromberg, 2003; Piperno, 2006; Fahmy, 2008; Mercader <i>et al.</i> , 2010.
c) Bilobate concave outer margin short Shank (BCCSS)c.f. BI-7	Bilobate with caved lobes connected with short shank <20µm.	Fig.1f	Stromberg, 2003; Piperno, 2006; Fahmy, 2008; Barboni and Bremond, 2009; Mercader <i>et al.</i> , 2010.
d) Bilobate concave outer margin long Shank (BCCLS) c.f. BI-6	Bilobate with caved lobes connected with long shank >20µm		Stromberg, 2003; Fahmy, 2008; Barboni and Bremond 2009; Mercader <i>et al.</i> , 2010.
e) Bilobate flattened outer margin short shank (BFSS)c.f. BI-1, BI-6	Bilobate with outer margins squared, shank<20 µm	Fig.1g	Stromberg, 2003; Piperno and Pearsall, 1998; Fahmy, 2008; Mercader <i>et al.</i> , 2010.
f) Bilobate flattened outer margin long Shank (BFLS) c. f. BI-6	Bilobates with outer margin squared with shank >20µm		Piperno and Pearsall, 1998; Stromberg, 2003; Fahmy, 2008; Mercader <i>et al.</i> , 2010.
g) Bilobate Panicoid type c.f. BI-8	Symmetrical bilobate with outer margin concave wide Shank <20 µm		Stromberg, 2003; Piperno, 2006; Fahmy, 2008; Mercader <i>et al.</i> , 2010.
2. Saddles (SAD) Chloridoideae	Grass short silica cell with two opposite convex edges and two straight or concave edges (Twiss <i>et al.</i> , 1969; Mulholland, 1989).		Twiss <i>et al.</i> , 1969; Mulholland, 1989; Piperno and Pearsall, 1998; Stromberg, 2003; Madella <i>et al.</i> , 2005; Rossouw, 2009.
a) Saddle long (SADL) Arundinoideae (e.g. <i>Phragmites</i> sp.) BI-14	Saddles with long convex edges. Described as, bilobate	Fig.1m	Stromberg, 2003; Barboni and Bremond, 2009;

	category (Stromberg, 2003)		Rossouw, 2009; Mercader <i>et al.</i> , 2010.
b) Saddle ovate (SADO) Aristidoideae (e.g. <i>Aristida</i> spp)	Rondels rounded /rounds (Piperno and Pearsall, 1998; Mercader <i>et al.</i> , 2010). Described as symmetry B bilobate (Stromberg, 2003)		(Piperno and Pearsall, 1998; Mercader <i>et al.</i> , 2010)Stromberg, 2003; Barboni and Bremond, 2009; Mercader <i>et al.</i> , 2010, Kinyanjui, 2013
c) Saddle squat (SADS) c.f.BI-15 Arundinoideae (e.g. in <i>Phragmites</i> sp.)	Saddles with short convex edges. Described as collapsed saddle (Stromberg, 2003, Piperno 2009)		Stromberg, 2003; Piperno, 2009; Barboni and Bremond, 2009; Rossouw, 2009; Mercader <i>et al.</i> , 2010.
d) Saddle plateau (SADp) c.f. BI-15 Chloridoideae (e. g. in <i>Eragrostis</i> sp.)	Saddle with side notches and much longer.		Twiss <i>et al.</i> , 1969; Stromberg 2003; Barboni and Bremond, 2009; Mercader <i>et al.</i> , 2010.
3. Cross/quadra-lobate (QCR) c.f CR4-2, 6 Panicoideae (e.g. in <i>Melinis</i> spp., <i>Coelarichis</i> spp.)	Grass short silica cell with four lobates, symmetrical or asymmetrical (Twiss <i>et al.</i> , 1969; Mulholland and Rapp, 1992)	Fig.1i	Twiss <i>et al.</i> , 1969; Mulholland and Rapp, 1992; Piperno and Pearsall, 1998; Stromberg, 2003; Madella <i>et al.</i> , 2005; Barboni and Bremond, 2009; Mercader <i>et al.</i> , 2010; Kinyanjui, 2013.
4. Polylobate (PLY) c.f. PO Panicoideae e.g. <i>Panicum</i> sp.	Grass short silica cell with more than two lobes	Fig 1j	Twiss <i>et al.</i> , 1969; Stromberg, 2003; Madella <i>et al.</i> , 2005; Mercader, 2009; Kinyanjui, 2013.
5. Rondels (ROND) cf. KR; keeled rondel	Grass silica short cells with conical, keeled and pyramidal forms, described in Twiss <i>et al.</i> , (1969).	Fig.1v	Twiss <i>et al.</i> , 1969; Twiss, 1992; Fredlund and Tieszen, 1994; Stromberg, 2003; Madella <i>et al.</i> , 2005.

6. Towers (TW) c.f. BI-3-4	Variants of rondel categories; Stromberg, (2003); variants of trapeziforms in Bremond <i>et al.</i> , (2008); Rossouw, (2009).		Stromberg, 2003; Bremond <i>et al.</i> , 2008; Rossouw, 2009; Mercader <i>et al.</i> , 2010; Kinyanjui, 2013.
a) Tower horned (TWH) c.f. BI-4 Panicoidae (e. g <i>Hyparrhenia</i> sp.)	Rondels with apex ends in one or two outward apices/ top truncated Described as bilobate variant” in Stromberg (2003); “saddle variant 1” (Rossouw, 2009); “rondel” (Neumann <i>et al.</i> , 2009).	Fig.1p	Stromberg 2003; Barboni and Bremond, 2009; Mercader <i>et al.</i> , 2010.
b) Tower wide (TWD) BI-10-11	Rondel elliptical base/ tall body with tapering/flat apex; its base is at least three times wider than the apex. Described as “conical rondel” (Stromberg, 2003); “reniform” (Rossouw, 2009).	Fig.1q	Stromberg, 2003; Barboni and Bremond, 2009; Mercader <i>et al.</i> , 2010; Kinyanjui, 2013.
7. Trapeziforms sinuate/elongates/tabular crenate (TABCRE) (Panicoidae e.g. <i>Oplismenus</i> sp., Chloridoideae .e.g. <i>Cynodon</i> sp.)	Elongate body with trapezoidal cross-section and wavy edges. Described as crenate in Stromberg (2003); trapeziform polylobate (Rossouw, 2009); “trapezoid sinuate” (Neumann <i>et al.</i> , 2009).	Fig.1r	Stromberg, 2003; Rossouw, 2009; Barboni and Bremond, 2009; Neumann <i>et al.</i> , 2009; Mercader <i>et al.</i> , 2010; Kinyanjui, 2013.
8. Bulliforms	Epidermal cells located in mesophyll, usually three dimensional in appearance, highly silicified and are associated with moisture storage in the plants leaf. Also called-fan-		Pearsall and Dinan, 1992; Piperno, 2006 P. 74 fig 3,9d.

shaped cells in some studies.

Non-grass morphotypes (Dicot morphotypes)

9. Tracheid elements (TRCH)	Silicified vein-sheath cells		Fahn, 1990; Albert, 1999; Piperno, 2006; Albert et al., 2009; Neumann et al., 2009; Novello et al., 2012.
10. Sclereids (SCLD)	Tracheary elements and other related silicified cells (Stromberg, 2003)	Fig 4b	Piperno, 2006
11. Globular morphotypes	Also identified as spheroids in various publications		Stromberg, 2003; Mercader <i>et al.</i> , 2000; Madella <i>et al.</i> , 2005; Albert et al., 2009; Barboni and Bremond, 2009; Neumann et al., 2009; Novello et al., 2012,
a) Globular psilate (GBHS)	Globular, smooth/sub-smooth surface.	Fig 4f	Albert, 1999; Madella <i>et al.</i> , 2005.
b) Globular echinate (GBHEC)	Globular, with spikes/pricks	Fig 4j	Albert <i>et al.</i> , 2009; Barboni and Bremond, 2009, Novello and Barboni, 2015.
c) Globular granulate (GBHESC)	Globular, with granular surface	Fig 4k-l	Albert, 1999; Piperno, 2006.
d) Globular verrucate (GBHEVE)	Globular, rough irregular surface.	Fig 5a-b	Albert, 1999; Madella <i>et al.</i> , 2005; Piperno, 2006; Neumann et al., 2009.

Non-grass morphotypes (Herbaceous and other non-grass taxa)

12. Ellipsoids/Oblong	Longer than broad and with nearly parallel side		Albert, 1999; Madella <i>et al.</i> , 2005; Albert et al., 2009.
a) Ellipsoid psilate (ELLPS)	Ellipsoid with smooth surface		Albert, 1999; Madella <i>et al.</i> , 2005.

b) Ellipsoid scabrate (ELLSC)	Ellipsoid with granular surface	Albert, 1999; Madella <i>et al.</i> , 2005.
c) Ellipsoid verrucate (ELLVE)	Ellipsoid with rough irregular surface	Albert, 1999; Madella <i>et al.</i> , 2005.
13. Honeycomb Assemblages	Net-like-connected cells in situ. Categorized as “spherical and sub-spherical bodies” (Stromberg, 2003).	Bozarth 1992; Albert, 1999; Madella <i>et al.</i> , 2005.
a) Honeycomb elongates (HYE)	Network of elongates silica cells	Albert, 1999; Madella <i>et al.</i> , 2005.
b) Honeycomb globular (HYGB)	Network of circular/semi-circular cells. Described as “verrucate silica” (Stromberg, 2003).	Albert, 1999; Madella <i>et al.</i> , 2005; Kinyanjui, 2103.
14. Silica skeletons (SC)	Silicified sections of epidermal cells	Bozarth, 1992; Rosen 1992; Albert, 1999.
15. Irregular forms (IRRF)	Silica cells with no defined shape/don’t belong to any of the above category	Albert, 1999; Stromberg, 2003; Madella <i>et al.</i> , 2005.
a) Irregular verrucate (IRRVE)	Irregular forms with rough surfaces	Albert, 1999; Madella <i>et al.</i> , 2005.
b) Irregular scabrate (IRRSC)	Irregular forms with granulate surface	Albert, 1999; Madella <i>et al.</i> , 2005.
16. Epidermal appendages		Albert, 1999v
17. Epidermal appendages	Silicified mesophyll, epidermal & Parenchyma cells	Albert, 1999; Piperno, 2005.
a) Hair base (HB)	Silicified mesophyll cells with radial outline	Albert, 1999; Mercader <i>et al.</i> , 2009.
b) Hair (HR)	Silicified elongated outgrowths from mesophyll	Fig 1w Albert, 1999; Mercader <i>et al.</i> , 2009.

c) Stomata (STMT)	Intercellular guard & subsidiary cells		Mercader <i>et al.</i> , 2009
18. Parallelepiped (P)	Tabular body with opposite sides parallel to each other		Madella <i>et al.</i> , 2005.
a) Parallelepiped thin crenate (PPTCR)	With psilate texture and scalloped edges	Fig 5j	Albert, 1999; Madella <i>et al.</i> , 2005; Mercader <i>et al.</i> , 2010.
b) Parallelepiped verrucate (PPVE)	With rough irregular surface	Fig 5k	Albert, 1999; Madella <i>et al.</i> , 2005; Mercader <i>et al.</i> , 2010.
c) Parallelepiped dendritic (PPDT)	With finely branched processes		Albert, 1999; Madella <i>et al.</i> , 2005; Mercader <i>et al.</i> , 2010.
d) Parallelepiped thin psilate (PPTP)	With smooth surface, width<length		Albert, 1999; Madella <i>et al.</i> , 2005; Mercader <i>et al.</i> , 2010.
e) Parallelepiped blocky psilate (PPBP)	With smooth surface, width >length		Albert, 1999; Madella <i>et al.</i> , 2005; Mercader <i>et al.</i> , 2010
f) Parallelepiped blocky scabrate (PPBS)	With granular surface, width>length		Albert, 1999; Madella <i>et al.</i> , 2005; Mercader <i>et al.</i> , 2010.
g) Parallelepiped facetate (PPFC)	With scalloped edges		Albert, 1999; Mercader <i>et al.</i> , 2010.
19. Cyperaceae phytoliths			
a) Papillae (PAPL)	Hat-shaped silica bodies in sedges.	Fig 4d	Ollendorf, 1992; Novello <i>et al.</i> , 2012; Piperno, 2006; Mercader <i>et al.</i> , 2010; Kinyanjui, 2013.
b) Achene (ACHN)	Cone shaped silica bodies in sedges.	Fig 4e	Ollendorf, 1992; Piperno, 2006; Mercader <i>et al.</i> , 2010; Kinyanjui, 2013

4.2.4. Data analyses

Methods considered under this section were based on the ability to address the following questions: 1) the ability of the method to give the relationship between grass-derived morphotypes and forest indicator morphotypes more accurately, 2) and determine the composition of the grass-derived phytoliths (GSSCs) within the assemblage to determine the open-arid grasslands versus moist-closed grasslands and 3) determine the presence of specific habitats on the palaeolandscapes such as wetlands, gallery forests etc. The results will help reconstruct the vegetation structure and determine changes through time and between the two prehistoric basins.

4.2.4.1. General approach (Abundance diagrams)

These are abundance diagrams generated by computer programs; software packages called TILIA and TILIA GRAPH (Grimm, 2007). On the Tilia diagram, each morphotype is plotted in a single graph in relation to the total morphotypes within the assemblage. The horizontal axis represents the relative frequencies of each morphotype identified and tallied while the vertical axis represent sample/depth/age of the samples in which the morphotypes have been preserved. More so, for an easier interpretation of the data analysed, morphotypes indicating similar ecological and taxonomic affiliation can be grouped together, hence visual analyses of various habitats can be interpreted. Temporal zones are created using a Constrained Incremental Sum-of-Squares Cluster analysis (CONISS) which is one of the packages within the TILIA software.

This analysis helped determine what morphotypes (grasses versus trees & shrubs) dominated the assemblage at any given level (per sample) and their percentage occurrence. Although phytoliths cannot show species richness in a given sample/level, Tilia graphs help identify the levels with the highest morphotype diversity.

The visual characterization seen in Tilia diagrams help interpret vegetation cover changes as indicated by changes in the plotted morphotypes. These changes are discussed in relation to each other along the stratigraphic and chronological profile of the samples analysed where relative age or absolute dates are provided. For the Ologesailie basin, dates are provided for every sample/level analysed while for the Koobi Fora samples in the Turkana basin, relative dates are used based on the available dated geological markers such as volcanic ashes and paleosols. Comparison of the vegetation structure present in both basins during the same time frame is noted and discussed in next chapters.

4.2.4.2. Phytolith indices

This approach is applied to describe the vegetation types indicated by the phytolith data and correlate this with climatic parameters such as temperatures and moisture gradient (Alexandre et al., 1997; Barboni et al., 1999; 2007; Bremond et al., 2005a, b; 2008; Alexandre and Bremond, 2009). They are

valuable tools to trace vegetation changes in tropical ecosystems as well as determining the prevailing climates, particularly for the grasslands and savannas (Neumann et al., 2009).

Selected grass and dicotyledons morphotypes are considered for these analyses. Three indices are often used: 1) Ic index (Twiss 1969) is the relative proportion of C₃ high elevation grasses versus C₄ grasses reflecting temperature gradient (Bremond et al 2008), 2) Iph index is relative proportion of Chloridoideae versus Panicoideae grasses reflecting the dominance of either the short-arid-grasses or the long-moist-grasses, hence determining the aridity-humidity gradient in savanna grasslands (Bremond et al., 2005b Novello et al., 2012), 3) Fs index is the percentage of the fan-shaped bulliforms versus the sum of grass phytoliths reflecting water stress conditions (Bremond et al., 2005) and D:P (Dicots:Poaceae) is the relative proportion of dicotyledons versus grasses, reflecting tree cover densities (Barboni et al., 2007).

The first three indices were developed based on the taxonomic significance of certain grass morphotypes to characterize grass subfamilies, originally defined by Twiss et al., (1969) and Twiss (1992). The following grass morphotypes are considered for the analyses:

- a) Saddles (Chloridoideae)
- b) Bilobates (dumbbells) and crosses (Panicoideae)

The index D:P has been debated ever since it was proposed (Alexandre et al., 1997) as a proxy to determine tree cover density, since more often it under-estimate the presence of woody components when compared to the actual proportions seen in the phytolith assemblages (e.g. Neumann et al., 2009; Novello et al., 2012). Consequently, the selected dicot indicator morphotypes have been inconsistent between vegetation regimes and studies with some researchers using only the globular granulate (Barboni et al., 2007; Bremond et al., 2008; Neumann et al., 2009), and others have included elongate faceted (Stromberg, 2002). The above studies demonstrated that the morphotypes considered may vary for the temperate environments and for the tropical environments. This is because the main dicot morphotype considered as key forest-indicator (woody dicots) the globular granulate type is rare or absent in temperate ecosystems (see Neumann et al., 2009).

Nevertheless, recent studies which analysed modern phytolith assemblages have shown the D: P coupled with other indices and general approach, would be a valuable tool to determine and reconstruct changes in tree/shrub cover densities in grasslands and savanna grasslands (Bremond et al., 2008; Neumann et al., 2009; Novello et al., 2012).

This study uses D: P index as the ratio of the sum of globular granulate morphotype versus total sum of selected GSSCs morphotypes (saddles, bilobates short shank and crosses). Also included are

morphotypes such as rondels, trapeziform bilobates and trapeziform short cell (after Bremond et al., 2008; Neumann et al., 2009; Novello et al., 2012)

For the purpose of this study, we applied two indices, the aridity index (Iph) and the tree cover density index (D: P) but we didn't consider climate index (Ic) because of rarity or lack of Pooideae-indicator morphotypes in the fossil assemblage. Both indices were calculated as follows:

- a) $I_{ph} = \frac{\text{Globular granulate}}{\text{saddles} + \text{bilobates short shanks} + \text{crosses}}$.
- b) $D:P = \frac{\text{Globular granulate}}{\text{saddles} + \text{bilobates short shank} + \text{crosses}}$

Due to the wide range of D: P values in the fossil assemblages, the degree of vegetation openness/closeness was categorised into three vegetation structure/composition. The description of the categories also considered the general abundance of the selected morphotypes. The criterion used is as follows:

- a) D:P values ≤ 1 reflect low tree –cover-density, open grasslands
- b) D:P values ≤ 1 reflect moderate tree –cover-density, wooded grasslands
- c) D:P values \geq reflect high tree –cover-density, woodlands/forests

Part II: Results

CHAPTER FIVE: MODERN PHYTOLITH REFERENCE COLLECTION

5.1. Introduction

Although phytolith research has grown and developed for over two decades now, there still a few taxonomic challenges that exist especially in developing a standard nomenclature that includes all plant species or vegetation habitats and which can be globally applied (e.g. a case of saddle plateau in Neumann et al, 2009). Modern reference collection therefore is an essential prerequisite to interpret the Pleistocene assemblages.

Phytolith were extracted from sixty three individual plant species collected from different altitudes and habitats as stated in appendix II. Plants that were observed to dominate in different habitats and are considered to characterise these habitats were collected so that they can qualify to be reliable analogues for the fossil assemblages. All plant parts indicated for each individual plant, were processed and analysed. A total of 100 different morphotypes were identified and counted as shown in the appendix III. The data is part of work in progress geared to developing a phytolith database for the palynology and paleobotany section, Earth sciences Department at the National Museums of Kenya.

5.2. Description of the morphotypes selected to reconstruct Early Pleistocene-Holocene vegetation cover.

Correspondence Analyses (CA) was ran through the whole phytolith data for both grass and non-grass plants to determine whether there is clear trend in the species clusters identified by similar morphotypes (Figure 18). The assignments of GSSCs morphotypes analysed from 42 grass species was determined by various statistical analyses performed on the modern reference collection (Correspondence analyses (CA), Frequency graphs) see Figure 20. Note that, more emphasis is put in grass analyses because of the strong relation between GSSCs and their taxonomical & ecological affiliation. Hence, the analyses provide more elaborate and important habitat information. Frequency graph for morphotypes identified in non-grass species are also presented.

5.2.1. Analyses of woody dicots, herbaceous and GSSCs morphotypes

Correspondence Analyses (CA) for all individual plant species show a clear division between grass and non-grass species. Presence of diagnostic GSSCs in grasses and their rarity or/and absence in woody and herbaceous taxa is the determining factor of the first two groups (I and II). Diagnostic; papillae

(PAPL) morphotype present in Cyperaceae and is rare to absent in the plant categories and the underlying factor responsible for the third group (III), in Figure 19.

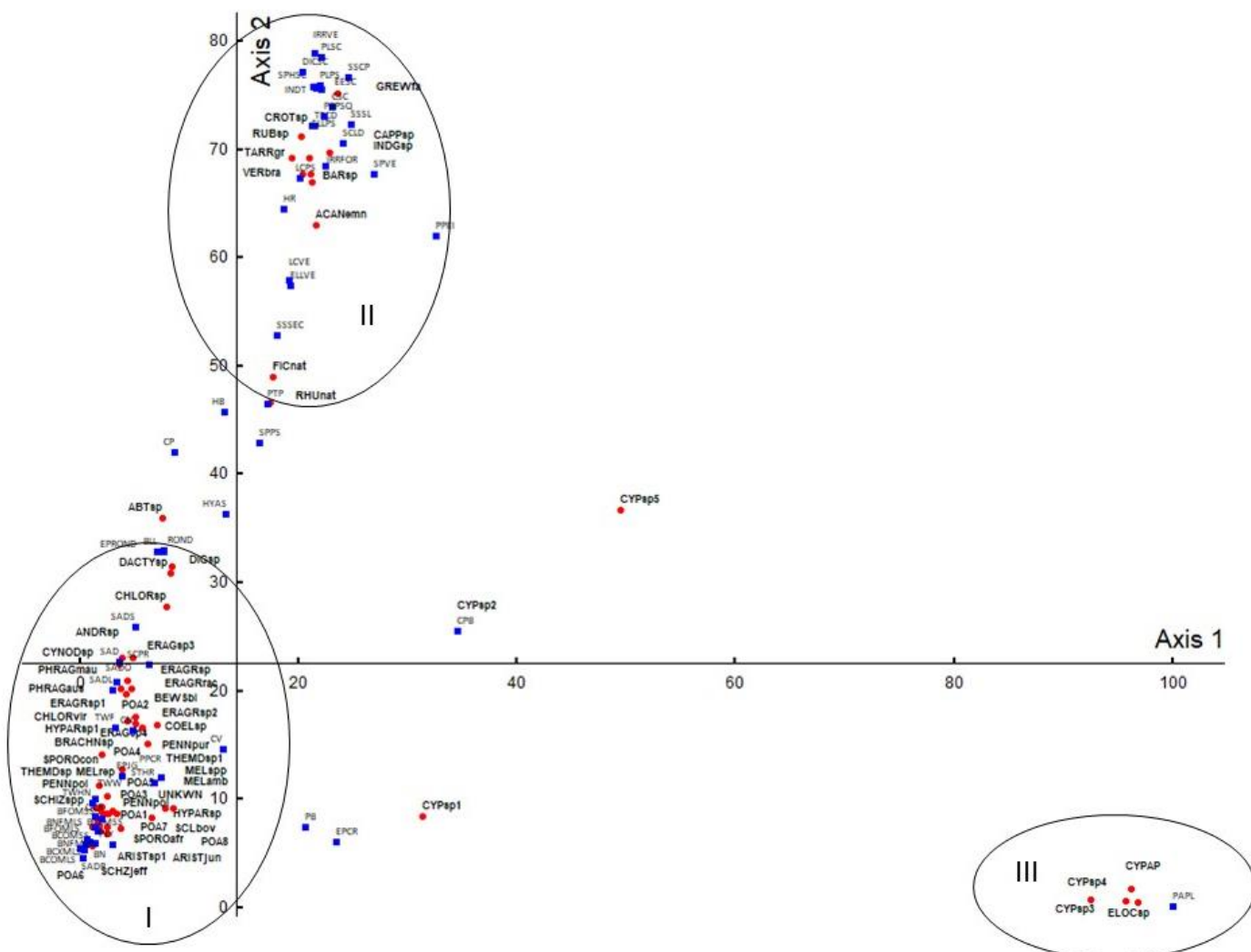


Figure 20. A scatter plot of Correspondence Analyses (CA) showing the relationship between the identified morphotypes and their parent species. Three clusters according to plants form and habits are identified.

5.2.1.1. Cluster I-Grasses

Cluster I consist mainly of all the grass species and their corresponding morphotypes. Morphotypes and the parent plant cluster faithfully with no notable outlier.

5.2.1.2. Cluster II-Woody and herbaceous taxa

Cluster II consist morphotypes derived from woody dicot and herbaceous taxa. The cluster is clearly defined except for one outlier, *Abutilon sp.* (**ABTsp**) which is a very poor phytolith accumulator, produces only two morphotypes that are non-diagnostic. The plants within cluster II, although are not

as good phytoliths producers as grasses, they seem to behave in a similar manner hence, fall under the same cluster.

5.2.1.3. Cluster III-Sedges

Out of the seven sedges analysed, four falls under this cluster. The other three are not well defined clusters. The four in cluster III include three species of the genus *Cyperus* and one species of the genus *Eleocharis*. The main morphotypes responsible for the cluster is Papillae (**PAPL**) which is common in the four species and are rare to absent the outlying species.

5.2.2. Analyses of GSSCs morphotypes-Poaceae

Figure 21 shows four main clusters of species which are influenced by similar morphotypes both in occurrence and in abundance.

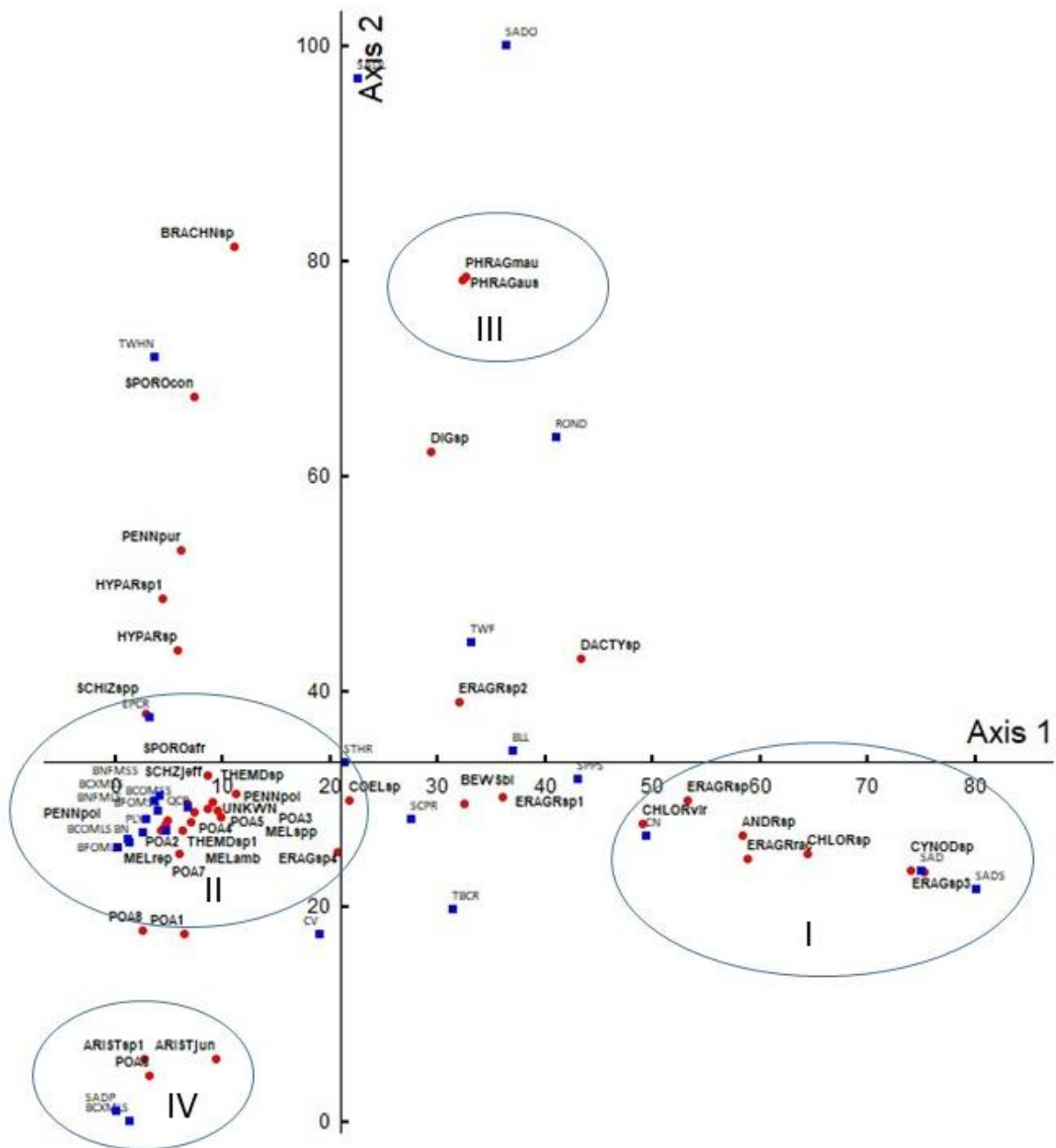


Figure 21. A scatter plot of Correspondence Analyses (CA) showing the relationship between GSSCs morphotypes and grass species. Four clusters are defined which corresponds to the four grass sub-families analysed.

5.2.2.1. Cluster I

This cluster is influenced by high frequency of saddles (SAD) and saddle squat (SADS). These morphotypes were abundant in *Eragrostis* (5 species) *Chloris* (2 species), *Cynodon* (1 species) and *Andropogon* (1 species). The first three genera are all in Chloridoideae sub-family while *Andropogon* is in the Panicoideae subfamily. 84.9% of the total saddles were observed in Chloridoideae species

(*Eragrostis*, sp., *E. racemosa*, & *Chloris* sp.), while 15.1% were observed in Panicoideae (*Andropogon* sp.) grasses. 97.7% of the SADS were observed in Chloridoideae while 2.3% in Panicoideae (*Digitaria* sp.).

5.2.2.2. Cluster II

This cluster is influenced by bilobate variants (bilobate convex short shank (BCXMSS), bilobate concave short shank (BCOMSS), bilobate concave long shank (BCOMLS), bilobate nodular (BN), bilobate flattened short shank (BFOMSS)), polylobate (PLY) and crosses (QRC). The morphotypes were abundant in *Melinis repens*, *Themeda* spp., *Pennisetum polystachion*, *Hyparrhenia* spp. and *Schizachyrium* spp. all of which are Panicoideae grasses. Two species in this subfamily however did not produce these morphotypes; such as *Andropogon* sp. and *Digitaria* sp. These morphotypes were not exclusively observed in Panicoideae grasses only, they were also observed in low frequencies in one *Aristida* sp. (Aristidoideae) and in one *Eragrostis* sp. (Chloridoideae). Bilobate concave short shank was the most abundant type (47.5%) in the Panicoideae grasses.

5.2.2.3. Cluster III

The cluster is highly influenced by two GSSCs morphotypes; saddle ovate (SADO) and saddle long (SADL). They were abundant in the two *Phragmites* species (Arundinoideae sub-family) and one *Brachyachne* sp. (Chloridoideae subfamily). Interestingly, 59.4% of the total SADL was observed in *Brachyachne* sp. while 29.7% were observed in the two *Phragmites* species. SADO on the other hand, occur in high abundance (94.5%) in *Phragmites* species but absent or rare in other grass species.

5.2.2.4. Cluster IV

The cluster is influenced by saddle plateau (SADP) and bilobate convex long shank (BCXMLS). *Aristida* species produced these morphotypes: 87.3% SADP and 75.9% bilobate convex long shank.

5.2.3. Summarised results of GSSCs analyses

Results of the grass morphotypes occurrence in the three sub-families represented by the grass species processed in this study is presented in the figure 22 below.

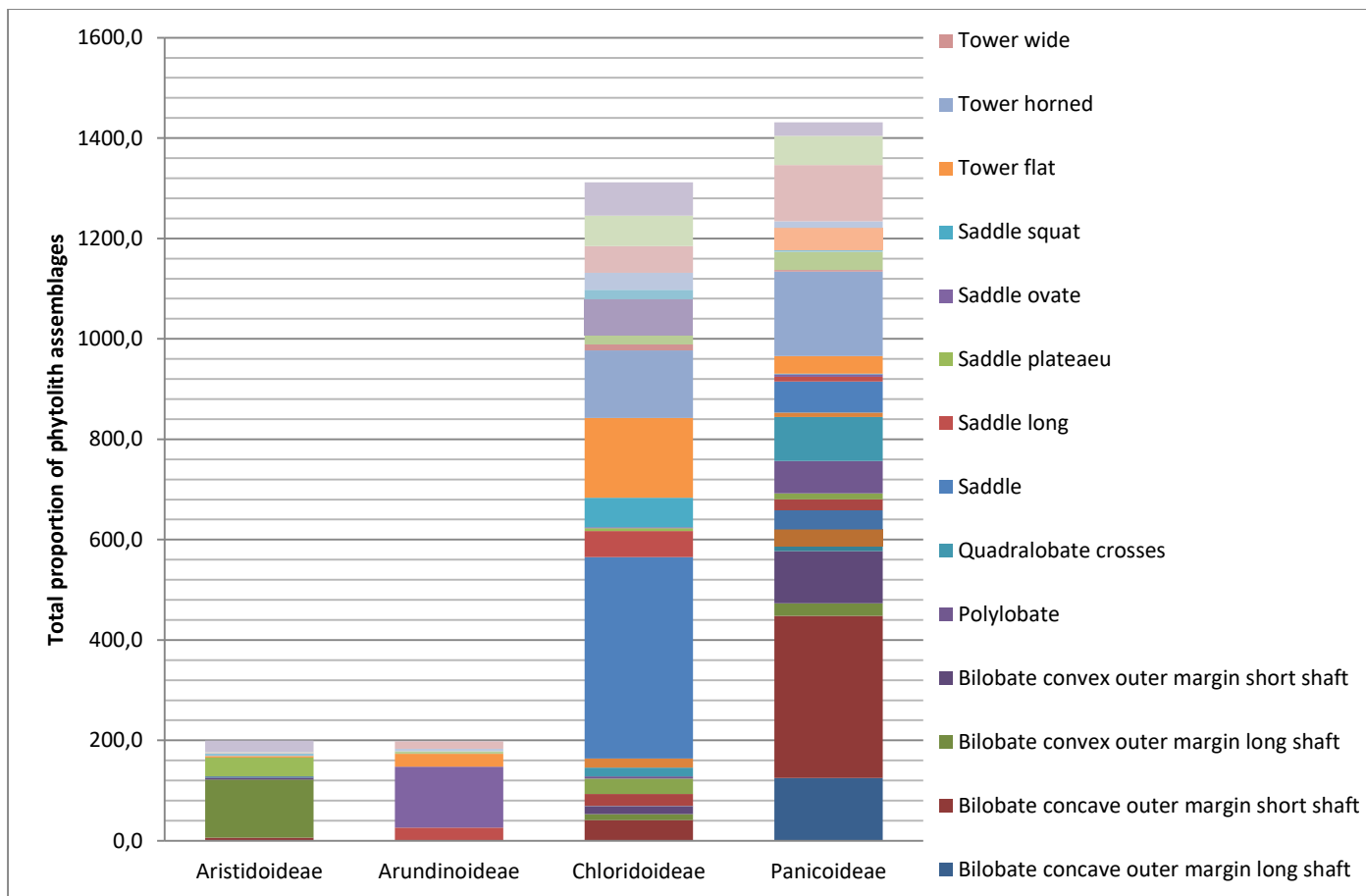


Figure 22. Relative abundance of phytoliths observed in grass sub-families.

Panicoideae grasses exhibit the greatest diversity of morphotypes (n=1431). Bilobates accounted for 47.6% of the total proportion. The following morphotypes are considered as possible key indicator of the family in order of abundance; bilobate concave short shank (22.2%), tower horned (11.7%), bilobate concave long shank (8.6%) and bilobate convex short shank (7.3%). Also considered in this category are cross/quadra-lobate and polylobate morphotypes which are exclusively abundant in the Panicoideae grasses (87.6% and 65% respectively) of the total assemblage.

Chloridoideae grasses ranks second in morphotypes diversity and proportions (n= 1312). Results suggest the following morphotypes as the possible key identifier of the sub-family: saddle (30.6%), tower flat (12.1%) and saddle squat (4.4%).

In the Aristidoideae grasses, the most represented morphotypes are bilobate convex long shank (58.1%) and saddle plateau (18.6%). In Arundinoideae grasses, saddle ovate (61.3%) is the most presented morphotype which remains rare in other grasses subfamilies.

5.2.4. Analyses of non-GSSCs morphotypes

The results presented here were analysed from the leaves of six herbaceous and seven woody species that accumulated silica in their cellular network.

There was no identified trend or relationship between morphotypes produced by the dicot category, both woody and herbaceous species. There was variation in which different species produced phytoliths. This study, categorise plants species into two broad categories depending on plant form; 1) herbaceous and 2) woody taxa.

5.2.4.1. Herbaceous taxa

All six herbaceous taxa processed for modern reference phytoliths produced significant amounts of phytoliths but assemblages varied from one species to the other (see figure 23). We therefore highlight the morphotypes that were significant in either one or more species. Irregular forms have a significant presence in three species; *Barleria sp* (22.3%), *Acanthus eminens* (13.6%) and *Vernonia brachaetis* (16.7%). However, this morphotype was absent in *Indigofera sp.*, *Crotalaria sp.* and *Abutilon sp.*

Each species shows uniqueness in silica production. Among the herbaceous species, *Acanthus eminens* has the most variable morphotypes, with the most abundant type being cylindroid psilate forms (9.5%). *Abutilon sp.* on the hand produces only two morphotypes, cylindroid psilate (57.9%) and blocky polyhedral (42.1%). Other species have particular morphotypes dominating their assemblages as follows: *Barleria sp.* (platelets scabrate-29.7%), *Vernonia brachaetis* (irregular forms-16.7%, sclereids-11.7%), *Indigofera sp.* (globular granulate- 44.6%) and *Crotalaria sp.* (irregular verrucate-34.7%). Of the 22 morphotype categories identified from these plants, 81.8% are non-diagnostic and 18.2% diagnostic i.e. globular granulate, tracheids, sclereids and irregular verrucate.

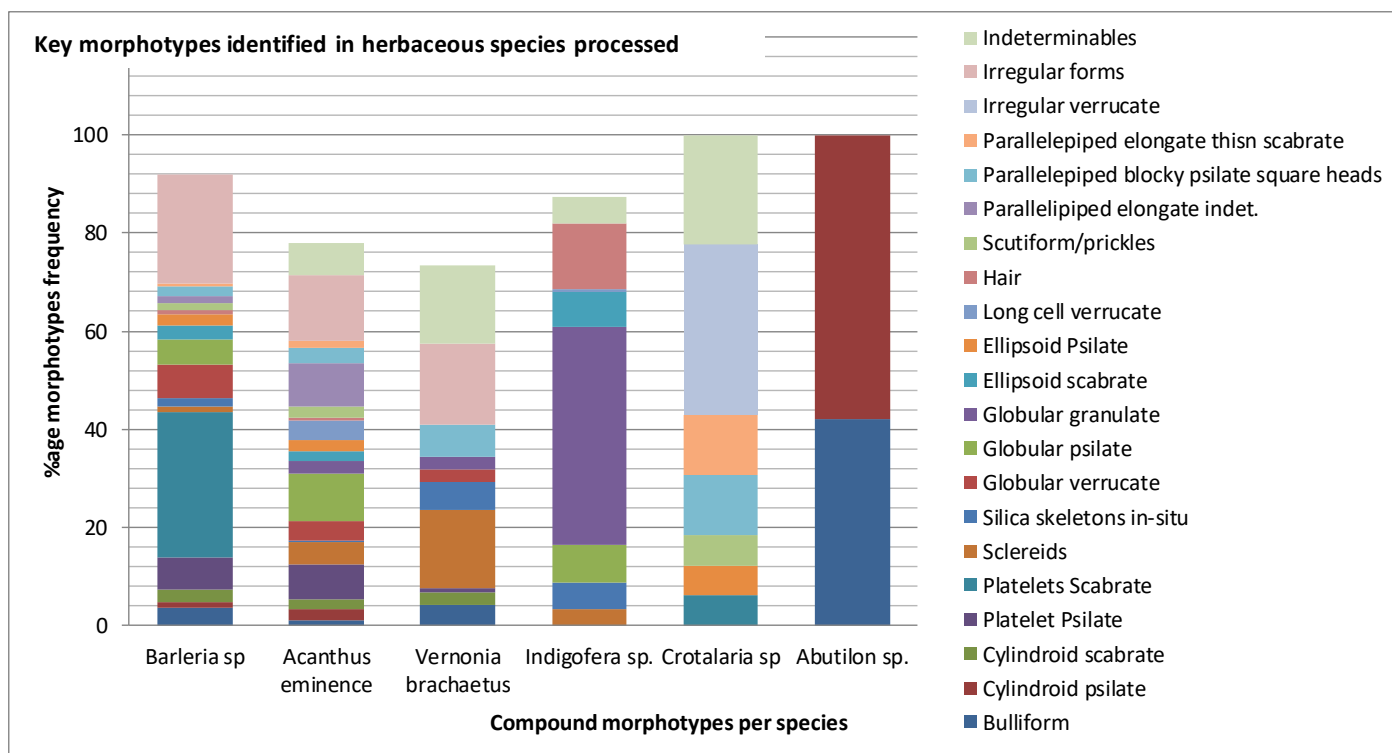


Figure 23. Relative abundance of phytolith assemblages observed in herbaceous taxa

5.2.4.2. Woody taxa

Woody dicots exhibit the highest variation in silica production. All the seven species processed show some uniqueness in the types of morphotypes they produce (Figure 24). Diagnostic morphotypes (globular granulate, tracheid and sclereids) remain rare in most of the woody dicots processed.

Phytolith assemblage produced in *Capparis* sp. is dominated by indeterminate (32.0%), parallelepiped elongates (16.3%) and irregular verrucate (9.8%). Other morphotypes include sclereids (7.2%) and platelets (7.2%). The *Acacia* sp. contains 100% ellipsoid scabrate. *Rhus natalensis* contains globular psilate (52.3%), platelets psilate (8.2%) and irregular forms (3.9%). *Ficus natalensis* is dominated by sclereids (40%), long cells verrucate (14.6%), silica skeletons with globular (6.2%) and silica skeletons psilate (4.6%). *Tarrena graveolens* is dominated by indeterminate (17.9%), irregular forms (16.6%), platelets psilate (13.8%), ellipsoid scabrate (9.0%) and platelets scabrate (7.6%). *Rubus* sp. is dominated by indeterminate (35.7%), globular granulate (14.3%), blocky polyhedral (14.3%) and irregular forms (7.1%). *Grewia fallax* is dominated by sclereids (25.8%), silica skeleton in-situ (25.8%), platelets scabrate (19.4%) and silica skeletons long cells (17.7%).

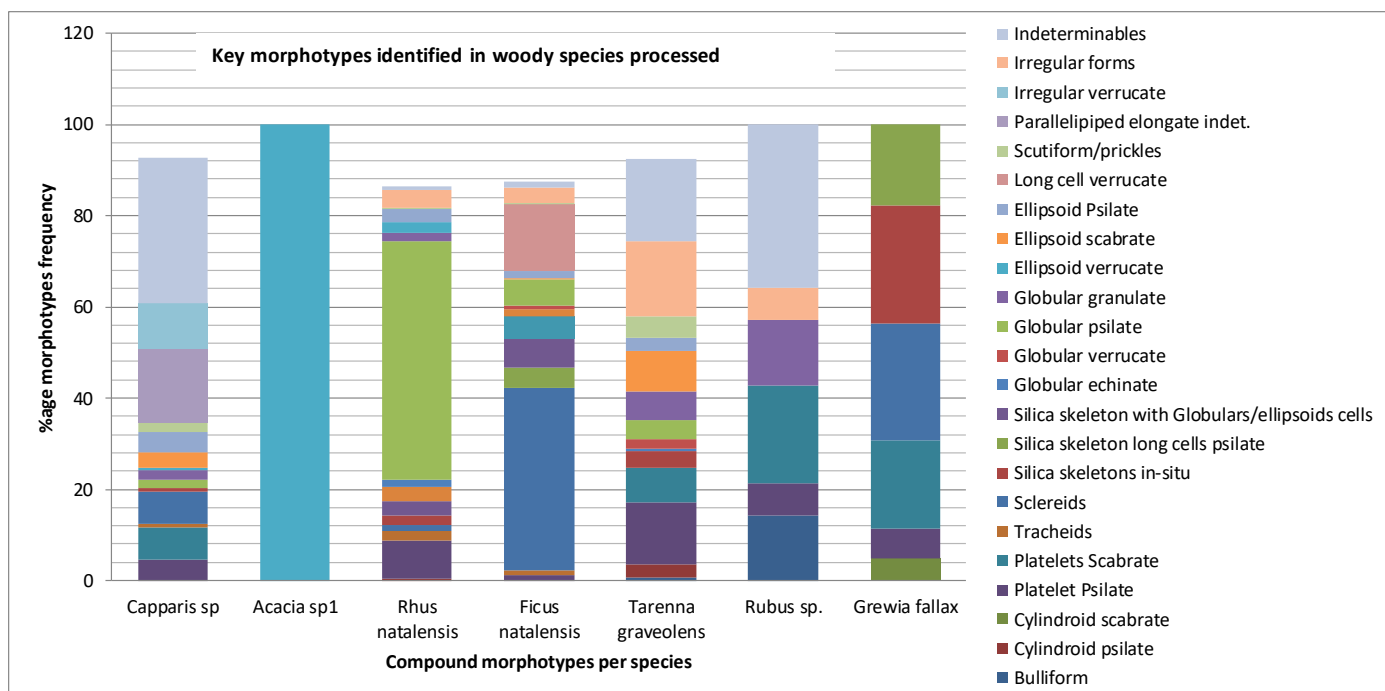


Figure 24. **Relative abundance of phytolith assemblages in the seven woody species analysed**

4.2.4.3. Sedges (*Cyperaceae*)

Among the eight sedges processed (Figure 25), *Cyperus elatus* and *Scleria bovinni* are the only Cyperaceae that didn't produce the known sedge indicator morphotype: papillae. The other three species produced papillae morphotypes in abundance. *Cyperus papyrus* contained papillae (94.7%). *Cyperus congensis* contained epidermal crenate (29.8%), papillae (14.9%), cylindroid verrucate (12.3%), stomata (11.9%) and tabular crenate (8.9%). *Cyperus elatus* contained tabular trapezoid (63.1%) and cylindroid psilate bulbous (4.0%). *Cyperus elephantinus* contained papillae (95.4%) and stomata (4.6%). *Kyllinga* sp. contained papillae (22.2%), parallelepiped elongate (13.3%), cylindroid psilate bulbous (8.1%). *Scleria bovinni* contained tabular sinuate (67.8%), epidermal jig-saw (12.7%) and tabular crenate (11.7%). *Eleocharis* sp. contained papillae (94.9%) and tabular crenate (3.4%).

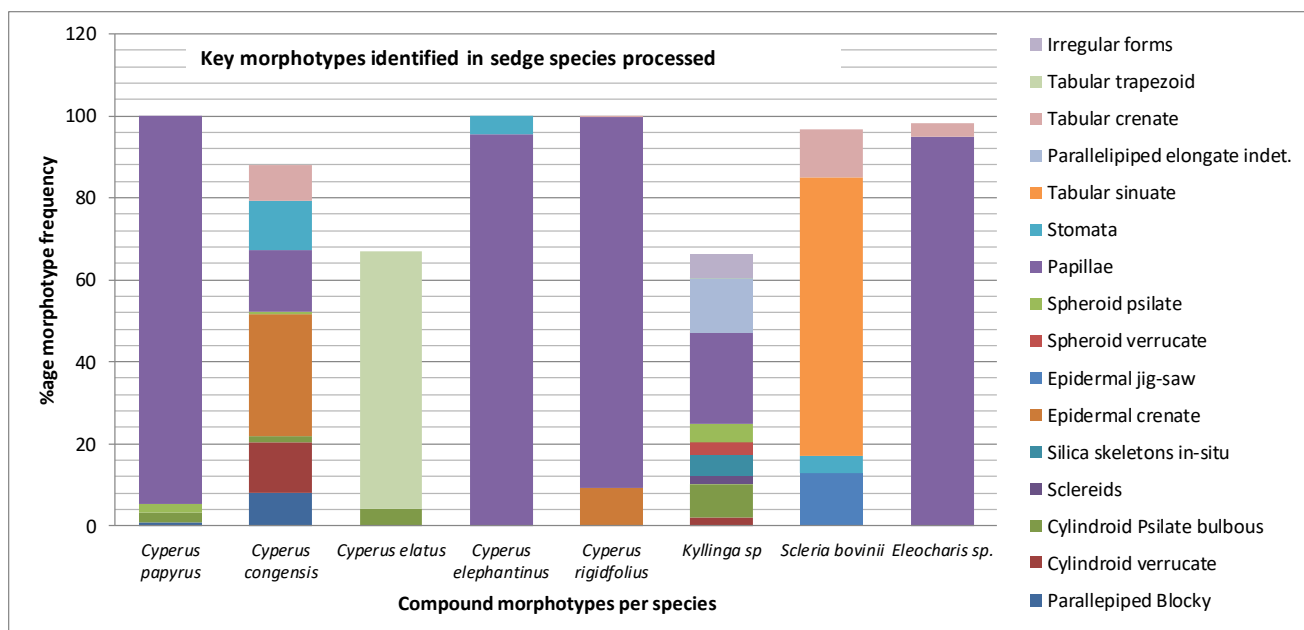


Figure 25. Relative abundance of phytolith assemblages observed in Cyperaceae

5.2.5. Summarised results of non-grass analyses

The results show that woody and herbaceous taxa accumulate less silica compared to grasses. The results do not show a clear difference between phytolith assemblages produced in the herbaceous and woody taxa processed. Ellipsoid verrucate, globular granulate, irregular forms and sclereids were mostly observed in woody taxa. No unique morphotypes were noted on the herbaceous taxa only. Other exceptions noted are the abundance of globular psilate observed in *Rhus natalensis* which is a tree while globular granulate was observed in abundance in *Indigofera sp.*

In the Cyperaceae species, papillae are the most represented morphotype in six of the eight species, but absent in two species. This morphotype can be considered as a direct key indicator of the Cyperaceae in a fossil assemblage. Morphotypes such as tabular sinuates, tabular trapezoids and epidermal crenate can only be applied with caution.

5.2.6. Testing the significance of the modern reference data as a benchmark to interpret fossil assemblage in this study

The results in Table 9 show the confidence level of the modern phytolith collection to interpret the three different categories of plants analysed in this study. Despite the variation in the number of individual species processed in each category, the diversity and frequency of morphotypes identified, the level of confidence in each category is the same, 95.0%.

Table 9. Table showing three main plants' categories and their corresponding statistical attributes.

Grasses		Sedges		Woody dicots & herbs	
Mean	135,5495	Mean	21,35135	Mean	22,54054
Standard Error	28,85533	Standard Error	10,40367	Standard Error	4,493453
Median	9	Median	0	Median	3
Mode	0	Mode	0	Mode	0
Standard Deviation	304,0098	Standard Deviation	109,6094	Standard Deviation	47,34146
Sample Variance	92421,96	Sample Variance	12014,23	Sample Variance	2241,214
Kurtosis	14,51865	Kurtosis	97,0794	Kurtosis	14,87903
Skewness	3,451122	Skewness	9,588239	Skewness	3,570833
Range	1992	Range	1129	Range	306
Minimum	0	Minimum	0	Minimum	0
Maximum	1992	Maximum	1129	Maximum	306
Sum	15046	Sum	2370	Sum	2502
Count	111	Count	111	Count	111
Confidence Level(95.0%)	57,1845	Confidence Level(95.0%)	20,61763	Confidence Level(95.0%)	8,904969

CHAPTER SIX: OLOGESAILIE PHYTOLITH ASSEMBLAGE

6.1. Introduction

Results presented here are analysed from 272 sediment samples taken at 48cm sampling interval from a 166m core. A total of 48,638 phytolith were identified into 70 morphotype categories. 93% (N=153) of the samples yielded phytoliths. However, only 36.4% (N=99) of the samples yielded more than 200 morphotypes. Of the 70 morphotype categories, 50% (n=35) are non-diagnostic morphotypes, 34.3% (n=24) are GSSCs, 11.4% (n=8) are diagnostic woody (dicots and palms) morphotypes and 2.9% (n=2) sedge morphotypes (see appendix III for more details).

Table 10 categorises the major morphotypes into four broad abundance categories depending on the frequencies occurrence throughout the core.

Table 10. Showing identified morphotypes from the ODP core assemblages of 48,638 categorised into four broad abundance classes (% of the total assemblage) 'abundant' (>10%), 'common' (>1-10%), 'Uncommon' (0.1-1.0%) and 'rare' (<0.1%).

a) Abundant (>10%)

Globular granulate, tracheids

b) Common (>1-10%)

Rondels, saddles, bilobate convex shortshank, bilobate flattened short sShank, bilobate panicoid, saddle long, saddle plateau, bulliforms, sclereids, globular verrucate, globular echinate, globular psilate, epidermal long cells, irregular scabrate, scutiform

c) Uncommon (0.1-1%)

Achene, bilobate concave long sshank, bilobate concave short shank, bilobate flattened long shank, crosses/quadra-lobate, polylobate, saddle collapse, saddle squat, tower variants, globular regulate, ellipsoid psilate ellipsoid scabrate, facetate, hair cell, irregular psilate, polyhedrals, prickle

d) Rare (<0.1%)

Papillae, bilobate concave long shank, saddle tall, trapezoid, globular scalloped, cylindroid variants, ellipsoid scabrate, honeycomb assemblage, mesophyll, parallelepiped variants, stomatal cells

6.2. ODP phytolith spectra: Individual key morphotypes

Phytolith assemblages identified and analysed from the ODP core are presented using a Tilia diagram while zones and sub-zones are identified by CONISS, a numerical clustering package within TILIA software (Figure 26 & 27).

The quantity of phytoliths identified in the lower part of the ODP core dated between 425kyr and 975kyr were scarce compared to the upper part of the core (~425-~75kyr) see figure 26 in some levels, phytoliths were completely absent

6.2.1. Zone ODP I (975-675kyr)

This zone has a low phytolith concentration, particularly the GSSCs morphotypes that are very rare to absent in most of the samples. Saddles, however are sporadically present at percentages of <20%. Forest indicators such as tracheids, sclereids, globular granulate and globular echinate are significantly present in most of the samples ranging between >20% and 60%. Globular echinate (Palm) morphotype significantly present in this zone registering >30% in one of the samples.

The zone is sub-divided into two sub-zones by what appears to be a hiatus around 900kyr (NO DATA PHASE). Although similar morphotype assemblages are present in both subzones, ODP Ia has less forest indicator (FI) morphotypes such as globular echinate, globular regulate, sclereid and tracheids compared to subzones ODP Ib while there are GSSCs, particularly the saddle morphotype in subzone ODP Ia. Globular echinate (Palm-type) contributes largely on the sub-division of the zone.

6.2.2. Zone ODP II (675-325kyr)

This zones show a marked increase in phytolith assemblages both in diversity and concentration in most samples. Key diagnostic morphotypes identifying four categories; wetlands (achene, papillae), grasslands (saddles, bilobate convex short shank, saddle plateau), gallery forests (palm globular echinate) and forests (globular echinate, tracheid) are significantly present in most samples. Most distinctive is the high presentation of globular granulates in most samples ranging between >20% and 100%. Another additional feature noted in this zone is the sporadic appearances of various morphotypes indicative of woody and herbaceous dicotyledons. Palm globular echinate however, are distinctively absent or very rare in the zone. Saddles, tracheids and globular granulate are the prominent morphotypes that defines this zonation.

Two distinct sub-zones are identified based on phytolith abundance and diversity at different levels. ODP IIa, by contrast has lower phytolith percentages and a notable hiatus around 600kyr compared to sub-zone ODP IIb.

6.2.3. Zone ODP III (325-77kyr)

The zone marks an increased proportion of GSSCs. Forest indicators remain significantly present in almost all the samples analysed. Woody and herbaceous dicotyledons indicators are much more in quantities and diversity than any other zone. Most samples in this zone have the highest quantity of unidentified morphotypes, the indeterminate.

Two subzones are identified in the zone most likely due to the abrupt reduction to absence of most of the morphotypes around 175kyr. Sub-zone ODP IIIa contrasts with ODP IIIb in that samples are much richer in phytolith assemblages of all the categories. Also notable is the absence of achene phytoliths in sub-zone ODP IIIb while they are present though in only a few samples (with a peak of >20%). Another contrast observed is the increased proportion of Panicoideae morphotypes such as bilobate convex short shank, bilobate concave short shank and crosses in ODP IIIa. Chloridoideae morphotypes are abundant in ODP IIIa and much reduced in abundance in ODP IIIb.

6.3. Phytolith Indices-ODP

Two phytolith indices are used in order to trace and understand changes in vegetation structure and composition such as woodland features and dominant grass subfamilies (table 11). Majority of samples had relevant morphotypes used to calculate the indices, however, there were levels with very poor preservation or no phytoliths present and were assumed to represent bare ground. Here the indices values are presented and discussed temporally according to the zonation already identified above in the abundance diagrams.

6.3.1. D: P index

The D: P (tree cover density) was prominent in the ODP core with an average value of 7.4. D: P values are categorized into three groups: D: P ≤ 1 , reflect low tree-cover-density/ open grasslands, D: P ≤ 10 , moderate tree-cover-density/ wooded grasslands, D: P > 10 , high tree-cover-density/woodlands/forests. The infinite value (∞) on the D:P index is the results of the absence of GSSCs indicating absence of GSSCs and dense wooded vegetation, where the abundance of globular granulate is greater than 10 but for those levels with a zero are considered “not significant” (see table 11 for details).

6.3.1.1. ODP zone 1 (976.7-657.9kyr)

There are six phases of high tree cover density, seven phases of moderate tree-cover-density and three phases of low tree cover densities. Between ~976kyr and ~944kyr, is a low tree cover density phase interrupted by a high peak of tree cover density (24.8) at ~966kyr. The vegetation structure is mostly open grasslands. Vegetation fluctuation rate during this period is low, but the shift from low- high-low tree cover density at ~966kyr, is drastic.

Between ~933kyr and ~850kyr, D: P shifts between high to moderate phases. The rate of fluctuation is high, switching between each sampling level. Around 830kyr, a low D: P phase interrupts this trend briefly which reappear again from ~817.6kyr to ~658kyr. This zone is characterised by high to moderate tree-cover-density cover. Before ~850kyr, the fluctuation rate between low to high tree-cover-density is higher than from ~817kyr to ~658kyr. The most conspicuous low tree-cover-density phase in this zone happened around 830.2kyr (0.1).

6.3.1.2. ODP zone II (644.0-325.9kyr)

There are five phases of high tree-cover-density, fifteen phases of moderate tree-cover-density and fourteen phases of low tree-cover-density phases. The period between ~644kyr and ~612kyr, is high to moderate D: P phase, the shift is gradual through time. Between ~585kyr and ~488kyr, is a moderate to low the D: P phase with high fluctuation rates. The period between ~475kyr and ~419kyr shows a high rate and strong fluctuations phases; from high to moderate, high to low and moderate to high shifts. The period between ~410kyr and 378kyr is a moderate to low D: P phase, fluctuation rate is high in the beginning but stabilises in the last three levels with moderate D: P phase. Between 375.9kyr and 325.9kyr, a high fluctuation rate is noted from high to moderate to low D: P. In the beginning, the D: P drops rapidly from high to low followed by sequence of moderate-low D: P phase to ~325kyr but which is interrupted by a high D: P index at ~355kyr.

This zone is characterised by moderate to low tree-cover-density; wooded grasslands to open grasslands vegetation structure. Of the five high tree cover density phases, the 630kyr record the highest D: P value indicating highly dense woodland/forest phase.

6.3.1.3. ODP zone III (322-77.5kyr):

There are about twenty two phases of high tree-cover-density, twenty one phases of moderate D: P phases and nine low D: P phases. There are quite a number of samples that did not yield the required morphotypes to calculate the D: P index, particularly the GSSCs, and this levels have an infinite D: P value (∞). Four of these phases are worth mentioning since they are prolonged: (~322kyr to 302kyr), (299.7kyr to 83kyr), (214.4kyr to 213.8kyr) and (212.67kyr to 212.65kyr). The period between ~300kyr and ~250kyr is low D:P phase with low fluctuation. This changes suddenly to a high D:P phase from ~246kyr to ~244kyr, it is worth noting the absence of GSSCs morphotypes while globular granulates are significantly present. Between ~243.1kyr and ~230kyr is a low-moderate D:P phase which interrupted occasionally by high D:P phases occurring between 235.7kyr and 232.3ky. The period between ~255kyr and 215.3kyr is mainly a high to moderate D:P value with a few punctuations of low and infinite D:P phases. The period is characterised by high rate fluctuation between phases. The period between ~213.8kyr and 212.6kyr is generally without GSSCs morphotypes with occasional moderate-high D:P phases. Between 212.5 and 77kyrs is a low-moderate-high D:P phases which fluctuates gradually through time except for an abrupt shift from low D:P value (0.4) to a high D:P value (217.0) around 103.9kyr and 101.3kyr. Another significant D:P change is noted at ~188.7kyr with high peak of 86.5. The vegetation structure therefore gradually shifts from woodlands to wooded grasslands to open grasslands in the upper part of the core.

6.3.2. Iph index

Similarly, the Iph indices are presented following the zones already identified. They range between 0 (low aridity; where Panicoideae dominate over the Chloridoideae grasses) and 1 (high aridity; where Chloridoideae dominated over the Panicoideae grasses), Iph index value of 0.5 suggest equal or almost equal representation of both grass sub-families as shown in table 11.

6.3.2.1. ODP I (976.7-657.9kyr)

Iph indices range between 0.6 and 1, general indication of more Chloridoideae than Panicoideae grasses, hence high aridity index. Two phases of high aridity are identified as follows: 976.7-884.6kyr (0.7-1) and 830.24-771.0kyr (0.6-1). Medium aridity (0.5) phases are two identified around 850.4kyr and 713.1kyr. Only one phase of low aridity is clearly identified in this zone around 861.0kyr with Iph value of Zero. The other samples did not yield diagnostic GSSCs.

6.3.2.2. ODP II (644.0-325.9kyr)

There are thirteen phases of high aridity (0.6-1) in this zone, with two of them occurring for a longer period between 574.2kyr and 548.0kyr, and the second one occurring between 370.5kyr and 356.0kyr. Eight phases of medium aridity are identified in the zone, no prolonged period; most likely these are transition phases. There are nine phases of low aridity (0.0-0.2) which are brief. The other samples did not yield diagnostic GSSCs.

6.3.2.3. ODP III (322-77.5kyr)

There are twenty one low aridity (0.0-0.3) phases. Most of them represent brief events except for two prolonged ones: between 208.4kyr and 164.7kyr and between 138.1kyr and 79.4kyr. There are numerous samples that did not yield diagnostic morphotypes resulting in huge “no significant” gaps between the following dates: 319.5-308.0kyr, 246.1-244.0kyr, 236.9-232.3kyr, 229.7-225.4kyr, 223.2-220.0kyr and 216.1-212.6kyr. Generally, aridity index in this zone indicate grasslands with high Panicoideae proportions.

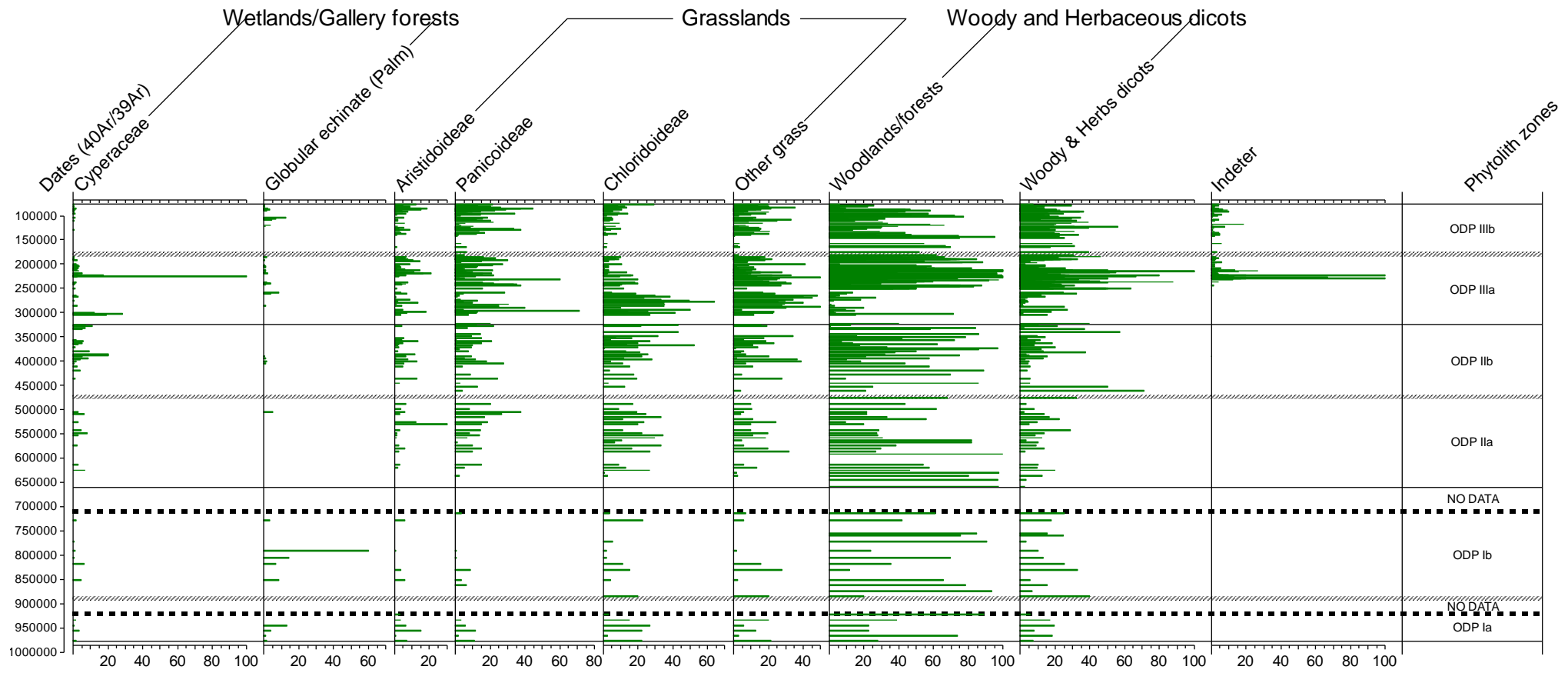


Figure 27. Relative abundance of key identified vegetation types /habitat versus age (left). Zones identified by CONISS in TILIA

Table 11. Showing aridity (Iph) and tree cover density (D:P) of the ODP core calculated from the selected GSSCs and globular granulate (modified from Bremond et al., 2008). Shading follows the D:P indices, not the aridity indices from the grasses. Note that the two do not correlate.

Age (kyr)	Depth	Panicoideae	Chloridoideae	Globular granulate	Panicoideae+Chloridoideae	Iph	D:P	Interpretation	Iph	D:P
77,50	27,03	56	60	17	116	0,5	0,1	Medium aridity, P=C	Low tree density, Open grasslands	
79,40	27,51	22	11	16	33	0,3	0,5	Low aridity, P>C	Low tree density, Open grasslands	
81,45	27,98	89	51	41	140	0,4	0,3	Low aridity, P>C	Low tree density, Open grasslands	
83,25	28,35	99	48	17	147	0,3	0,1	Low aridity, P>C	Low tree density, Open grasslands	
84,74	28,95	91	22	15	113	0,2	0,1	Low aridity, P>C	Low tree density, Open grasslands	
85,61	29,43	128	12	14	140	0,1	0,1	Low aridity, P>C	Low tree density, Open grasslands	
86,29	29,91	140	26	14	166	0,2	0,1	Low aridity, P>C	Low tree density, Open grasslands	
86,90	30,39	121	44	25	165	0,3	0,2	Low aridity, P>C	Low tree density, Open grasslands	
87,46	30,87	29	9	90	38	0,2	2,4	Low aridity, P>C	Moderate density, wooded grasslands	
88,10	31,44	51	10	115	61	0,2	1,9	Low aridity, P>C	Moderate density, wooded grasslands	
88,57	31,83	37	9	88	46	0,2	1,9	Low aridity, P>C	Moderate density, wooded grasslands	
89,18	32,32	41	5	58	46	0,1	1,3	Low aridity, P>C	Moderate density, wooded grasslands	
89,87	32,8	29	6	165	35	0,2	4,7	Low aridity, P>C	Moderate density, wooded grasslands	
90,90	33,34	41	8	88	49	0,2	1,8	Low aridity, P>C	Moderate density, wooded grasslands	
91,52	33,82	25	1	139	26	0,0	5,3	Low aridity, P>C	Moderate density, wooded grasslands	
92,63	34,31	19	18	75	37	0,5	2,0	Medium aridity, P=C	Moderate density, wooded grasslands	
95,57	35,75	240	86	39	326	0,3	0,1	Low aridity, P>C	Low tree density, Open grasslands	
96,67	36,21	22	16	142	38	0,4	3,7	Low aridity, P>C	Moderate density, wooded grasslands	
98,04	36,68	61	34	178	95	0,4	1,9	Low aridity, P>C	Moderate density, wooded grasslands	
100,50	37,18	15	7	357	22	0,3	16,2	Low aridity, P>C	High tree density, woodlands	
101,30	37,66	1	0	217	1	0,0	217,0	Low aridity, P>C	High tree density, woodlands	
103,86	38,15	45	11	22	56	0,2	0,4	Low aridity, P>C	Low tree density, Open grasslands	
106,26	38,63	38	7	48	45	0,2	1,1	Low aridity, P>C	Moderate density, wooded grasslands	
107,81	39,11	53	19	120	72	0,3	1,7	Low aridity, P>C	Moderate density, wooded grasslands	
110,17	39,6	82	11	54	93	0,1	0,6	Low aridity, P>C	Low tree density, Open grasslands	
113,50	40,21	13	0	9	13	0,0	0,7	Low aridity, P>C	Low tree density, Open grasslands	

Age (kyr)	Depth	Panicoideae	Chloridoideae	Globular granulate	Panicoideae+Chloridoideae	Iph	D:P	Interpretation	Iph	D:P
115,73	40,67	10	13	59	23	0,6	2,6 Medium aridity, P=C	Moderate density, wooded grasslands		
117,68	41,16	1	0	25	1	0,0	25,0 Low aridity, P>C	High tree density, woodlands		
119,80	41,66	10	0	170	10	0,0	17,0 Low aridity, P>C	High tree density, woodlands		
121,76	42,12	31	18	82	49	0,4	1,7 Low aridity, P>C	Moderate density, wooded grasslands		
123,77	42,65	3	1	25	4	0,3	6,3 Low aridity, P>C	Moderate density, wooded grasslands		
125,51	43,06	20	4	79	24	0,2	3,3 Low aridity, P>C	Moderate density, wooded grasslands		
127,73	43,57	72	18	49	90	0,2	0,5 Low aridity, P>C	Low tree density, Open grasslands		
129,79	44,05	155	11	50	166	0,1	0,3 Low aridity, P>C	Low tree density, Open grasslands		
132,32	44,54	26	0	70	26	0,0	2,7 Low aridity, P>C	Moderate density, wooded grasslands		
134,94	45,02	46	4	152	50	0,1	3,0 Low aridity, P>C	Moderate density, wooded grasslands		
138,07	45,5	31	17	68	48	0,4	1,4 Low aridity, P>C	Moderate density, wooded grasslands		
139,95	45,99	4	6	123	10	0,6	12,3 High aridity P<C	High tree density, woodlands		
141,42	46,47	4	0	236	4	0,0	59,0 Low aridity, P>C	High tree density, woodlands		
144,06	46,96	0	0	30	0	∞	∞ not significant, No grasses	High tree density, woodlands		
145,66	47,44	0	0	12	0	∞	∞ not significant, No grasses	High tree density, woodlands		
157,20	47,92	3	2	38	5	0,4	7,6 Low aridity, P>C	Moderate density, wooded grasslands		
161,81	48,4	0	0	29	0	∞	∞ not significant, No grasses	High tree density, woodlands		
164,74	48,89	13	4	125	17	0,2	7,4 Low aridity, P>C	Moderate density, wooded grasslands		
174,93	49,45	4	0	27	4	0,0	6,8 Low aridity, P>C	Moderate density, wooded grasslands		
180,74	49,85	0	0	23	0	∞	∞ not significant, No grasses	High tree density, woodlands		
184,29	50,34	1	0	32	1	0,0	32,0 Low aridity, P>C	High tree density, woodlands		
185,07	50,82	23	9	36	32	0,3	1,1 Low aridity, P>C	Moderate density, wooded grasslands		
185,82	51,3	37	4	253	41	0,1	6,2 Low aridity, P>C	Moderate density, wooded grasslands		
186,66	51,78	57	11	58	68	0,2	0,9 Low aridity, P>C	Low tree density, Open grasslands		
188,94	52,38	2	0	173	2	0,0	86,5 Low aridity, P>C	High tree density, woodlands		
189,09	52,76	20	6	32	26	0,2	1,2 Low aridity, P>C	Moderate density, wooded grasslands		
189,14	52,87	21	5	134	26	0,2	5,2 Low aridity, P>C	Moderate density, wooded grasslands		
189,24	53,13	0	0	122	0	∞	∞ not significant, No grasses	High tree density, woodlands		
189,32	53,35	2	1	47	3	0,3	15,7 Low aridity, P>C	High tree density, woodlands		
189,41	53,58	3	2	26	5	0,4	5,2 Low aridity, P>C	Moderate density, wooded grasslands		
189,48	53,76	19	1	181	20	0,1	9,1 Low aridity, P>C	Moderate density, wooded grasslands		
189,50	53,83	13	4	151	17	0,2	8,9 Low aridity, P>C	Moderate density, wooded grasslands		

Age (kyr)	Depth	Panicoideae	Chloridoideae	Globular granulate	Panicoideae+Chloridoideae	Iph	D:P	Interpretation	Iph	D:P
191,32	54,32	57	3	38	60	0,1	0,6	Low aridity, P>C Low tree density, Open grasslands		
193,02	54,8	41	3	159	44	0,1	3,6	Low aridity, P>C Low tree density, Open grasslands		
195,65	55,52	8	0	216	8	0,0	27,0	Low aridity, P>C High tree density, woodlands		
197,06	55,83	2	0	29	2	0,0	14,5	Low aridity, P>C High tree density, woodlands		
200,47	56,39	67	22	17	89	0,2	0,2	Low aridity, P>C Low tree density, Open grasslands		
202,74	56,87	54	3	104	57	0,1	1,8	Low aridity, P>C Moderate density, wooded grasslands		
203,50	57,36	39	10	144	49	0,2	2,9	Low aridity, P>C Moderate density, wooded grasslands		
205,53	57,84	35	9	147	44	0,2	3,3	Low aridity, P>C Moderate density, wooded grasslands		
208,44	58,49	4	0	49	4	0,0	12,3	Low aridity, P>C High tree density, woodlands		
209,22	58,95	0	0	76	0	∞	∞	not significant, No grasses High tree density, woodlands		
209,83	59,31	1	0	41	1	0,0	41,0	Low aridity, P>C High tree density, woodlands		
210,13	59,86	0	0	36	0	∞	∞	not significant, No grasses High tree density, woodlands		
210,43	60,4	11	0	108	11	0,0	9,8	Low aridity, P>C Moderate density, wooded grasslands		
212,47	61,52	30	5	24	35	0,1	0,7	Low aridity, P>C Low tree density, Open grasslands		
212,56	62	0	0	16	0	∞	∞	not significant, No grasses High tree density, woodlands		
212,65	62,49	0	0	0	0	∞	∞	not significant, No grasses Not significant		
212,67	62,97	0	0	1	0	∞	∞	not significant, No grasses Not significant		
212,67	63,45	0	0	1	0	∞	∞	not significant, No grasses Not significant		
212,67	63,93	0	0	0	0	∞	∞	not significant, No grasses Not significant		
212,67	64,41	0	0	0	0	∞	∞	not significant, No grasses Not significant		
212,67	64,89	0	0	0	0	∞	∞	not significant, No grasses Not significant		
212,67	65,36	0	0	0	0	∞	∞	not significant, No grasses Not significant		
212,83	65,77	0	0	86	0	∞	∞	not significant, No grasses High tree density, woodlands		
213,05	65,91	8	7	132	15	0,5	8,8	Medium aridity, P=C Moderate density, wooded grasslands		
213,31	66,34	0	0	142	0	∞	∞	not significant, No grasses High tree density, woodlands		
213,39	66,83	0	0	2	0	∞	∞	not significant, No grasses Not significant		
213,46	67,31	0	0	7	0	∞	∞	not significant, No grasses Not significant		

Age (kyr)	Depth	Panicoideae	Chloridoideae	Globular granulate	Panicoideae+Chloridoideae	Iph	D:P	Interpretation	Iph	D:P
213,54	67,8	4	0	0	31	4	0,0	7,8 Low aridity, P>C	Moderate density, wooded grasslands	
213,61	68,36	0	0	0	7	0	∞	∞ significant, No grasses	Not significant	
213,61	68,76	0	0	0	13	0	∞	∞ significant, No grasses	High tree density, woodlands	
213,62	69,24	0	0	0	1	0	∞	∞ significant, No grasses	Not significant	
213,67	69,73	0	0	0	0	0	∞	∞ significant, No grasses	Not significant	
213,76	70,28	0	0	0	46	0	∞	∞ significant, No grasses	High tree density, woodlands	
213,82	70,7	0	0	0	0	0	∞	∞ significant, No grasses	Not significant	
213,82	71,18	0	0	0	5	0	∞	∞ significant, No grasses	Not significant	
214,21	71,66	0	0	0	6	0	∞	∞ significant, No grasses	Not significant	
214,37	72,14	0	0	0	0	0	∞	∞ significant, No grasses	Not significant	
214,42	72,62	0	0	0	4	0	∞	∞ significant, No grasses	Not significant	
215,79	73,72	0	0	0	28	0	∞	∞ significant, No grasses	High tree density, woodlands	
215,86	74,25	0	0	0	12	0	∞	∞ significant, No grasses	High tree density, woodlands	
216,10	74,39	0	0	0	0	0	∞	∞ significant, No grasses	Not significant	
216,30	74,51	11	2	2	21	13	0,2	1,6 Low aridity, P>C	Moderate density, wooded grasslands	
216,61	74,69	11	21	21	37	32	0,7	1,2 High aridity P<C	Moderate density, wooded grasslands	
217,46	75,17	4	4	4	49	8	0,5	6,1 Medium aridity, P=C	Moderate density, wooded grasslands	
218,31	75,65	37	0	0	71	37	0,0	1,9 Low aridity, P>C	Moderate density, wooded grasslands	
218,46	75,82	0	0	0	26	0	∞	∞ significant, No grasses	High tree density, woodlands	
218,93	76,13	8	1	1	5	9	0,1	0,6 Low aridity, P>C	Low tree density, Open grasslands	
220,11	76,61	0	0	0	50	0	∞	∞ significant, No grasses	High tree density, woodlands	
221,17	77,09	0	0	0	64	0	∞	∞ significant, No grasses	High tree density, woodlands	
221,90	77,51	0	0	0	87	0	∞	∞ significant, No grasses	High tree density, woodlands	
221,95	77,57	0	0	0	114	0	∞	∞ significant, No grasses	High tree density, woodlands	
222,29	78,05	0	0	0	0	0	∞	∞ significant, No grasses	Not significant	
222,37	78,51	0	0	0	31	0	∞	∞ significant, No grasses	High tree density, woodlands	

Age (kyr)	Depth	Panicoideae	Chloridoideae	Globular granulate	Panicoideae+Chloridoideae	Iph	D:P	Interpretation	Iph	D:P
222,68	78,96	0	0	0	0	0	∞	not significant, No grasses		
222,90	79,25	0	0	11	0	0	∞	not significant, No grasses		
223,08	79,5	0	0	0	0	0	∞	not significant, No grasses		
223,17	79,64	7	11	10	18	0,6	0,6	High aridity P<C		
223,35	79,98	9	0	54	9	0,0	6,0	Low aridity, P>C		
223,70	80,46	0	0	19	0	∞	∞	Medium aridity, P=C		
223,83	80,94	15	11	7	26	0,4	0,3	Low aridity, P>C		
224,08	81,64	0	0	0	0	0	∞	not significant, No grasses		
224,44	82,13	0	0	0	0	0	∞	not significant, No grasses		
224,72	82,57	12	10	31	22	0,5	1,4	Medium aridity, P=C		
225,03	82,87	1	0	28	1	0,0	28,0	Low aridity, P>C		
225,31	83,36	0	0	1	0	0	∞	not significant, No grasses		
225,64	83,84	0	0	0	0	0	∞	not significant, No grasses		
225,86	84,2	0	0	0	0	0	∞	not significant, No grasses		
226,14	84,69	0	0	0	0	0	∞	not significant, No grasses		
226,39	85,17	0	0	0	0	0	∞	not significant, No grasses		
226,55	85,46	0	0	3	0	0	∞	not significant, No grasses		
226,80	85,91	0	0	0	0	0	∞	not significant, No grasses		
226,93	86,39	0	0	0	0	0	∞	not significant, No grasses		
227,04	86,87	0	0	1	0	0	∞	not significant, No grasses		
227,35	87,35	0	0	5	0	0	∞	not significant, No grasses		
227,68	87,84	0	0	0	0	0	∞	not significant, No grasses		
227,99	88,22	0	0	0	0	0	∞	not significant, No grasses		
228,46	88,8	0	0	0	0	0	∞	not significant, No grasses		
228,92	89,28	0	0	6	0	0	∞	not significant, No grasses		
229,25	89,76	0	0	0	0	0	∞	not significant, No grasses		

Age (kyr)	Depth	Panicoidae	Chloridoideae	Globular granulate	Panicoidae+Chloridoideae	Iph	D:P	Interpretation	Iph	D:P
229,55	90,24	0	0	2	0	∞	∞ significant, No grasses	not significant		
229,73	90,73	0	0	1	0	∞	∞ significant, No grasses	not significant		
230,01	91,21	1	0	11	1	0,0	11,0 Low aridity, P>C	High tree density, woodlands		
230,33	91,79	1	0	4	1	0,0	4,0 Low aridity, P>C	Moderate density, wooded grasslands		
230,56	92,18	2	0	2	2	0,0	1,0 Low aridity, P>C	Low tree density, Open grasslands		
230,84	92,62	1	0	2	1	0,0	2,0 Low aridity, P>C	Moderate density, wooded grasslands		
231,24	93,14	3	1	0	4	0,3	0,0 Low aridity, P>C	Low tree density, Open grasslands		
232,32	93,62	0	0	55	0	∞	∞ significant, No grasses	High tree density, woodlands		
233,47	94,1	0	0	11	0	∞	∞ significant, No grasses	High tree density, woodlands		
234,64	94,59	0	0	0	0	∞	∞ significant, No grasses	Not significant		
235,72	95,07	0	0	19	0	∞	∞ significant, No grasses	High tree density, woodlands		
236,15	95,55	0	0	2	0	∞	∞ significant, No grasses	not significant		
236,46	96,04	0	0	1	0	∞	∞ significant, No grasses	not significant		
236,65	96,52	0	0	15	0	∞	∞ significant, No grasses	High tree density, woodlands		
236,65	97,01	0	0	0	0	∞	∞ significant, No grasses	not significant		
236,65	97,49	0	0	0	0	∞	∞ significant, No grasses	not significant		
236,88	97,88	0	0	1	0	∞	∞ significant, No grasses	not significant		
237,97	98,46	25	27	9	52	0,5	0,2 Medium aridity, P=C	Low tree density, Open grasslands		
238,92	98,94	15	12	46	27	0,4	1,7 Low aridity, P>C	Moderate density, wooded grasslands		
239,87	99,42	38	35	21	73	0,5	0,3 Medium aridity, P=C	Low tree density, Open grasslands		
240,83	99,9	41	16	10	57	0,3	0,2 Low aridity, P>C	Low tree density, Open grasslands		
241,85	100,38	84	21	14	105	0,2	0,1 Low aridity, P>C	Low tree density, Open grasslands		
243,06	100,86	48	11	5	59	0,2	0,1 Low aridity, P>C	Low tree density, Open grasslands		
244,40	101,34	1	1	88	2	0,5	44,0 Medium aridity, P=C	High tree density, woodlands		
244,40	101,82	0	0	62	0	∞	∞ significant, No grasses	High tree density, woodlands		
244,40	102,3	0	0	25	0	∞	∞ significant, No grasses	High tree density, woodlands		
245,32	102,78	0	0	65	0	∞	∞ significant, No grasses	High tree density, woodlands		

Age (kyr)	Depth	Panicoideae	Chloridoideae	Globular granulate	Panicoideae+Chloridoideae	Iph	D:P	Interpretation	Iph	D:P
246,14	103,26	0	0	40	0	∞	∞	not significant, No grasses	High tree density, woodlands	
249,83	104,23	0	0	1	0	∞	∞	not significant, No grasses	Not significant	
250,09	104,72	11	8	32	19	0,4	1,7	Low aridity, P>C	low tree density, Open grasslands	
250,52	105,2	0	0	46	0	∞	∞	Medium aridity, P=C	High tree density, woodlands	
250,95	105,68	0	0	8	0	∞	∞	Medium aridity, P=C	Not significant	
258,96	107,18	27	5	9	32	0,2	0,3	Low aridity, P>C	Low tree density, Open grasslands	
261,31	107,58	8	31	15	39	0,8	0,4	High aridity P<C	Low tree density, Open grasslands	
264,03	108,05	1	15	2	16	0,9	0,1	High aridity P<C	Low tree density, Open grasslands	
266,73	108,53	2	90	9	92	1,0	0,1	High aridity P<C	Low tree density, Open grasslands	
269,62	109,01	0	28	33	28	1,0	1,2	High aridity P<C	Moderate density, wooded grasslands	
272,18	109,49	2	47	26	49	1,0	0,5	High aridity P<C	Low tree density, Open grasslands	
274,84	109,97	25	96	5	121	0,8	0,0	High aridity P<C	Low tree density, Open grasslands	
277,40	110,45	2	27	0	29	0,9	0,0	High aridity P<C	Low tree density, Open grasslands	
279,96	110,94	8	25	0	33	0,8	0,0	High aridity P<C	Low tree density, Open grasslands	
282,48	111,42	21	21	1	42	0,5	0,0	Medium aridity, P=C	Low tree density, Open grasslands	
285,13	111,9	31	44	3	75	0,6	0,0	High aridity P<C	Low tree density, Open grasslands	
287,80	112,39	1	0	0	1	0,0	0,0	Low aridity, P>C	Low tree density, Open grasslands	
290,53	112,87	4	1	2	5	0,2	0,4	Low aridity, P>C	Low tree density, Open grasslands	
293,15	113,36	1	11	2	12	0,9	0,2	High aridity P<C	Low tree density, Open grasslands	
295,10	113,84	5	0	1	5	0,0	0,2	Low aridity, P>C	Low tree density, Open grasslands	
297,56	114,32	3	7	0	10	0,7	0,0	Medium aridity, P=C	Low tree density, Open grasslands	
300,27	114,79	7	23	0	30	0,8	0,0	Medium aridity, P=C	Low tree density, Open grasslands	
302,61	115,28	0	0	5	0	∞	∞	not significant, No grasses	Not significant	
305,20	115,76	1	7	4	8	0,9	0,5	Medium aridity, P=C	Low tree density, Open grasslands	
308,81	116,43	0	0	0	0	∞	∞	not significant, No grasses	Not significant	
311,66	116,87	0	0	0	0	∞	∞	not significant, No grasses	Not significant	
314,09	117,35	0	0	0	0	∞	∞	not significant, No grasses	Not significant	
316,86	117,84	0	0	0	0	∞	∞	not significant, No grasses	Not significant	
319,50	118,32	0	0	0	0	∞	∞	not significant, No grasses	Not significant	
322,01	118,8	1	0	2	1	0,0	2,0	Low aridity, P>C	Moderate density, wooded grasslands	

Age (kyr)	Depth	Panicoideae	Chloridoideae	Globular granulate	Panicoideae+Chloridoideae	Iph	D:P	Interpretation	Iph	D:P
325,93	119,5	7	25	7	32	0,8	0,2	High aridity P<C	Low tree density, Open grasslands	
328,17	119,91	28	31	1	59	0,5	0,0	Medium aridity, P=C	Low tree density, Open grasslands	
330,86	120,36	3	0	13	3	0,0	4,3	Low aridity, P>C	Moderate density, wooded grasslands	
334,41	120,8	0	0	6	0	∞	∞	not significant, No grasses	Not significant	
340,19	121,36	0	3	0	3	1,0	0,0	High aridity P<C	Low tree density, Open grasslands	
343,51	121,84	2	0	12	2	0,0	6,0	Low aridity, P>C	Moderate density, wooded grasslands	
347,29	122,47	3	10	5	13	0,8	0,4	High aridity P<C	Low tree density, Open grasslands	
350,27	122,96	0	1	9	1	1,0	9,0	High aridity P<C	Moderate density, wooded grasslands	
353,12	123,44	11	12	26	23	0,5	1,1	Medium aridity, P=C	low tree density, Open grasslands	
355,98	123,92	1	9	122	10	0,9	12,2	High aridity P<C	High tree density, woodlands	
358,73	124,37	51	65	17	116	0,6	0,1	High aridity P<C	Low tree density, Open grasslands	
361,84	124,89	8	11	8	19	0,6	0,4	High aridity P<C	Low tree density, Open grasslands	
364,75	125,37	1	15	50	16	0,9	3,1	High aridity P<C	Moderate density, wooded grasslands	
367,68	125,85	6	33	10	39	0,8	0,3	High aridity P<C	Low tree density, Open grasslands	
370,46	126,33	8	14	24	22	0,6	1,1	High aridity P<C	Low tree density, Open grasslands	
373,21	126,81	3	2	256	5	0,4	51,2	Low aridity, P>C	High tree density, woodlands	
375,85	127,28	1	0	36	1	0,0	36,0	Low aridity, P>C	High tree density, woodlands	
378,69	127,78	4	7	27	11	0,6	2,5	Medium aridity, P=C	Moderate density, wooded grasslands	
381,73	128,26	0	5	9	5	1,0	1,8	High aridity P<C	Moderate density, wooded grasslands	
384,78	128,74	0	15	19	15	1,0	1,3	High aridity P<C	Moderate density, wooded grasslands	
387,82	129,23	0	0	9	0	∞	∞	not significant, No grasses	Not significant	
390,70	129,71	27	64	48	91	0,7	0,5	High aridity P<C	low tree density, Open grasslands	
393,73	130,2	6	13	54	19	0,7	2,8	High aridity P<C	Moderate density, wooded grasslands	
396,74	130,68	18	48	17	66	0,7	0,3	High aridity P<C	Low tree density, Open grasslands	
399,70	131,16	35	2	34	37	0,1	0,9	Low aridity, P>C	Low tree density, Open grasslands	
403,62	131,65	32	13	52	45	0,3	1,2	Low aridity, P>C	Moderate density, wooded grasslands	
410,40	132,13	10	36	139	46	0,8	3,0	High aridity P<C	Moderate density, wooded grasslands	
419,26	132,61	0	0	23	0	∞	∞	not significant, No grasses	High tree density, woodlands	
428,12	133,1	2	4	16	6	0,7	2,7	High aridity P<C	Moderate density, wooded grasslands	
436,49	133,58	21	17	8	38	0,4	0,2	Low aridity, P>C	Low tree density, Open grasslands	
444,99	134,07	1	1	27	2	0,5	13,5	Medium aridity, P=C	High tree density, woodlands	
453,19	134,55	1	1	2	2	0,5	1,0	Medium aridity, P=C	Low tree density, Open grasslands	

Age (kyr)	Depth	Panicoideae	Chloridoideae	Globular granulate	Panicoideae+Chloridoideae	Iph	D:P	Interpretation	Iph	D:P
460,97	135,03	1	0	5	1	0,0	5,0	Low aridity, P>C	Moderate density, wooded grasslands	
475,09	135,81	0	0	37	0	∞	∞	not significant, No grasses	High tree density, woodlands	
488,39	136,3	6	5	13	11	0,5	1,2	Medium aridity, P=C	Moderate density, wooded grasslands	
497,51	136,79	12	13	91	25	0,5	3,6	Medium aridity, P=C	Moderate density, wooded grasslands	
504,19	137,27	53	27	30	80	0,3	0,4	Low aridity, P>C	Low tree density, Open grasslands	
509,44	137,79	25	23	20	48	0,5	0,4	Medium aridity, P=C	Low tree density, Open grasslands	
514,48	138,24	1	2	2	3	0,7	0,7	High aridity P<C	Low tree density, Open grasslands	
519,96	138,72	0	1	5	1	1,0	5,0	High aridity P<C	Moderate density, wooded grasslands	
524,97	139,21	19	25	10	44	0,6	0,2	High aridity P<C	Low tree density, Open grasslands	
529,84	139,69	3	4	4	7	0,6	0,6	High aridity P<C	Low tree density, Open grasslands	
542,96	140,8	8	7	18	15	0,5	1,2	Medium aridity, P=C	Moderate density, wooded grasslands	
547,95	141,25	13	35	46	48	0,7	1,0	High aridity P<C	Low tree density, Open grasslands	
553,28	141,79	27	68	56	95	0,7	0,6	High aridity P<C	Low tree density, Open grasslands	
557,68	142,22	5	21	22	26	0,8	0,8	High aridity P<C	Low tree density, Open grasslands	
562,50	142,69	0	7	53	7	1,0	7,6	High aridity P<C	Moderate density, wooded grasslands	
567,94	143,17	1	6	56	7	0,9	8,0	High aridity P<C	Moderate density, wooded grasslands	
574,16	143,66	31	91	126	122	0,7	1,0	High aridity P<C	Low tree density, Open grasslands	
579,78	144,14	12	7	26	19	0,4	1,4	Low aridity, P>C	Moderate density, wooded grasslands	
585,20	144,63	4	11	11	15	0,7	0,7	High aridity P<C	Low tree density, Open grasslands	
591,16	145,11	0	0	5	0	∞	∞	not significant, No grasses	Not significant	
612,84	146,87	10	5	36	15	0,3	2,4	Low aridity, P>C	Moderate density, wooded grasslands	
618,57	147,35	3	7	29	10	0,7	2,9	High aridity P<C	Moderate density, wooded grasslands	
624,51	147,83	0	2	7	2	1,0	3,5	High aridity P<C	Moderate density, wooded grasslands	
630,23	148,31	0	1	101	1	1,0	101,0	High aridity P<C	High tree density, woodlands	
636,64	148,8	1	1	24	2	0,5	12,0	Medium aridity, P=C	High tree density, woodlands	
644,03	149,28	0	0	50	0	∞	∞	not significant, No grasses	High tree density, woodlands	
657,86	149,73	0	0	205	0	∞	∞	not significant, No grasses	High tree density, woodlands	
713,13	151,27	1	1	17	2	0,5	8,5	Medium aridity, P=C	Moderate density, wooded grasslands	
726,86	151,66	0	21	42	21	1,0	2,0	High aridity P<C	Moderate density, wooded grasslands	
755,50	152,43	0	0	54	0	∞	∞	not significant, No grasses	High tree density, woodlands	
758,50	152,78	0	0	21	0	∞	∞	not significant, No grasses	High tree density, woodlands	

Key

	Low aridity P<C		High tree density, woodlands
	Medium aridity, P=C		Moderate density, wooded grasslands
	High aridity, P>C		Low tree density, Open grasslands
	not significant, No grasses		Not significant

6.3.3. Dynamism in both Iph and D/P indices

Indices for all samples were plotted as a line graph (Figure 28) to visualize what phytolith assemblages can inform in terms of change frequency. The graph shows two major phases; rapid phase; the lower and top party of the core, where both indices fluctuates between the two extreme values more often (as shown by arrows in the figure 28) than the mid part of the core, where indices seem to have shifts that are more moderate.

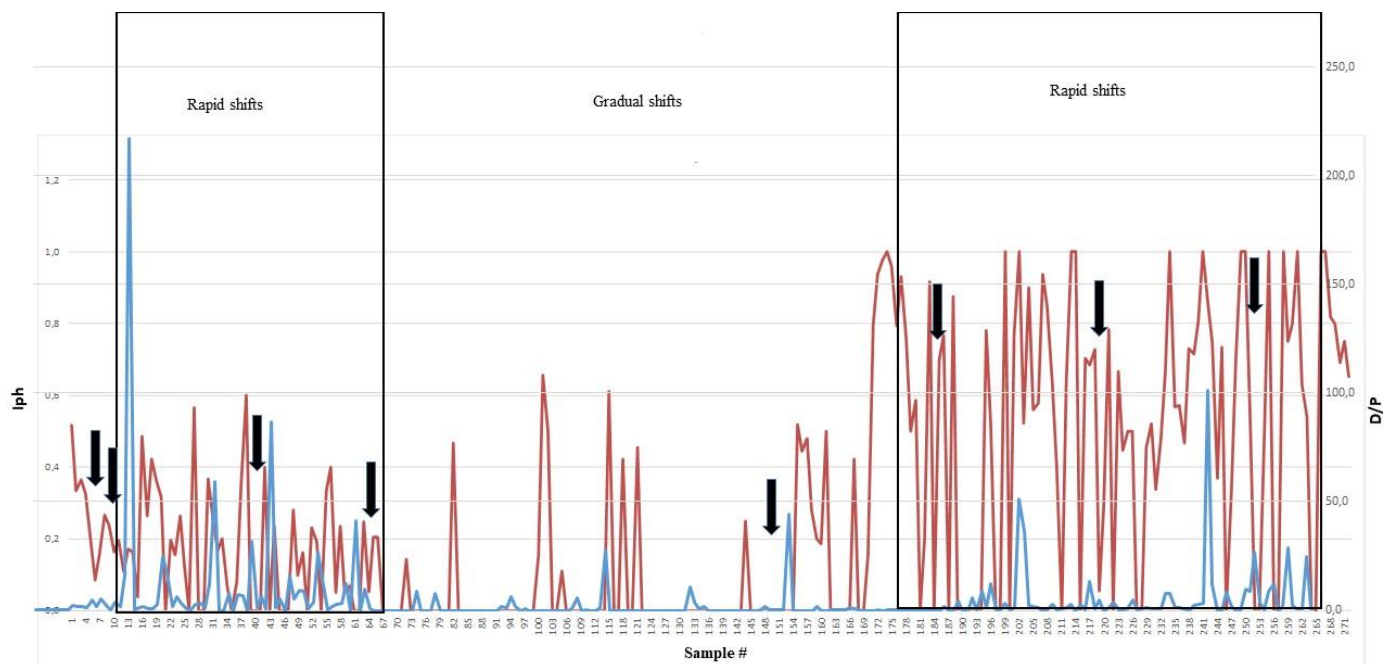


Figure 28. A graph showing rapid and gradual shifts in aridity (Iph, in red) and tree cover density (D/P, in blue) indices of the ODP core. The arrows shows the levels with wide range of vertical change.

5.3.2. ODP Phytolith assemblages, $\delta^{18}O$ and eccentricity

ODP core provided a great opportunity to analyse phytolith assemblages in order to identify abrupt environmental changes and test how this relates to the known climatic shifts.

Three analyses were run on the phytolith data: (1) correspondence analysis (CA) on raw abundances, (2) principal coordinates analysis (PCoA) on a similarity matrix obtained using chord distance (a measure of dissimilarity for abundance data), and (3) Bayesian change point analysis (CPA) on the first coordinate of the PCoA. Any sample with less than five identified specimens was excluded. For the CA and PCoA, the first three axes/coordinates that describe the majority of the variance through the sequence were recorded; these values summarize the major changes in taxonomic composition across the sequence.

CPA is used to identify abrupt shifts in the mean value of a time series. This was conducted only on the first coordinate of the PCoA. The relevant output is the *Probability of a Change*, which ranges between 0 and 1, with higher values indicating that an abrupt shift has likely occurred as shown in figure 29 (Data presented on a table in appendix IV).

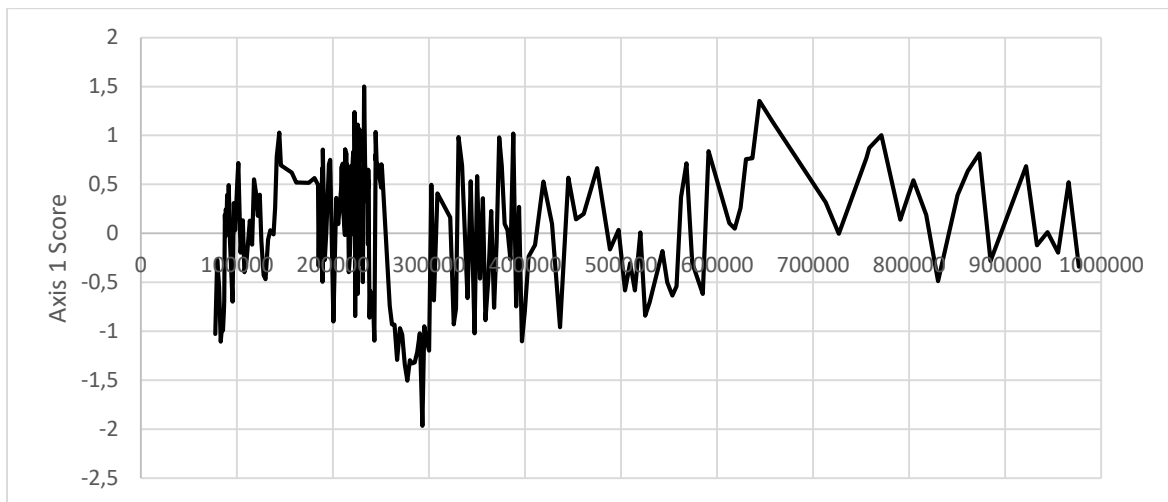


Figure 29. Showing woody cover (positive values) versus grasses (negative values). Phytolith data indicate more persistent woody signature at the top of the core and grassland expansion ~275kyr to 300kyr (at ~110m, depth).

CHAPTER SEVEN: KOOBI FORA PHYTOLITH ASSEMBLAGES

7.1. Introduction

This chapter present phytolith data extracted and processed from modern soil samples collected from different vegetation habitats and fossil phytolith data analysed from Early Pleistocene and Holocene sediments of the Koobi Fora basin.

Although this was not mentioned in the previous chapter on the Olorgesailie basin, the results of phytolith assemblages analysed from the modern soil samples are reliable in interpreting the vegetation habitats they were collected from and therefore are reliable modern analogous for classifying paleo-habitats for the fossil assemblage, for both the Olorgesailie and Koobi Fora basins.

7.2. Phytolith Assemblages: Site-based results

Results of phytolith analyses from different sites/ time periods varied remarkably and due to lack of temporal continuity, phytolith data for each temporal period is presented separately. The most prominent key morphotypes identified and used to indicate various vegetation types included: 1). grasses-bilobates, rondels, saddles, crosses, bulliforms and towers, 2). woody dicots-tracheids, schlereids, globular granulate, globular echinate, 3) Palms-globular echinate-palm type, 4). Sedges-papillae, achene and 5). Herbaceous-other non-diagnostic morphotypes listed in appendix IV. In addition, fossil pollen, diatoms and sponges identified in the sediments are also considered as part of results to identify terrestrials and aquatic habitats.

Phytolith data is presented as tibia diagrams which shows occurrence frequency of the identified morphotypes between samples. Morphotypes identified to indicate similar plant communities are grouped together to identify various vegetation types. For comparison purposes, four broad phytolith-identified taxa/habitats are considered: grasslands, woodlands, woody & herbaceous dicots and wetlands. Later in the section, changes in abundance/presence of key morphotypes through time are described as visualised in the composite abundance Tilia generated diagram. Absolute count data is shown in appendix IV.

7.2.1. Early-Pleistocene assemblages

Phytolith assemblages from twelve Early Pleistocene and Pleistocene paleosols with estimated dates between 1.525 and 1.51Ma consist of similar morphotype compositions except for three samples. Woodland indicators are the most prominent followed by GSSCs and lastly by other woody and herbaceous morphotypes. Sedges and wetlands indicators are rare.

Out of 12 samples, six samples have similar phytolith assemblages with substantial representation of three major phytoliths categories i.e. FI, GSSCs and other non-diagnostic woody & herbaceous

morphotypes. These samples are not significantly different except for the following that are highlighted for their distinctive unique phytolith composition (figure 31):

- 1) 14A-8A-GS-2-RK-1 & 14A-8A-GS-5-RK-4- These two samples were collected from area 8A. The two sample are distinctively different in terms of the phytolith assemblages. The former consists of 80% GSSCs and 20% other non-diagnostic phytoliths that identify woody & herbaceous taxa. Forest indicators (FI) such as schelreids, tracheids, globular granulate and globular morphotypes are completely absent in the sample, making this sample unique for lacking FI morphotypes. The latter is dominated with FI at 53.1% and non-diagnostic woody & herbaceous morphotypes; 43.8% with a notable rarity in GSSCs at 3.1% only.
- 2) AV-ET-11-1-RK-18-This sample was collected from area 1A. It consists of 60% forest indicator-morphotypes, 30% other non-diagnostic woody & herbaceous morphotypes and 10% sedges. This sample is distinctly lacking GSSCs morphotypes.
- 3) AV-ET-11-1RK-19-This sample was collected from area 1A. It consists of 15.6% GSSCs, 68.8% forest indicators morphotypes and 12.5% wetland/aquatic indicators such as papillae, diatoms and sponges indicating sedges, lichens and sponges respectively.
- 4) 1A-Du-ET-11-02-RK11 & AV-ET-11-1-RK-17-These samples were collected from area 1A and are dominated with FI morphotypes $\geq 80\%$ with $<15\%$ GSSCs.



Figure 30. Percentage diagram of major habitats identified by phytolith assemblages in site FxJj-14E, Area 1A (the top ten samples) and Area 8A (the bottom two samples)- Early-Pleistocene paleosols.

7.2.2. Early Holocene assemblages

Six samples collected from FxJj108 (dated between ~9.6kyr and ~6kyr) consist of distinct phytolith compositions, differing remarkably from other sites studied. Morphotypes indicating riparian/gallery forests and aquatic habitats are notably present in all the samples analysed. Woodland morphotypes and GSSCs (especially Panicoideae indicators) are prominently present throughout the profile (figure 32).

FI indicators contribute the highest percentages: 82.2% in RK-1, 56.8% in RK-2, 51.6% in RK-3, 43.2% in RK-4, 61.2% in RK-5 and 62.6% in RK-6. GSSCs morphotypes in contrast were present in all samples with 10.3% in RK-1, 10.3% in RK-2, 32.4% in RK-3, 17.9% in RK-4, 21.4% in RK-5 and 17.6% in RK-6. Non-diagnostic woody and herbaceous morphotypes are uncommon in the samples, with the highest occurrence of 16% in RK-2. Palm-globular-echinate morphotypes are rare but significantly present with 5.3%, 1.8% and 1% in RK-5, RK-3 and RK-4 respectively. Similarly sedge (achene) morphotypes are rare but significantly present in all the samples. They are most prominent in RK-1 with 8.6% and in RK-4 with 6.3%. Other aquatic indicators (sedges, diatoms and sponge spicules) occur significantly present in all samples, especially in RK-4 at 25.3%, in RK-6 at 8.4%, and >2.5% in the rest of the samples.

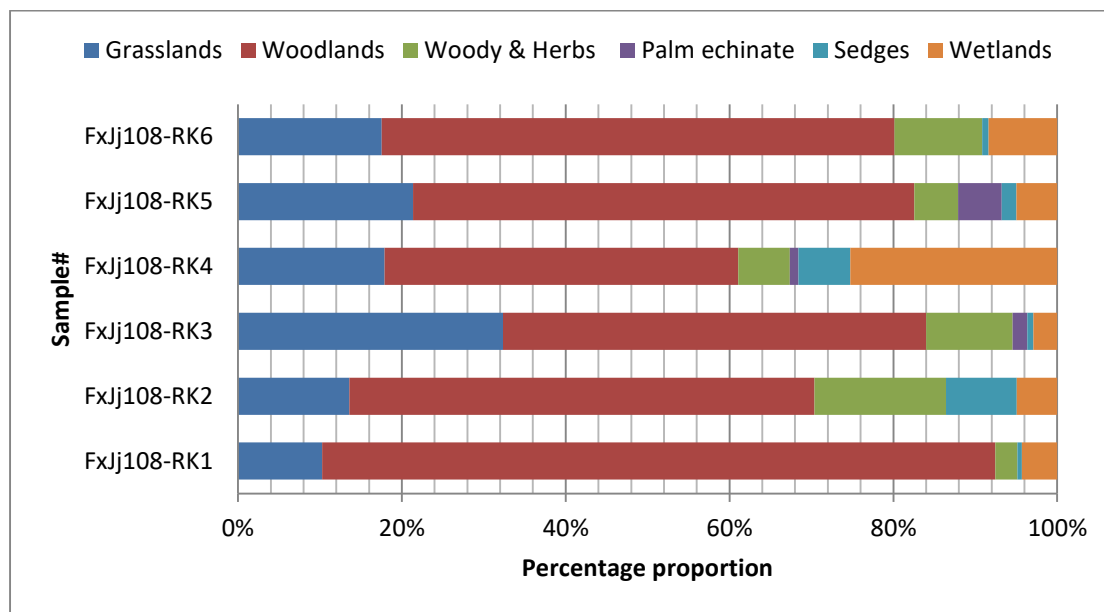


Figure 31. Percentage diagram of major habitats identified by phytolith assemblages in site FxJj108, an early Holocene site.

7.2.3. Early-mid-Holocene phytolith assemblages

FxJj27 site is dated between ~9.3kyr and ~4.2kyr with archaeological evidence suggesting transition from fisher-gatherers to Pastoral-Neolithic economic occupations (Ndiema, 2011). The most dominant morphotypes are FI t (figure 33): 37.8% in RK-1, 90.6% in RK-2 and 80.2% in RK-3. GSSCs account for 28.9% in RK-1, 4.4% in RK-1, 4.4% in RK-2 and 15.3% in RK-3. Other non-diagnostic woody and

herbaceous morphotypes account for 33.3% in RK-1, 4.4% in RK-2 and 3.6% in RK-3. Aquatic morphotypes including diatoms and sponges are the rarest, with <1% in samples RK-2 and RK-3.

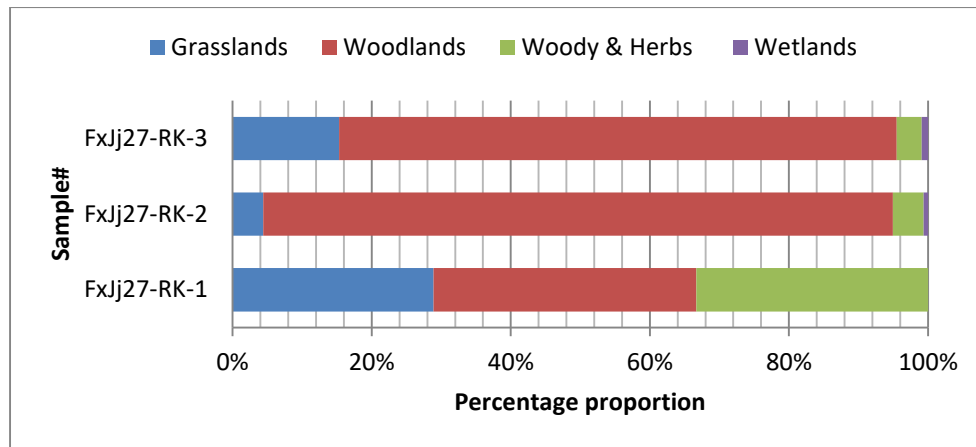


Figure 32. Percentage diagram of major habitats identified by phytolith assemblages in site FxJj27, an early-mid-Holocene transition site.

7.2.4 Mid-late-Holocene phytolith assemblages

These are from three archaeological sites dated between ~4.2kyr and ~0.93kyr. Phytolith assemblages across samples are predominantly woodlands indicators (globular granulate, tracheids and sclereids) with >60% occurrence. Wetland indicators (papillae, diatoms and sponge spicules) are the rarest across the sites, occurring in only one sample and one site (see figure 34).

In site GaJj4 (~4.2kyr- ~3.9kyr), forest indicator morphotypes dominate with percentages of 77.7% in RK-1, 70.2% in RK-2, 63.6% in RK-4 and lastly 62% in RK-3. GSSCs are less common with percentages of 23.8% in RK-2, 14.8% in RK-3, 8.3% in RK-4 and lastly 7.4% in RK-1. Other non-diagnostic woody and herbaceous dicots are uncommon with percentages of 28.2% in RK-4, 23.1% in RK-3, 15.3% in RK-1 and 2.4% in RK-2. Papillae and other aquatics such as diatoms and sponges types occur only in RK-2 at 3.6%.

In site FwJj25 (~4.2kyr- ~1.34kyr), GSSCs morphotypes are predominantly present with percentages of 75% in RK-3, then 31.3% in RK-1 and lastly 15.6% in RK-2. Woody morphotypes dominate in RK-2 at 67.2%, then 62.5% in RK-1 and lastly 12.5% in RK-3. Other non-diagnostic woody and herbaceous morphotypes have a lower presence as follows: 17.2% in RK-2, 12.5% in RK-3 and 6.3% in RK-1

In site FwJj5 (~0.93kyr), GSSCs are variably common in all the samples: 100% in RK-2, followed by 60.7% in RK-3 and 31.8% in RK-1. Forest indicator phytoliths are significantly present with 54.5% in RK-1 and 39.3% in RK-3. Aquatic indicators are only present in RK-1 with a percentage of 13.6%.

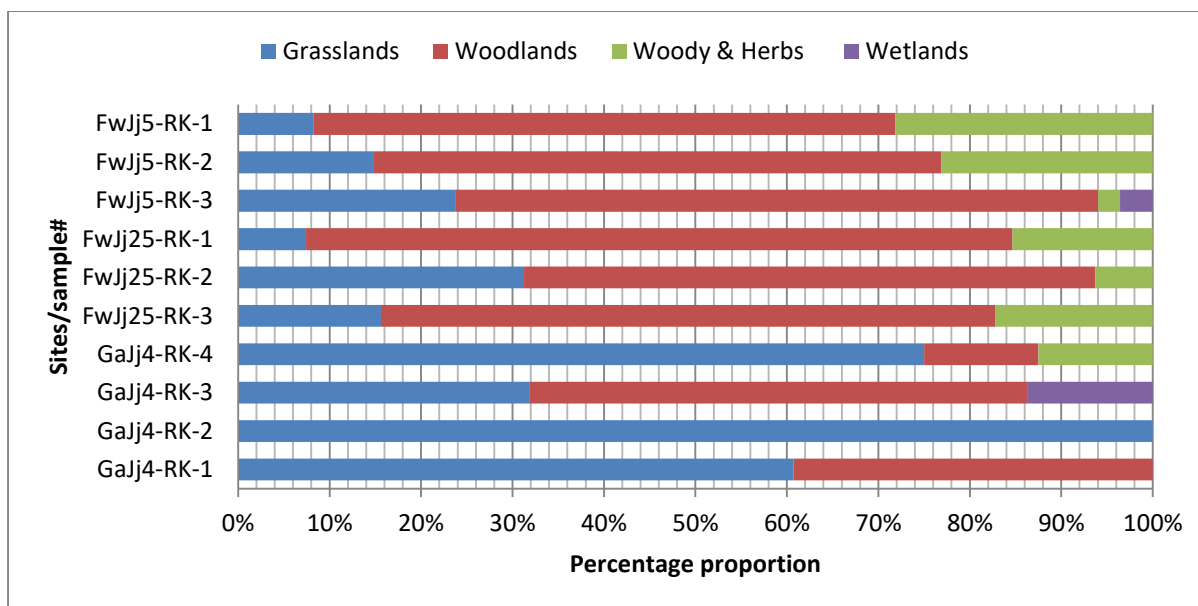


Figure 33. Percentage diagram of major habitats identified by phytolith assemblages in mid-late-Holocene sites.

7.2.5. Modern phytolith surface samples

Results of the four modern surface samples have varied percentage composition of each key taxa (Figure 35). As expected, GSSCs dominate in the open grassland (sample-SS4) with 69.2%, followed by 32.7% occurrence in *Barleria sp.* scrubland (sample-SS3), then 11% occurrence in the *Acacia-Syzygium-Sanseveria* riverine forest and least at 2% in *Acacia-Commiphora* shrubland (SS1). The woody morphotypes dominate with 94.3% in the gallery forest (sample SS2), followed by 80% in the *Acacia-Commiphora* shrubland (SS1), then 53.8% in *Barleria sp.* (SS3) scrubland and lastly by 11.1% occurrence in the open grasslands (SS4). Other woody & herbaceous dicots occur sparingly in all samples: 19.7% in open grasslands (SS4), 9.6% in *Barleria sp.* scrubland (SS3), 5.7% in *Acacia-Commiphora* shrubland (SS1) and lastly, 3.7% in gallery forest (SS2).

The results of the phytolith assemblage composition for each sample accurately corresponds to the habitats, from which they were collected, hence are applicable as modern analogues for the fossil assemblages in this study. This concurs with other published studies (for example, Neumann et al., 2009). These results are consistent with previous studies on modern soils in Africa (Runge 1999, Bremond et al., 2005, 2005, 2008; Barboni et al., 2007, Mercader et al., 2011, Aleman et al., 2012, 2014, Novello et al., 2012, 2016, 2017).

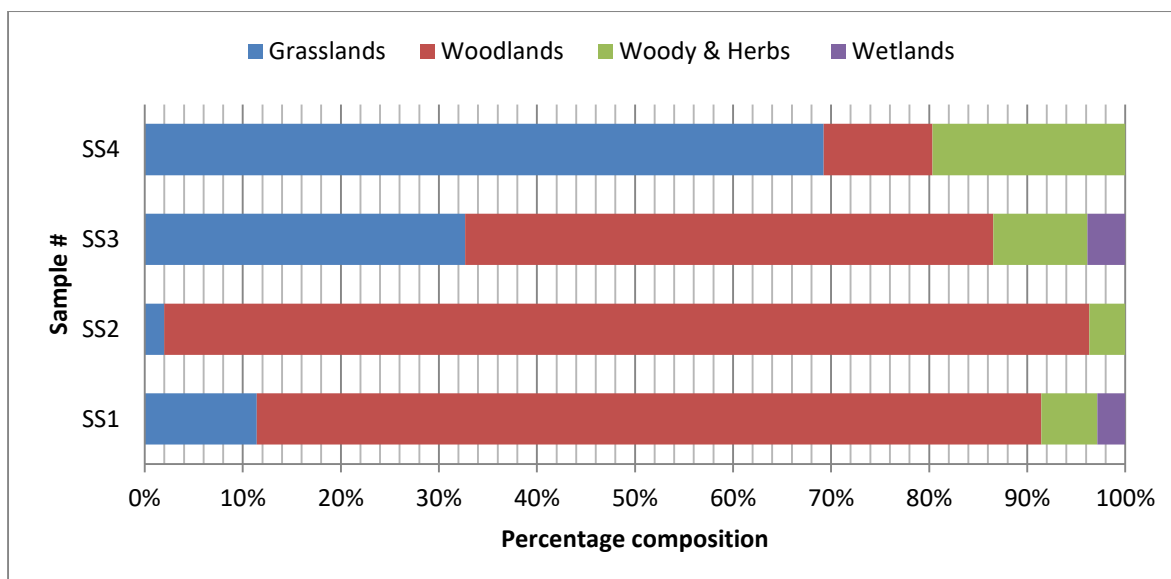


Figure 34. Percentage diagram of major habitats identified by phytolith assemblages in modern surface samples.

7.3. Temporal changes in phytolith assemblage of the Koobi Fora sequence

This section describes phytolith assemblages identified from Early Pleistocene sediments of the Koobi Fora Formation and the Holocene Galana Boi deposits presented in the Tilia diagram. Zonation of the abundance diagram follows the chronology of the samples (Figure 36).

7.3.1. Early Pleistocene

This zone present phytolith assemblages of paleosols associated with Ileret tuff complex. The assemblage is dominated with woody morphotypes with significance presence of non-diagnostic woody and herbaceous morphotypes. GSSCs morphotypes become prominently present though in low abundance <20% in samples below 1.52Ma, particularly saddles (Chloridoideae). Assemblages from samples between 1.53Ma and 1.52Ma do not vary too, both in abundance and in diversity.

Samples below 1.51Ma, consisted of woody morphotypes, non-diagnostic woody and herbaceous morphotypes and significant presence of Panicoidae (Panicoid bilobates, crosses, polylobate) morphotypes >30%.

7.3.2. Early Holocene

Woody morphotypes are the most common with >60% presence. Diagnostic GSSCs morphotypes indicating Chloridoideae and Panicoidae grass are sparingly present <10%. However, non-diagnostic GSSCs morphotypes and much more >20%. Other non-diagnostic woody and herbaceous morphotypes are low. The samples are distinctively characterised by the presence of wetland and/or riverine indicators such as: Palms, sedges, sponge spicules and diatoms. Panicoid bilobates, crosses & polylobate morphotypes s are also prominent in the samples.

7.3.3. Early-Mid transition

Woody morphotypes remain common during the transition from the early- to mid-Holocene period. Wetland indicators are completely absent while GSSCs morphotypes especially saddles, bilobates and crosses (Chloridoideae and Panicoideae) rare but present <5%. Other non-diagnostic GSSCs, woody and herbaceous morphotypes are significantly present.

7.3.4. Mid-Holocene

The oldest sample from mid-Holocene sediments consists mainly of non-diagnostic GSSCs morphotypes, sedge-type and well preserved pollen grains of the following taxa: *Hyphaene*, Acanthaceae, Capparaceae, and Agavaceae; contrasting strongly with other samples preceding and after this deposition level (NB: The occurrence of pollen grains in this level during microscopic analysis was not ignored and I decided to have it included in the analyses). Notably, samples within the ~4.2kyr period are dominated by forest indicators, with an admixture of morphotypes from other non-diagnostic woody & herbaceous and Panicoideae morphotypes.

7.3.5. Late Holocene

Between ~1.34kyr and ~0.93kyr the conspicuous feature in this zone is the high abundance of Chloridoideae morphotypes (saddles). Woody, non-diagnostic woody, herbaceous and GSSCs morphotypes are also sparingly present, declining towards 0.93kyr. Diatoms and *Typha* are also present in this zone.

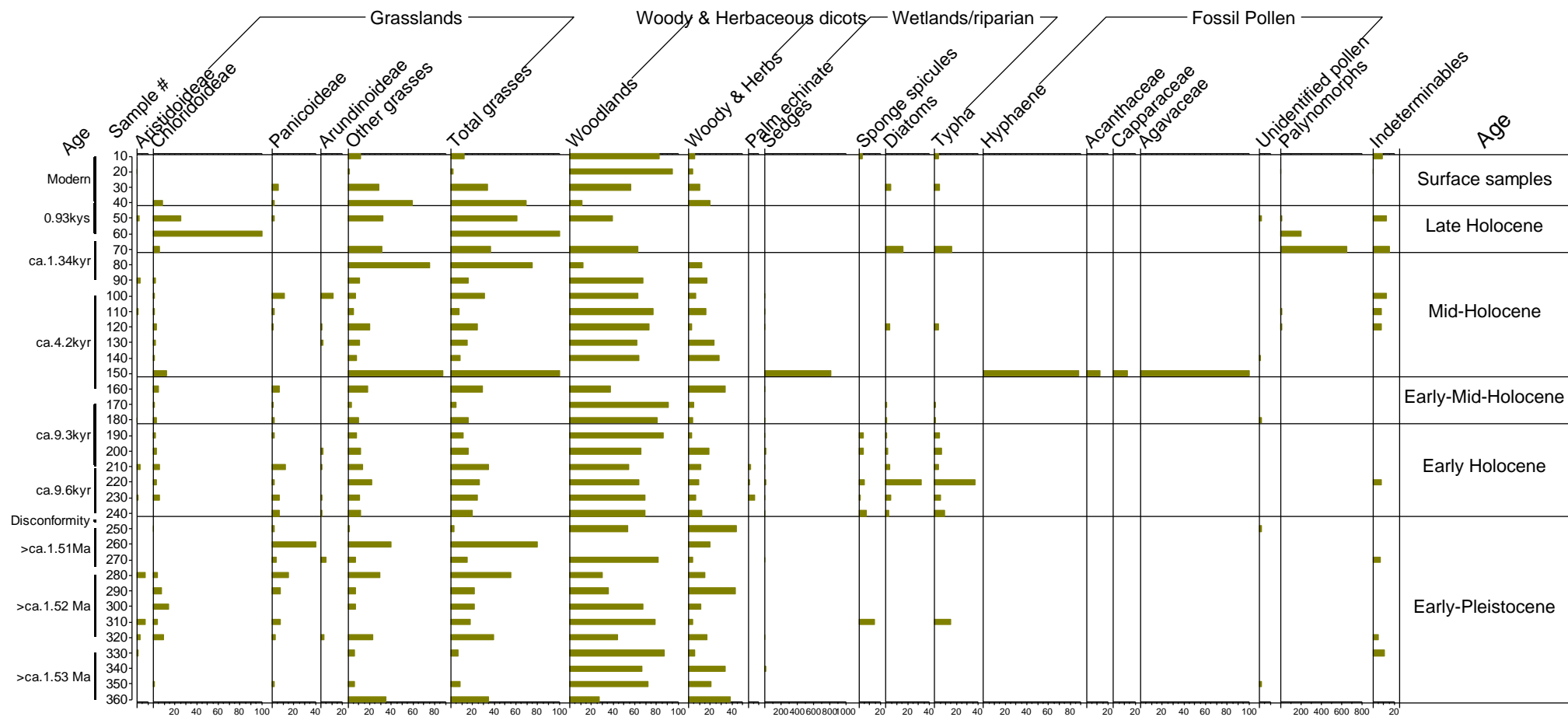


Figure 35. Relative abundance of key phytolith types, main vegetation habitats versus sample # and estimated age (right) of the Koobi Fora samples

7.4 Phytolith Indices-KOOBI FORA

In general, Koobi Fora samples have very low GSSCs morphotype concentrations and the absolute counts as seen in Table 12. Nevertheless, the available data was used to calculate aridity (I_{ph}) and tree-cover-density (D:P) indices to estimate changes in moisture and tree cover temporally. Although the indices alone are not fully reliable to accurately reconstruct paleo-vegetation and palaeoenvironmental changes, when coupled with general abundance analyses, a better understanding of changes in habitats and paleoenvironments can be achieved especially on a broader scale (Stromberg, 2002; Barboni et al., 2007; Bremond et al., 2008; Neumann et al., 2009).

7.4.1. The D:P index

The range of D:P values varied between 0 and 85. The values are used to describe relative closeness of the habitats and are categorised as follows: D:P value ≤ 1 -low tree-cover-density, D:P ≤ 10 moderate tree-cover-density and D:P ≥ 20 high tree-cover-density (see table 12). These categories are only used to describe temporal changes in palaeo-habitats of the Koobi Fora landscapes.

7.4.1.1. Early-Pleistocene samples

The D:P of the Early Pleistocene samples below lower Ileret tuff (1.525Ma) have infinite D:P value except for sample 14A-8A-GS-2-RK-1 with D:P value=9.7. One of the samples above the 1.52Ma tuff have infinite D:P value while the other two have 0.7 and 2.3 respectively.

Area 1A samples collected below 1.52Ma have D:P value ranging between 0.0 and 20.5, while the sample above it has a value of 21.6.

7.4.1.2. Holocene samples

Early Holocene samples (FxJj108) have a D:P value ranging between 0.1 and 1.5. Samples from FxJj27, a site representing a transition from early to mid-Holocene period have D:P values ranging between 2.0 and 2.5. Mid-Holocene samples (GaJj4) have the largest D:P value range between 2.7 and 85.0. There is one exception with D:P value of 0.0. Lastly, the late-Holocene samples (FwJj5), have D:P values ranging between 0 and 0.2.

7.4.1.3. Modern samples

The D:P values of the modern surface samples varied between samples as expected. Samples SS1 and SS2 collected from *Acacia-Commiphora* and gallery forest respectively have an infinite D:P value. Sample SS3 collected from *Barleria sp* scrublands has D:P value of 6.7, while sample SS4 collected from open grassland habitat has a D:P value of 0.

7.4.2. Iph index

The proportion of the diagnostic GSSCs morphotypes allowed the calculation of the aridity index in most of the fossil assemblages (Table 12). However, some samples did not yield diagnostic Chloridoideae and Panicoideae morphotypes leading to an infinite Iph value which is considered here insignificant in terms of reflecting aridity conditions. Those samples that yielded diagnostic morphotypes have aridity values range between 0 and 1; with 0.1 reflecting low aridity while 1 reflects high aridity.

7.4.2.1. Early-Pleistocene samples

Samples from the Early-Pleistocene period have variable Iph values ranging between 0.2 and 1. Most of the samples have aridity value less than 0.5. Samples below 1.525Ma have infinite Iph value except for sample 14A-8A-GS-2-RK1 with Iph value of 0.3. While the three samples above this tuff have Iph values drop from infinite to 0.3. The decreasing trend continues in samples below 1.52 Ma where Iph value decrease from 1.0 to 0.0 and then to ∞ . The sample above 1.52Ma have Iph value of 0.2.

7.4.2.2. Holocene samples

Early Holocene samples (FxJj108) have variable Iph values ranging between 0 and 1. Most samples have an Iph value lower than 0.5. Of significant are samples FxJj108-3 and FxJj108-5 have Iph values of 0.7 and 1 respectively.

Early-mid-Holocene samples (FxJj27) have Iph values decreasing gradually from 0.6 to 0.4.

Mid-Holocene samples (GaJj4) have Iph values ranging between 0.3 and 1. The oldest sample has the lowest Iph value of 0.3 which increased through 0.7 to 1.0. In site FwJj25, the aridity value increases sharply from 0.1 to 1, then drops to zero. Late Holocene samples (FwJj5) have Iph values ranging between 0.9 and 1.

7.4.2.3. Modern samples

Samples SS1 and SS2 collected from Acacia-Commiphora and riparian habitats have ∞ Iph value while samples SS3 and SS4 collected from Barleria scrubland and open grasslands have Iph values of 0.8 and 0.0 respectively.

Table 12. *Iph* and *D:P* indices of the phytolith assemblages of the Koobi Fora samples. Shading is according to different sites. NB: The two indices do not correlate

Sample#	Age	Chloridoideae	Panicoidae	Globular granulate	Grasslands	<i>Iph</i>	<i>D:P</i>	Interpretation	<i>Iph</i>	<i>D:P</i>
SS1	Acacia-Commiphora shrublands	0	0	16	0	∞	∞	Not significant high tree density, foresst/woodlands		
SS2	Gallery/riparian forest	0	0	270	0	∞	∞	Not significant high tree density, foresst/woodlands		
SS3	Barleria scrubland	0	3	20	3	0	6,7	Not significant moderate tree density, wooded grasslands		
SS4	Open grasslands	10	2	0	12	0,8	0,0	High aridity, P<C low tree density, open grasslands		
FwJj5-RK-3	~0.93kyr	14	1	3	15	0,9	0,2	High aridity, P<C low tree density, open grasslands		
FwJj5-RK-2	~0.93kyr	1	0	0	1	1,0	0,0	High aridity, P<C low tree density, open grasslands		
FwJj5-RK-1	~0.93kyr	1	0	0	1	1,0	0,0	High aridity, P<C low tree density, open grasslands		
FwJj25-RK-3	~4.2-1.34kyr	0	0	0	0	0,0	0,0	Not significant low tree density, open grasslands		
FwJj25-RK-2	~4.2-1.34kyr	1	0	25	1	1,0	25,0	High aridity, P<C high tree density, foresst/woodlands		
FwJj25-RK-1	~4.2-1.34kyr	1	11	55	12	0,1	4,6	Low aridity, P>C moderate tree density, wooded grasslands		
GaJj4-RK-5	~4.2kyr	1	0	0	1	1,0	0,0	High aridity, P<C low tree density, open grasslands		
GaJj4-RK-4	~4.2kyr	1	0	85	1	1,0	85,0	High aridity, P<C high tree density, foresst/woodlands		
GaJj4-RK-3	~4.2kyr	5	0	137	5	1,0	27,4	High aridity, P<C high tree density, foresst/woodlands		
GaJj4-RK-2	~4.2kyr	2	1	8	3	0,7	2,7	High aridity, P<C moderate tree density, wooded grasslands		
GaJj4-RK-1	~4.2kyr	1	3	29	4	0,3	7,3	Low aridity, P>C moderate tree density, wooded grasslands		
FxJj27-RK-3	~9.3-4.2kyr	4	6	25	10	0,4	2,5	Low aridity, P>C moderate tree density, wooded grasslands		
FxJj27-RK-2	~9.3-4.2kyr	1	1	4	2	0,5	2,0	Medium aridity, P=C moderate tree density, wooded grasslands		
FxJj27-RK-1	~9.3-4.2kyr	7	4	28	11	0,6	2,5	High aridity, P<C moderate tree density, wooded grasslands		
FxJj108-6	~9.6 -6kyr	3	3	7	6	0,5	1,2	Medium aridity, P=C moderate tree density, wooded grasslands		
FxJj108-5	~9.6 -6kyr	2	0	3	2	1,0	1,5	High aridity, P<C moderate tree density, wooded grasslands		
FxJj108-4	~9.6 -6kyr	14	31	12	45	0,3	0,3	Low aridity, P>C low tree density, open grasslands		
FxJj108-3	~9.6 -6kyr	2	1	3	3	0,7	1,0	High aridity, P<C low tree density, open grasslands		
FxJj108-2	~9.6 -6kyr	13	16	2	29	0,4	0,1	Low aridity, P>C low tree density, open grasslands		
FxJj108-1	~9.6 -6kyr	0	8	5	8	∞	0,6	Low aridity, P>C low tree density, open grasslands		

Sample#	Age	Chloridoideae	Panicoidae	Globular granulate	Grasslands	I:ph	D:P	Interpretation	I:ph	D:P
1A-Du-ET-11-02-RK-15	Younger than 1.52Ma	1	4	108	5	0,2	21,6	Low aridity, P<C high tree density, woodlands/forest	Dark Green	Light Green
1A-Du-ET-11-02-RK-21	Older than 1.52Ma	0	2	0	2	∞	0,0	Not significant low tree density, open grasslands	Grey	Yellow
AV-ET-11-1-RK-18	Older than 1.52Ma	0	2	41	2	0,0	20,5	Low aridity high tree density, woodlands/forest	Dark Green	Light Green
AV-ET-11-1-RK-17	Older than 1.52Ma	1	4	2	5	0,2	0,4	Low aridity, P>C low tree density, open grasslands	Dark Green	Yellow
AV-ET-11-1-RK-20	Older than 1.52Ma	1	1	0	2	0,5	0,0	Medium aridity P=C low tree density, open grasslands	Light Green	Yellow
AV-ET-11-1-RK-19	Older than 1.52Ma	4	0	5	4	1,0	1,3	High aridity, P<C moderate tree density, wooded grasslands	Orange	Light Green
AV-ET-11-1-RK-14	Younger than 1.525Ma	1	2	7	3	0,3	2,3	Low aridity, P>C moderate tree density, wooded grasslands	Dark Green	Light Green
1A-Du-ET-11-02-RK-13	Younger than 1.525Ma	8	2	7	10	0,8	0,7	High aridity, P<C low tree density, open grasslands	Orange	Light Green
1A-Du-ET-11-02-RK-12	Younger than 1.525Ma	0	0	46	0	∞	∞	Not significant high tree density, woodlands/forest	Grey	Dark Green
1A-Du-ET-11-02-RK-11	Older than 1.525Ma	0	0	5	0	∞	∞	Not significant high tree density, woodlands/forest	Grey	Dark Green
14A-8A-GS-2-RK-1	Older than 1.525Ma	1	2	29	3	0,3	9,7	Low aridity, P>C moderate tree density, wooded grasslands	Dark Green	Light Green
14A-8A-GS-5-RK-4	Older than 1.525Ma	0	0	3	0	∞	∞	Not significant high tree density, woodlands/forest	Grey	Dark Green

Legend.

Dark Green	Low aridity P<C	Light Green	High tree density, woodlands
Light Green	Medium aridity, P=C	Light Green	Moderate density, wooded grasslands
Orange	High aridity, P>C	Yellow	Low tree density, Open grasslands
Grey	not significant, No grasses	Grey	Not significant

7.4.3. Dynamism in both I:ph and D:P indices

I:ph and D:P indices were plotted to visualize the aridity and tree-cover-density changes from one geological time period to another in Figure 37. Aridity index fluctuates more rapidly between samples than D:P index. D:P index on the other hand is gradual with only one significant rise during the mid-Holocene.

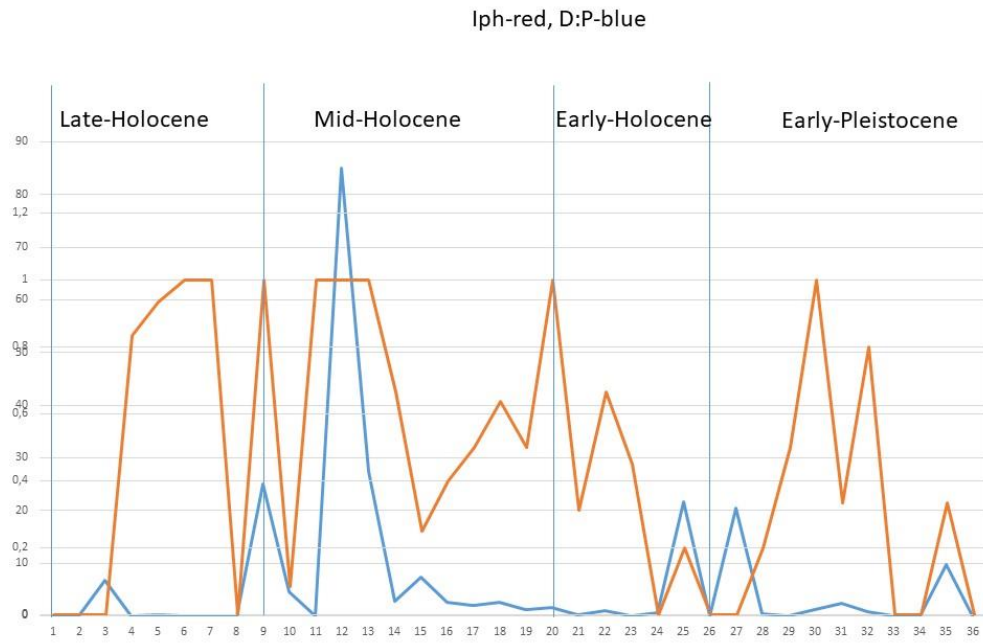


Figure 36. Shows a graph of both Iph and D:P indices and their variation between Early-Pleistocene to late-Holocene samples.

Part III: Interpretation and Discussion

In this section, the phytolith data from both the Ologesailie and Koobi Fora basins is interpreted and thereafter discussed. Chapter SEVEN reports on the interpretation of the phytolith assemblage of the ODP core, Ologesailie basin. Significance of the results is also discussed. Chapter EIGHT presents interpretation of the Koobi Fora phytolith assemblage from each site. The significance of the results is discussed later in the chapter. Chapter NINE, discusses the significance of these results in the context of East African paleoclimatic and paleoenvironmental context.

CHAPTER EIGHT: VEGETATION HISTORY AND ENVIRONMENTAL CHANGES IN THE OLOGESAILIE BASIN AND THE SURROUNDING ENVIRONS.

8.1. INTEPRETATION

The following section interprets the phytolith assemblage results and discusses the significance of the vegetation structure and environmental conditions reconstructed during Pleistocene period of the Ologesailie basin.

8.1.1. Understanding the last 1Ma of vegetation structure using the general approach

Vegetation composition of the Ologesailie basin, identified by key indicator morphotypes are summarised as a Tilia abundance diagram in figure 26. CONNISS cluster identified similar zonation pattern for both individual morphotype and the identified taxa diagrams. NO DATA levels possibly non-deposition phases (hiatus) are distinct and they coincide with the zonation boundaries (Figures 26 & 27).

Owing to the detailed outcrop research findings and the unfortunate lack of deposit continuity both temporally and spatially, the ODP team led by Potts, planned and executed the drilling of a long continuous sediment core that is close enough to be correlated with data acquired from the Ologesailie Formation. This is hoped to capture a missing gap due to a major deposition unconformity in the past ~500kyr and also will be ideal to correlate the acquired data with the existing outcrop findings.

Two distinct sections are identified based on the abundance and diversity of phytoliths in the samples analysed. Samples collected in the lower part of the core, dated between 975kyr and 675kyr have low phytolith percentages and occur in fewer samples contrasting the upper part (675-77kyr) of the core

where higher phytolith abundance and diversity is observed in most of the samples analysed. Grasses in particular are rare to absent in most of the samples in the lower part of the core, figure 25.

Woody and herbaceous dicotyledons are the most prominent vegetation feature throughout the sequence, but are more stable after 675kyr than in earlier periods. Mixed grasslands also appear to be a common feature in the upper part of the core. Zooming in to particular phytolith- stratigraphy, it is noted that assemblages fluctuated between samples as follows:

The phytolith assemblage of ODP Ia (~ 975-900kyr) indicates mixed C₃ and C₄ vegetation structure that resembles today's savanna woodlands. The presence of palm phytoliths indicates presence of freshwater environments on the landscape during the same period (Albert et al., 2009; Ashley et al., 2010).

Since the phytolith data here have a mixture of both local (terrestrial) and regional (lacustrine) input, it therefore suggests that wooded grasslands and open grasslands were widespread across the landscape. The grass component included both tall (Panicoideae) and short (Chloridoideae and Aristidoideae) sub-families. Fossil and archaeological data that coincide with this period include *Homo erectus* cranial remains associated with a high concentration of Acheulean hand-axes and other mammalian remains (Potts et al., 2004). The significance of the above mentioned heterogeneous vegetation structure is that it indicates variable food resources, diverse habitats that would have reduced the competition among herbivores and hominins and availability of fresh water resources.

After an erosional phase identified after ~900kyr (ODP Ib), vegetation becomes increasingly wooded, particularly palms and subtle presence of sedges indicating continued presence gallery forests (Albert et al., 2009; Neumann et al., 2009), while grasslands become rare up to ~670kyr.

Another unconformity is recorded around 700kyr; the vegetation structure continues to be woody dominated with increased mixed grasslands occurring in most of the levels. This is interrupted by a "NO DATA" phase (~ 600kyr) then more stable wooded grasslands habitats re-appear briefly between ~400kyr and 350kyr. The gaps noted in this sub-zone (ODP IIa) could be a result of brief expanding and receding of the lake margin (Owen et al., 2008). Lithological studies show this phase was predominantly terrestrial, hence phytolith assemblages reflect mostly local vegetation structure.

Phytolith assemblages in the subzone (ODP IIa) show a series of vegetation shifts from open grasslands to open woodlands to wooded grasslands (~670kyr to ~435kyr), with instances of dense woodlands with admixture of other herbaceous dicots and sedges, a significant component of the undergrowth with significant decline to total absence of grasslands (~400kyr to ~325kyr). Generally, the vegetation structure during this period was quite unstable.

Immediately after ~325kyr, a ~25kyr sedimentation break is identified, hence no phytolith data. This is followed by vegetation structure dominated by grasslands which are predominantly Chloridoideae C₄ short grasses while woodlands declined significantly, an indication of savanna grasslands with scattered woody elements (~300kyr to ~250kyr). Interestingly, these environments had fresh water resources possibly springs, as indicated by the presence of palms and sedges around this period.

The scenario changed around 250kyr, with a sudden decrease of grasslands, especially Chloridoideae types while Panicoideae grasses remain significantly present coupled by increase in wooded vegetation structure. Perhaps of significance is a sudden rise of Cyperaceae and reappearance of palms, an indication of increased moisture and/or underground water resources during this period.

The presence of Panicoideae grasses coupled with sedges and palms indicate wetlands/swampy habitats and higher humidity than the preceding period. Sedges and palms were significantly present, though sedges were more prominent indicating swampy habitats as opposed to gallery forests. The vegetation structure persisted up to ~180kyr when grasslands diminished almost completely (ODP IIIa). This signal is mostly regional since the predominant depositional environment is lacustrine (Behrensmeier et al., *in progress*).

One very significant change is the increased grass morphotypes noted between ~300kyr and 250kyr while woody and herbaceous dicotyledons decrease rapidly. Around this period, Chloridoideae grasses are the most prominent feature in the assemblage (zone ODP IIa).

Immediately after ~180kyr, is a "NO DATA" phase. However, similar vegetation structure as indicated in the previous sub-zone continues to persist up to ~77kyr. Generally Chloridoideae grasses are relatively low compared to the Panicoideae grasses but which is not quite consistent between samples. Another significant change is the absence of Cyperaceae during this period, although, palms are still present but rare. This could possibly indicate presence of underground water or it marks the beginning of a drier period, responsible for diminishing wetlands/swampy habitats. Sedges, unlike palms are herbaceous and are likely to diminish almost immediately after the swamps/wetlands diminishes, but palms can persist longer, especially if water table is high.

Stratigraphic analyses show the environmental setting during ~ 250kyr to ~77kyr is predominantly lacustrine (Behrensmeier et al., *in progress*); hence the vegetation reflected here is both local and regional terrestrial signal, including palms and sedges which would be associated with lake-margin settings. Towards ~77kyr, Chloridoideae grasses increased while woodlands and Panicoideae grasses decreased.

8.1.1.1. Summary

Phytolith assemblages analysed from the ODP core identified two main phases of vegetation structure based on the differences in phytolith composition and abundance. The period between ~970kyr and ~300kyr (zones ODP I and II), phytolith abundance was relatively low compared to the period after ~300kyr (zone ODP III). Although the general pattern shows that woody and herbaceous dicots were more prominent than grasslands before ~700kyr, vegetation structure was not quite stable; there are specific periods when grasslands expanded and were dominated by Chloridoideae grasses. On the other hand, the primary lithologies suggest more terrestrial environments punctuated by shorter periods of lacustrine environments, suggesting phytolith assemblages were primarily local representations rather than regional. Geochronology studies have identified at least two unconformities (Behrensmeyer et al., *in progress*), coinciding with the “NO DATA” zone reflected by the phytolith data.

Following primary lithostratigraphic and geochronological data obtained from the ODP core which show a series of depositional environments which include: terrestrial, fluvial, lacustrine and volcanistic environments (Behrensmeyer et al., 2007; Deino et al., *in progress*) and, the phytolith zonation, a general trend of the changes in the vegetation cover has been interpreted the best way possible. The implication of these changes in understanding the palaeoenvironments with which early hominins interacted with and determine the possible driving factors that controlled technological transitions recorded in the Olorgesailie basin can be discussed comfortably.

8.1.2. Application of indices: D:P and Iph

The calculation of the phytolith indices is mainly to determine the climatic parameters affecting the vegetation structure identified by the general assemblages, as well as vegetation composition. However, the use of a few specific morphotypes which could be extremely rare or be overrepresented in different vegetation habitats remain a major limitation in realizing the said objective (Stromberg, 2004; Bremond et al, 2008; Neumann et al., 2009). Such morphotypes include: globular granulate (woody dicots), saddles (Chloridoideae subfamily) and bilobates short cells, crosses & polylobates (Panicoidae subfamily). Nevertheless, when present in the phytolith assemblages, they are valuable tools in determining and estimating important climatic parameters such as aridity-moisture gradient (Iph) and woodlands/grasslands proportions of the identified vegetation structure.

In this study phytolith assemblages indicate high variability in vegetation structure through time showing a general trend of woody and herbaceous dicots dominating most of the palaeolandscapes. Considering phases identified by the assemblages, the D:P index points to shifts between high to moderate tree cover density around ~978kyr to ~658kyr. In contrast the Iph index indicates that Chloridoideae grasses were more prominent than the Panicoidae grasses suggesting events of high

aridity persisted during this period. But around 860kyr, a period of Panicoideae dominated vegetation structure is reflected, suggesting high moisture events occurred.

Between ~645kyr and ~325kyr, tree cover density shifted between moderate to low, suggesting wooded grasslands to open grasslands with an abrupt interruption phase of high tree-cover-density around 630kyr. These changes seem sudden temporally from one level to the other. The aridity index oscillated between medium to high aridity, suggesting Chloridoideae grasses were more dominant.

The most arid period happens between ~264kyr and ~275kyr peaking at ~266kyr. The vegetation cover during this period was mainly open arid grasslands with less or no tree cover. Phytolith assemblages in this period reflect both local and regional vegetation cover as two deposition environments are identified: fresh water shallow lakes and terrestrial (Behrensmeier et al., *in progress*). Another similar brief event with high aridity occurs between ~250kyr and 245kyr, after which vegetation structure changed abruptly to mixed wooded tall grasslands, indicating warm but moister climates.

Around ~100kyr, the climates became humid with denser vegetation cover and riverine forests as indicated by the presence of palms trees. Interestingly, phases of open grasslands, wooded grasslands and dense woodlands do not seem to last for long, they were variable throughout Pleistocene period, suggesting the climates were highly variable.

8.1.2.1. Summary

In summary, the aridity index (Iph), is significant in this study as it discriminated the distribution of tall grasslands (Panicoideae) versus short (Chloridoideae) throughout the core. More so, the aridity-moisture gradient is well reflected and complements the assemblage abundance data. Although the Iph signal is more reliable than the D:P signal, when combined, estimates of climatic parameters, especially moisture gradient, and environmental inference has been made possible.

8.2. DISCUSSION

8.2.1. Significance of vegetation structure and the Palaeoenvironments of the Ologesailie basin

As mentioned in previous chapters, the ODP sediment core has a continuous high resolution $^{40}\text{Ar}/^{39}\text{Ar}$ chronology that gives a new opportunity to acquire a detailed palaeoenvironmental and palaeoclimatic record for the last 1Ma Deino et al, *work in progress*). For more than six decades, there have been numerous studies undertaken in the Ologesailie basin geared to identify the environmental settings that supported early human populations and understand the linkages between climate change /variability and human evolution (Potts, 1994, 1996, 1998, 2001, 2004, 2007; Sikes et al., 1999; Behrensmeier, et al., 2002; Brooks et al., 2007; Owen et al., 2008; Kinyanjui, 2013).

The existing rich and unique prehistoric findings that have contributed largely to addressing critical questions on the role of palaeoenvironments and Palaeoclimates in modelling the human evolution history and their adopted evolving technologies, have been analysed from Olorgesailie Formation. These deposits span between ~1.2Ma to 0.49Ma (Deino and Potts, 1990; 1991; Potts, 1998), and are found within exposed outcrops that are eroded periodically and at different times exposing new research opportunities.

Comparing these results with those analysed from the outcrops (Kinyanjui, 2013), ODP core provided a higher resolution chronology of vegetation change. However on general trend, the results are consistent with phytolith data from the Olorgesailie Formation.

The vegetation structure identified from the phytolith assemblage between ca. 975-900kyr was bushlands dominated with woody component, almost similar to present day's savannah woodland. Previous studies on vegetation cover using Carbon isotope describes vegetation cover of the immediate preceding period ca. 990kyr, as more open C₄ grasslands (Sikes et al., 1999). Additionally, diatom assemblage analysed from the paleolake sediments indicate that during this period the Olorgesailie basin was covered by lake that underwent a series of shifts involving the disappearance, reappearance and expansion of the lake margin (Potts, 1998; Owen et al., 2008), which was influenced mainly by geological processes such volcanic eruptions farther north (Behrensmeyer et al., 2002).

These processes resulted in three landscape changes: fluvial, fluctuating lake-margins and stable terrestrial environments (Potts, 1998). Ongoing research from the core is investigating the role of climate in influencing the changes (Potts et al., *in progress*). Nevertheless such scenarios could have affected the taphonomy of phytolith deposition/preservation in the levels that either did not yield or had very low phytolith counts. Diatom and other trace fossils data from the Olorgesailie Formation dated within the same time bracket (~974kyr and ~780kyr) had broken diatoms due to poor preservation (Owen et al, 2008).

Sedimentological, limnological and trace fossils analyses indicate unstable mid-Pleistocene period with a sequence of extreme droughts between 601kyr and 493kyr recorded in the upper Member 12 and Member 13 of the Olorgesailie Formation (Melson and Potts, 2001; Owen et al., 2008, 2009). This coincides with diminishing of the Acheulean technology in the southern rift, especially at the basin, where a transition technology is noted from Acheulean to Middle Stone Age transition (MSA) (Potts, 1994; Potts et al., *in progress*). Additionally, fossil fauna that are related to the modern mammals such as: *Equus grevyi* (grazers), *Laxodontat africana* (browsers), *Papio anubis* (omnivore), *Phacochoerus aethiopicus* and *Hippotamus amphibious* appear around this period (~340kyr) in the Olorgesailie basin (Potts, 2007). Vegetation data indicate expansion of grasslands on the landscape around this period (ca.

340kyr) and continued being prominent in the region towards 70kyr. Hence, more grazers appearing on the landscape.

Phytolith assemblage from the paleosols dated between ~320kyr and ~220kyr of the post-Olorgesailie FM (Olkesiteti and Oltepesi beds) indicate a heterogeneous vegetation structure across the mid-Pleistocene landscapes similar to the present vegetation cover (Kinyanjui, 2013). The archaeological record suggests increased modern grazers on the landscape and oldest evidence of MSA technology is found in the basin dates to ~320kyr (Potts, 1994; Potts et al., 1999, Brooks et al., 2007).

The sudden vegetation cover changes around 250kyr could be attributed to change in paleoclimate which probably led to transitions in the archaeological record which shows an increased toolkit innovation and hominin mobility in the African region, as hypothesized by Rick Potts that, sudden environmental changes and or high variability may have been a major driving factor in toolkit transitions and human behavioural change (Potts, 1998; see Basell, 2008 and references therein).

Around 250kyr, diversity in MSA technology is recorded (Basell, 2008) and most importantly the emergence of the anatomically modern man (*Homo sapiens*) ca 200kyr (White et al., 2003; Haile-Selassie et al., 2004).

In summary, phytolith assemblages from the ODP core provide a unique opportunity to understand temporal vegetation changes with continuous geochronological data that can accurately characterise the Pleistocene environments in relation to hominin behaviour, human and other fauna evolutionary history and test the available hypotheses about role of climatic variability (high/low) to the aforementioned subjects.

The major advantage of the ODP phytolith is their good preservation in most of the samples and their potential to identify various habitats that are critical in understanding the vegetation dynamics in the Olorgesailie basin. Although other woody and herbaceous dicotyledons are identified, their role in the vegetation could not be fully exploited due to the ambiguity of the morphotypes used to identify this group.

8.2.2. Phytolith data, $\delta^{18}\text{O}$ and eccentricity

In the previous chapter, ODP phytolith assemblages were compared with the following data sets $\delta^{18}\text{O}$ and eccentricity (Figure 38). CA Axis 1 tracks the amount of woody cover (positive values) vs. grasses (negative values). The time series shows frequent fluctuations between wooded vegetation and grasslands especially the lower part of the core.

Like observed in the Tilia diagrams previously, distinct boundaries are visible and are worth highlighting at the following depth: I) ~635kyr (148.80, 1.28), II) ~397kyr (130.68, -1.19), III) ~293kyr

(113.36, -2.39), IV) ~232kyr (93.62, 1.39), V) ~200kyr (56.39, -0.89), VI) ~144kyr (46.96, 0.95) and VII) ~83kyr (28.35, -1.16). Hence the vegetation cover fluctuated from densely wooded to grasslands with some woody elements to increased open grasslands then abruptly shifted to wooded vegetation around 232kyr. Thereafter mixed vegetation became more prominent towards 83kyr.

Comparing the time series (phytolith data set) with $\delta^{18}\text{O}$ record and eccentricity cycle (Tyler et al., *in progress*) shows that there is a strong relationship between changes in the phytolith assemblages and that of the two proxies (see figure 38 a & b). There is high variability; frequent shifts from very wet to very dry. Woody dominated vegetation appears to be within phases of high orbital eccentricity while grasslands dominated appear to be within phases of low orbital eccentricity. When compared with $\delta^{18}\text{O}$, although not obvious the relationship between phytolith data and orbital eccentricity, a trend is observed where grasslands dominate during cooler temperatures phase when more water was locked in ice volume while woody elements dominate during warmer temperatures when less water was locked in the ice volume.

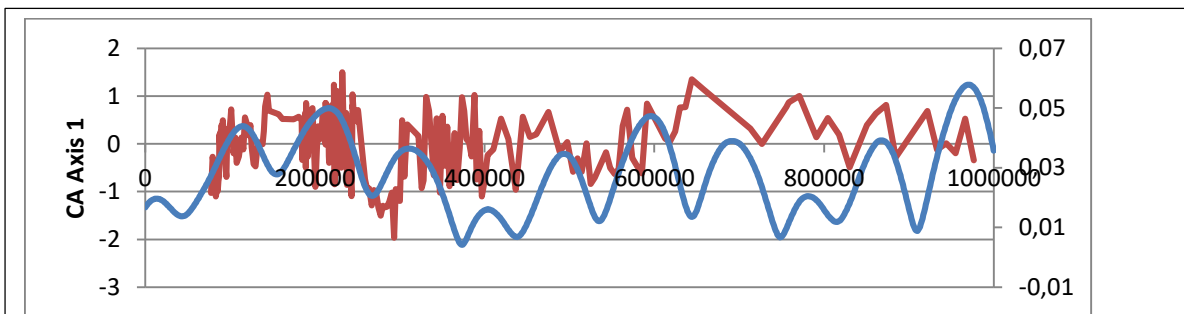


Figure 36-z. Phytolith data (red) arrayed against orbital eccentricity (blue)

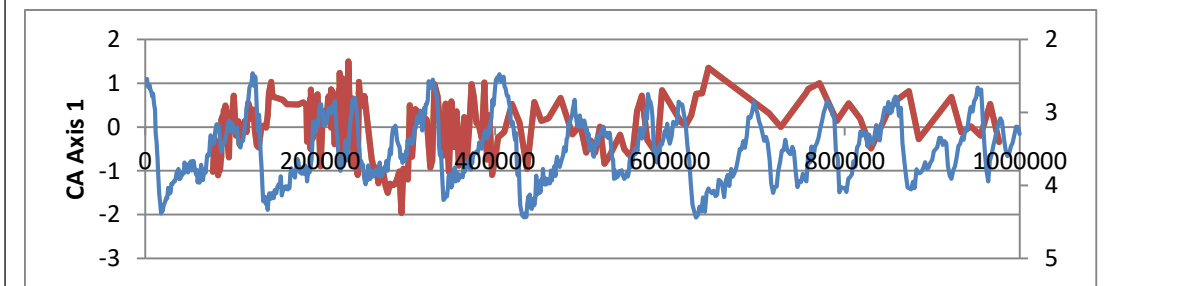


Figure 36-b. Phytolith data (red) arrayed against $\delta^{18}\text{O}$ (blue)

Figure 37. Preliminary results indicate vegetation structure fluctuations a) correspond with a) orbital eccentricity cycle b) grasslands expansion correspond are in phase with $\delta^{18}\text{O}$ record (Tyler et al., *in progress*).

8.3. Significance of the ODP phytolith data in relation to other proxies studied from the Olorgesailie Formation and surrounding regions.

The vegetation structure comprised open grasslands, wooded grasslands, woodland/forest, and wetland/riparian/riverine habitats. These habitats fluctuated from one palaeolandscape to the other, hence the environments were unstable. The rate of fluctuations changed from high to low throughout the Olorgesailie sequence. The indices further indicated variation in composition of vegetation cover and guided in estimating the environmental and climatic parameters controlling these changes.

The presence of varied vegetation habitats implies availability of varied resources required by hominins occupying these landscapes. Therefore variations and fluctuation rate of the vegetation structure through time would have most likely affected hominin-environment interactions. Keeping in mind that the archaeological sites in the Olorgesailie basin have been interpreted as occupations or stable camps of ancient hominins who were mainly hunters/meat eaters (Isaac, 1977; Potts, 1989), we highlight current inference of vegetation structure of specific time periods with known published data from the Olorgesailie Formation and discuss their relationship below: 7.3.1. ~970kyr to ~900kyr period.

This represents the Olorgesailie Formation, from the boundary between Members 6/7 and Member 5. During this period, cranial remains of the only hominin; *Homo erectus*, was excavated in association of other mammalian fossils and high concentration of Acheulean hand-axes (Potts et al., 2004). Phytolith data indicate vegetation structure during this period fluctuated between open to wooded savanna grasslands which was under high aridity environments, implying that the Hominin interacted with arid environments. The presence of large herbivores such as; *Elephas reckii* and *Equus oldowayensis* which are browsers and grazers (Potts, 1989), suggest wooded habitats and grasslands respectively (Kinyanjui, 2013), agreeing with this inference. More archaeological findings interpreted that Members 7, 10 and 11 artefacts were associated with ephemeral stream channels with seasonal fresh water (Owen and Renault, 1981). The presence of palm phytoliths during this period further affirms these findings.

8.3.1. ~500kyr to ~350kyr period

This covers the period of Members 11 through 14 of the Koobi Fora Formation. Archaeological data indicate demise of Acheulean technology (Brooks et al., 2007) while limnological analyses indicate fluctuating lake levels and with changing salinity (Owen et al., 2009). Trace fossils showed a drier period during Member 13 environments and a wet period during Member 14 environments. ODP phytolith data suggest a highly fluctuating vegetation structure through time. The aridity indices fluctuate between low-medium-high, but the fluctuation rates do not correlate with D:P fluctuations. The hypothesis that rapid environmental and palaeoclimatic events were the driving factors for innovation of new and complex technologies such as MSA is supported by this study (Potts, 1998; 2013). Previous phytoliths study did not fully capture this phase due to erosion (Kinyanjui, 2013).

8.3. 2. ~350kyr to 300kyr period

Archaeological evidence shows the first appearance of the Middle Stone Age (MSA) technology (approx. age 320kyr) in the basin suggesting hominin behavioural change leading to technological innovations which were more complex than the earlier Acheulean tools (McBrearty and Brooks, 2000). The complexities of the MSA toolkit, particularly the presence of these tools in sites with raw material sources far from the sites, have been interpreted to indicate long distance exchange/mobility and economic intensification (McBrearty and Brooks, 2000). In addition, evidence comes from the initial transition of mammalian faunas from extinct populations to relatives of the modern mammals (Brooks et al., 2007). ODP phytolith data show vegetation structure ranging between open grasslands to wooded-grasslands around 350kyr to 320kyr, followed by either paleolandscapes with no vegetation cover or a phase of erosional events/ unconformity phase. Iph indices indicate grasslands dominated by Chloridoideae grasses, hence arid environments. Probably increased aridity and open vegetation structure was the main driver to complete extinction or speciation of previous faunal communities.

8.3.3. 225ky to 200kyr period

Outcrop sediments are geologically described as post-Olorgesailie Formation which consist of the Olkesiteti beds (Behrensmeyer, 2010). Archaeological evidence from the post-Olorgesailie Formation (Olkesiteti beds) on the outcrops indicates a high concentration of MSA technology (Brooks et al., 2007). This period also is critical because it has the earliest known appearance of *Homo sapiens* in East African region currently (White et al., 2003; Haile Selassie et al., 2004; McDougall et al., 2005). Phytolith data analysed from different localities across the basin suggest the existence of heterogeneous vegetation structure on the paleolandscapes (Kinyanjui, 2013) which is ideal for availability of varied resources. ODP phytolith data suggest vegetation structure that was predominantly wooded-to open-grasslands. High rate of aridity fluctuations occurred during this period, with generally high aridity environments persisting over this period. Availability of fresh water resources on the landscape is indicated by the presence of sedges and palms in the phytolith assemblages, providing attractive spots for the hominins on the otherwise arid landscape.

8.3.4. 200kyr to 100kyr period

This period is represented by post-Olorgesailie deposits (Oltepesi beds) that have undergone a series of superimposed channel fills dating between ~220kyr and <12kyr, which altered the landscapes (Behrensmeyer, 2010). Several MSA sites have been found associated with these deposits distributed laterally across the basin. Lithostratigraphic analyses indicated an arid palaeolandscape during this period with channel substrates which were likely used by the hominins. Elsewhere, evidence of the first “Out Of Africa” to the north and later to the world around 110kyr and 90kyr is recorded (Osborne et al. 2008). For this particular time period phytolith data indicate that around 110kyr the vegetation cover

was dense woodlands and humid environments. Chloridoideae grasses were absent during this time while palm phytoliths were notable. After 110kyr, the vegetation cover again became moderately wooded with mixed grasslands with much lower fluctuation rates.

8.4. Role of Olorgesailie vegetation cover on the Hominin landscapes

The ODP core provides a unique opportunity to understand the role of vegetation dynamics and environmental conditions faced by the early hominins over the last ~1Ma. This is so partly because of the long continuous sediments sequence which is well dated and partly because of the ongoing multidisciplinary and multi-proxy research. Preliminary analyses show a strong relationship identified between the phytolith assemblages, $\delta^{18}\text{O}$ record and the eccentricity cycles, show that woodland dominated during high orbital eccentricity while grasslands during period of low eccentricity (ODP team, *analyses in progress*).

In addition grasslands dominated during cold periods while woodlands coincided with period of warm temperature which was more humid (Kingston et al., 1994; DeMenocal, 1995; DeMenocal and Blomendal, 1995).

There data shows phases of both high and low variability in both assemblage composition and diversity which is attributed to be driven mainly by Pleistocene climate scenario which is considered to influence the behaviour of humans and other mammals in East Africa rift valley (Potts, 1998; Basell, 2008).

Understanding the vegetational environments with which early hominins interacted will help understand their foraging behaviour and land-use patterns. In the Olorgesailie basin, the vegetation structure provided a variety of habitats from riparian forests, wooded grasslands to open grasslands providing a variety of resources that attracted and sustained hominins on these landscapes. Such plants resources that were likely exploited include food, shelter/shade and refuge from predators. Other secondary resources included meat resources from animals supported/specialised to interact with these vegetation habitats, making the basin preferable home bases for hunters and gatherers, Acheulean tool makers.

CHAPTER NINE: EARLY-PLEISTOCENE AND HOLOCENE VEGETATION DYNAMICS IN KOOBI FORA BASIN.

Here the vegetation structure of the Koobi Fora basin is interpreted chronologically following site by site sequence. Although vegetation reconstruction from the Koobi Fora basin is a bit challenging due to discontinuous geochronological sequence, site-based-age correlation whose dates have been obtained from either selected tuffs that are related to the Early Pleistocene samples (Brown and Feibel, 1991; Brown and McDougall, 2011) or dates obtained from archaeological horizons of different Holocene deposits (Ashley et al., 2011) made it possible.

9.1. INTERPRETATION

9.1.1. Early Pleistocene vegetation structure

Phytolith assemblages from paleosols deposited between 1.525Ma and 1.52Ma suggest a general vegetation cover dominated by woodlands which shifted to woody mixed grasslands that resemble present savanna habitats. A moister grassland habitat is also reflected between 1.52Ma and 1.51Ma. The presence of sponge spicules, though rare, further indicate occurrence of seasonal high humidity events (Neumann et al., 2006). A few exceptions are indicated when the vegetation cover was entirely mixed grasslands with admixture of other woody and herbaceous species not long before 1.525Ma.

Phytolith assemblages reported here are within the Ileret complex dated tuffs. Sedimentological analyses have shown a series of depositional environments such as fluvial, lacustrine and terrestrial environments (Brown et al., 2006; Gathogo and Brown, 2006). More specifically, the phytolith data is associated with fluvial and terrestrial environments, since the Ileret tuffs were deposited at a time when the lake's most northward margin was near the Koobi Fora region, south of Ileret, and the Omo River was flowing through the Ileret region to drain to the lake (Brown et al., 2006).

Such environments were conducive to supporting a vegetation structure which would be highly unstable, that would vary depending on dynamism of the river system. It is therefore not surprising, to have incidences of abrupt vegetation shifts from woodlands to open grasslands as observed in some of the levels. In addition, the existence of riverine/riparian habitats would be paramount at some point during the Early Pleistocene period.

These findings are consistent with conclusions made in Quinn and Lepre, (2005), that the region underwent periodic water table rise influenced by distal flood waters allowing "woodlands and scrub to colonize wet-dry grasslands". The Early Pleistocene vegetation of the Ileret region was mainly controlled by the dynamism of the ancestral Omo River, resulting in the existence of grassland and woodland mosaic environments (Quinn and Lepre, 2005).

9.1.2. Holocene vegetation change and palaeoenvironments.

Early Holocene (~9.6kyr to ~9.3kyr) assemblages suggest almost similar vegetation cover as indicated in Early Pleistocene palaeolandscapes. However, the woodlands were denser and more so, Palm trees were present suggesting riverine/riparian environments and possible fresh/spring water resources (Albert et al., 2009; Ashley et al., 2010).

The presence of aquatic indicators such as sedges, sponge spicules and diatoms further suggest wetlands/swampy habitats. Moisture-loving grasslands are also significantly present. These results are consistent with ongoing sedimentological and archaeological studies indicating high lake stand at the site FxJj108 and FxJj27. Available faunal data point out that the main economic strategy was fishing as evidenced by the presence of numerous ichthyofaunal remains and bone harpoons in-situ (Forman et al., 2014; Wright et al., 2015; Ndiema et al., *in progress*).

During the transition period from early- to mid-Holocene (~9.3kyr to ~4.2kyr), vegetation cover remain consistently dominated by woodlands with low mixed grasslands, creating mosaic environments. The presence of Panicoideae and Arundinoideae, although in low percentages indicate the humid environments.

Archaeological evidence suggests a transition in economic subsistence from fishing to pastoralism; ichthyofaunal remains declined rapidly, replaced with caprine bone remains suggesting animal domestication (Ndiema, 2011). This period experienced rapid changes in lake levels after 9kyr; however evidence of human settlements associated with lake margins from cultural findings pointing to pastoralist-fisher-forager economies (Wright et al., 2015).

Phytolith assemblages during mid-Holocene (~4.2kyr) indicate a more stable vegetation structure dominated especially by woodlands. The most likely habitats indicated by the assemblage are terrestrial environments bordered by two palaeolandscapes that contrast strongly with those in between. The phytolith assemblage in the oldest sample is unique; suggesting open but undefined grasslands, with a notable presence of sedges and fossilized pollen grains (*Hyphaene*, Capparaceae and Agavaceae taxa). Comparing with other studies, this is not surprising because from the same site, organic charcoal has been found well preserved and in fact was used for AMS dating (Ashley et al., 2011). This suggests the environments were conducive for preservation of organic plant materials with low oxidation activity.

A clear vegetation shift is noted during the late Holocene period (~1.34ky to 0.93kyr), where woodlands declined while Chloridoideae grasses increased significantly indicating arid habitats similar to present-day savanna grasslands. Although aquatic indicators (sedges and diatoms) are not consistently present in all the palaeolandscapes, their occurrence cannot be ignored because they indicate availability of wetlands resources in the midst of arid habitats. Geological evidence from the site (FwJj5) indicates

existence of fresh/spring water inferred from the carbonate-cemented sand (tufa) analysed from the site (Ashley et al., 2011).

9.1.3. Phytolith Indices

To understand the vegetation and environmental dynamism of the Koobi Fora region, a systematic interpretation of the phytolith indices from Early Pleistocene and Holocene deposits is presented below:

9.1.3.1. D:P index

Interpretation of D:P and the Iph indices of the Koobi Fora phytolith assemblages was limited because of rarity and/or absence of the recommended morphotypes that are used in the calculations. Nevertheless, a general vegetation composition for different levels was possible to infer. During Early Pleistocene period, the D:P indices suggest moderate to high tree cover density indicating the wooded grasslands to woodlands vegetation structure. Only two palaeolandscapes were the exception with low tree cover density, suggesting more open grasslands.

Early Holocene period (9.6-6kyr) was covered predominantly with open grasslands. Towards upper levels, tree-cover-density increased to moderate. During the Early-Mid Holocene transition (9.3-4.2kyr), the vegetation cover shifts from open grasslands to wooded grasslands. Mid-Holocene period (4.2kyr) have varied habitats. Similar wooded grasslands noted in the previous sequence continue to persist before shifting to wooded vegetation structure with less grasslands but changing to open grasslands in the youngest sample. While Late Holocene period is dominantly open grasslands.

The D:P values for modern soil samples varied as expected, with their values reflecting the modern vegetation cover above them. SS1 and SS2 both collected from wooded vegetation had their D:P value at ∞ , indicating high tree-cover-density while SS3 and SS4 collected from scrubland and grasslands reflected moderate and low tree-cover-density respectively.

9.1.3.2. Iph Index

The aridity index of the Early Pleistocene samples indicate low aridity situation with less grasses on the landscapes. Two sample were exceptional, having an aridity value greater than 0.5: sample 1A-DU-ET-11-02-RK-13 collected above lower Ileret tuff (1.525Ma) has an aridity value of 0.8 while sample AV-ET-11-1-RK-19 collected above lower Ileret tuff (1.52Ma) has a value of 1.0. suggesting grasslands dominated by Chloridoideae short grasses.

Early Holocene period experienced high aridity environmental conditions unlike the preceding early Pleistocene period. However, the conditions changed gradually with decreasing aridity around Early-Mid Holocene transition phase. The scenario of low aridity conditions persisted through mid-Holocene becoming more arid towards late Holocene period.

Aridity indices for the modern soil samples were reflective of the habitat conditions from which they were collected. Sample collected from the open grasslands which was predominantly Chloridoideae short grasses had the highest Iph value (0.8).

9.2. DISCUSSION

9.2.1. Significance of vegetation structure and the Palaeoenvironments of the Koobi Fora basin

The Koobi Fora region has preserved a long record of human and behavioural evolution from the Pliocene (~6Ma) to Holocene (~10kyr-3kyr) period. The region has experienced a series of rapid geological processes of erosional and sediment infillings resulting in rich and unique preservation of fossils. The fossil bearing deposits are well studied and have provided valuable information on the past human evolutionary history in biological, behavioural and cultural aspects (Barthelme, 1985; Brown and Feibel, 1986; 1991; Leakey et al., 2001; Quinn and Lepre, 2005; Braun et al., 2010; Ashley et al., 2011; Ndiema, 2011; Archer et al., 2014).

The Plio-Pleistocene to Pleistocene deposits belongs stratigraphically to the Koobi Fora Formation while the Holocene deposits are classified as Galana Boi Formation. Between these two formations is ~40-10kyr hiatus (Brown and Feibel, 1986; Owen and Renaut, 1986; Garcin et al., 2009). The faulting and rifting processes resulted in changes in the basin's topography which eventually impacted on vegetation cover, shifting from tropical forests to arid grasslands through time and across the landscapes (Wright et al., 2009). Phytolith data suggest transition of woodlands to woody grasslands during Early Pleistocene period creating mosaic environments.

Dramatic changes in Holocene paleoclimates are well documented in the East African region, and the Galana Boi deposits in the Koobi Fora region are not left out (Owen et al., 1982; Ashley et al., 2011). Lake Turkana basin has also provided a rich archive of the Holocene paleoclimate proxies which are well studied and have confirmed that the region was equally affected by the rapid climatic changes (Halfman, et al., 1992; Garcin et al., 2009; Wright et al., 2009; Forman et al., 2014).

Early Holocene (~12-9kyr) was a wet phase and the Turkana lake level was 80m higher than present day (1976) level (Owen et al., 1982). During this period the archaeological record demonstrates that the main economic subsistence was gathering-fishing-hunting of aquatic and wild terrestrial fauna; this is evidenced by the occurrence of aquatic and wild terrestrial faunal remains, bone harpoons, decorated and undecorated pottery shards. These sites are associated with beach /lake-shore line environments and are labelled as fish-camps (Barthelme, 1985; Ashley et al., 2011; Ndiema, 2011). Phytolith data indicate vegetation structure indicative of humid environments, fresh water resources and woodland vegetation cover during this period. Vegetation shifted towards open grasslands with well-developed

herbaceous cover, described as “sub-desert steppe” similar to present day open grassy *Barleria* dominated scrubland (Owen et al., 1982). These results are consistent with Owen et al., (1982) pollen data which indicated vegetation cover was mainly

The mid-Holocene (~5-4kyr) climate became exceedingly drier with lake level falling by 25m to 55m a. s. l (Halfman et al., 1992). This period records the first evidence of domesticated animals dated to 4kyr. These sites are mostly found adjacent to the lake margins and fluvial environments (Ashley et al., 2011). The sites are labelled as pastoral camps and have yielded domesticated faunal remains (goats, sheep) in association with pottery and lithic artefacts (Barthelme, 1985; Ndiema, 2011).

Archaeological research demonstrates that during this period, increased mobility of humans in search of raw materials and toolkit exchange across the landscapes (Ndiema et al., 2011). Phytolith data suggest vegetation structure dominated by woodlands with a decline in grasslands. Considering the climatic parameters, one would expect more grasslands than woodlands. However, it is possible that the decline in grasslands was as a result of intensive grazing from the domesticated animals, reducing grass components on the landscape. This scenario can be compared with present day vegetation cover which is more heavily impacted by grazing than by prevailing arid climates.

Late Holocene was a period of high climatic variability; humid events are recorded at 3.0kyr and 2-1.3kyr (Forester et al., 2012). Drought phases are recorded at 3.3kyr and 2.5kyr when the lake levels declined abruptly. Archaeological records suggest humans adapted to specialized nomadic pastoralism, new land-use patterns and cultural resilience in response to extreme ecological changes (Forman et al., 2014). Phytolith data indicate increased grasslands dominated by Chloridoideae short grasses that indicate high aridity conditions. Short events of increased moisture during this period, are not identified in the phytolith data.

In summary, interpretation of the phytolith assemblage clearly shows that the vegetation structure changed in response to changing environmental settings that was mainly influenced by climatic factors especially changes in precipitation. The influence could either be primary; when increased rainfall resulted into vegetation shift from arid grasslands to woodlands/forest, or be a secondary influence of the lake levels and flooding Omo River discharge (Halfman et al., 1992).

9.3. Significance of the phytolith data in relation to other studies in Koobi Fora region.

Little is known about the vegetation component of the Early Pleistocene and Holocene landscapes of the Koobi Fora region, and more especially for the famous foot print site located at Ileret. This data has provided critical information of the general vegetation dynamics of the region. At least broad

palaeoenvironmental reconstructions have been undertaken using various sedimentological and geological proxies (Behrensmeyer, 1970; Cohen, 1982; Brown and Feibel, 1986; 1991; Gathogo and Brown, 2006; Ashley et al., 2011), fossil vertebrates including hominids (Feibel et al., 1989; Quinn and Lepre, 2005; Bennet et al., 2009) and archaeological evidence (e.g. Bunn, 1994; Ndiema, 2011; Archer et al., 2014).

This study is the first attempt to utilise phytolith assemblages to reconstruct the vegetation history of the Koobi Fora region. The good preservation of phytoliths in most of the sediments is a great advantage in this study. The discussion of the phytolith data in the Early-Pleistocene palaeoenvironmental context is quite challenging due to unavailability of comparable datasets. However, the Holocene data is consistent with previous palaeoclimatic interpretations of various datasets.

Since diagnostic morphotypes are reliable in identifying specific vegetation type, it provided a great opportunity to reconstruct the vegetation structure of the Koobi Fora region and how this changed through time. Considering the indices, tree-cover-density and aridity indices provided crucial information regarding environmental conditions (Alexandre, et al., 1999; Stromberg, 2004; Barboni et al., 2007).

However, the following are important points noted and discussed on application of indices in this study. The D:P indices have accurately reflected the tree cover density (Bremond et al., 2008). It is therefore not surprising to have over-representation of globular granulate in savanna shrublands or short woodlands, with few grasses and more shrubs. This is the most likely vegetation structure that existed on the Turkana basin palaeolandscapes during Early Pleistocene period.

The Iph index was not quite consistent with the D:P index, showing high aridity conditions in levels that the D:P values showed high tree-cover-density. Such scenario can be interpreted as phases of wooded grasslands that are dominated by Chloridoideae grasses. Similar disparity was noted in the Holocene phytolith assemblages.

This study therefore shows that phytolith indices alone cannot be relied upon to reconstruct vegetation dynamics; they are valuable tools in complementing the abundance data to more accurately reconstruct vegetation structure using phytolith data. More often, climatic parameters can be estimated especially when Panicoideae and Chloridoideae grasses are represented in the assemblage. In summary, application of phytolith indices requires a lot of caution when determining vegetation structure and palaeoclimatic parameters from fossil assemblages. Such limitations have also been pointed out in previous phytolith studies (e.g. Stromberg, 2004; Neumann et al., 2009).

CHAPTER TEN: VEGETATION STRUCTURE OF THE OLOGESAILIE AND KOOBI FORA BASIN AND HOW IT CHANGED THROUGH PLEISTOCENE –HOLOCENE PERIODS

10.1. Introduction

Based on modern phytolith analogues (Chapter four) and previously published modern phytolith data (e. g Alexandre et al., 1997; Bremond et al., 2008; Mercader et al., 2009; Rossouw and Scott, 2011), four vegetation categories were identified as follows: wetlands (sedges, globular echinate palm), grasslands (Chloridoideae, Panicoideae, Aristidoideae and undifferentiated grasses), woodlands/forests (globular granulate, schlereids, tracheids, globular verrucate) and other woody and herbaceous dicotyledons (globular variants, polyhedrals, facetates etc.). These categories were used to determine the vegetation changes through time depending on the present assemblages per sample/level.

Additionally, two phytolith indices; D:P and Iph were calculated and used to trace changes in the proportions of forest/woodlands versus grasses (tree cover index) and changes in proportions of Panicoideae versus Chloridoideae grasses (aridity-humidity gradient) respectively (Alexandre et al., 1997; Bremond et al., 2005; Barboni et al., 2007) for the fossil assemblages.

10.2. Significance of the vegetation changes in the Ologesailie Basin during the Pleistocene Period to Human evolution History

The ODP sediment core provided a valuable opportunity to acquire continuous phytolith data that have given insights to the vegetation changes of the Ologesailie basin during the Pleistocene period. Although not all levels yielded phytolith data most likely due to taphonomic limitations in some of the sediments, the majority of the samples yielded phytolith data that were significant enough to make inferences regarding the vegetation structure.

10.3. Significance of the vegetation changes in the Koobi Fora Basin during Early-Pleistocene and Holocene Periods to Human evolution History

This study is the first attempt to reconstruct vegetation history of the Koobi Fora region using phytolith data as the only proxy. Phytolith assemblages analysed from modern soil surface samples from four main vegetation habitats found in the basin were used to interpret vegetation habitats in the fossil assemblage. The resolution of temporal vegetation structure reconstruction is quite coarse, because it is limited to the available dates that are site based. The main criterion of site choice is the availability of well dated stratigraphy and archaeological horizons. The significance of vegetation structure reconstructed here is therefore discussed based on archaeological sites and the available dates.

10.3.1. Early Pleistocene (FwJi14E)

Also known as the “foot print” site located at Ileret. The age of the site is correlated with Ileret complex tuffs; the lower tuff dated ~1.53Ma and the upper tuffs dated 1.52 to 1.51Ma (Findlater, 1978; Bennett et al., 2009).

Geological studies demonstrated that the site is associated with flood deposits with evidence of palaeosol development within this time bracket. Traces of hominin activities are found associated with a variety of ecological settings (Harris et al., 2002; Braun et al., 2010). The association of faunal fossils and stone tools with deltaic environments, lake-shore-lines has been argued to be a deliberate choice by the hominins as occupation sites (Bunn et al., 1980).

Pollen data from an almost similar site (site 50) indicated a fairly open vegetation structure, composed of dry *Acacia-Commiphora* savanna with more than 80% grasslands (Vincens, 1979 in Bunn et al., 1980). Riparian/gallery forests were also indicated by the presence of species such as *Ficus* sp., *Salvadora* sp. and *Acacia* sp. (Bunn et al., 1980). These species occur in the area today so the possibility of contamination must be considered.

Phytolith data indicate wooded grassland and dense woodlands and semi-arid environments. The presence of sponge spicules and diatoms indicate occurrence of seasonal high humidity (Neumann et al., 2009). The data therefore suggest that *Homo erectus* living on these landscapes interacted with a variety of vegetational environments that were largely controlled by local topography and hydrology, other than external climatic factors.

10.3.2. Holocene

Koobi Fora and the entire Lake Turkana basin have been well studied in the context of Holocene paleoclimates, paleoenvironments and human behavioural and cultural dynamics (Ashley et al., 2011; Ndiema, 2011; Ndiema et al., 2011; Garcin et al., 2012; Forman et al., 2014). These studies demonstrated that the basin, just like other parts in tropical Africa, was not in isolation from the influence of dramatic climatic fluctuations, extremes and transitions (Garcin et al., 2012).

The Holocene climatic history of tropical Africa impacted largely on the ecosystems shifting from arid to semi-arid environments, consequently affecting demographic and socioeconomic shifts (Brooks, 2006; Ndiema, 2011). In the Koobi Fora basin, three distinct climatic phases are shown and distinguished by different lake levels identified by the shifting beach-line and, well-preserved archaeological evidence (Ashley et al., 2011; Ndiema et al., 2011; Ndiema, 2011).

The early Holocene period, the lake level was at the highest, 80m above the 1976 level. This was period of high humidity and the cultural-socio-economic strategies were hunter-fisher-gatherer reliance

(Ndiema, 2011). The vegetation reconstructed during this period was mainly dense woodland with a possibility of riparian/gallery forests as indicated by palms trees and sedges. Such vegetation structure was a great resource for hunting and gathering activities.

The mid Holocene period is marked by decreased humidity, with the lake level falling to 55m (above the 1976 level) and lake food resources became increasingly scarce leading to domestication of animals (Ndiema, 2011) Vegetation composition was mostly savanna woodlands. Grasslands were scarce on the landscape but this could be probably due to increased grazing by the domesticated animals and other wild herbivores.

The environments became increasing dry in late Holocene, and communities adopted specialised nomadic pastoralism which has persisted up to present. Wooded to open grasslands dominated with Chloridoideae arid grasses but which have been declining towards the present day, and most probably have long been replaced by the present *Barleria* sp. scrubland mixed with arid *Acacia-Commiphora* shrublands, mainly due to intensive overgrazing across the landscapes. Fresh water resources were available on the semi-arid landscapes as indicated by the presence of “tufa” (Ashley et al., 2011) and, sedges and diatoms in this study.

10.4. How similar/different is the vegetation structure in Koobi Fora and Olorgesailie basins?

To address the research question about how similar or dissimilar Koobi Fora and Olorgesailie basins are, could not be fully addressed. This is partly because of the available dates from both basins could not be correlated and partly because the available sampling strategies. However, the study has demonstrated that both basins were covered with vegetation cover that was dynamic. The indices also show varied environmental parameters, hence the paleoenvironments were unstable in general. With availability of a continuous phytolith profile capturing similar geological periods from the Koobi Fora region, more and better comparisons can be discussed.

CHAPTER ELEVEN: CONCLUSIONS AND FUTURE RESEARCH DIRECTIONS

11.1 CONCLUSIONS

Phytolith assemblages derived from two major hominin sites in Kenya's rift system were used to reconstruct I) Pleistocene vegetation of the Olorgesailie basin (~1Ma to 77kyr) and, II) the Pleistocene–Holocene periods of the Koobi Fora basin (1.525-1.51Ma, ~9.6kyr-0.93kyr). Vegetation structure changed through time depending on the availability of moisture or hydrological changes.

Correlation of these changes was limited by dissimilarity in sampling strategies and sample chronology.

Determining the preservation status of phytolith assemblage as initially planned was not possible because the initially targeted palaeosol profiles were not always available in both samples. Instead, sampling was done in profiles with available dates which were critical to achieve the main goal of this study.

In Koobi Fora, Pleistocene vegetation structure consisted of higher proportion of wooded plants and was more stable compared to Holocene vegetation cover. More vegetation variability is recorded in the Holocene environments and appear to be controlled mostly by changing climates. Holocene archaeological and geological record indicate climate was more variable in the region.

ODP core on the other hand, phytolith record show the vegetation structure varied through time. More so, the rate of variability was much higher during mid-Pleistocene period ~500-300kyr.

10.2. FUTURE RESEARCH DIRECTION

This study is the first attempt to utilize phytolith analyses as the only proxy to reconstruct the vegetation history of the Koobi Fora prehistoric basin. The study has demonstrated that phytolith data is a valuable tool to determine vegetation habitats especially so, because they preserve better in most of the depositional environments and they identify grasslands beyond family level. In addition, a broader perspective of the past environments are deduced and their significance extrapolated. However, vegetation reconstruction was site-based and limited to the available dates due to lack of continuous chronology. For future research therefore, need to explore the possibilities of long sediment core from the adjacent Lake Turkana which will offer opportunity to have a higher resolution phytolith data from which continuous vegetation reconstruction can be made.

REFERENCES

- Agnew, A.D.Q., and Agnew, S., 1994. Upland Kenya Wild Flowers. A Flora of the Ferns and Herbaceous Flowering plants of Upland Kenya. Pp.374. East Africa Natural History Society, Nairobi.
- Ahmed, M., Hassan, F.U., Qadeer, V., Aslam, M. A. 2011b. Silicon application and drought tolerance mechanism of sorghum. *Afric. J. Agric. Res.* **6**: 594-607.
- Albert, R.M., 1999. Study of Ash Layers through Phytolith Analyses from the Middle Palaeolithic levels of Kebara and Tabun Caves. PhD dissertation, (Faculty of Geography and History, University of Barcelona, Spain.). Pp 227.
- Albert, R.M., and Weiner, S., 2001. Study of phytoliths in prehistoric ash layers from Kebara and Tabun caves using a quantitative approach. In: Meunier, J.D., Colin, F. (Eds.), *Phytolith: Applications in Earth sciences and Human History*. A.A Balkema Published, Lisse, Pp. 251-266.
- Albert, R.M., Weiner, S., Bar-Yosef, O. and Meignen, L., 2000. Phytoliths in the Middle Palaeolithic deposits of Kebara Cave, Mt, Carmel, Israel: study of the plant materials used for fuel and other purposes. *Journal of Archaeological Science* **27**: 931-947.
- Albert, R.M., Bamford, M.K. and Cabanes, D. 2006. Taphonomy of Phytolith and macroplants in different soils from Olduvai Gorge (Tanzania) and the application to Plio-Pleistocene Palaeoanthropological samples. *Quaternary International* **148**:78-94.
- Albert, R. M., Shahack-Gross, R., Cabanes, D., Gilboa, A., Lev-Yadun, S., Portillo, M.m Sharon, I., Boaretto, E., Weiner, S. 2008. Phytolith-rich layers from the Late Bronze and Iron Ages at Tel Dor (Israel): mode of formation and archaeological significance. *Journal of Archaeological Sciences* **35** (1): 57-75.
- Albert, R.M., Bamford, M.K., and Cabanes, D., 2009. Palaeoecological significance of palms at Olduvai Gorge, Tanzania, based on Phytolith remains. *Quaternary International* **193**: 41-48.
- Alexandre, A., Meunier, J.-D., Lézine, A.-M., Vincens, A. and Schwartz, D. 1997. Phytoliths: indicators of grasslands dynamics during the late Holocene in intertropical Africa. *Palaeogeography, Palaeoclimatology, Palaeoecology* **136**: 213-229.
- Alexandre, A. and Brémond, L. 2009. Comment on the Paper in *Quaternary International*: “Methodological concerns for Analysis of phytolith assemblages: Does count size matter?” (C.A.E. Strömberg). *Quaternary International* **193**: 141-142.

- Archer, W., Braun, D.R., Harris, J.W.K., McCoy, J.T., Richmond, B.G., 2014. Early Pleistocene aquatic resource use in Turkana Basin. *Journal of Human Evolution*, 1-14.
- Asani, G.C., and Kinuthia, J.H. 1979. Diurnal variation of Precipitations in East Africa-Nairobi, Kenya. *Metrological Department Research Report*, 8.
- Asfaw, B., White, T., Lovejoy, O., Latimer, B., Simpson, S. And Suwa, G. 1999. *Australopithecus garhi*: A New Species of Early Homind from Ethiopia. *Science* **289**: 629-635.
- Ashley, G.M., Mworira, M.J., Muasya, A.M., Owen, R.B., Driese, S.G., Hover, V.C., Renault, R.W., Goman, M. F., Mathai, S. Blatt, S.H. 2004. Sedimentation and recent history of a freshwater wetland in a semi-arid environment: Lobo Swamp, Kenya, East Africa
- Ashley, G. M., Tactikos, J.C., Owen, R.B. 2009. Hominin use of trees and wetlands: Paleoclimate and archaeology records from Olduvai Gorge (1.79-1.74 Ma). *Palaeogeography, Palaeoclimatology, Palaeoclimatology* **272**: 1-16
- Ashley, G.M., Barboni, D., Dominguez-Rodrigo, M., Bunn, H.T., Mabulla, A.Z.P., Diez-Martin, F., Barba, R. and Baquedano, E. 2010a. A Spring and wooded habitats at FLK Zinj and their relevance to origins of Human behaviour. *Quaternary Research* **74**(3): 304-314
- Ashley, G.M., Barboni, D., Dominguez-Rodrigo, M., Bunn, H.T., Mabulla, A.Z.P., Diez-Martin, F., Barba, R. 2010b. Paleoenvironmental and Paleoecological reconstruction of a fresh water oasis in Savannah grasslands at FLK North, Olduvai Gorge Tanzania. *Quaternary Research* **74** (3): 333-343
- Ashley, G., Ndiema, E.K., Spencer, J.Q.G., Harris, J.W.K., Kiura, P.W. 2011. Paleoenvironmental context of Archaeological Sites, Implications for Subsistence strategies under Holocene Climate Change, Northern, Kenya. *Geoarchaeology: an International Journal* 1-29
- Bamford, M.K., Albert, R.M., and Cabanes, D. 2006. Plio-Pleistocene macroplant fossil remains and phytoliths from Lowermost Bed II in the eastern palaeolake margin of Olduvai Gorge, Tanzania. *Quaternary International* **148**:95-112
- Barboni, D., Bonnefille, R., Alexandre, A. and Meunier, J. D.1999. Phytoliths as paleoenvironmental indicators, West Side Awash Valley, Ethiopia. *Palaeogeography, Palaeoclimatology, Palaeoclimatology* **152**: 87-100.
- Barboni, D., Bremond, L. and Bonnefille, R. 2007. Comparative study of modern phytolith assemblages from inter-tropical Africa. *Palaeogeography, Palaeoclimatology, Palaeoclimatology* **246**: 454-470.

Barboni, D. and Bremond, L. 2009. Phytoliths of East African grasses: An assessment of their environmental and taxonomic significance based on floristic data. *Review of Palaeobotany and Palynology* **158**: 29-41.

Barboni, D., Ashley, G.M., Dominguez-Rodrigo, M. and Bunn, H.T., Mabulla, A. Z.P and Baquedano, E. 2010. Phytoliths infer locally dense and heterogeneous paleovegetation at FLK North and surrounding localities during upper Bed I time, Olduvai Gorge, Tanzania. *Quaternary Research* **74**: 344-354

Barthelme, J.W. (1985). Fisher-Hunters and Neolithic Pastoralists in East Turkana, Kenya. B.A.R. Cambridge Monographs in African Archaeology, 13.

Baker, B.H. and Mitchel, J.G. 1976. Volcanic stratigraphic and geochronology of the Kedong-Olorgesailie area and evolution of the South Kenya rift valley. *Journal of Geological Society London* **132**:467-484.

Baker, R.G., Fredlund, G.G., Mandel, R.D., Beltis III, E.A. 2000. Holocene environments of the Central Great Plains: Multi-proxy evidence from alluvial sequences, Southeastern Nebraska. *Quaternary International* **67**: 75-88.

Basell, L. 2008. Middle Stone Age (MSA) site distributions in eastern Africa and their relationship to Quaternary environmental change, refugia and the evolution of *Homo sapiens*. *Quaternary Science Reviews* **27**: 2484-2498

Beentjie, H.J., 1994. Kenya Trees, Shrubs and Lianas. National Museums of Kenya, Nairobi, Kenya. Pp. 722.

Behrensmeyer, A.K. 1970. Preliminary geologic interpretation of a new hominid site in the Lake Rudolf basin. *Nature* **226**: 225-226.

Behrensmeyer, A.K., Todd, N.E., Potts, R. and McBrinn, G.E. 1997. Late Pliocene faunal turnover in the Turkana Basin, Kenya and Ethiopia. *Science* **278**: 1589-1594

Behrensmeyer, A.K., Todd, N.E., Potts, R. and McBrinn, G.E. 1997. Late Pliocene faunal turnover in the Turkana Basin, Kenya and Ethiopia. *Science* **278**: 1589-1594

Behrensmeyer, A.K., Potts, R., Deino, A. and Ditch field, P. 2002. Olorgesailie, Kenya: a million years in the life of a rift basin. In Renault, R.W. and Ashley, G. (Eds.), *Sedimentation in continental rifts*. SEPM Specl. Publication, **73**:99-106.

Behrensmeyer, A.K. 2006. Climate change and human evolution. *Science* **311**:476-478

- Behrensmeyer, A.K., Potts, R. and Deino, A. 2007. Cycles of erosion and deposition in the Pleistocene Olorgesailie Basin of southern Kenya and their impact of paleoanthropological record. Abstract with programs, Annual Meeting of the Geological society of America, vol. **125** (2): 343.
- Behrensmeyer, A.K. 2010. Revised Report on Locality B stratigraphy and Age relationship. Unpublished field report Pp5.
- Bennett, M.R., Harris, J.W.K., Richmond, B.G., Braun, D.R., Mbua, E., Kuira, P., Olago, D., Kibunjia, M., Omuombo, C., Behrensmeyer, A.K., Huddart, D., Gonzalez, S. 2009. Early Hominin foot Morphology based on 1.5 million year old footprints from Ileret, Kenya. *Science* **323**(5918): 1197-1201.
- Bergner, A, G.N. and Trauth, M.H.2004. Comparison of the hydrologic and hydrochemical evolution of lake Naivasha (Kenya) during three highstands between 175 and 60 kyr BP. *Palaeogeography, Palaeoclimatology, Palaeoecology* **125**: 17-36.
- Bergner, A.G.N., Trauth, M.H. and Bookhagen, B. 2003. Magnitude of precipitation/evaporation changes in the Naivasha Basin (Kenya) during the last 150kyrs. *Global Planetary Change* **36**:117-135.
- Bergner, A.G.N., Loutre, M.F. and Mélice, J.L. 2006. Equatorial insolation: from precession harmonics to eccentricity frequencies. *Clim. Past* **2**:131-136.
- Bergner, A.G.N., Strecker, M.R., Trauth, M.H., Deino, A., Gasse, F., Blisniuk, P. and Dühnforth, M. 2009. Tectonic and climatic control on evolution of rift lakes in the Central Kenya Rift, East Africa. *Quaternary Science Reviews* **28**:2804-2816.
- Birks, H.J.B., and Gordon, A.D. 1985. Numerical methods in Quaternary Pollen Analysis. Academic Press, London.
- Blinnikov, M. Busacca, A. and Whitlock, C. 2002. Reconstruction of the Late Pleistocene Grassland of the Columbia Basin, Washington, USA, Based on Phytolith Records in Loess. *Palaeogeography, Palaeoclimatology, Palaeoecology* **177**:77-101.
- Blumenshine, R.J., Masao, F.T. 1991. Living sites at Olduvai Gorge, Tanzania? Preliminary landscape archaeology results in the basal Bed II lake margin zone. *Journal of Human Evolution* **21**: 451-462
- Bobe, R., Behrensmeyer, A.K. and Chapman, R. 2002. Faunal Change, environmental variability and late Pliocene hominin evolution. *Journal of Human Evolution*. **42**. 475-497.

- Bobe, R. and Behrensmeyer, A. K. 2004. The expansion of grassland ecosystems in Africa in relation to mammalian evolution and the origin of the genus *Homo*. *Palaeogeography, Palaeoclimatology, Palaeoecology* **207**: 399-420.
- Bobe, R. 2006. The evolution of arid ecosystems in eastern Africa. *Journal of Arid Environments* **66**: 564-584
- Bonnefille, R. 1995. A reassessment of the Plio-Pleistocene pollen record of East Africa. In: Vrba, E.S., Denton, G.H., Partridge, T.C. and Burcle, L.H. (eds.): *Paleoclimate and Evolution with Emphasis on Human Origins*. New Haven: Yale University press. Pp 299-310.
- Bonnefille, R. and DeChamps, R. 1983. Data on fossil flora. In J de Heinzelin (ed.): *The Omo group: Archives of the International Omo Research Expedition*. Tervuren: Musée Royal de l'Afrique Centrale, pp191-207.
- Bonnefille, R. and Riollet, G. 1987. Palynological spectra from the upper Laetoli Beds. In Leakey, M.D. and Harris, J.M (eds.): *Laetoli: A Pliocene site in Northern Tanzania*. Oxford: Clarendon pp 52-61.
- Bonnefille, R., Vincens, A., Butchet, G. 1987. Palynology, Stratigraphy and palaeoenvironment of a Pliocene Hominid site (2.9-3.3M.Y) at Hadar, Ethiopia. *Palaeogeography, Palaeoclimatology, Palaeoecology*, **60**:249-282
- Bozarth, S.R.1992. Classification of Opal Phytoliths Formed in Selected Dicotyledons Native to the Great Plains. In: Rapp, G. Jr. and Mulholland, S.C. 1992. *Phytolith Systematics, Emerging Issues: Advances in Archaeological and Museum Science* **1**:193-214.
- Bozarth, S.R. 1993. Biosilicate Assemblages of Boreal forests and Aspen Parklands. In: Pearsall, D.M. and Piperno, D.R. *Current Research in Phytolith Analysis: Applications in Archaeology and Paleocology* Pp. 95-105.
- Bozarth, S.R. 1996. Pollen and opal phytolith evidence of pre-historic agriculture and wild plant utilization in lower Verde River, Arizona PhD Thesis, university of Kansas.
- Braun, D.R. 2006. *Ecology of Oldowan Technology: Koobi Fora and Kanjera South.*, Rutgers, Unpublished PhD Dissertation, The State University Of New Jersey, New Brunswick, New Jersey.

Braun, D.R., Harris, J.W.K., Levin, N.E., McCoy, J.T., Herris, A.I.R., Bamford, M. K., Bishop, L.C., Richmond, B.G., Kibunjia, M. 2010. Early hominin diet included diverse terrestrial and aquatic animals 1.95Ma in East Turkana, Kenya. *Proc. Natl. Acad. Scie.* 107:10002.

Brauer, G., 1984. A craniological approach to the origin of anatomically modern *Homo sapiens* in Africa and implications for the appearance of modern Europeans. In: Smith, F.H., Spencer, F. (Eds.), *The Origins of Modern Humans: A World Survey of the Fossil Evidence*. Alan R. Liss Inc., New York, pp. 327–410.

Bremond, L., Alexandre, A., Hély, C., and Guiot, J. 2005a. A Phytolith index as a proxy of tree cover density in tropical areas: calibration with Leaf Area Index along a forest-savanna transect in southeastern Cameroon. *Global and Planetary Change* **45** (4). 277-293.

Bremond, L., Alexandre, A., Hély, C., and Guiot, J. 2005b. Grass water stress estimated from phytoliths in West Africa. *Journal of Biogeography* **32**: (2). 311-327.

Bremond, L., Alexandre, A., Wooller, M. J., Hély, C., Williamson, D., Schäfer, P. A., Majule, A. and Guiot, J. 2008. Phytolith indices as proxies of grass subfamilies on the East African tropical mountains. *Global and Planetary Change* **61**:209-224.

Brink, J.S. and Lee-Thorp, J.P., 1992. The feeding niche of an extinct springbok, *Antidorcas bondi* (Antilopini Bovidae) and its palaeoenvironmental meaning. *South African Journal of Science* **88**: 227-229.

Brooks, N. 2006. Cultural responses to aridity in the Middle Holocene and increased social complexity. *Quaternary International* **151**: 29-49

Brooks, A., Behrensmeyer, A.K., Yellen, Y., Deino, A., Sharp, W., and Potts, R., 2007. After the Acheulean: stratigraphy, dating and archaeology of two new formations in the Olorgesailie basin, southern rift. *Paleoanthropology*. Internet journal of the paleoanthropology Society, P.A5

Brown, D. 1984. Prospects and Limits of a Phytolith Key for grasses in the Central United States. *Journal of Archaeological Science*, **11**: 221-243.

Brown, F.H., Feibel, C.S., 1985. Stratigraphic notes on the Okote Tuff Complex Koobi Fora Formation. *Nature*: 794-797

Brown, F.H., Feibel, C.S. 1986. Revision of lithostratigraphic nomenclature in the Koobi Fora region, Kenya. *Journal of the Geological Society, London* **143**: 297-310.

- Brown, F., and Feibel, C.S., 1991. Stratigraphy, depositional environments, and paleogeography of Koobi Fora Formation. In: Harris, J.M. (Ed.), Koobi Fora Research Project, Vol. 3. Clarendon Press, Oxford, Pp1-30.
- Bunn, H., Harris, J.W.K., Isaac, G., Kaufulu, Z., Kroll, E., Schick, K., Toth, N. and Behrensmeyer, A.K. 1980. FxJj 50: an Early Pleistocene site in northern Kenya. *World Archaeology* 12(2) 109-141.
- Bunn, H.T. 1994. Early Pleistocene hominid foraging strategies along the ancestral Omo River at Koobi Fora, Kenya. *Journal of Human Evolution* 27: 247-266.
- Butzer, K.W. 1980. The Holocene lake plain of north Rudolf, East Africa. *Physical Geography* 1:42-58.
- Butzer, K.W. (1982). *Archaeology as Human Ecology: Method and Theory for Contextual Approach*. Cambridge: Cambridge University Press.
- Cabanes, Dan, Mallol, Expósito Isabel, and Baena Javier, 2010. Phytolith evidence for hearths and beds in the late Mousterian occupations of Esquilieu cave (Cantabria, Spain). *Journal of Archaeological Science* 37 (11): 2947-2957.
- Campisano, C.J. and Feibel, C.S. 2007. Connecting local environmental sequences to global climate patterns: evidence from hominin-bearing Hadar Formation, Ethiopia. *Journal of Human Evolution* 53: 515-527.
- Cerling, T.E., Bowman, J.R., O'Neil, J.R. 1988. An Isotopic study of a fluvial-lacustrine sequences, East Africa. *Palaeogeography, Palaeoclimatology, Palaeoecology*, 63: 335-356.
- Cerling, T.E., 1992. Development of grasslands and savannas in East Africa during the Neogene. *Palaeogeography, Palaeoclimatology, Palaeoecology* 97: 241-247.
- Cerling, T.E., Levin, N.E., Quade, J., Wynn, J.G., Fix, D.L., Kingstone, J.D., Klein, R.G. and Brown, F.H. 2010. Comment on the Palaeoenvironments of *Ardipithecus ramidus*. *Science* 328: 1105d. DOI:10.1126/science.1185274.
- Chang, S.J., Tzeng, D.D., Li, C.C. 2002. Effects of silicon nutrient on bacterial blight resistance of rice (*Oryza sativa*, L.). Abstract of second Silicon in Agriculture conference PP 31-33
- Clark, J.D., 1988. The Middle Stone Age of East Africa and the Beginnings of Regional Identity. *Journal of World Prehistory* 2: 235-305.

- Clement, A.C., Hall, A., Broccoli, A.J., 2004. The importance of precessional signals in the tropical climate. *Clim. Dyn.* **22**, 327e341.
- Codron D.L., Brink, J.S., Rossouw, L. and Clauss, M. 2008. The Evolution of Ecological Specialization in Southern African ugulates completion-or physical Environmental Turnover? *Oikos* **117**: 344-353
- Conway, D., 2002. Extreme rainfall events and lake level changes in East Africa: Recent events and historical proceedings. In: Odada, E.O., Olago, D.O. (Eds.), *The East African Great Lakes: Limnology, palaeolimnology and biodiversity*. Kluwer Academic Publishers, Dordrecht, 63-92.
- Cohen, A., 1982. Palaeoenvironments of root casts from Koobi Fora Formation, Kenya. *Journal of Sedimentary Petrology* **52**(2): 0401-0414.
- Cohen, A.S., Stone, J.R., Beuning, K.R., Park, L.E., Reinthal, P.N., Dettman, D., Scholz, C.A., Johnson, T.C., King, J.W., Talbot, M.R., Brown, E.T., Ivory, S.J. 2007. Ecological consequences of Early Late Pleistocene megadroughts in Tropical Africa. *P. Natl. Acad. Sci. USA* **104**: 16422-16427.
- Cooke, J., Leishman, M.R. 2011. Silicon concentration and leaf longevity: Is silicon a player in the leaf dry mass spectrum? *Functional Ecology* **25**(6):1181-1188.
- Damnati, B. and Taieb, M. 1995. Solar and ENSO signatures in laminated deposits from Lake Magadi (Kenya) during the Pleistocene/ Holocene transition. *Journal of African Earth Sciences* **21**(3): 373-382.
- de Heinzelin, J. 1983. The Omo Group. *Musée Royal de l'Afrique Centrale, Tervuren, Belgique. Annales, Serie in 8, Sciences Geologiques* **85**.
- Deino, A., and Potts, R. 1990. Single-crystal $^{40}\text{Ar}/^{39}\text{Ar}$ dating of Olorgesailie Formation, southern Kenya Rift. *Journal of Geophysical Research* **95**: 8453-8470.
- Deino, A. and Potts, R. 1992. Age-probability spectra for examination of single crystal $^{40}\text{Ar}/^{39}\text{Ar}$ dating results: examples from Olorgesailie, southern Kenya rift. *Quaternary International* **13-14**:47-53.
- deMenocal, P. 1995. Plio-Pleistocene African Climate. *Science* **270**:53-59.
- deMenocal, P.B., and Bloemendal, J. 1995. Plio-Pleistocene climatic variability in subtropical Africa and the paleoenvironment of hominid evolution: a combined data-model approach. In: Vrba, E.S., Denton, G.H., Partridge, T.C., and Burkle, L. H. Eds. 1995. *Paleoclimate and Evolution*. Yale University Press, New Haven, Conn. Pp262-288.
- deMenocal, P.B. 2004. African Climate Change and Faunal evolution during the Pliocene-Pleistocene. *Earth and Planetary Science Letters* **220**:3-24.

Driese, S.G., Ashley, G.M., Li, Z.-H., Hover, V.C. and Owen, R.B. (2004) Possible Late Holocene equatorial palaeoclimate record based upon soils spanning the Medieval Warm Period and Little Ice Age, Lobo Plain, Kenya Palaeogeography, Palaeoclimatology, Palaeoecology.

Faegeri, K., and Inversen. 1975. Textbook of Pollen Analysis, 3rd ed. Blackwell, Oxford. 295Pp.

Fahmy, A. G. 2008. Diversity of lobate phytoliths in grass leaves from Sahel region, West Tropical Africa: Tribe Paniceae. Plant Systematics and Evolution **270**: 1-23.

Fahn, A. 1990. Plant Anatomy 4th edn, Oxford: Pergamon Press.

Faith, J. T., Potts, R., Plummer, T.W., Bishop, L.C., Marean, C.A., and Tryon, C.A. 2012. New perspectives on middle Pleistocene change in the large mammal faunas of East Africa: *Damaliscus hypsodon* sp. nov. (Mammalia, Artiodactyla) from Lainyamok, Kenya. Palaeogeography, Palaeoclimatology, Palaeoecology **361/362**:84–93.

Faith, J. T., Tryon, C.A., Peppe, D.J. and Fox, D.L. 2013. The fossil history of Gravy's zebra (*Equus grevyi*) in equatorial East Africa. Journal of Biogeography 40:359–369.

Feibel, C.S. 1988. Paleoenvironments from the Koobi Fora Formation Turkana Basin, northern Kenya. PhD dissertation, University of Utah.

Feibel, C.S., Brown, F.H., McDougall, I. 1989. Stratigraphic context of fossil hominids from the Omo Group deposits, northern Turkana Basin, Kenya and Ethiopia. American Journal of Physical Anthropology **78**: 595-622.

Feibel, C.S., Harris, J.M. and Brown, F.H. 1991. Palaeoenvironmental context for the late Neogene of the Turkana Basin. In: Harris, J.M. (Ed.): Koobi-Fora Research project, Oxford: Clarendon. **3**: 321-370.

Feibel, C.S. 1999. Basin Evolution, sedimentary dynamics, and hominid habitats in East Africa. In: Bromage, T.G. and Schrenk, F. (Eds.), African Biogeography, Climate Change and Human Evolution. Oxford University Press, Oxford, Pp.276-281.

Ferguson, A.J.D., Harbolt, B.J. 1982. Geographical, physical and chemical aspects of Lake Turkana project, 1972-1975. Overseas Development Administration, London, England pp. 1-110.

Findlater, I.C. 1978. Stratigraphy. In Leakey, M.G. & Leakey, R.E. (eds.) Koobi Fora Research Project, Vol.1; The fossil hominids and an introduction to their context, 1968-1974, Clarendon Press, Oxford, 14-31.

- Foerster, V., Junginger, A., Langkamp, O., Gebru, T., Asrat, A., Umer, M., Lamb, H.F., Wennrich, V., Rethemeyer, J., Nowaczyk, N., Trauth, M.H., Schaebitz, F., 2012. Climate change recorded in the sediments of the Chew Bahir basin, southern Ethiopia during the last 45,000years. *Quaternary International* **274**: 25-37.
- Forman, S.L., Wright, D.K., Bloszies, C. 2014. Variations in water level for lake Turkana in the past 8,500 years near Mt. Porr, Kenya and the transition from the African Humid Period to Holocene aridity. *Quaternary Science Reviews* **97**: 84-101.
- Fredlund, G.G. and Tieszen, L.T. 1994. Modern Phytolith Assemblages from the North American Great Plains. *Journal of Biogeography* **21**:321-335.
- Fredlund, G.G. and Tieszen, L.T. 1997. Calibrating Grass Phytolith Assemblages in Climatic Terms: Application to Late Pleistocene Assemblage from Kansas and Nebraska. *Palaeogeography, Palaeoclimatology, Palaeoecology* **136**:199-211.
- Frostick, L.E. 1997. The east African rift basin. In R.C. Selley (series Editor; K.J. Hsu). *African Basins: Sedimentary Basins of the World 3*. Pp: 187-209
- Garcin, Y., Junginger, A., Melnick, D., Olago, D., Strecker, M.R., Trauth, M.H. 2009. Late Pleistocene-Holocene rise and collapse of lake Suguta, Northern Kenya Rift. *Quaternary Science Reviews* **28**: 911-925.
- Garcin, Y., Melnick, D., Strecker, M.R., Olago, D., Tiercelin, J-J. 2012. East African Mid-Holocene wet-dry transition recorded in palaeo-shoreline of Lake Turkana, northern Kenya Rift. *Earth and Planetary Science letters* (**331-332**): 322-334
- Gathogo, P.N. and Brown, F.H. 2006. Stratigraphy of the Koobi Fora Formation (Pliocene and Pleistocene) in the Ileret region of northern Kenya. *Journal of African Earth Sciences* **45**: 369-390.
- Greenacre, M.J. 1984. *Theory and Applications of Correspondence Analysis*. Academic press, London.
- Gregory, J.W. 1921. *The Rift Valleys and Geology of East Africa*. Seeley service, London.
- Grimm, E.C. 2007. *Tilia 1.01 and Tilia Graph*. Illinois State University, Illinois.
- Griffiths, J.F. 1958. Climatic Zones of East Africa. *East African Agricultural Journal* **23**:179-185.
- Griffiths, J.F. 1972. Climates of Africa, *World survey of Climatology*. **10**:313-347.
- Grün, R., Stringer, C.B. 1999. Electron spin Resonance dating and the evolution of Modern Humans. *Archaeometry* **33** (2): 153-199.

- Haile-Selassie, Y., Asfaw, B., White, T.D., 2004. Hominid cranial remains from Upper Pleistocene Deposits at Aduma, Middle Awash, Ethiopia. *American Journal of Physical Anthropology* **123**: 1–10.
- Haines, R.W. and Lye, K.A. 1983. The sedges and Rushes of East Africa. A Flora of the Families Juncaceae and Cyperaceae in East Africa-with a particular Reference to Uganda. East Africa Natural History Society, Nairobi. Pp404.
- Halfman, J.D., Jacobson, D.F., Cannella, C.M., Haberyan, K.A., Finney, B.P. 1992. Fossil diatoms and the mid to late Holocene paleolimnology of Lake Turkana, Kenya: a reconnaissance study. *Journal of paleolimnology* **7**: 23-35
- Halfman, J.D., Johnson, T.C., Showers, W.J., & Lister, G.S. (1989). Authigenic low-Mg calcite in Lake Turkana, Kenya. *Journal of African Earth Sciences* **8**(2-4): 533-540.
- Hart, D.M. 1988. The plant Opal content in the vegetation and sediment of swamp at Oxford Falls, New South Wales, Australia. *Australian Journal of Botany* **36**: 159-170.
- Harris, J.M., Brown, F.H., Leakey, M.G., Walker, A., Leakey, R.E., 1988. Pliocene and Pleistocene hominid-bearing sites from west of Turkana, Kenya. *Science* **239**: 27-33.
- Harvey, C.P.D., and Grove, A.T. 1982. A Prehistoric Source of the Nile. *The Geographical Journal*, **148**(3): 327-336.
- Hijmans, R.J., S.E. Cameron, J.L Parra, P.G. Jones & A. Jarvis 2005. Very high resolution interpolated climate surfaces for global land areas. *International Journal of Climatology* **25**: 1965–1978.
- Hill, I. D. 1973. “Algorithm AS 66: The Normal Integral” *Applied Statistics*, **22**:424-427
- Hills, R.C. 1978. The structure of the Inter-Tropical Convergence Zone in Equatorial Africa and its relationship to East Africa rainfall. *Transaction of the Institute of British Geographers, New series* **4** (3): 329-352.
- Honaine, M. F., Zucol, A. F. And Osterrieth, M. L. 2006. Phytolith Assemblages and Systematic Associations in Grassland species of South-Eastern Pampean Plains, Argentina. *Annals of Botany* **98**: 1155-1165.
- Ibrahim, K.M. and Kabuye, C.H.S. 1987. *An Illustrated Manual of Kenya Grasses*. Food and Agriculture Organisation of the United Nations. Rome, 1987. Pp765.
- Isaac, G.L., Leakey, R.E.F. and Behrensmeyer, A.K. 1971. Archaeological traces of early hominid activities, east of Lake Rudolf, Kenya. *Science* **173**: 1129-1134

- Isaac, G. L. 1978. The Olorgesailie Formation: stratigraphy, tectonics and the paleogeographic context of the middle Pleistocene archaeological sites. In: W.W. Bishop, Ed. Geological Background to Fossil Man: Pp173-206. Edinburgh: Scottish Academic Press.
- Isaac, G. L. 1977. Olorgesailie, Archaeological studies of Middle Pleistocene Lake Basin in Kenya. 272pp University of Chicago press.
- Kaufman, P.B. Dayanandan, B.P., Franklin, C.L., Takeoka, Y. 1985. Structure and function of silica bodies in the epidermal system of grass shoots. *Annals of Botany* **55**: 487-507.
- Kealhofer, L., Torrence, R. and Fullagar, R. 1999. Integrating Phytoliths within Use-Wear/Residue Studies of Stone Tools. *Journal of Archaeological Science* **26**:527-546.
- Kenworthy, J.M. 1966. Temperature conditions in the tropical highland climates in East Africa. *E. Afr. Geogr. Rev.* **4**:1-11.
- Kingston, J.D., Marino, B.D. and Hill, A. 1994. Isotopic evidence for Neogene hominid palaeoenvironments in the Kenya Rift Valley. *Science* **264**:955-959.
- Kingstone, J.D., Deino, A.L., Edgar, R.K., Hill, A. 2007. Astronomically forced climate change in the Kenyan Rift Valley 2.7-2.55 Ma: implications for the evolution of early hominin ecosystems. *Journal of Human Evolution* **53**: 487-503.
- King'uyu, S.M., Ogallo, L.A., Anyamba, E.K., 2000. Recent trends of minimum and maximum surface temperatures over eastern Africa. *Journal of Climate* **13**: 2876-2886.
- Kinyanjui, R. N. 2013. Phytolith Analysis as a paleoecological tool for reconstructing Mid-Late Pleistocene environments in the Olorgesailie Basin, Kenya. MSc. Dissertation at University of Cape Town, Environmental and Geographical Sciences department. Pp 130.
- Klein, R. G. 1984. The large mammals of southern Africa: late Pleistocene to recent. - In: Klein, R. G. (ed.), *South African prehistory and palaeoenvironments*. A. A. Balkema, Rotterdam, pp. 107-146.
- Kondo, R., Childs, C. and Atkinson, I. 1994. *Opal Phytoliths of New Zealand*. Manaaki Press, Lincoln, New Zealand.
- Lahr, M.M and Foley, R. 1994. Multiple Dispersal and modern Human Origins. *Evolutionary Anthropology* 48-60
- Lahr, M.M., Foley, R. 1998. Towards a theory of modern human origins: geography and diversity in recent human evolution. *Year Physical Anthropology* **41**: 137-176.

- Lahr, M. and Foley, R. 2016. Human evolution in Late Quaternary eastern Africa. In S. C. Jones & B. A. Stewart (Eds.), *Africa from MIS 6-2: Population dynamics and paleoenvironments* (pp. 215–231). Dordrecht: Springer.
- Lamb, H., 2001. Multi-proxy records of Holocene climate and vegetation change from Ethiopian crater lakes, in: *Biology and environment. Proceedings of the Royal Irish Academy* **101B**: 35-46.
- Lamb, H.D and Verschuren, D. 2003. Vegetation response to rainfall variation and human impact in the central Kenya during the past 1100 years. *The Holocene* **13**:285-292.
- Leakey, M.D. 1970. Early artefacts from the Koobi Fora area. *Nature (London)* **226**: 228-230
- Leakey, M.G., Feibel, C.S., McDougall, I. and Walker, A.C. 1995. New four-million-year-old hominid species from Kanapoi and Allis Bay, Kenya. *Nature* **376**:565-571.
- Leakey, M.G., Feibel, C.S., Bernol, R.L., Harris, J.M., Cerling, T.E., Stewart, K.M., Storrs, G.W., Walker, A., Werdelin, L. and Winkler, A.J. 1996. Lothagam: A record of faunal change in the late Miocene of East Africa. *Journal of Vertebrate Palaeontology* **6**:556-570.
- Leakey, M.G., Spoor, F., Brown, F.H., Gathogo, P.N., Kiarie, C., and Leakey, L.N. (2001). New hominin genus from eastern Africa shows diverse middle Pliocene lineages. *Science* **410**(6827):433-440.
- Lee-Thorp, J., Sponheimer, M. and Luyt, J. 2007. Tracking changing environments using stable carbon isotopes in fossils tooth enamel: an example from the South African hominin sites. *Journal of Human Evolution* **53**: 595-601.
- Lepš, J. and Šmilauer, P., 2003. *Multivariate Analysis of Ecological Data of Ecological Data Using CANOCO*. United Kingdom: University Press, Cambridge. Pp.269.
- Lepre, C.J., Quinn, R.L., Joordens, J.C.A., Swisher III, C.C. and Feibel, C.S. 2007. Plio-Pleistocene facies environments from the KBS Member, Koobi Fora Formation: Implications for climate controls on the development of lake-margin hominin habitats in the northeast Turkana Basin (northern Kenya). *Journal of Human Evolution* **53**:504-524.
- Levin, N.E., Brown, F.H., Behrensmeier, A.K., Bobe, R., Cerling, T.E. 2011. Paleosol carbonates from the Omo Group: Isotopic records of local and regional environmental change in East Africa. *Palaeogeography, Palaeoclimatology, Palaeoecology* **307**: 75-89
- Livingstone, D.A and Clayton, W.D. 1979. An Altitudinal Cline in Tropical African Grass Floras and its Paleoecological Significance. *Quaternary Research*, **13**: 392-402.

- Mabulla, A., 1996. Middle and Later Stone Age land-use and lithic technology in the Eyasi Basin, Tanzania. Unpublished PhD thesis, University of Florida
- Madella, M., Alexandre, A., and Ball, T. 2005. International Code for Phytolith Nomenclature 1.0. *Annals of Botany* **96**: 253-260.
- Malhorta, C.H., Kapoor, R.T., Ganjewala, D. 2016. Alleviation of Abiotic and Biotic stresses in plants by Silicon supplementation. *Sci. Agri.* **13**(2): 59-73
- Marchant, R., Taylor, D., 1998. Dynamics of montane forest in central Africa during the late Holocene: a pollen based record from western Uganda. *The Holocene* **8**: 375-381.
- Marchant, R.A., Mumbi, C., Behera, S., and Yamagata, T. 2006. The Indian Ocean Dipole- the unsung driver of climatic variability in East Africa. *African Journal of Ecology* **45**: 4-16.
- Maruo, S., 2002. Differentiation of subsistence farming patterns among the Haya banana growers in northwestern Tanzania. *African Study Monographs* **23**: 147-175.
- Maslin, M. A., and Christensen, B., 2007. Tectonics, orbital forcing, global climate change, and human evolution in Africa: introduction to the African paleoclimate special volume. *Journal of Human Evolution* **53**: 443-463.
- Maslin, M.A., and Trauth, M.H., 2009. Plio-Pleistocene east African pulsed climate variability and its influence on early human evolution, in “the first humans-origins of the genus Homo”. In: Grine, F.E., Leakey, R.E., Fleagle, J.G. (Eds.), *Vertebrate, Paleobiology and Paleanthropology Series*. Springer Verlag, Pp. 151-158.
- Massey, F.P., Ennos, A.R., Hartley, S.E. 2007. Herbivore specific induction of Silica-based plant defences. *Oecologia* **152**: 677-683.
- Massey, F.P., Hartley, S.E. 2009. Physical defences wear you down: Progressive and irreversible impacts of Silica on insect herbivores. *Journal of Animal Ecology* **78**: 281-291.
- Mbaluka, J.K., Brown, F.H. 2016. Vegetation of The Koobi Fora Region Northeast Of Lake Turkana, Marsabit County, Northern Kenya. *Journal of East African Natural History* **105**: 21-50.
- McBrearty, S., Brooks, A., 2000. The revolution that wasn't: a new interpretation of the origin of modern human behaviour. *Journal of Human Evolution* **39** 453–563.
- McBrearty, S. 2007: Down with the revolution. In K. Boyle, O. Bar-Yosef, & C. Stringer (Eds.), *Rethinking the human revolution: New behavioural and biological perspectives on the origin and*

dispersal of modern humans (pp. 133–152). Cambridge: McDonald Institute for Archaeological Research Monographs.

McDougall, I., Maier, R., Sutherland-Hawkes, P., Gleadow, A.J.W., 1980. K-Ar age estimate for the KBS Tuff, East Turkana, Kenya. *Nature* **284**: 230-234.

McDougall, I., Davies, T., Maier, R., Rudowski, R., 1985. Age of the Okote Tuff Complex at Koobi Fora, Kenya. *Nature* **316**: 792-794.

McDougall, I., Brown, F.H., Fleagle, J.G., 2005. Stratigraphic placement and age of modern humans from Kibish, Ethiopia. *Nature* **433**, 733e736.

McDougall, I., Brown, F.H., 2006. Precise $^{40}\text{Ar}/^{39}\text{Ar}$ geochronology for the upper Koobi Fora Formation Turkana basin, northern Kenya. *Journal of the Geological Society, London* **163**:205-220.

Mehlman, M.J., 1987. Provenience, age and associations of archaic *Homo sapiens* crania from Lake Eyasi, Tanzania. *Journal of Archaeological Science* **14**:133–162.

Mehlman, M.J., 1991. Context for the emergence of modern man in Eastern Africa: some new Tanzanian evidence. In: Clark, J.D. (Ed.), *Cultural Beginnings: Approaches to Understanding Early Hominid Life-Ways in the African Savanna*. Habelt, Bonn, pp. 177–196.

Mercader, J., Runge, F., Vrydaghs, L., Doutrelepon, H., Ewango, C. E. N. and Tresseras, J. J. 2000. Phytolith from Archaeological Sites in the Tropical Forest of Ituri, Democratic Republic of Congo. *Quaternary Research* **54**: 102-112.

Mercader, J., Bennett, T., Esselmont, C., Simpson, S. and Walde, D. 2009. Phytoliths in woody plants from the Miombo woodlands of Mozambique. *Annals of Botany* **104**(1): 91-113.

Mercader, J., Astudillo, F., Barkworth, M., Bennett, T., Esselmont, C., Kinyanjui, R., Grossman-Laskin, D., Simpson, S. and Walde, D. 2010. Grass and Sedge phytoliths from Niassa, Mozambique. *Journal of Archaeological Science* **37** (8):1953-1967.

Mercader, J., Bennett, T., Esselmont, C., Simpson, S., Walde, D. 2011. Soil phytoliths from miombo woodlands in Mozambique. *Quaternary Research* **75**: 138-150.

Metcalf, C.R. 1960. *Anatomy of Monocotyledons. I. Gramineae*. Oxford, Clarendon Press: 731Pp.

Moore, P.D. and Webb, J.A. 1978. *An Illustrated guide to pollen analysis*. Hodder and Stoughton, 133Pp.

- Mudelsee, M. and Statteger, K. 1997. Exploring the Structure of the Mid-Pleistocene revolution with advance methods of time-series analysis. *Geol. Rundsch.* **86**:499-511
- Mulholland, S.C. 1989. Phytolith shape frequencies in North Dakota grasses: A comparison to general patterns. *Journal of Archaeological Science* **16**: 489-511.
- Mulholland, S.C. and Rapp, G. Jr. 1992a. Phytolith Systematic: An Introduction. In: Rapp, G. Jr. and Mulholland, S.C. 1992. Phytolith Systematics, Emerging Issues: Advances in Archaeological and Museum Science **1**:1-13. Plenum Press, New York.
- Mulholland, S. C. and Rapp, G. Jr. 1992b. A morphological classification of grass silica-bodies. In Rapp, G. Jr. and Mulholland, S.C. 1992. Phytolith Systematic, Emerging Issues: Advances in Archaeological and Museum Science **1**:65-89. Plenum Press, New York.
- Mutai, C.C and Ward, M.N. 2000. East African rainfall and the tropical circulation/convection on interseasonal to interannual timescales. American Meteorological Society. *Journal of Climate* **13**:315-3939.
- Mworia, J., Dallmeijer, A. and Jacobs, B. 1988. Vegetation and Modern Pollen Rain at Ologesailie, Kenya. *Utafiti* **1**(1): 1-22.
- Mworia-Maitima, J. 1997. Prehistoric fires and land-cover change in western Kenya: evidences from pollen, charcoal, grass cuticles and grass phytoliths. *The Holocene* **7-4**: 409-417.
- Mworia-Maitima, J. 1999. Preliminary Report on Preservation status of Organic plant remains in Ologesailie basin. Unpublished report at National Museums of Kenya.
- Ndiema, E. (2011). Mobility and subsistence patterns among mid Holocene pastoralists at Koobi Fora, northern Kenya: New archaeological sites and evidence from obsidian sourcing and geochemical characterization. New Brunswick, NJ: Rutgers University Press.
- Ndiema, K.E., Dillan, C.D., Braun, D.R., Harris, J.W.K and Kiura, P.W. 2011. Transport and subsistence patterns at the transition to pastoralism, Koobi Fora, Kenya. *Archeometry*
- Neumann, K., Fahmy, A., Lespez, L., Ballouch, A., Huysecom, E. 2009. The Early Holocene Palaeoenvironment of Ounjougou (Mali): Phytolith in a multiproxy context. *Palaeogeography, Palaeoclimatology, Palaeoclimatology* **276**:87-106.
- Nicholson, S.E. 1996. A review of Climate Dynamics and Climate Variability in eastern Africa. In: Johnson, T.C. and Odada, E.O. (Eds.) *The Limnology, Climatology and Paleoclimatology of the East Africa Lakes*. Gordon and Breach Publishers, The Netherlands.

- Nicholson, S.E., Kim, J., 1997. The relationship of the El-Nino Southern Oscillation to African rainfall. *International Journal of Climatology* **17**:117-135.
- Nicholson, S.E. 2000.
- Novello, A., Barboni, D., Berti-Equille, L., Mazur, J-C. 2012. Phytolith signal of aquatic plants and soils in Chad, Central Africa. *Review of Palaeobotany and Palynology* **178**: 43-58
- Novello, A., Barboni, D. 2015. Grass inflorescence phytoliths of useful species and wild cereals from sub-Saharan Africa. *Journal of archaeological science* **59**: 10-22
- Novello, A., Lebatard, A.E., Moussa, A., Barboni, D., Sylvestre, F., Bourles, D.L., Pailles, C., Buchet, G., Dacarreau, A., Düringer, P., Ghienne, J.F., Malev, J., Mazur, J-C., Roquin, C., Schuster, M., Vignaud, P. 2016. Corrigendum to “Diatom, phytolith and pollen records from a ¹⁰Be/⁹Be dated lacustrine succession in the Chad basin: Insight on the Miocene-Pliocene paleoenvironmental changes in Central Africa- Palaeogeography, Palaeoclimatology, Palaeoclimatology **430**:85-103.
- Novello, A., Barboni, D., Sylvestre, F., Lebatard, A-E., Pailles, C., Bourles, D.L., Lilius, A., Mackaye, H. T., Vignaud, P., Brunet, M. 2017. Phytoliths indicate significant arboreal cover at *Sahelanthropus* type locality TM266 in northern Chad and a decrease in later sites. *Journal of Human Evolution* **106**:66-83.
- Ollendorf, A.L., Mulholland, S.C. and Rapp, G. Jr. 1988. Phytolith Analysis as a Means of Plant Identification: *Arundo donax* and *Phragmites communis*. *Annals of Botany* **61**:209-214.
- Ollendorf, A.L. 1992. Toward classification Scheme of Sedge (Cyperaceae) Phytoliths. In Rapp, G. Jr. and Mulholland, S.C. 1992. *Phytolith Systematics, Emerging Issues: Advances in Archaeological and Museum Science* **1**:91-111. Plenum Press, New York.
- Olago, D.O., Odada, E.O. 2000. An inter-basinal comparison of the sedimentary of late Holocene to recent sediments in Rift valley, Lake Turkana. *Journal of African Earth Sciences* **32**(2): 237-252.
- Olago, D., Opere, A. and Barongo, J. 2009. Holocene palaeohydrology, groundwater and climate change in the lake basins of the Central Kenya Rift. *Hydrological Sciences Journal* **54**(4):765-780.
- Owen, R.B., Renaut, R.W. 1981. Paleoenvironments and sedimentology of the Middle Pleistocene Olorgesailie Formation, Southern Kenya Rift Valley. *Palaeoecol.* **13**: 147-174.
- Owen, R., Barthelme, J., Renaut, R., & Vincens, A. (1982). Palaeolimnology and archaeology of Holocene deposits north-east of Lake Turkana, Kenya. *Nature*, **198**: 523-529.

- Owen, R.B., Renaut, R.W. 1986. Sedimentology, stratigraphy and palaeoenvironments of the Holocene Galana Boi Formation, NE Lake Turkana, Kenya. In: Frostick, L.E., Renaut, R.W., Reid, I., Tiercelin, J.J (Eds.), *Sedimentation in the African Rifts*, Geological Society Special Publication 25. Blackwell.
- Owen, R. B., Potts, R., Behrensmeier, A. K. and Ditchfield, P. 2008. Diatomaceous sediments and environmental change in the Pleistocene Olorgesailie Formation, southern Kenya rift Valley. *Palaeogeography, Palaeoclimatology, Palaeoclimatology* **269**: 17-37.
- Pallister, J.W. 1971. The Tectonics of East Africa, *Tectonique de l'Afrique*, Earth Sciences **6**: 511-542). South Africa UNESCO.
- Pearsall, D.M. 1989. *Paleoethnobotany: A Handbook of Procedures*. Academic Press, San Diego.
- Pearsall, D.M. 2000. *Paleoethnobotany: A Handbook of procedure*. Academic press, San Diego
- Pearsall, D.M. and Dinan, E.H. 1992. Developing a Phytolith Classification System. In Rapp, G. Jr. and Mulholland, S.C. 1992. *Phytolith Sytematics: Emerging Issues*, Advances in Archaeological and Museums Science **1**:37-64. Plenum Press, New York.
- Piperno, D.R.1988. *Phytolith Analysis: An Archaeological and Geological Perspective*. Academic Press, San Diego. Pp 280.
- Piperno, D.R. 1989. The Occurrence of Phytoliths in Reproductive Structures of Selected Tropical Angiosperms and their Significance in Tropical Paleocology, *Paleoethnobotany, and Systematic. Review of Palaeobotany and Palynology* **61**:147-173.
- Piperno, D.R. 1993. Phytolith and charcoal records from deep lake cores in the American tropics. In. *archaeology and paleocology MASCA Research Papers in Science and Archaeology* 10. University Museum of Archaeology and Anthropology, University of Pennsylvania, Philadelphia pp 58-71.
- Piperno, D.R., 1994. Phytolith and Charcoal Evidence for Prehistoric Slash-and-Burn Agriculture in the Darien Rain Forest of Panama. *The Holocene* **4**:321-325.
- Piperno, D.R. 2001. Phytoliths. In: Smol, J.P., Birks, H.J.B. and Last, W.M. *Tracking (Eds.) Environmental Change Using Lake Sediments. Terrestrial, Algal, and Siliceous Indicators. Vol.3*: 235-251. Kluwer Academic Publishers, Dordrecht, Netherlands.
- Piperno, D.R. 2006. *Phytoliths: A Comprehensive guide for Archaeologists and Paleoecologists*. Pp238. Altamira Press, Oxford.

- Piperno, D.R., Bush, M.B. and Colinvaux, P.A. 1990. Palaeoenvironments and Human Occupation in Late-Glacial Panama. *Quaternary Research* **33**:108-116.
- Piperno, D.R. and Pearsall, 1993. The nature and status of phytolith analysis application in archaeology and paleoecology MASCA Research Papers in Science and Archaeology 10. University Museum of Archaeology and Anthropology, University of Pennsylvania, Philadelphia pp9-18.
- Piperno, D. R. and Pearsall 1998. The Silica Bodies of Tropical American Grasses: Morphology, Taxonomy, and Implications for Grass Systematics and Fossil Phytolith Identification. *Smithsonian Contributions to Botany*. **5**. Pp 45.
- Piperno, D.R., Holst, I., Wessel-Beaver, L. and Andres, T.C. 2002. Evidence for the Control of Phytolith Formation in Curcubita Fruits by the Hard Rind (Hr) Genetic Locus: Archaeological and Ecological Implications. *Proceedings of the National Academy of Sciences USA* **99**:10923-10928.
- Potts, R.1989. Olorgesailie: new excavations and findings in Early and Middle Pleistocene contexts, southern Kenya rift Valley. *Journal of Human Evolution* **18**: 477-484.
- Potts, R. 1994. Variables versus models in early Pleistocene hominid land use. *Journal of Human Evolution*. **27**: 7-24.
- Potts, R., 1996. Evolution and climate variability. *Science* **273**: 922-923.
- Potts, R. 1998. Environmental Hypotheses of Hominin Evolution. *Yearbook of Physical Anthropology* **41**:93-136.
- Potts, R. 2002. Complexity and Adaptability in Human Evolution. In: Goodman, M. and Moffat, A.S. (Eds.) 2002. *Probing Human Origins*, pp 33-57.
- Potts, R., 2007. Environmental context of Pliocene human evolution in Africa. In: Bobe, R., Alemseged, Z., Behrensmeyer, A.K. (Eds.), *Hominin Environments in the East African Pliocene: An Assessment of the Faunal Evidence*. Springer, New York, pp. 25–48.
- Potts, R., Ditchfield, P., Hicks, J. and Deino, A.1997. Palaeoenvironments of late Miocene and early Pliocene strata of Kanam, western Kenya. *American Journal of Physical Anthropology* **24**:188-189.
- Potts, R., Behrensmeyer, A. K., and Ditchfield, P. 1999. Paleolandscape variation and Early Pleistocene hominid activities: Members 1and 7, Olorgesailie Formation, Kenya. *Journal of Human evolution* **37**: 747-788.

- Potts, R., Behrensmeyer, A.K., Deino, A., Ditchfield, P., and Clark, J. 2004. Small Mid-Pleistocene Hominin Associated with East African Acheulean Technology. *Science* **305**: 75-78.
- Potts, R., Faith, T. 2015. Alternating high and low climate variability: The context of natural selection and speciation in Plio-Pleistocene hominin evolution. *Journal of Human Evolution* **87**:5-20
- Plummer, T.W et al., 2009. Oldest evidence of toolmaking hominins in grassland dominated ecosystem. *PLOS ONE* **4**, e7199
- Quinn, R., Lapre, C. 2005. Environmental context of early Pleistocene hominins from Ileret sub-region (Area 1a) of Koobi Fora, Kenya. *American Journal of physical Anthropology (Suppl.40)*: p174.
- Quinn, R.L., Lepre, C.J., Wright, J.D. and Feibel, C.S. 2007. Paleogeographic variations of pedogenic carbonate ^{13}C values from Koobi Fora, Kenya: implications for floral compositions of Plio-Pleistocene hominin environments. *Journal of Human Evolution* **53**: 560-573
- Rapp, G. Jr., and Mulholland, S.C. 1992. *Phytolith Systematics: Emerging Issues*. Advances in Archaeological and Museums Science. Plenum Press, New York. Pp 350.
- Robertshaw P., Taylor D., 2000. Climate change and the rise of political complexity in western Uganda. *Journal of African History* **41**:1-28
- Robertshaw, P., Taylor, D., Doyle, S., Marchant, R., 2004. Famine, climate and crisis in Western Uganda. In: Battarbee, R.W., Gasse, F., Stickley, C.E. (Eds.), *Past climate variability through Europe and Africa*. Springer-Verlag, Berlin, 535-549.
- Roger, A.R. and Jorde, L.B. 1995. Genetic Evidence on Modern Human origins. *Human Biology* **67** (1):1-36
- Rogers, M.J., Feibel, C.S. and Harris J.W.K. 1994. Changing Patterns of land use by Plio-Pleistocene hominids in the Lake Turkana Basin. *Journal of Human Evolution* **27**: 139-158.
- Rogers, M.J. 1997. A landscape archaeological study at East Turkana, Kenya. Unpublished PhD Thesis Rutgers University, New Brunswick.
- Rosen, A.M. 1992. Preliminary Identification of Silica Skeletons from Near Eastern Archaeological Sites: An Anatomical Approach. In: Rapp, G. Jr., and Mulholland, S.C. 1992 (Ed) *Phytolith Systematic: Emerging issues*, Advances in Archaeological and Museum Science. Plenum Press, New York 1: 129-147.

Rossouw and Scott 2011. Phytoliths and pollen, the microscopic plant remains in Pliocene volcanic sediments around Laetoli, Tanzania. In: T. Harrison (ed), *Paleontology and Geology of Laetoli: Human Evolution in context*. Volume 1. Geology, Geochronology, Paleocology and paleoanthropology. DOI 10.1007/978-90-481-9956-3-9.

Rossouw, L. 2009. The application of fossil grass-phytolith analysis in the reconstruction of Cainozoic environments in the South African interior, PhD dissertation, (Faculty of Natural and Agricultural Sciences, University of the Free State, Bloemfontein) Pp 329.

Rovner, I. 1971. Potential of Opal Phytoliths for use in Paleocological Reconstruction. *Quaternary Research* **1**:343-359.

Rucina S.M., Muiruri, V.M., Downton, L., Marchant, R. 2010. Late-Holocene savanna dynamics in the Amboseli Basin, Kenya. *The Holocene* **20**(5): 667-677.

Ruff, C.B. and Walker, A., 1993. Body size and body shape. In: Walker, A. and Leakey, R.E. (Eds.), *The Nariokotome Homo erectus Skeleton*. Harvard University Press, Cambridge. Pp.234-265.

Runge, F. 1995. The Opal Phytolith for Use in Paleocological Reconstruction in the Humid Tropics of Africa. *Zeitschrift für Geomorphologie N.F. supplementbände* **99**:53-64.

Runge, F 1999. The Opal Inventory of Soils in Central Africa-Quantities, Shapes, Classification, and Spectra. *Review of Palaeobotany and Palynology* **107**:23-53.

Russell, J.M., Johnson, T.C., 2005. A high-resolution geochemical record from Lake Edward, Uganda-Congo, and the timing and causes of tropical African drought during the late Holocene. *Quaternary Science Reviews* **24**, 1375-1389.

Russell, J.M., Johnson, T.C., 2007. Little Ice Age drought in equatorial Africa: Intertropical Convergence Zone migrations and El Nino-Southern Oscillation variability. *Geology* **35**, 21-24.

Sansom, H.W. 1954. The climate of East Africa based on Thornthwaite's classification. *E.Afri. Meteorol. Dept. Mem.* **3**:1-49

Schefuß, E., Schouten, S., Jansen, J.H.F. and Sinninghe Damsté, J.S., 2003. Africa vegetation controlled by tropical sea surface temperatures in the mid-Pleistocene period. *Nature* **422**: 418-421.

Scholz, C.A., Johnson, T.C., Cohen, A.S., King, J.W. Peck, J.A., Overpeck, J.T., Talbot, M.R., Brown, E.T., Kalindekaffe, L., Amoako, P.L.O. Lyons, R.P., Shanahan, T.M., Castañeda, I.S., Heil, C.W., Forman, S.L., McHargue, L.R., Beuning, K.R., Gomez, J. and Pierson, J. 2007. East African

megadroughts between 135 and 75 thousand years ago and on early-modern human origins. *National Academy of Science of USA (PNAS)* **104** (42): 16416-16421.

Shillito, L. 2012. Grains of truth or transparent blindfolds? A review of current debates in archaeological phytolith analysis. *Vegetation History Archaeobotany*

Sikes, N.E., 1994. Early hominid habitat preference in East Africa: Paleosol carbon isotopic evidence. *Journal of Human Evolution* **27**:25-45.

Sikes, N.E., Potts, R. and Behrensmeyer, A.K., 1997. Isotopic study of Pleistocene palaeosols from the Olorgesailie Formation, southern Kenya rift. *Journal of Human Evolution* **32**: A21-A21

Sikes, N. E., Potts, R. and Behrensmeyer, A.K., 1999. Early Pleistocene habitat in Member 1 Olorgesailie based on palaeosol stable isotopes. *Journal of Human Evolution* **37**: 721-746.

Sikes, N. E., and Ashley, G. M., 2007. Stable Isotopes of pedogenic carbonates as indicators of paleoecology in the Plio-Pleistocene (Upper Bed I), western margin of Olduvai Basin, Tanzania. *Journal of Human Evolution* **53**: 574-594.

Soares, P., Rito, T., Pereira, L., & Richards, M. B. (2016). A genetic perspective on African prehistory. In S. C. Jones & B. A. Stewart (Eds.), *Africa from MIS 6-2: Population dynamics and paleoenvironments* (pp. 383–405). Dordrecht: Springer.

Somer, B.F. 2003. A Late Pleistocene and Holocene phytolith Record, Lower Salmon River Canyon, Idaho. Unpublished MA thesis, (Department of Anthropology, University of Alberta, Edmonton, Alberta). Pp 186.

Ssemmanda, I., Ryves, D.B., Bennike, O., Appleby, P.G., 2005. Vegetation history in western Uganda during the last 1200 years: a sediment-based reconstruction from two crater lakes. *The Holocene* **15**: 119-132.

Stager, J.C., Cumming, B.F., Meeker, L., 2003. A 10,200-year high resolution diatom record from Pilkington Bay, Lake Victoria, East Africa. *Quaternary Research* **59**: 172-181.

Stager, J.C., Ryves, D., Cumming, B.F., Mecker, L.D., Beer, J. 2005. Solar Variability and the levels of Lake Victoria, East Africa, during the last millennium. *Journal of Paleolimnology* **33**: 243-251.

Stewart, B.A, Jones, S.C. 2016 Africa from MIS 6-2: The Florescence of Modern Humans. In Sacha C. Jones and Brian A. Stewart (eds.), *Africa from MIS 6-2: Population Dynamics and Paleoenvironments, Vertebrate Paleobiology and Paleoanthropology*, DOI 10.1007/978-94-017-7520-5_1

Strömberg, C.A.E. 2003. The Origin and the spread of grass-dominated ecosystems during the Tertiary of North America and how it relates to the evolution of hyposodonty in equids, PhD Thesis, Integrative Biology, Berkeley: University of California.

Strömberg, C.A.E., 2004. Using Phytolith assemblages to reconstruct the origin and spread of grass-dominated habitats in the great plains of North America during the late Eocene to early Miocene. *Palaeogeography, Palaeoclimatology, Palaeoecology* **207**:239-275

Strömberg, C.A.E., 2009. Methodological concerns for analysis of phytolith assemblages: Does count size matter? *Quaternary International* **193**: 124-140.

Taylor, D., Robertshaw, P., Marchant, R., 2000. Environmental change and economic upheaval in precolonial western Uganda. *The Holocene* **10**: 527-536.

Timberlake, J. Chidumayo, E. and Sawadogo, L. 2010. Distribution and characteristics of African Dry Forests and woodlands. In: Chidumayo E.N. and Gumbo, D.J. *The dry forest and woodlands of Africa. Managing for products and services* 2010. Pp 11-42.

Thorn, V.C. 2004. Phytolith evidence for C₄-dominated grassland since the early Holocene at Long Pocket, northeast Queensland, Australia. *Quaternary Research* **61**:168-180.

Tieszen, L.L., Senyimba, M.M., Imbamba, S.K. and Troughton, J.H. 1979. The distribution of C₃ and C₄ grasses and carbon isotope discrimination along an altitudinal and moisture gradient in Kenya. *Oecologia* **37**:337-350

Trauth, M. H., Deino, A., and Strecker, M.R., 2001. Response of the East African climate to orbital forcing during the last interglacial (130-117 ka) and the early last glacial (117-60 ka). *Geology* **29**: 499-502.

Trauth, M.H., Deino, A., Bergner, A.G.N., and Strecker, M. R., 2003. East African climate change and orbital forcing during the last 175kyr BP. *Earth Planetary Science Letters* **206**: 297-313.

Trauth, M. H., Maslin, M.A., Deino, A. and Strecker, M. R. 2005. Late Cenozoic Moisture History of East Africa. *Science* **309**: 2051-2053.

Trauth, M. H., Maslin, M., Deino, A., Strecker, M.R., Bergner, A.G.N., and Duhnforth, M., 2007. High- and low-latitude forcing of Plio-Pleistocene East African climate and human evolution. *Journal of Human Evolution* **53**: 475-486.

Twiss, P.C., Suess, E. and Smith, R.M. 1969. Morphological Classification of Grass Phytoliths. *Soil Science Society of America Proceedings* **33**:109-115.

Twiss, P.C. 1983. Dust Deposition and Opal Phytoliths in the Great Plains. *Transactions of the Nebraska Academy of Science* **11**:73-82.

Twiss, C. 1992. Predicted World Distribution of C₃ and C₄ Grass Phytoliths. In: Rapp, G. Jr. and Mulholland, S.C. 1992. *Phytolith Systematics, Emerging Issues Advanced in Archaeological and Museum Science* **1**:113-128. Plenum Press, New York.

Tryon, C.A., Faith, J.T., Peppe, D.J., Fox, D.L., McNulty, K.P., Peppe, D.J., Fox, D.L., McNulty, K.P., Jenkins, K., Dunsworth, H., Harcourt-Smith, W. 2010. The Pleistocene archaeology and environments of the Wasirya Beds, Rusinga Island, Kenya. *Journal of Human Evolution* **59**:657-671

Trauth, M.H., Deino, A.L., Bergner, A.G.N. and Strecker, M.R. (2003) East African climate change and orbital forcing during the last 175 kyr BP. *Earth Planet. Sci. Lett.*, **206**, 297–313.

Umer, M., Legesse, D., Gasse, F., Bonniefille, R., Lamb, H., & Leng, M.J. (2004). Late Quaternary Climate Changes in the Horn of Africa. In *Past Climate Variability through Europe and Africa* (R.W. Battarbee, F. Gasse and C. Stickley Eds.), (159-180). New York: Springer.

Verschuren, D., Laird, K.R. and Cumming B.F. 2000. Rainfall and drought in equatorial East Africa during the last 1,100 years. *Nature* **403**:410-414.

Verschuren, D. 2001. Reconstructing fluctuations of shallow East African Lake during the past 1800yrs from sediment stratigraphy in a submerged crater basin. *Journal of Paleolimnology* **25**: 297-311.

Verschuren, D., Damtse, J.S.S., Moernaut, J. Kristen, I., Blaaum, M., Fagot, M., Haug, G.H, CHALLACEA project members 2009. Half-Precessional dynamic of monsoon rainfall near the East Africa Equator. *Nature* **462**: 637-641.

Verschuren, D., and Charman, D.J. 2009. Latitudinal linkages in late Holocene moisture-balance variation. In: Richard W. Battarbee and Heather A. Binney. *Natural Climate perspective* Eds.

Vrba, E.S., 1985. Environmental and evolution: Alternative causes of the temporal distribution of evolutionary events. *South Africa Journal of Science* **81**: 229-236

Vrba, E.S., 1995. The fossil record of African antelopes (Mammalia, Bovidae) in relation to human evolution and paleoclimate. In: Vrba, E.S., Denton, G.H., Partridge, T.C., Burckle, L. H. (Eds.), *Paleoclimate and Evolution, with Emphasis on Human Origins*. Yale University Press, New Haven, Pp. 385-424.

Vrba, E.S. 2000. Major features of Neogene mammalian evolution in Africa. In Partridge, T.C. and Maud, R.R. (Eds.) *The Cenozoic of Southern Africa*. Oxford University Press, New York, Pp. 277-304.

Wallis, L.A. 2003. An Overview of Leaf Phytolith Production Patterns in Selected Northwest Australian Flora. *Review of Palaeobotany and Palynology* 125:201-248.

Walter, R.C., Manega, P.C., Drake, R.E. and Curtis, G.H. 1991. Laser-Fusion $^{40}\text{Ar}/^{39}\text{Ar}$ dating of Bed I, Olduvai Gorge, Tanzania. *Nature* **354**: 145-149.

White, F., 1983. The vegetation Map of Africa- a Descriptive Memoir to Accompany the UNESCO/AETFAT/UNSO vegetation map of Africa. U.N. (Eds.). Scientific and Cultural Organization, Paris. **20**: Pp.356.

White, T.D., 1995. African Omnivore: global climatic change and Plio-Pleistocene hominids and suids. In: Vrba, E. S. Denton, G.H., Partridge, T.C., Burckle, L. H. (Eds.), *Paleoclimate and Evolution, with Emphasis on Human Origins*. Yale University Press, New Haven, Pp. 385-424.

White, T.D., Asfaw, B., DeGusta, D., Giblbert, H., Richards, G.D., Suwa, G., Howell, F.C., 2003. Pleistocene *Homo sapiens* from Middle Awash, Ethiopia. *Nature* **423**: 742–747.

White, T.D., WoldeGabriel, G., Asfaw, B., Gilbert, H., Haile-Selassie, Y., Hart, W.K., Hlusko, L.J., Howell, F.C., Kono, R.T., Lehmann, T., Louchart, A., Lovejoy, C.O., Renne, P.R., Saegusa, H., Vrba, E.S., Wesselman, H. and Suswa, G. 2006. Asa Issie, Aramis and origin of *Australopithecus*. *Nature* **440**: 883-889.

White, T.D., Ambrose, S.H., Suwa, G. And WoldeGabriel, G. 2010. Response to Comment on Palaeoenvironments of *Ardipithecus ramidus*. *Science* **328**: 1105-e. DOI: 10.1126/science. 1185466.

Willoughby, P.R. 2007. *The evolution of modern humans in Africa: a comprehensive guide* New York: Altamira Press.

Winkler, A.J. 1995. Small mammals from the early Pliocene at Kanapoi, West Turkana, northern Kenya. *Journal of Vertebrate Palaeontology* 15(3): 60A.

WoldeGabriel, G., White, T.D., Suwa, G., Renne, P., deHeinzelin, J., Hart, W.K. and Helken G. 1994. Ecological and temporal placement of early Pliocene hominids at Aramis, Ethiopia. *Nature* **371**:330–333.

WoldeGabriel, G., Ambrose, S.H., Barboni, D., Bonnefille, R., Bremond, L., Currie, B., DeGusta, D., Hart, W.K., Murray, A.M., Renne, P.R. Jolly-Saad, M.C., Stewart, K.M. and White, T.D. 2009. The Geological, Isotopic, Botanical, Invertebrate and Lower Vertebrate Surroundings of *Ardipithecus ramidus*. *Science* 326: 65e5. DOI:10.1126/science.1175812.

Wright, D.K., Forman, S.L., Kiura, P., Bloszies, C., Beyin, A. 2015. Lakeside view: Sociocultural Responses to changing water levels of lake Turkana, Kenya. *African Archaeological Review* 1-34.

Wright, D. K., 2017. Humans as Agents in the Termination of the African Humid Period. *Frontiers in Earth Sciences*, **5**(4):1-14.

Wynn, J.G. 2004. Influence of Plio-Pleistocene aridification on human evolution from paleosols of the Turkana Basin, Kenya. *American Journal of Physical Anthropology*. **123**: 106-118

Yuretich, R.F., Cerling, T.E. 1983. Hydrogeochemistry of lake Turkana Kenya: mass balance and Mineral reactions in an alkaline lake. *Geochem, Cosmochem, Acts* **47**: 1099-1109.

Zurro, D., Madella, M., Briz, I., Vila, A. 2016. Variability of the phytolith record in fisher–hunter–gatherer sites: An example from the Yamana society (Beagle Channel, Tierra del Fuego, Argentina). *Quaternary International* **193**: 184-194

APPENDICES

Appendix I. Age versus depth of the ODP core; the model assigns depth age on a cm-by-cm scale (Deino et al., *in progress*)

Slide number	Depth (meter below surface)	Z prime (m)	Z prime (cm)	Age (years BP)	Age (years BP)	Age (year BP)	Age (years BP)	Age (years BP)
				95% CI lower bound 2.50%	80% CI lower bound 10%	<u>Most probable age</u> 50%	80% CI upper bound 90%	95% CI upper bound 97.50%
1	27.03	27.030	2703	58,177.6	67,605.5	77,498.6	85,518.8	88,561.0
2	27.51	27.510	2751	62,434.3	70,556.6	79,400.6	86,301.9	89,540.4
3	27.98	27.980	2798	67,266.5	73,696.6	81,449.8	87,490.6	90,650.4
4	28.35	28.296	2829.6	71,758.9	76,256.5	83,246.7	88,677.5	91,792.2
5	28.95	28.662	2866.2	75,219.5	78,273.0	84,739.9	89,777.2	92,811.6
6	29.43	29.142	2914.2	76,616.5	79,231.3	85,606.3	90,659.9	93,513.9
7	29.91	29.622	2962.2	77,620.5	80,031.5	86,290.4	91,348.7	94,017.1
8	30.39	30.102	3010.2	78,236.1	80,812.3	86,896.8	91,857.1	94,470.8
9	30.87	30.582	3058.2	79,002.3	81,626.8	87,461.7	92,354.3	94,829.6
10	31.44	31.152	3115.2	79,777.5	82,545.5	88,100.5	92,916.8	95,679.1
11	31.83	31.542	3154.2	80,266.8	83,207.6	88,567.7	93,448.2	96,256.7
12	32.32	32.032	3203.2	80,681.6	83,840.8	89,176.6	94,039.2	97,030.7
13	32.8	32.512	3251.2	81,459.9	84,480.2	89,865.7	94,761.6	97,590.7
14	33.34	33.052	3305.2	82,572.3	85,537.0	90,899.7	95,617.9	98,347.5
15	33.82	33.266	3326.6	83,233.9	86,277.9	91,519.9	96,234.8	99,134.8
16	34.31	33.686	3368.6	84,713.5	87,703.1	92,627.7	97,399.8	100,748.3
17	35.75	35.116	3511.6	88,614.9	91,183.2	95,574.4	101,129.8	105,777.0
18	36.21	35.576	3557.6	89,660.7	92,027.6	96,667.4	102,208.3	107,534.1
19	36.68	36.046	3604.6	90,936.1	93,264.7	98,043.9	103,923.3	110,252.4

20	37.18	36.412	3641.2	93,127.3	95,516.9	100,502.0	108,774.7	119,019.7
21	37.66	36.536	3653.6	93,780.9	96,198.0	101,304.6	110,407.9	121,520.8
22	38.15	36.970	3697	95,308.3	97,881.4	103,855.7	116,033.9	126,260.3
23	38.63	37.450	3745	96,597.9	99,563.6	106,264.0	120,637.7	130,567.4
24	39.11	37.769	3776.9	97,185.0	100,527.1	107,805.4	122,739.9	132,228.5
25	39.6	38.250	3825	98,203.8	101,905.9	110,166.0	125,313.3	134,794.1
26	40.21	38.860	3886	99,376.2	103,553.3	113,502.6	128,479.3	137,900.3
27	40.67	39.320	3932	100,086.6	104,690.2	115,727.1	131,288.3	140,493.6
28	41.16	39.810	3981	101,029.5	105,805.2	117,681.4	133,740.2	142,720.0
29	41.66	40.310	4031	102,218.0	107,172.6	119,798.8	135,969.1	144,288.3
30	42.12	40.770	4077	103,229.9	108,645.4	121,756.7	138,081.9	146,227.9
31	42.65	41.300	4130	104,298.1	110,622.1	123,773.0	140,445.4	148,355.1
32	43.06	41.710	4171	105,426.6	112,296.3	125,508.9	142,227.4	149,782.3
33	43.57	42.220	4222	107,512.3	114,378.0	127,730.5	144,443.4	151,772.7
34	44.05	42.700	4270	109,701.4	116,354.6	129,788.4	146,578.4	153,795.3
35	44.54	43.190	4319	112,142.7	118,742.5	132,321.6	148,801.5	156,063.9
36	45.02	43.670	4367	115,459.6	121,527.3	134,938.9	151,094.6	158,460.2
37	45.5	44.150	4415	119,198.1	124,360.4	138,068.4	154,004.3	161,550.4
38	45.99	44.374	4437.4	121,053.8	125,831.1	139,953.6	155,737.1	163,564.5
39	46.47	44.512	4451.2	122,558.6	127,135.3	141,415.3	156,954.2	164,867.2
40	46.96	44.591	4459.1	125,593.2	130,275.1	144,057.4	158,550.3	165,984.5
41	47.44	44.639	4463.9	127,437.0	132,182.9	145,662.7	159,520.1	166,663.4
42	47.92	44.984	4498.4	140,689.1	145,894.7	157,200.9	166,490.3	171,542.8
43	48.4	45.205	4520.5	146,719.4	151,680.7	161,813.0	169,778.8	173,861.7
44	48.89	45.352	4535.2	150,602.9	155,373.7	164,736.6	171,905.1	175,362.3
45	49.45	45.844	4584.4	167,081.9	169,890.0	174,928.8	178,600.6	180,172.0
46	49.85	46.244	4624.4	176,671.0	178,125.2	180,737.0	183,527.5	186,226.9
47	50.34	46.734	4673.4	181,288.8	182,231.3	184,292.7	188,069.8	192,289.7

48	50.82	46.934	4693.4	181,748.2	182,747.2	185,071.1	189,386.2	193,383.5
49	51.3	47.126	4712.6	182,110.7	183,217.8	185,815.4	190,369.5	194,243.8
50	51.78	47.345	4734.5	182,477.4	183,739.9	186,662.5	191,323.6	195,111.7
51	52.38	47.927	4792.7	183,345.5	185,072.7	188,943.5	193,363.0	196,795.7
52	52.76	47.965	4796.5	183,399.7	185,158.4	189,093.2	193,484.4	196,890.9
53	52.87	47.976	4797.6	183,415.3	185,183.3	189,136.5	193,519.5	196,918.4
54	53.13	48.002	4800.2	183,452.5	185,242.1	189,238.6	193,603.1	196,982.9
55	53.35	48.024	4802.4	183,485.4	185,294.0	189,322.2	193,678.6	197,030.2
56	53.58	48.047	4804.7	183,519.8	185,348.3	189,409.5	193,757.6	197,079.7
57	53.76	48.065	4806.5	183,546.7	185,390.7	189,477.9	193,819.4	197,118.5
58	53.83	48.072	4807.2	183,557.2	185,407.3	189,504.5	193,843.4	197,133.5
59	54.32	48.553	4855.3	184,268.6	186,550.9	191,318.8	195,489.5	198,192.1
60	54.8	49.033	4903.3	184,972.2	187,799.7	193,023.1	197,095.7	199,467.1
61	55.52	49.753	4975.3	187,840.3	190,684.8	195,651.4	199,940.8	202,315.3
62	55.83	50.063	5006.3	189,797.9	192,292.3	197,061.0	201,489.3	203,874.6
63	56.39	50.623	5062.3	194,298.4	196,152.4	200,465.1	204,940.4	207,170.4
64	56.87	51.033	5103.3	196,366.3	198,700.2	202,736.8	206,702.9	208,973.0
65	57.36	51.180	5118	196,993.3	199,479.8	203,502.1	207,378.7	209,546.3
66	57.84	51.569	5156.9	198,771.7	201,538.1	205,533.4	209,216.7	211,172.3
67	58.49	52.111	5211.1	201,984.8	204,359.6	208,440.9	212,169.6	214,285.3
68	58.95	52.249	5224.9	202,769.2	205,062.8	209,217.9	212,991.5	215,219.3
69	59.31	52.357	5235.7	203,383.0	205,613.1	209,825.9	213,634.8	215,950.3
70	59.86	52.411	5241.1	203,690.0	205,888.3	210,129.9	213,956.5	216,315.7
71	60.4	52.465	5246.5	203,996.9	206,163.5	210,434.0	214,278.1	216,681.2
72	61.52	53.396	5339.6	205,882.1	208,410.3	212,474.8	216,317.6	218,338.2
73	62	53.444	5344.4	205,963.8	208,508.0	212,561.2	216,410.2	218,400.0
74	62.49	53.493	5349.3	206,047.2	208,607.7	212,649.4	216,504.7	218,463.2
75	62.97	53.506	5350.6	206,070.3	208,633.8	212,671.4	216,527.8	218,478.8

76	63.45	53.506	5350.6	206,070.3	208,633.8	212,671.4	216,527.8	218,478.8
77	63.93	53.506	5350.6	206,070.3	208,633.8	212,671.4	216,527.8	218,478.8
78	64.41	53.506	5350.6	206,070.3	208,633.8	212,671.4	216,527.8	218,478.8
79	64.89	53.506	5350.6	206,070.3	208,633.8	212,671.4	216,527.8	218,478.8
80	65.36	53.506	5350.6	206,070.3	208,633.8	212,671.4	216,527.8	218,478.8
81	65.77	53.606	5360.6	206,257.0	208,829.7	212,827.6	216,688.3	218,588.4
82	65.91	53.746	5374.6	206,518.2	209,104.0	213,046.3	216,912.9	218,742.0
83	66.34	53.915	5391.5	206,833.6	209,435.1	213,310.2	217,184.0	218,927.3
84	66.83	53.964	5396.4	206,925.1	209,531.1	213,386.8	217,262.6	218,981.0
85	67.31	54.012	5401.2	207,015.3	209,621.9	213,462.9	217,335.8	219,031.7
86	67.8	54.061	5406.1	207,109.5	209,704.9	213,544.3	217,398.8	219,077.6
87	68.36	54.101	5410.1	207,186.4	209,772.7	213,610.7	217,450.2	219,115.0
88	68.76	54.101	5410.1	207,186.4	209,772.7	213,610.7	217,450.2	219,115.0
89	69.24	54.107	5410.7	207,197.9	209,782.9	213,620.6	217,457.9	219,120.6
90	69.73	54.138	5413.8	207,257.5	209,835.4	213,672.1	217,497.7	219,149.6
91	70.28	54.193	5419.3	207,363.2	209,928.5	213,763.4	217,568.4	219,201.0
92	70.7	54.229	5422.9	207,432.4	209,989.5	213,823.1	217,614.6	219,234.7
93	71.18	54.229	5422.9	207,432.4	209,989.5	213,823.1	217,614.6	219,234.7
94	71.66	54.460	5446	207,876.4	210,380.8	214,206.6	217,911.4	219,450.7
95	72.14	54.564	5456.4	208,029.8	210,550.2	214,365.4	218,040.1	219,547.8
96	72.62	54.601	5460.1	208,074.1	210,608.9	214,418.8	218,084.8	219,582.2
97	73.72	55.492	5549.2	209,503.4	212,032.2	215,793.0	219,153.5	220,412.4
98	74.25	55.532	5553.2	209,571.1	212,107.5	215,860.4	219,193.4	220,451.4
99	74.39	55.672	5567.2	209,799.3	212,380.7	216,098.4	219,326.2	220,589.3
100	74.51	55.792	5579.2	209,994.9	212,615.0	216,302.4	219,440.0	220,707.4
101	74.69	55.972	5597.2	210,288.3	212,966.3	216,608.4	219,610.8	220,884.7
102	75.17	56.452	5645.2	211,435.2	213,795.2	217,455.1	220,180.5	221,355.0
103	75.65	56.932	5693.2	212,417.5	215,022.4	218,312.4	220,831.4	221,923.9

104	75.82	57.012	5701.2	212,596.9	215,237.4	218,457.7	220,943.1	222,020.5
105	76.13	57.252	5725.2	213,459.3	215,932.8	218,932.0	221,310.0	222,308.5
106	76.61	57.732	5773.2	215,861.8	217,608.4	220,110.1	222,232.7	223,132.6
107	77.09	58.102	5810.2	217,975.9	219,054.0	221,167.1	223,059.5	223,903.9
108	77.51	58.389	5838.9	219,012.1	220,011.2	221,904.7	223,618.7	224,362.7
109	77.57	58.407	5840.7	219,077.1	220,071.2	221,951.0	223,653.8	224,391.4
110	78.05	58.542	5854.2	219,542.2	220,510.9	222,287.4	223,897.2	224,594.7
111	78.51	58.578	5857.8	219,653.2	220,621.8	222,370.8	223,950.5	224,641.5
112	78.96	58.713	5871.3	220,069.2	221,038.0	222,683.7	224,150.5	224,817.1
113	79.25	58.807	5880.7	220,358.9	221,327.7	222,901.6	224,289.7	224,939.3
114	79.5	58.882	5888.2	220,590.1	221,558.9	223,075.5	224,400.8	225,036.8
115	79.64	58.924	5892.4	220,719.5	221,688.3	223,172.8	224,463.0	225,091.4
116	79.98	58.999	5899.9	220,950.7	221,919.5	223,346.7	224,574.1	225,188.9
117	80.46	59.143	5914.3	221,409.4	222,347.3	223,697.3	224,824.5	225,417.3
118	80.94	59.199	5919.9	221,587.9	222,513.6	223,833.8	224,921.9	225,506.2
119	81.64	59.301	5930.1	221,912.9	222,816.6	224,082.2	225,099.5	225,668.2
120	82.13	59.448	5944.8	222,381.4	223,253.2	224,440.3	225,355.3	225,901.6
121	82.57	59.601	5960.1	222,805.8	223,597.4	224,720.9	225,647.6	226,212.2
122	82.87	59.804	5980.4	223,325.8	223,978.9	225,030.3	226,053.3	226,670.4
123	83.36	59.988	5998.8	223,797.1	224,324.6	225,310.7	226,421.0	227,085.8
124	83.84	60.468	6046.8	223,998.2	224,617.5	225,637.9	226,912.4	227,765.6
125	84.2	60.828	6082.8	224,156.2	224,784.0	225,860.4	227,187.1	228,071.4
126	84.69	61.318	6131.8	224,328.2	224,973.4	226,137.1	227,529.2	228,437.2
127	85.17	61.798	6179.8	224,471.1	225,137.9	226,394.7	227,847.6	228,890.4
128	85.46	62.088	6208.8	224,557.3	225,236.9	226,552.1	228,036.1	229,195.2
129	85.91	62.538	6253.8	224,697.3	225,400.4	226,803.4	228,330.3	229,623.7
130	86.39	62.766	6276.6	224,802.7	225,513.1	226,932.0	228,517.9	229,769.5
131	86.87	62.952	6295.2	224,888.7	225,605.1	227,036.9	228,670.9	229,888.4

132	87.35	63.432	6343.2	225,090.9	225,813.7	227,350.0	229,050.8	230,277.8
133	87.84	63.922	6392.2	225,263.4	226,043.7	227,677.7	229,534.8	230,754.5
134	88.22	64.302	6430.2	225,588.1	226,333.9	227,986.7	229,993.5	231,290.2
135	88.8	64.770	6477	225,967.3	226,773.7	228,461.7	230,696.7	232,578.6
136	89.28	65.250	6525	226,270.4	227,152.5	228,918.5	231,362.5	233,956.3
137	89.76	65.730	6573	226,513.0	227,394.5	229,251.1	231,889.5	234,904.8
138	90.24	66.210	6621	226,732.6	227,609.5	229,551.4	232,450.2	235,596.5
139	90.73	66.476	6647.6	226,867.7	227,738.4	229,728.1	232,790.9	235,859.3
140	91.21	66.949	6694.9	226,987.6	228,015.4	230,007.1	233,482.9	236,483.1
141	91.79	67.529	6752.9	227,138.8	228,342.7	230,332.9	234,150.2	237,234.2
142	92.18	67.919	6791.9	227,312.9	228,530.3	230,560.7	234,683.1	237,862.8
143	92.62	68.359	6835.9	227,514.0	228,748.4	230,839.2	235,291.5	238,680.2
144	93.14	68.879	6887.9	227,853.7	229,040.9	231,238.5	236,198.3	239,488.3
145	93.62	69.359	6935.9	228,745.6	229,880.1	232,317.8	237,889.8	241,073.5
146	94.1	69.839	6983.9	229,548.5	230,838.1	233,471.9	239,207.4	242,178.0
147	94.59	70.329	7032.9	230,396.2	231,710.5	234,643.0	240,149.0	242,929.0
148	95.07	70.799	7079.9	231,085.9	232,483.3	235,723.4	241,080.3	243,602.2
149	95.55	70.992	7099.2	231,324.3	232,793.9	236,150.3	241,483.9	243,872.2
150	96.04	71.139	7113.9	231,472.6	232,977.1	236,462.1	241,684.6	244,061.1
151	96.52	71.226	7122.6	231,559.2	233,083.7	236,646.2	241,799.7	244,172.4
152	97.01	71.226	7122.6	231,559.2	233,083.7	236,646.2	241,799.7	244,172.4
153	97.49	71.226	7122.6	231,559.2	233,083.7	236,646.2	241,799.7	244,172.4
154	97.88	71.336	7133.6	231,668.7	233,218.5	236,879.0	241,945.3	244,313.0
155	98.46	71.866	7186.6	232,453.7	233,990.9	237,972.6	242,652.3	244,975.1
156	98.94	72.346	7234.6	233,109.9	234,740.9	238,918.6	243,410.1	245,451.7
157	99.42	72.826	7282.6	233,603.3	235,558.6	239,871.3	244,092.3	245,829.2
158	99.9	73.306	7330.6	234,419.5	236,452.2	240,829.6	244,767.0	246,555.2
159	100.38	73.786	7378.6	235,433.0	237,551.6	241,848.1	245,486.5	247,499.4

160	100.86	74.266	7426.6	236,804.3	239,075.0	243,058.9	246,610.2	248,592.5
161	101.34	74.586	7458.6	238,529.6	240,727.1	244,401.2	247,897.0	249,768.0
162	101.82	74.586	7458.6	238,529.6	240,727.1	244,401.2	247,897.0	249,768.0
163	102.3	74.586	7458.6	238,529.6	240,727.1	244,401.2	247,897.0	249,768.0
164	102.78	74.700	7470	239,739.7	241,776.0	245,320.0	248,672.6	250,544.4
165	103.26	74.802	7480.2	240,822.3	242,714.6	246,142.1	249,366.4	251,239.0
166	104.23	75.232	7523.2	244,567.3	246,352.0	249,834.4	254,969.0	259,911.4
167	104.72	75.260	7526	244,765.7	246,571.2	250,087.4	255,482.6	260,795.3
168	105.2	75.308	7530.8	245,105.7	246,946.8	250,521.1	256,363.1	262,310.6
169	105.68	75.356	7535.6	245,445.7	247,322.5	250,954.8	257,243.6	263,825.9
170	107.18	76.613	7661.3	249,613.6	252,073.6	258,962.5	276,740.4	287,548.4
171	107.58	77.013	7701.3	250,494.8	253,174.6	261,310.3	281,413.2	292,443.9
172	108.05	77.483	7748.3	251,428.8	254,550.2	264,033.5	285,172.6	299,319.6
173	108.53	77.913	7791.3	252,219.7	255,646.7	266,729.8	287,503.1	301,973.3
174	109.01	78.393	7839.3	253,137.9	256,810.2	269,618.5	290,867.9	304,782.7
175	109.49	78.873	7887.3	254,190.1	257,967.3	272,179.2	294,466.0	308,015.4
176	109.97	79.353	7935.3	255,060.1	259,452.4	274,842.6	297,083.1	310,155.4
177	110.45	79.833	7983.3	255,931.1	261,200.9	277,401.3	299,449.0	312,084.3
178	110.94	80.323	8032.3	256,913.0	262,926.4	279,963.3	301,947.5	314,207.3
179	111.42	80.803	8080.3	257,817.8	264,687.9	282,479.3	304,556.4	316,401.4
180	111.9	81.283	8128.3	258,764.7	266,364.1	285,125.9	306,946.8	318,162.1
181	112.39	81.773	8177.3	259,932.5	267,948.7	287,796.6	309,206.6	320,086.9
182	112.87	82.253	8225.3	260,990.8	269,646.8	290,530.8	311,556.1	321,808.5
183	113.36	82.703	8270.3	262,083.0	271,348.7	293,153.7	313,660.4	322,997.2
184	113.84	83.063	8306.3	263,336.5	272,755.5	295,104.7	315,132.3	324,016.7
185	114.32	83.543	8354.3	265,718.3	274,997.5	297,563.6	316,934.5	325,650.8
186	114.79	84.013	8401.3	267,255.7	276,841.8	300,268.1	318,773.8	326,999.1
187	115.28	84.503	8450.3	269,298.0	279,256.1	302,610.2	320,448.3	328,082.0

188	115.76	84.983	8498.3	270,868.8	282,119.6	305,199.3	322,069.2	329,424.6
189	116.43	85.623	8562.3	274,970.8	285,897.1	308,809.8	324,292.5	330,542.0
190	116.87	86.063	8606.3	277,970.9	288,797.9	311,659.6	325,764.9	331,300.0
191	117.35	86.543	8654.3	280,676.6	291,823.2	314,092.3	327,752.6	332,619.2
192	117.84	87.033	8703.3	284,512.5	295,530.4	316,859.6	329,153.5	333,665.6
193	118.32	87.513	8751.3	288,243.2	299,474.9	319,497.0	330,598.2	335,032.4
194	118.8	87.993	8799.3	292,036.1	303,015.6	322,009.4	331,958.4	336,032.5
195	119.5	88.693	8869.3	298,904.7	310,846.1	325,927.3	334,012.4	337,711.2
196	119.91	89.103	8910.3	304,180.5	315,462.4	328,168.0	335,556.0	338,808.3
197	120.36	89.553	8955.3	310,929.0	321,083.0	330,864.8	337,545.6	340,524.3
198	120.8	89.993	8999.3	325,641.5	328,732.1	334,407.6	340,215.5	342,892.4
199	121.36	90.553	9055.3	330,391.5	333,499.2	340,194.8	350,698.4	364,757.6
200	121.84	91.033	9103.3	332,449.8	335,712.5	343,510.0	358,210.9	369,699.0
201	122.47	91.663	9166.3	334,608.1	338,394.0	347,285.1	365,247.3	376,119.8
202	122.96	92.153	9215.3	336,027.3	340,276.4	350,267.7	369,610.9	380,088.1
203	123.44	92.633	9263.3	337,163.6	341,900.9	353,117.7	372,504.8	382,977.5
204	123.92	93.113	9311.3	338,206.0	343,482.8	355,976.4	375,664.1	385,108.1
205	124.37	93.563	9356.3	339,394.1	345,307.5	358,727.7	378,675.0	387,581.6
206	124.89	94.083	9408.3	340,733.6	347,234.6	361,842.2	381,150.2	389,933.2
207	125.37	94.563	9456.3	341,703.6	349,034.8	364,746.3	383,329.0	391,792.0
208	125.85	95.043	9504.3	342,697.4	350,756.9	367,675.1	385,560.9	393,029.7
209	126.33	95.523	9552.3	344,149.3	352,358.5	370,455.1	387,642.0	394,864.5
210	126.81	96.003	9600.3	345,562.9	354,347.1	373,212.6	389,963.5	396,270.9
211	127.28	96.453	9645.3	346,870.9	356,846.5	375,849.6	391,562.9	397,265.4
212	127.78	96.893	9689.3	349,183.4	359,254.2	378,692.1	393,602.7	398,317.1
213	128.26	97.373	9737.3	351,990.5	361,672.3	381,734.2	395,343.9	399,422.0
214	128.74	97.853	9785.3	354,568.3	364,280.7	384,783.4	396,952.2	400,364.1
215	129.23	98.343	9834.3	357,436.2	367,460.1	387,817.4	398,359.9	401,495.7

216	129.71	98.823	9882.3	360,935.0	370,624.9	390,704.7	399,638.5	402,730.8
217	130.2	99.313	9931.3	364,486.9	374,533.7	393,726.0	401,005.9	403,916.7
218	130.68	99.793	9979.3	368,430.9	379,765.7	396,737.7	402,514.2	405,255.2
219	131.16	100.273	10027.3	374,575.5	387,074.6	399,700.8	404,197.3	406,985.3
220	131.65	100.763	10076.3	390,145.1	397,255.4	403,618.2	407,857.3	413,105.5
221	132.13	101.243	10124.3	403,457.0	405,769.1	410,404.3	421,828.9	435,144.4
222	132.61	101.723	10172.3	407,704.2	410,748.2	419,264.0	439,709.4	458,334.1
223	133.1	102.213	10221.3	411,002.3	415,133.5	428,116.3	451,049.1	467,125.1
224	133.58	102.693	10269.3	414,079.2	419,741.3	436,485.4	459,390.6	473,431.2
225	134.07	103.183	10318.3	417,637.2	424,465.4	444,989.0	466,433.8	479,350.7
226	134.55	103.663	10366.3	421,382.2	429,119.9	453,189.4	473,561.7	484,630.5
227	135.03	104.143	10414.3	425,763.9	434,220.4	460,965.5	481,303.4	490,818.9
228	135.81	104.923	10492.3	435,918.2	445,633.1	475,094.9	495,471.8	502,847.4
229	136.3	105.413	10541.3	446,403.8	459,986.6	488,387.6	509,704.5	524,768.8
230	136.79	105.893	10589.3	453,964.6	468,147.3	497,513.9	524,687.3	547,618.3
231	137.27	106.373	10637.3	460,009.3	473,748.8	504,188.9	538,233.8	565,579.5
232	137.79	106.843	10684.3	463,416.7	478,412.4	509,437.5	549,252.3	577,400.3
233	138.24	107.293	10729.3	465,935.7	481,971.5	514,475.1	558,840.2	584,823.9
234	138.72	107.773	10777.3	469,922.7	485,084.4	519,958.4	567,444.4	593,004.4
235	139.21	108.263	10826.3	473,608.3	487,831.8	524,973.1	574,456.4	602,297.3
236	139.69	108.743	10874.3	476,018.2	491,277.6	529,840.8	581,382.4	610,372.4
237	140.8	109.853	10985.3	482,647.3	500,221.0	542,960.9	594,749.0	622,189.1
238	141.25	110.303	11030.3	485,689.3	503,338.3	547,953.9	599,570.6	625,511.1
239	141.79	110.843	11084.3	488,399.7	507,481.5	553,282.2	605,740.8	630,204.5
240	142.22	111.273	11127.3	490,253.9	510,823.2	557,681.9	610,040.3	634,787.6
241	142.69	111.743	11174.3	491,918.9	514,552.3	562,500.9	614,970.9	639,537.5
242	143.17	112.223	11222.3	494,458.4	518,531.5	567,944.7	619,791.2	644,125.9
243	143.66	112.713	11271.3	498,108.3	522,155.7	574,155.5	624,308.1	648,592.0

244	144.14	113.193	11319.3	501,470.5	525,849.3	579,775.2	628,941.0	652,205.9
245	144.63	113.683	11368.3	505,810.0	530,174.4	585,201.2	633,440.3	655,488.4
246	145.11	114.163	11416.3	510,134.6	534,484.3	591,159.0	638,822.0	659,132.3
247	146.87	115.923	11592.3	529,307.9	553,063.8	612,840.9	655,151.4	671,990.8
248	147.35	116.403	11640.3	534,885.0	559,333.0	618,574.9	660,438.2	675,368.7
249	147.83	116.883	11688.3	539,236.2	565,656.7	624,506.6	665,741.2	678,543.3
250	148.31	117.363	11736.3	543,263.4	574,041.7	630,226.3	670,899.0	682,110.6
251	148.8	117.853	11785.3	547,679.8	585,457.1	636,640.7	675,740.2	685,800.6
252	149.28	118.333	11833.3	556,446.7	602,839.6	644,032.6	681,983.5	690,321.2
253	149.73	118.783	11878.3	577,988.6	625,292.9	657,858.5	693,764.8	708,129.4
254	151.27	120.323	12032.3	657,886.5	679,254.7	713,132.3	736,008.3	748,600.2
255	151.66	120.713	12071.3	668,105.5	691,603.9	726,859.0	745,137.5	755,050.3
256	152.43	121.483	12148.3	706,936.2	716,313.0	755,498.8	770,419.0	775,642.5
257	152.78	121.543	12154.3	712,091.0	721,235.1	758,497.0	774,301.7	782,890.5
258	153.2	121.773	12177.3	733,990.1	744,498.0	770,997.5	791,658.9	818,659.5
259	153.69	122.263	12226.3	768,030.3	775,641.0	790,780.0	831,527.6	873,605.0
260	154.17	122.743	12274.3	781,288.3	785,846.9	804,364.4	864,569.8	908,245.4
261	154.65	123.223	12322.3	785,512.8	791,050.7	817,636.0	886,891.6	932,083.3
262	155.13	123.703	12370.3	789,340.8	795,628.7	830,243.6	904,886.8	948,620.5
263	156.01	124.583	12458.3	794,586.9	803,663.9	850,386.6	932,939.9	979,029.2
264	156.49	125.063	12506.3	797,536.4	808,279.7	861,016.1	945,713.6	994,784.9
265	156.98	125.553	12555.3	800,482.9	812,927.8	873,247.5	956,469.9	1,003,828.0
266	157.45	126.023	12602.3	803,262.2	817,751.0	884,607.6	969,990.2	1,012,605.0
267	159.05	127.623	12762.3	816,065.4	840,778.9	921,820.1	1,002,393.0	1,039,764.0
268	159.54	128.113	12811.3	820,469.2	848,415.4	933,234.1	1,013,967.0	1,045,406.0
269	159.99	128.563	12856.3	823,185.8	854,764.4	944,196.1	1,021,732.0	1,049,146.0
270	160.5	129.073	12907.3	827,315.5	862,188.1	955,139.2	1,030,765.0	1,056,893.0
271	160.99	129.563	12956.3	835,291.8	872,280.7	966,203.9	1,037,906.0	1,062,305.0

272 161.47 130.043 13004.3 842,822.0 886,723.0 976,668.0 1,044,208.0 1,067,361.0

Appendix II: List of plants species analysed for modern phytolith reference data

Family	Species	Habitats/Altitude range/ site collected	Plant part
Poaceae	<i>Aristida junciformis</i> Trin. & Rupr.	400-2100m (Olorgesailie); poor eroded or stony soils	Whole
Poaceae	<i>Aristida sp.</i>	930-2000m (Olorgesailie)	Whole
Poaceae	<i>Aristida congesta</i> Roem. & Schult.	900-2100m (Taita hills); deciduous bushland often on eroded slopes	Whole
Poaceae	<i>Phragmites mauritianus</i> Kunth	0-1500m (Taita hills), shallow water streams, river banks & lakes, and swampy places	whole
Poaceae	<i>Phragmites australis</i> (Cav.) Steud.	600-1500m (Taita hills) shallow water streams, river & lake banks, in swampy places.	Whole
Poaceae	<i>Eragrostis racemosa</i> (Thunb.) Steud.	300-2300m (Olorgesailie); often on sandy/shallow stony soils	Whole
Poaceae	<i>Sporobulus africanus</i> (Poir) Robyns & Tournay	1300-2600m (Mt. Kenya), disturbed grounds/alongside paths	Whole
Poaceae	<i>Sporobulus consimilis</i> Fresen.	390-1950m (Mt Kenya) flood plains and lake shores	Whole
Poaceae	<i>Chloris virgata</i> Sw.	10-2000m (Mt. Kenya), Wooded grasslands, bushlands & disturbed habitats	Flowers
Poaceae	<i>Sporobulus angustifolius</i> A. Rich	1300-2600m (Mt. Kenya) Deciduous bushlands	Whole
Poaceae	<i>Chloris mossambicensis</i> K. Schum	400-2000m (Olorgesailie) Wooded grasslands	Whole
Poaceae	<i>Bewsia biflora</i>	2000-2400m (Mt Kenya)	Whole
Poaceae	<i>Cynodon aethiopicus</i> Clayton & Harlan	0-2000m (Olorgesailie); mostly in disturbed places	Whole
Poaceae	<i>Cynodon sp.</i>	~1000m Olorgesailie	Whole
Poaceae	<i>Brachyachne patentiflora</i> (Stent & Rattray) C.E. Hubbard	2100m (Taita hills) shallow soils over rocky bed	Whole
Poaceae	<i>Dactyloctenium aegyptium</i> (L.) Willd.	0-2100m (Taita Hills) open grasslands & woodlands	Whole
Poaceae	<i>Harpachne schimperi</i> A. Rich.	200-2000m (Olorgesailie) bushlands and grasslands	Whole

Poaceae	<i>Coelachyrum longiglume</i> Napper	230-1500m (Olorgesailie) Dry grasslands	Whole
Poaceae	<i>Cypholepis yemenica</i> (Schweinf.) Chiov.	250-2070m (Olorgesailie) Grasslands, bushlands mostly on rocky ground	Whole
Poaceae	<i>Tripogon curvatus</i> S.M. Phillips & Launert	1700-1950m (Olorgesailie) open grasslands	Whole
Poaceae	<i>Eragrostis pilosa</i> (L.) P.	0-2000m (Olorgesailie), dry grasslands	Whole
Poaceae	<i>Eragrostis superba</i> Peyr.	0-1800m (Olorgesailie); open thicket/ wooded grasslands, often in disturbed ground	Whole
Poaceae	<i>Ischaemum rugosum</i> Salisb. <i>c</i> ₄	1000-2600m (Taita hills) water logged grasslands	Whole
Poaceae	<i>Hyparrhenia drageana</i> (Nees) Stent	2200-2500m (Mt. Kenya); Open bushed and wooded grassland	Whole
Poaceae	<i>Schizachyrium jeffreysii</i>	0-900m (Olorgesailie) wooded grasslands on moist places	Whole
Poaceae	<i>Coelorhachis lepidura</i> Stapf	0-2300m (Taita hills); swampy grasslands	Whole
Poaceae	<i>Themeda triadra</i> Forssk	0-3200m (Mt. Kenya) Deciduous bushland/wooded grasslands.	Whole
Poaceae	<i>Hyparrhenia hirta</i> (L.) Stapf	1300-2700m (Mt. Kenya) wooded grasslands	Whole
Poaceae	<i>Schizachyrium brevifolium</i> (Sw.) Buse	0-900m (Olorgesailie) along stream banks	Whole
Poaceae	<i>Themeda villosa</i> (Poir.) A. Camus	0-3200m (Mt. Kenya) open grasslands & deciduous bushland	Whole
Poaceae	<i>Echinochloa sp.</i>	~ 1800m Taita hills	Whole
Poaceae	<i>Cymbopogon caesius</i> (Hock. & Arn.) Stapf	100-1300m (Olorgesailie), deciduous bushland and semi-arid grasslands	Whole
Poaceae	<i>Melinis ambigua</i> Hack.	1000-1720m (Taita hills) upland grasslands	Whole
Poaceae	<i>Melinis minutiflora</i> P.Beauv.	1000-1720m (Taita hills) open grasslands on rocky hills.	Whole
Poaceae	<i>Pennisetum purpureum</i> Schumach.	0-2000m (Mt. Kenya) Forest margins & riverine	Whole
Poaceae	<i>Pennisetum polystachion</i> (L.) Schult.	2000-2730m (Mt. Kenya) open grasslands & bushlands in disturbed areas	Whole
Poaceae	<i>Pennisetum polystachion</i>	2000-2730m (Mt. Kenya) open grasslands & bushlands in disturbed areas	Whole
Poaceae	<i>Melinis repens</i>	930-2520m (Mt, Kenya) wooded grasslands	Whole

Poaceae	<i>Digitaria ciliaris</i> (Retz.) Koel.	150-600m (Olorgesailie); open grasslands	Whole
Poaceae	<i>Setaria sphacelata</i> (Schumach.) Moss	300-3300m (Mt. Kenya) grasslands & bushlands, stony hillside to river banks	Whole
Poaceae	<i>Panicum eickii</i> Mez	2800m (Mt. Kenya) Forest edges, swamp grasslands (uplands)	Whole
Poaceae	<i>Setaria poiretiana</i> (Schult.) Kunth	300-2300m (Mt. Kenya) Bushed-grasslands	Whole
Poaceae	<i>Setaria plicatilis</i> (Hochst.) Engl.	900-2400m (Mt. Kenya) Forest shade	Whole
Poaceae	<i>Setaria incrassata</i> (Hochst.) Hack.	0-2400m (Olorgesailie) Balck caly soils in open bushlands	Whole
Poaceae	<i>Oplismenus compositus</i> (L.) P. Beauv.	0-2300m (Mt. Kenya) forest shade	Whole
Poaceae	<i>Oplismenus hirtellus</i> (L.) P. Beauv.	0-2500m (Mt. Kenya) forest shade	Whole
Poaceae	<i>Panicum maximum</i> Jacq.	0-2400 (Olorgesailie) wooded grasslands, forest edges	Whole
Poaceae	<i>Brachiaria cf. semiundulata</i>	0-1200m (Taita hills)	Whole
Cyperaceae	<i>Cyperus dives</i>	700-2000 (Olorgesailie) swampy areas	Whole
Cyperaceae	<i>Cyperus papyrus</i> L.	650-2000m (Olorgesailie) swampy areas	Flowers
Cyperaceae	<i>Cyperus sp.</i>	930-2000m (Olorgesailie)	Whole
Cyperaceae	<i>Cyperus spp.</i>	1800-2200 (Mt. Kenya)	Stem, leaves, flowers
Cyperaceae	<i>Kyllinga odorata</i> Vahl	1140-1500 (Mt Kenya) Moist soils, forest edges	Stem/Leaf
Cyperaceae	<i>Scleria boivinii</i> Steudel	1140-1160m (Mt. Kenya) swampy forest edges	Leaf
Cyperaceae	<i>Eleocharis spp.</i>	950-1200 (Olorgesailie) marshes at low altitudes	Whole
Acanthaceae	<i>Barleria titensis</i> S. Moore	350-1050 (Taita hills), dry bushland/woodland	Whole
Acanthaceae	<i>Acanthus eminens</i> C.B.CL.	1500-2650m (Mt. Kenya), Moist or dry forests	stem, flowers roots
Anarcadiaceae	<i>Rhus natalensis</i> Krauss	450-2700 (Mt. Kenya), Dry forest margins, thickets and wooded grassland	stem, leaves, fruits
Anarcadiaceae	<i>Rhus Vulgaris</i> Meikle	1200-2700m (Olorgesailie), wooded grassland, thickets, bushed grasslands in rocky sites.	stems, leaves
Anthericaceae	<i>Anthericum sp.</i>	1980-2450m (Mt, Kenya)	Leaves

Asteraceae	<i>Vernonia brachycalyx</i> O.Hoffm.	~1100m (Olorgesailie) riverine along lugga	Stem, leaves, flowers
Capparaceae	<i>Cadaba farinosa</i> Forssk.	1-1900m (Olorgesailie) Dry <i>Acacia</i> bushland, riverine thickets	Leaves, fruits
Leguminosae-Mimosoideae	<i>Acacia brevispica</i> Harms	1-1800m (Olorgesailie), Dry <i>Acacia</i> bushland, woodland often on rocky or stony soil	Stems, leaves
Leguminosae-Papilionoideae	<i>Indigofera lupatana</i> Bak.f.	250-2100m (Taita hills), Evergreen or deciduous bushland, bushed grassland	leaves, flowers
Leguminosae-Papilionoideae	<i>Indigofera arrecta</i> A. Rich	350-2650 m (Olorgesailie), wooded grassland, forest margins in dry areas often near luggas	Leaves, fruits
Leguminosae-Papilionoideae	<i>Crotalaria lachnocarpoides</i> Engl.	1200-2650 m (Mt. Kenya), forest margins, bushed grassland	leaves, flowers
Leguminosae-Papilionoideae	<i>Rhynchosia hirta</i> (Andr.) Meikle & Verdc.	450-1850m (Olorgesailie), Bushed or wooded grasslands, forest margins	Leaves, flowers
Malvaceae	<i>Abutilon hirtum</i> (Lam.)Sweet	1-1800m (Olorgesailie), Dry <i>Acacia</i> bushland, usually near luggas or riverine	Leaves, flowers
Moraceae	<i>Ficus natalensis</i> Hochst.	900-1800m (Olorgesailie), Riverine and ground water forest	stem, leaves, fruits
Rosaceae	<i>Rubus apetalus</i> Poir.	1450-2700m (Mt. Kenya), Forest margins, secondary bush/grasslands, riverine forest	Stem, leaves, fruits
Rubiaceae	<i>Tarrena graveolens</i> (S.Moore) Brem.	1-2100m (Taita hills), bushland on rocky hills, drier forest margins, bushed grassland	stem, leaves, fruits
Rubiaceae	<i>Canthium dyscriton</i> Bullock	750-1600m (Taita hills), rocky outcrops	Stem, leaves, fruits
Tiliaceae	<i>Grewia fallax</i> K. Schum.	350-1500m (Olorgesailie), Dry bushland, bushed grassland near luggas or rivers	Leaves
Myrsinaceae	<i>Maesa lanceolata</i> Forssk.	1300-280 m (Mt. Kenya) Often in secondary forests	Leaves, fruits
Salvadoraceae	<i>Salvadora persica</i> L.	1-1850m (Olorgesailie) along rivers, luggas, lakes or wells, dry <i>Acacia</i> bushland/wooded grassland	Leaves, fruits
Iridaceae	<i>Gladiolus candidus</i> (Rendle)	1300-2800 m (Mt. Kenya) forest edges, wooded grasslands	Whole

Appendix III: Table showing raw counts of phytolith assemblage identified in modern plants species.

See also phytolith/plants codes and their corresponding names

Family	Photosynthetic pathway	Species	Codes	Bilobate concave outer margin long shank	Bilobate concave outer margin short shank	Bilobate convex outer margin long shank	Bilobate convex outer margin short shank	Bilobate flattened outer margin long shank	Bilobate flattened outer margin short shank	Bilobate nodular	Bilobate notched/flared outer margin long shank	Bilobate notched/flared outer margin short shank	Polylobate	Quadralobate/crosses	Rondel	Saddle	Saddle long	Saddle ovate	Saddle plateau	Saddle squat	Tower flat	Tower horned	Tower wide	
				BCOMLS	BCOMSS	BCXMLS	BCXMSS	BFOMLS	BFOMSS	BN	BNFMLS	BNFMSS	PLY	QCR	ROND	SAD	SADL	SADP	SADO	SADS	TWF	TWHN	TWW	
Cyperaceae	n/a	<i>Cyperus papyrus</i>	CYP pap	0	0	0	0	0	0	0	0	0	0	0	0	0	0	0	0	0	0	0	0	
Cyperaceae	n/a	<i>Cyperus dives</i>	CYP div	0	0	0	0	0	0	0	0	0	0	0	0	0	0	0	0	0	0	0	0	
Cyperaceae	n/a	<i>Cyperus spp.</i>	CYP sp1	0	0	0	0	0	0	0	0	0	0	0	0	0	0	0	0	0	0	0	0	
Cyperaceae	n/a	<i>Cyperus spp.</i>	CYP sp2	0	0	0	0	0	0	0	0	0	0	0	0	0	0	0	0	0	0	0	0	
Cyperaceae	n/a	<i>Scleria boivinii</i>	SCL boiv	0	0	0	0	0	0	0	0	0	139	0	0	0	0	0	0	0	0	0	0	0
Cyperaceae	n/a	<i>Cyperus spp.</i>	CYP sp3	0	0	0	0	0	0	0	0	0	0	0	0	0	0	0	0	0	0	0	0	0
Cyperaceae	n/a	<i>Eleocharis spp.</i>	ELOC sp	0	0	0	0	0	0	0	0	0	0	0	0	0	0	0	0	0	0	0	0	0
Cyperaceae	n/a	<i>Kyillinga ordarata</i>	KYIL orda	0	0	0	0	0	0	0	0	0	1	0	0	0	0	0	0	0	0	0	0	0
Poaceae	C4	<i>Andropogon</i>	ANDRsp	0	0	0	0	0	0	0	0	0	0	0	0	235	0	0	0	0	24	0	0	0
Poaceae	C4	<i>Aristida congesta</i>	ARISTsp1	0	24	185	14	1	0	9	0	0	0	0	0	0	127	0	0	0	12	0	0	0
Poaceae	C4	<i>Aristida junciformis</i>	ARISTjun	0	0	143	0	0	0	0	0	0	0	0	0	0	8	0	0	0	0	0	0	0
Poaceae	C4	<i>Bewisia biflora</i>	BEWBif	0	1	0	0	0	0	0	0	0	0	0	0	0	0	0	0	0	57	0	0	0
Poaceae	C4	<i>Brachiaria c.f semiundulata</i>	BRACHsp	1	7	210	9	0	0	0	0	0	0	0	0	0	59	0	0	8	0	0	0	0
Poaceae	C4	<i>Brachyachne patentiflora</i>	BRACHNpaten	2	32	0	2	0	0	0	0	0	0	1	0	73	0	0	0	0	109	0	0	0
Poaceae	C4	<i>Brachyachne spp.</i>	BRACHNsp	0	0	0	0	0	0	0	0	0	0	0	0	191	0	0	0	0	0	238	0	0
Poaceae	C4	<i>Chloris mossambicensis</i>	CHLORmoss	0	0	0	0	0	0	0	0	0	0	0	0	122	0	0	0	100	0	0	0	0
Poaceae	C4	<i>Chloris virgata</i>	CHLORvir	0	0	0	0	0	0	0	0	0	0	0	0	83	0	0	0	0	0	0	0	0
Poaceae	C4	<i>Coelorachis lepidura</i>	COELlep	0	5	0	0	0	0	0	0	1	0	49	0	0	0	0	0	0	0	0	0	0
Poaceae	C4	<i>Cymbopogon caesius</i>	CYMBOcaes	0	67	44	32	0	0	4	0	0	0	10	0	8	0	0	0	0	39	0	0	0
Poaceae	C4	<i>Cynodon aethiopicus</i>	CYNODeathi	0	0	0	0	0	0	0	0	0	0	0	0	218	0	0	0	0	0	0	0	0
Poaceae	C4	<i>Dactyloctenium spp.</i>	DACTY sp	0	0	1	26	0	0	0	0	0	0	6	34	70	30	0	9	0	8	0	0	0
Poaceae	C4	<i>Digitaria ciliaris</i>	DIGITcilia	0	1	0	0	0	0	0	0	0	0	0	38	11	38	0	21	6	51	36	0	0

Family	Photosynthetic pathway	Species	Codes	Tower wide	Epidermal short cells (Rondeis)	Epidermal Short cells (Saddles)	Epidermal Long cells (Bilobate)	Bulliform	Parallepiped Blocky	Blocky facetate	Conical	Cylindroid verrucate	Cylindroid Clavate/wavy	Cylindroid Psilate bulbous	Cylindroid psilate	Cylindroid rugulate	Cylindroid clavate	Platelet Psilate	Platelets rugulate	Platelets verrucate	Sclereids	Tracheids	Mesophyl	Silica skeletons sensu lato
				TWW	EPROND	EPISAD	EPIBI	BLL	PB	BF	CN	CV	CCW	CPB	CP	CSC	CYC	PLPS	PLSC	PLVE	SCLD	TRCD	MSPY	SSSL
Cyperaceae	n/a	<i>Cyperus papyrus</i>	CYP pap	0	0	0	0	0	2	0	0	0	0	6	0	0	0	0	0	0	0	0	0	0
Cyperaceae	n/a	<i>Cyperus dives</i>	CYP div	0	0	0	0	0	24	0	0	37	0	5	0	0	0	0	0	0	0	0	0	0
Cyperaceae	n/a	<i>Cyperus spp.</i>	CYP sp1	0	0	0	0	0	0	0	0	0	0	10	0	0	0	0	0	0	0	0	0	0
Cyperaceae	n/a	<i>Cyperus spp.</i>	CYP sp2	0	0	0	0	0	0	0	0	0	0	0	0	0	0	0	0	0	0	0	0	0
Cyperaceae	n/a	<i>Scleria boivinii</i>	SCL boiv	0	0	0	0	0	0	0	0	0	0	0	0	0	0	0	0	0	0	0	0	0
Cyperaceae	n/a	<i>Cyperus spp.</i>	CYP sp3	0	0	0	0	0	0	0	0	0	0	0	0	0	0	0	0	0	0	0	0	0
Cyperaceae	n/a	<i>Eleocharis spp.</i>	ELOC sp	0	0	0	0	0	0	0	0	0	0	0	0	0	0	0	0	0	0	0	0	0
Cyperaceae	n/a	<i>Kyillinga ordarata</i>	KYIL orda	0	0	0	0	0	0	0	0	9	3	36	2	2	0	0	0	0	0	10	0	22
Poaceae	C4	<i>Andropogon</i>	ANDRsp	0	0	0	0	83	0	0	0	0	0	0	0	0	0	0	0	0	0	0	0	0
Poaceae	C4	<i>Aristida congesta</i>	ARISTsp1	0	0	0	0	0	0	0	0	4	0	0	0	0	0	0	0	0	0	0	0	0
Poaceae	C4	<i>Aristida junciformis</i>	ARISTjun	0	0	0	0	0	0	0	0	9	0	0	0	0	0	0	0	0	0	0	0	0
Poaceae	C4	<i>Bewsia biflora</i>	BEWbif	0	0	0	0	4	0	0	94	58	0	0	0	0	0	0	0	0	0	0	0	0
Poaceae	C4	<i>Brachiaria c.f semiundulata</i>	BRACHsp	0	0	0	0	0	0	0	0	14	0	0	0	0	0	0	0	0	0	0	0	0
Poaceae	C4	<i>Brachyachne patentiflora</i>	BRACHNpaten	0	0	0	0	4	8	0	0	3	0	0	0	0	0	0	0	0	0	0	0	0
Poaceae	C4	<i>Brachyachne spp.</i>	BRACHNsp	0	0	0	0	0	0	0	0	0	0	0	0	0	0	0	0	0	0	0	0	0
Poaceae	C4	<i>Chloris mossambicensis</i>	CHLORmoss	0	0	0	0	0	0	0	0	1	0	5	0	0	0	0	0	0	0	0	0	0
Poaceae	C4	<i>Chloris virgata</i>	CHLORvir	0	0	0	0	0	0	0	123	0	0	0	0	0	0	0	0	0	0	0	0	0
Poaceae	C4	<i>Coelorachis lepidura</i>	COELlep	0	0	0	0	0	0	0	0	0	0	0	0	0	0	0	0	0	0	0	0	0
Poaceae	C4	<i>Cymbopogon caesius</i>	CYMBOcaes	0	0	0	0	3	0	0	0	0	0	20	0	0	0	0	0	0	0	0	0	0
Poaceae	C4	<i>Cynodon aethiopicus</i>	CYNODeathi	0	0	0	0	0	0	0	0	0	0	0	0	0	0	0	0	0	0	0	0	0
Poaceae	C4	<i>Dactyloctenium spp.</i>	DACTY sp	0	40	37	11	12	0	0	0	0	0	0	0	0	0	0	0	0	0	4	0	5
Poaceae	C4	<i>Digitaria ciliaris</i>	DIGITalia	0	64	3	0	1	0	0	0	0	0	0	1	4	0	0	0	0	0	3	0	14

Family	Photosynthetic pathway	Species	Codes	SSSL	SSCP	SSLCP	SSLCV	SSSEC	SSPC	SSIS	SSCCS	EPCR	EPJG	EPPY	GLEC	PSB	GB	HYEP	HYAS	HYEL	HYSP	SPEC	SPVE	SPPS	
				Silica skeletons sensu lato	Silica skeleton long cells psilate	Silica skeleton long cells psilate	Silica skeleton long cell verrucate	Silica skeleton with globulars/ellipsoids cells	Silica skeleton wt polyhedral cells	Silica skeleton jigsaw puzzle	Silica skeleton cylindrical cells sinous	Epidermal crenate	Epidermal jig-saw	Epidermal polygonal	Globular echinate irregular ridged	Psilate Bulbous	Globular folded	Honey comb elongate Psilate	Honey comb assemblage	Honeycomb elongates	Honey comb globular	globular echnate	globular verrucate	globular psilate	
Cyperaceae	n/a	<i>Cyperus papyrus</i>	CYP pap	0	0	0	0	0	0	0	0	0	0	0	0	0	0	0	0	0	0	0	0	5	
Cyperaceae	n/a	<i>Cyperus dives</i>	CYP div	0	0	0	0	0	0	0	0	90	0	0	0	0	0	0	0	0	0	0	0	0	2
Cyperaceae	n/a	<i>Cyperus spp.</i>	CYP sp1	0	0	0	0	0	0	0	0	0	0	0	0	0	6	0	0	0	0	0	0	0	0
Cyperaceae	n/a	<i>Cyperus spp.</i>	CYP sp2	0	0	0	0	0	0	0	0	0	0	0	0	0	0	0	0	0	0	0	0	0	0
Cyperaceae	n/a	<i>Scleria boivinii</i>	SCL boiv	0	0	0	0	0	0	0	0	0	26	0	7	0	0	0	0	0	0	0	0	0	0
Cyperaceae	n/a	<i>Cyperus spp.</i>	CYP sp3	0	0	0	0	0	0	0	0	23	0	0	0	0	0	0	0	0	0	0	0	0	0
Cyperaceae	n/a	<i>Eleocharis spp.</i>	ELOC sp	0	0	0	0	0	0	0	0	0	0	0	0	0	0	0	0	0	0	0	0	0	0
Cyperaceae	n/a	<i>Kyllinga ordarata</i>	KYL orda	22	4	8	0	0	0	0	0	0	0	0	0	0	0	0	6	0	7	0	14	19	
Poaceae	C4	<i>Andropogon</i>	ANDRsp	0	0	0	0	0	0	0	0	0	0	0	0	0	0	0	0	0	0	0	0	0	0
Poaceae	C4	<i>Aristida congesta</i>	ARISTsp1	0	0	0	0	0	0	0	0	0	0	0	0	0	0	0	0	0	0	0	0	0	0
Poaceae	C4	<i>Aristida junciformis</i>	ARISTjun	0	0	0	0	0	0	0	0	0	0	0	0	0	0	0	0	0	0	0	0	0	0
Poaceae	C4	<i>Bewisia biflora</i>	BEWBif	0	0	0	0	0	0	0	0	0	0	0	0	0	0	0	0	0	0	0	0	0	0
Poaceae	C4	<i>Brachiaria c.f semiundulata</i>	BRACHsp	0	0	0	0	0	0	0	0	0	0	0	0	0	0	0	0	0	0	0	0	0	0
Poaceae	C4	<i>Brachyachne patentiflora</i>	BRACHNpaten	0	0	0	0	0	0	0	0	0	0	0	0	0	0	0	0	0	0	0	0	0	0
Poaceae	C4	<i>Brachyachne spp.</i>	BRACHNsp	0	0	0	0	0	0	0	0	0	0	0	0	0	0	0	0	0	0	0	0	0	0
Poaceae	C4	<i>Chloris mossambicensis</i>	CHLORmoss	0	0	0	0	0	0	0	0	0	0	0	0	0	0	0	0	0	0	0	0	0	74
Poaceae	C4	<i>Chloris virgata</i>	CHLORvir	0	0	0	0	0	0	0	0	0	0	0	0	0	0	0	0	0	0	0	0	0	0
Poaceae	C4	<i>Coelorachis lepidura</i>	COELlep	0	0	0	0	0	0	0	0	0	0	0	0	0	0	0	0	0	0	0	0	0	4
Poaceae	C4	<i>Cymbopogon caesius</i>	CYMBOcaes	0	0	0	0	0	0	0	0	0	0	0	0	0	0	0	0	0	0	0	0	0	27
Poaceae	C4	<i>Cynodon aethiopicus</i>	CYNODEathi	0	0	0	0	0	0	0	0	0	0	0	0	0	0	0	0	0	0	0	0	0	0
Poaceae	C4	<i>Dactyloctenium spp.</i>	DACTY sp	5	0	8	0	0	0	0	0	0	0	0	0	0	0	0	4	0	0	0	0	0	0
Poaceae	C4	<i>Digitaria ciliaris</i>	DIGITcilia	14	0	0	0	0	1	0	0	0	19	0	0	0	0	0	0	14	0	0	0	0	0

Family	Photosynthetic pathway	Species	Codes	globular psilate	globular Colpate	globular rugulate	Ovate	Ellipsoid verrucate	Ellipsoid rugulate	Ellipsoid polylobate	Ellipsoid Psilate	Discoid Psilate	Discoid rugulate	Long cell wavy/polylobate	Long cell Psilate	long cell sinuate	Long cell dendritic	Long cell verrucate	Papillae	Achene	Hair bases	Hair	Stomata/Hair	Scutiform/prickles
				SPPS	SPCOL	SPHSC	Ovate	ELLVE	EESC	ELLPOL	ELLPS	DSCPSI	DICSC	LCWPL	LCPS	LCSI	LCDC	LCVE	PAPL	ECHN	HB	HR	STHR	SCPR
Cyperaceae	n/a	<i>Cyperus papyrus</i>	CYP pap	5	0	0	0	0	0	0	0	0	0	0	0	0	0	0	230	0	0	0	0	0
Cyperaceae	n/a	<i>Cyperus dives</i>	CYP div	2	0	0	0	0	0	0	0	0	0	0	0	0	0	0	45	0	0	0	36	0
Cyperaceae	n/a	<i>Cyperus spp.</i>	CYP sp1	0	0	0	0	0	0	0	0	0	0	0	0	0	0	0	0	0	0	0	0	0
Cyperaceae	n/a	<i>Cyperus spp.</i>	CYP sp2	0	0	0	0	0	0	0	0	0	0	0	0	0	0	0	249	0	0	0	12	0
Cyperaceae	n/a	<i>Scleria boivinii</i>	SCL boiv	0	0	0	0	0	0	0	0	0	0	0	0	0	0	0	0	0	0	0	9	0
Cyperaceae	n/a	<i>Cyperus spp.</i>	CYP sp3	0	0	0	0	0	0	0	0	0	0	0	0	0	0	0	224	0	0	0	0	0
Cyperaceae	n/a	<i>Eleocharis spp.</i>	ELOC sp	0	0	0	0	0	0	0	0	0	0	0	0	0	0	0	282	0	0	0	0	0
Cyperaceae	n/a	<i>Kyllinga ordarata</i>	KYIL orda	19	0	0	2	0	1	2	0	0	0	2	0	0	0	0	99	78	0	2	0	2
Poaceae	C4	<i>Andropogon</i>	ANDRsp	0	0	0	0	0	0	0	0	0	0	0	0	0	0	0	0	0	0	0	0	3
Poaceae	C4	<i>Aristida congesta</i>	ARISTsp1	0	0	0	0	0	0	0	0	0	0	0	0	0	0	0	0	0	0	0	0	3
Poaceae	C4	<i>Aristida junciformis</i>	ARISTjun	0	0	0	1	0	0	0	0	0	0	0	0	0	0	0	0	0	0	0	3	0
Poaceae	C4	<i>Bewisia biflora</i>	BEWBif	0	0	0	0	0	0	0	0	0	0	0	0	0	0	0	0	0	0	0	0	20
Poaceae	C4	<i>Brachiaria c.f semiundulata</i>	BRACHsp	0	0	0	0	0	0	0	0	0	0	0	0	0	0	0	0	0	0	0	5	0
Poaceae	C4	<i>Brachyachne patentiflora</i>	BRACHNpaten	0	0	0	0	0	0	0	0	0	0	0	0	0	0	0	0	0	0	0	0	113
Poaceae	C4	<i>Brachyachne spp.</i>	BRACHNsp	0	0	0	0	0	0	0	0	0	0	0	0	0	0	0	0	0	0	0	0	0
Poaceae	C4	<i>Chloris mossambicensis</i>	CHLORmoss	74	0	0	0	0	0	0	0	0	0	0	0	0	0	0	0	0	0	0	0	5
Poaceae	C4	<i>Chloris virgata</i>	CHLORvir	0	0	0	0	0	0	0	0	0	0	0	0	0	0	0	0	0	0	0	78	0
Poaceae	C4	<i>Coelorachis lepidura</i>	COELLEp	4	0	0	0	0	0	0	0	0	0	0	0	0	0	0	0	0	0	0	83	137
Poaceae	C4	<i>Cymbopogon caesius</i>	CYMBOcaes	27	0	0	0	0	0	0	0	0	0	0	0	0	0	0	0	0	0	0	0	57
Poaceae	C4	<i>Cynodon aethiopicus</i>	CYNODeathi	0	0	0	0	0	0	0	0	0	0	0	0	0	0	0	0	0	0	0	0	1
Poaceae	C4	<i>Dactyloctenium spp.</i>	DACTY sp	0	0	3	0	0	0	0	0	0	0	0	2	1	3	0	0	0	0	2	5	4
Poaceae	C4	<i>Digitaria ciliaris</i>	DIGITcilia	0	0	0	0	0	0	0	0	0	0	0	0	1	10	0	0	0	10	24	12	0

Family	Photosynthetic pathway	Species	Codes	Scutiform/prickles	Parallelepiped elongate verrucate	Parallelepiped facetate	Parallelepiped elongate indet.	Parallelepiped blocky psilate round heads	Parallelepiped blocky psilate square heads	Parallelepiped thin psilate	Parallelepiped elongate thin rugulate	Fibres sensu lato	Tabular crenate	Tabular dendriform	Tabular elongate	Tabular facetate	Tabular lanceolate	Tabular oblong	Tabular scrobiculate	Tabular sinuate	Tabular trapezoid	Trapeziform crenate	Irregular verrucate	Irregular Echnates	
				SCPR	PAELV	PARF	PPEI	PBPR	PBPSQ	PTP	PELTS	FBL	TBCR	TADE	TABELG	TABFAC	TABLAN	TABOBL	TABSCR	TABSI	TABTRP	TRAPCRE	IRRYE	IRRECH	
Cyperaceae	n/a	<i>Cyperus papyrus</i>	CYP pap	0	0	0	0	0	0	0	0	0	0	0	0	0	0	0	0	0	0	0	0	0	
Cyperaceae	n/a	<i>Cyperus dives</i>	CYP div	0	0	0	0	0	0	0	0	0	27	0	0	5	31	0	0	0	0	0	0	0	0
Cyperaceae	n/a	<i>Cyperus spp.</i>	CYP sp1	0	0	0	0	0	0	0	0	0	0	0	0	0	0	76	0	0	157	0	0	0	
Cyperaceae	n/a	<i>Cyperus spp.</i>	CYP sp2	0	0	0	0	0	0	0	0	0	0	0	0	0	0	0	0	0	0	0	0	0	
Cyperaceae	n/a	<i>Scleria boivinii</i>	SCL boiv	0	0	0	0	0	0	0	0	0	24	0	0	0	0	0	0	0	0	0	0	0	0
Cyperaceae	n/a	<i>Cyperus spp.</i>	CYP sp3	0	0	0	0	0	0	0	0	0	1	0	0	0	0	0	0	0	0	0	0	0	0
Cyperaceae	n/a	<i>Eleocharis spp.</i>	ELOC sp	0	0	0	0	0	0	0	0	0	10	2	0	0	0	0	3	0	0	0	0	0	0
Cyperaceae	n/a	<i>Kyllinga ordarata</i>	KYL orda	2	1	0	59	1	5	6	1	7	0	0	0	0	0	0	0	0	1	0	0	0	0
Poaceae	C4	<i>Andropogon</i>	ANDRsp	3	0	0	0	0	0	0	0	0	53	0	0	0	0	0	0	0	0	0	0	0	0
Poaceae	C4	<i>Aristida congesta</i>	ARISTsp1	3	0	0	0	0	0	0	0	0	1	0	0	0	0	0	0	0	0	0	0	0	0
Poaceae	C4	<i>Aristida junciformis</i>	ARISTjun	0	0	0	0	0	0	0	0	0	49	0	0	0	0	0	0	0	0	0	0	0	0
Poaceae	C4	<i>Bewisia biflora</i>	BEWbif	20	0	0	0	0	0	0	0	0	0	0	0	0	0	0	0	0	0	100	0	0	0
Poaceae	C4	<i>Brachiaria c.f semiunudulata</i>	BRACHsp	0	0	0	0	0	0	0	0	0	0	0	0	0	0	0	0	0	0	0	0	0	0
Poaceae	C4	<i>Brachyachne patentiflora</i>	BRACHNpaten	113	0	0	0	0	0	0	0	0	72	34	0	0	0	0	0	17	0	0	0	0	0
Poaceae	C4	<i>Brachyachne spp.</i>	BRACHNsp	0	0	0	0	0	0	0	0	0	0	0	0	0	0	0	0	0	0	0	0	0	0
Poaceae	C4	<i>Chloris mossambicensis</i>	CHLORmoss	5	0	0	0	0	0	0	0	0	20	0	0	0	0	0	0	0	0	0	0	0	0
Poaceae	C4	<i>Chloris virgata</i>	CHLORvir	0	0	0	0	0	0	0	0	0	0	0	0	0	0	0	0	0	0	0	0	0	0
Poaceae	C4	<i>Coelorachis lepidura</i>	COELlep	137	0	0	0	0	0	0	0	0	2	0	0	0	0	0	0	4	0	0	0	0	0
Poaceae	C4	<i>Cymbopogon caesius</i>	CYMBOcaes	57	0	0	0	0	0	0	0	0	67	0	0	0	0	0	0	0	0	0	0	0	0
Poaceae	C4	<i>Cynodon aethiopicus</i>	CYNODEathi	1	0	0	0	0	0	0	0	0	4	0	0	3	0	0	0	0	0	0	0	0	0
Poaceae	C4	<i>Dactyloctenium spp.</i>	DACTY sp	4	20	0	6	0	0	13	9	9	0	0	0	0	0	0	0	0	0	0	0	0	0
Poaceae	C4	<i>Digitaria ciliaris</i>	DIGITcilia	0	0	2	1	0	0	18	3	10	0	0	0	0	0	0	0	0	0	0	2	0	

Family	Photosynthetic pathway	Species	Codes	Irregular Echnates	Irregular forms	Cystoliths	Indeterminables	Total Sum
				IRRECH	IRRFOR	CYT	INDT	TOT
Cyperaceae	n/a	<i>Cyperus papyrus</i>	CYP pap	0	0	0	0	0
Cyperaceae	n/a	<i>Cyperus dives</i>	CYP div	0	0	0	0	0
Cyperaceae	n/a	<i>Cyperus spp.</i>	CYP sp1	0	0	0	0	0
Cyperaceae	n/a	<i>Cyperus spp.</i>	CYP sp2	0	0	0	0	0
Cyperaceae	n/a	<i>Scleria boivinii</i>	SCL boiv	0	0	0	0	0
Cyperaceae	n/a	<i>Cyperus spp.</i>	CYP sp3	0	0	0	0	0
Cyperaceae	n/a	<i>Eleocharis spp.</i>	ELOC sp	0	0	0	0	0
Cyperaceae	n/a	<i>Kyllinga ordarata</i>	KYIL orda	0	25	0	0	25
Poaceae	C4	<i>Andropogon</i>	ANDRsp	0	0	0	0	0
Poaceae	C4	<i>Aristida congesta</i>	ARISTsp1	0	0	0	0	0
Poaceae	C4	<i>Aristida junciformis</i>	ARISTjun	0	0	0	0	0
Poaceae	C4	<i>Bewisia biflora</i>	BEWbif	0	0	0	0	0
Poaceae	C4	<i>Brachiaria c.f semiunudulata</i>	BRACHsp	0	0	0	0	0
Poaceae	C4	<i>Brachyachne patentiflora</i>	BRACHNpaten	0	0	0	0	0
Poaceae	C4	<i>Brachyachne spp.</i>	BRACHNsp	0	0	0	0	0
Poaceae	C4	<i>Chloris mossambicensis</i>	CHLORmoss	0	0	0	0	0
Poaceae	C4	<i>Chloris virgata</i>	CHLORvir	0	0	0	0	0
Poaceae	C4	<i>Coelorachis lepidura</i>	COELLEp	0	0	0	0	0
Poaceae	C4	<i>Cymbopogon caesius</i>	CYMBOcaes	0	0	0	0	0
Poaceae	C4	<i>Cynodon aethiopicus</i>	CYNODEathi	0	0	0	0	0
Poaceae	C4	<i>Dactyloctenium spp.</i>	DACTY sp	0	23	0	3	26
Poaceae	C4	<i>Digitaria ciliaris</i>	DIGITcilia	0	0	0	10	10

Family	Photosynthetic pathway	Species	Codes	Bilobate concave outer margin long shank	Bilobate concave outer margin short shank	Bilobate convex outer margin long shank	Bilobate convex outer margin short shank	Bilobate flattened outer margin long shank	Bilobate flattened outer margin short shank	Bilobate nodular	Bilobate notched/flared outer margin long shank	Bilobate notched/flared outer margin short shank	Polylobate	Quadrilobate/crosses	Rondel	Saddle	Saddle long	Saddle ovate	Saddle plateau	Saddle squat	Tower flat	Tower horned
				BCOMLS	BCOMSS	BCXMLS	BCXMSS	BFOMLS	BFOMSS	BN	BNFMLS	BNFMSS	PLY	QCR	ROND	SAD	SADL	SADP	SADO	SADS	TWF	TWHN
Poaceae	C4	<i>Eragrostis pilosa</i>	ERAGRpil	0	0	0	0	0	0	0	0	0	0	0	0	273	0	0	0	62	0	0
Poaceae	C4	<i>Eragrostis racemosa</i>	ERAGROrac	0	25	0	0	0	0	0	0	0	0	0	0	162	0	0	0	26	1	0
Poaceae	C4	<i>Eragrostis superba</i>	ERAGRsup	1	19	0	1	0	0	0	0	0	0	0	0	17	0	0	0	0	190	0
Poaceae	C4	<i>Harpachne shimperi</i>	HARPshimp	0	0	0	0	0	0	0	0	0	0	0	0	137	0	0	0	0	74	0
Poaceae	C4	<i>Hyparrhenia hirta</i>	HYPARhir	7	98	0	0	1	1	0	0	0	0	8	0	0	1	0	0	0	4	92
Poaceae	C4	<i>Hyparrhenia drageana</i>	HYPARdrag	13	36	3	26	6	8	11	0	0	0	15	0	0	0	0	0	0	0	117
Poaceae	C4	<i>Melinis ambigua</i>	MELambi	42	48	0	48	3	4	12	0	27	36	18	0	0	0	0	0	0	0	0
Poaceae	C4	<i>Melinis minuteflora</i>	MELminut	21	76	0	3	0	0	38	0	2	101	25	0	0	0	0	0	0	0	0
Poaceae	C4	<i>Melinis repens</i>	MELrep	0	202	6	44	0	2	0	0	0	3	9	0	0	0	0	0	0	0	0
Poaceae	C4	<i>Oplismenus compositus</i>	OPLIScomp	37	46	6	4	0	14	0	1	0	0	1	0	0	0	112	0	0	0	0
Poaceae	C4	<i>Oplismenus hirtellus</i>	OPLIShirt	4	58	7	79	0	15	19	5	14	11	9	0	0	0	0	0	0	0	2
Poaceae	C4	<i>Panicum eickii</i>	PANICecki	72	108	1	14	0	6	5	1	0	0	13	0	0	0	0	0	0	0	2
Poaceae	C4	<i>Panicum maximum</i>	PANImax	55	133	0	64	0	0	13	2	0	0	2	0	0	0	0	0	0	0	0
Poaceae	C4	<i>Pennisetum polystachion</i>	PENNpol	36	59	6	39	0	5	25	4	1	37	24	0	0	0	0	0	0	0	0
Poaceae	C4	<i>Ischaemum rugosum</i>	ISCHARug	19	23	7	5	0	0	34	64	2	33	55	0	0	0	0	0	0	0	0
Poaceae	C4	<i>Pennisetum purpureum</i>	PENNpurp	0	2	13	57	0	0	0	0	0	0	1	0	0	1	0	0	0	2	151
Poaceae	C3	<i>Phragmites australis</i>	PHRAGaus	0	0	0	0	0	0	0	0	0	0	0	0	0	58	0	138	0	67	0
Poaceae	C3	<i>Phragmites mauritianus</i>	PHRAGmau	0	0	0	0	0	0	0	0	0	0	0	0	0	12	0	182	0	3	0
Poaceae	C4	<i>Schizachyrium brevifolium</i>	SCHIZbrevi	18	133	0	11	0	8	0	0	0	10	2	0	0	0	0	0	0	0	0
Poaceae	C4	<i>Schizachyrium jeffreysii</i>	SCHIZjeff	19	110	0	1	0	53	0	2	0	3	33	0	0	0	0	0	0	7	4
Poaceae	C4	<i>Schizachyrium spp.</i>	SCHIZspp	103	52	6	15	1	10	1	3	1	0	0	0	0	0	0	0	0	0	69
Poaceae	C4	<i>Setaria incrassata</i>	SETARincra	78	56	87	3	12	1	10	0	0	2	4	0	0	0	0	0	0	0	0
Poaceae	C4	<i>Setaria plicatilis</i>	SETARplic	69	91	0	31	6	3	46	24	0	0	16	0	0	0	0	0	0	0	0
Poaceae	C4	<i>Setaria poiretiana</i>	SETApoir	14	102	0	63	0	9	0	0	0	0	13	0	0	0	0	0	0	21	0

Family	Photosynthetic pathway	Species	Codes	Tower horned	Tower wide	Epidermal short cells (Rondels)	Epidermal Short cells (Saddles)	Epidermal Long cells (Bilobate)	Bulliform	Parallepiped Blocky	Blocky facetate	Conical	Cylindroid verrucate	Cylindroid Clavate/wavy	Cylindroid Psilate bulbous	Cylindroid psilate	Cylindroid rugulate	Cylindroid clavate	Platelet Psilate	Platelets rugulate	Platelets verrucate	Sclereids	Tracheids
				TWHN	TWW	EPROND	EPISAD	EPIBI	BLL	PB	BF	CN	CV	CCW	CPB	CP	CSC	CYC	PLPS	PLSC	PLVE	SCLD	TRCD
Poaceae	C4	<i>Eragrostis pilosa</i>	ERAGRpil	0	0	0	0	0	0	0	0	0	0	0	0	0	0	0	0	0	0	0	0
Poaceae	C4	<i>Eragrostis racemosa</i>	ERAGROrac	0	0	0	0	0	8	0	0	0	0	0	0	0	0	0	0	0	0	0	0
Poaceae	C4	<i>Eragrostis superba</i>	ERAGRsup	0	0	0	0	0	0	0	0	0	0	0	0	0	0	0	0	0	0	0	0
Poaceae	C4	<i>Harpachne shimperi</i>	HARPshimp	0	0	0	0	0	28	0	0	0	0	0	0	0	0	0	0	0	0	0	0
Poaceae	C4	<i>Hyparrhenia hirta</i>	HYPARhir	92	4	0	0	0	1	0	0	0	0	0	0	0	0	0	0	0	0	0	0
Poaceae	C4	<i>Hyparrhenia drageana</i>	HYPARdrag	117	0	0	0	0	6	0	0	0	0	0	0	0	0	0	0	0	0	0	0
Poaceae	C4	<i>Melinis ambigua</i>	MELambi	0	0	0	0	0	5	0	0	0	0	0	0	0	0	0	0	0	0	0	0
Poaceae	C4	<i>Melinis minuteflora</i>	MELminut	0	0	0	0	0	4	0	0	0	2	0	7	0	0	0	0	0	0	0	0
Poaceae	C4	<i>Melinis repens</i>	MELrep	0	0	0	0	0	0	0	0	0	0	0	0	0	0	0	0	0	0	0	0
Poaceae	C4	<i>Oplismenus compositus</i>	OPLIScomp	0	0	0	0	0	0	0	0	0	11	0	0	0	0	0	0	0	0	0	0
Poaceae	C4	<i>Oplismenus hirtellus</i>	OPLISHirt	2	0	0	0	0	7	0	0	0	0	0	1	0	0	0	0	0	0	0	0
Poaceae	C4	<i>Panicum eickii</i>	PANICEcki	2	0	0	0	0	13	0	0	0	0	0	0	0	0	0	0	0	0	0	0
Poaceae	C4	<i>Panicum maximum</i>	PANImax	0	0	0	0	0	9	0	0	0	3	0	0	0	0	0	0	0	0	0	0
Poaceae	C4	<i>Pennisetum polystachion</i>	PENNpol	0	0	0	0	0	0	0	0	0	0	0	0	0	0	0	0	0	0	0	0
Poaceae	C4	<i>Ischaemum rugosum</i>	ISCHARug	0	0	0	0	0	0	0	0	0	0	0	3	0	0	0	0	0	0	0	0
Poaceae	C4	<i>Pennisetum purpureum</i>	PENNpurp	151	7	0	0	0	11	0	0	0	0	0	0	0	0	0	0	0	0	0	0
Poaceae	C3	<i>Phragmites australis</i>	PHRAGaus	0	0	0	0	0	1	0	0	0	0	0	0	0	0	0	0	0	0	0	0
Poaceae	C3	<i>Phragmites mauritianus</i>	PHRAGmau	0	0	0	0	0	12	0	0	0	0	0	0	0	0	0	0	0	0	0	0
Poaceae	C4	<i>Schizachyrium brevifolium</i>	SCHIZbrevi	0	0	0	0	0	9	42	0	0	9	0	0	0	0	0	0	0	0	0	0
Poaceae	C4	<i>Schizachyrium jeffreysii</i>	SCHIZjeff	4	0	0	0	0	0	0	0	0	3	0	0	0	0	0	0	0	0	0	0
Poaceae	C4	<i>Schizachyrium spp.</i>	SCHIZspp	69	0	0	0	0	0	0	0	0	0	0	0	0	0	0	0	0	0	0	0
Poaceae	C4	<i>Setaria incrassata</i>	SETARincra	0	0	0	0	0	3	0	0	0	0	0	0	0	0	0	0	0	0	0	0
Poaceae	C4	<i>Setaria plicatilis</i>	SETARplic	0	0	0	0	0	2	0	0	0	0	0	0	0	0	0	0	0	0	0	0
Poaceae	C4	<i>Setaria poiretiana</i>	SETApoir	0	0	0	0	0	1	0	0	0	0	0	0	0	0	0	0	0	0	0	0

Family	Photosynthetic pathway	Species	Codes	Tracheids	Mesophyl	Silica skeletons sensu lato	Silica skeleton long cells psilate	Silica skeleton long cells psilate	Silica skeleton long cell verrucate	Silica skeleton with globulars/ellipsoids cells	Silica skeleton wt polyhedral cells	Silica skeleton jigsaw puzzle	Silica skeleton cylindrical cells sinuous	Epidermal crenate	Epidermal jig-saw	Epidermal polygonal	Globular echinate irregular ridged	Psilate Bulbous	Globular folded	Honey comb elongate Psilate	Honey comb assemblage	Honeycomb elongates	Honey comb globular	globular echinate
				TRCD	MSPY	SSSL	SSCP	SSLCP	SSLCV	SSSEC	SSPC	SSJS	SSCCS	EPCR	EPJG	EPY	GLEC	PSB	GB	HYEP	HYAS	HYEL	HYSP	SPEC
Poaceae	C4	<i>Eragrostis pilosa</i>	ERAGRpil	0	0	0	0	0	0	0	0	0	0	0	0	0	0	0	0	0	0	0	0	0
Poaceae	C4	<i>Eragrostis racemosa</i>	ERAGROrac	0	0	0	0	0	0	0	0	0	0	0	0	0	0	0	0	0	0	0	0	0
Poaceae	C4	<i>Eragrostis superba</i>	ERAGRsup	0	0	0	0	0	0	0	0	0	0	0	0	0	0	0	0	0	0	0	0	0
Poaceae	C4	<i>Harpachne shimperi</i>	HARPshimp	0	0	0	0	0	0	0	0	0	0	0	0	0	0	0	0	0	0	0	0	0
Poaceae	C4	<i>Hyparrhenia hirta</i>	HYPARhir	0	0	0	0	0	0	0	0	0	0	64	0	0	0	0	0	0	0	0	0	0
Poaceae	C4	<i>Hyparrhenia drageana</i>	HYPARdrag	0	0	0	0	0	0	0	0	0	0	0	0	0	0	0	0	0	0	0	0	0
Poaceae	C4	<i>Melinis ambigua</i>	MELambi	0	0	0	0	0	0	0	0	0	0	0	0	0	0	0	0	0	0	0	0	0
Poaceae	C4	<i>Melinis minutiflora</i>	MELminut	0	0	0	0	0	0	0	0	0	0	75	0	0	0	0	0	0	0	0	0	0
Poaceae	C4	<i>Melinis repens</i>	MELrep	0	0	0	0	0	0	0	0	0	0	0	0	0	0	0	0	0	0	0	0	0
Poaceae	C4	<i>Oplismenus compositus</i>	OPLIScomp	0	0	0	0	0	0	0	0	0	0	0	0	0	0	0	0	0	0	0	0	0
Poaceae	C4	<i>Oplismenus hirtellus</i>	OPLIShirt	0	0	0	0	0	0	0	0	0	0	0	0	0	0	0	0	0	0	0	0	0
Poaceae	C4	<i>Panicum eickii</i>	PANICecki	0	0	0	0	0	0	0	0	0	0	0	0	0	0	0	0	0	0	0	0	0
Poaceae	C4	<i>Panicum maximum</i>	PANImax	0	0	0	0	0	0	0	0	0	0	0	0	0	0	0	0	0	0	0	0	0
Poaceae	C4	<i>Pennisetum polystachion</i>	PENNpol	0	0	0	0	0	0	0	0	0	0	0	0	0	0	0	0	0	0	0	0	0
Poaceae	C4	<i>Ischaemum rugosum</i>	ISCHArug	0	0	0	0	0	0	0	0	0	0	0	0	0	0	0	0	0	0	0	0	0
Poaceae	C4	<i>Pennisetum purpureum</i>	PENNpurp	0	0	0	0	0	0	0	0	0	0	13	0	28	0	0	0	0	0	0	0	0
Poaceae	C3	<i>Phragmites australis</i>	PHRAGaus	0	0	0	0	0	0	0	0	0	0	0	0	0	0	0	0	0	0	0	0	0
Poaceae	C3	<i>Phragmites mauritanus</i>	PHRAGmau	0	0	0	0	0	0	0	0	0	0	0	0	0	0	0	0	0	0	0	0	0
Poaceae	C4	<i>Schizachyrium brevifolium</i>	SCHIZbrevi	0	0	0	0	0	0	0	0	0	0	62	0	7	0	0	0	0	0	0	0	0
Poaceae	C4	<i>Schizachyrium jeffreysii</i>	SCHIZjeff	0	0	0	0	0	0	0	0	0	0	0	0	0	0	0	0	0	0	0	0	0
Poaceae	C4	<i>Schizachyrium spp.</i>	SCHIZspp	0	0	0	0	0	0	0	0	0	0	0	0	0	0	0	0	0	0	0	0	0
Poaceae	C4	<i>Setaria incrassata</i>	SETARincra	0	0	0	0	0	0	0	0	0	0	0	0	0	0	0	0	0	0	0	0	0
Poaceae	C4	<i>Setaria plicatilis</i>	SETARplic	0	0	0	0	0	0	0	0	0	0	0	0	0	0	0	0	0	0	0	0	0
Poaceae	C4	<i>Setaria poiretiana</i>	SETApoir	0	0	0	0	0	0	0	0	0	0	0	0	0	0	0	0	0	0	0	0	0

Family	Photosynthetic pathway	Species	Codes	gloabular echnate	gloabular verrucate	gloabular psilate	gloabular Colpate	gloabular rugulate	Ovate	Ellipsoid verrucate	Ellipsoid rugulate	Ellipsoid polylobate	Ellipsoid Psilate	Discoid Psilate	Discoid rugulate	Long cell wavy/polylobate	Long cell Psilate	long cell sinuate	Long cell dendritic	Long cell verrucate	Papillae	Achene	Hair bases
				SPEC	SPVE	SPPS	SPCOL	SPHSC	Ovate	ELLVE	EESC	ELLPOL	ELLPS	DSCPSI	DICSC	LCWPL	LCPS	LCSI	LCDC	LCVE	PAPL	ECHN	HB
Poaceae	C4	<i>Eragrostis pilosa</i>	ERAGRpil	0	0	0	0	0	0	0	0	0	0	0	0	0	0	0	0	0	0	0	0
Poaceae	C4	<i>Eragrostis racemosa</i>	ERAGROrac	0	0	0	0	0	0	0	0	0	0	0	0	0	0	0	0	0	0	0	0
Poaceae	C4	<i>Eragrostis superba</i>	ERAGRsup	0	0	13	0	0	0	0	0	0	0	0	0	0	0	0	0	0	0	0	0
Poaceae	C4	<i>Harpachne shimperi</i>	HARPshimp	0	0	0	0	0	0	0	0	0	0	0	0	0	0	0	0	0	0	0	0
Poaceae	C4	<i>Hyparrhenia hirta</i>	HYPARhir	0	0	0	0	0	0	0	0	0	0	0	0	0	0	0	0	0	0	0	0
Poaceae	C4	<i>Hyparrhenia drageana</i>	HYPARdrag	0	0	0	0	0	0	0	0	0	0	0	0	0	0	0	0	0	0	0	0
Poaceae	C4	<i>Melinis ambigua</i>	MELambi	0	0	3	0	0	0	0	0	0	0	0	0	0	0	0	0	0	0	0	0
Poaceae	C4	<i>Melinis minuteflora</i>	MELminut	0	0	21	0	0	0	0	0	0	0	0	0	0	0	0	0	0	0	0	0
Poaceae	C4	<i>Melinis repens</i>	MELrep	0	0	11	0	0	0	0	0	0	0	0	0	0	0	0	0	0	0	0	0
Poaceae	C4	<i>Oplismenus compositus</i>	OPLIScomp	0	0	0	0	0	0	0	0	0	0	0	0	0	0	0	0	0	0	0	0
Poaceae	C4	<i>Oplismenus hirtellus</i>	OPLIShirt	0	0	0	0	0	0	0	0	0	0	0	0	0	0	0	0	0	0	0	0
Poaceae	C4	<i>Panicum eickii</i>	PANICecki	0	0	0	0	0	0	0	0	0	0	0	0	0	0	0	0	0	0	0	0
Poaceae	C4	<i>Panicum maximum</i>	PANImax	0	0	0	0	0	0	0	0	0	0	0	0	0	0	0	0	0	0	0	0
Poaceae	C4	<i>Pennisetum polystachion</i>	PENNpol	0	0	0	0	0	0	0	0	0	0	0	0	0	0	0	0	0	0	0	0
Poaceae	C4	<i>Ischaemum rugosum</i>	ISCHARug	0	0	0	0	0	0	0	0	0	0	0	0	0	0	0	0	0	0	0	0
Poaceae	C4	<i>Pennisetum purpureum</i>	PENNpurp	0	0	0	0	0	0	0	0	0	0	0	0	0	0	0	0	0	0	0	0
Poaceae	C3	<i>Phragmites australis</i>	PHRAGaus	0	0	8	0	0	0	0	0	0	0	0	0	0	0	0	0	0	0	0	0
Poaceae	C3	<i>Phragmites mauritianus</i>	PHRAGmau	0	0	5	0	0	0	0	0	0	0	0	0	0	0	0	0	0	0	0	0
Poaceae	C4	<i>Schizachyrium brevifolium</i>	SCHIZbrevi	0	0	0	0	0	9	0	0	0	0	0	0	0	0	0	0	0	0	0	0
Poaceae	C4	<i>Schizachyrium jeffreysii</i>	SCHIZjeff	0	0	4	0	0	0	0	0	0	0	0	0	0	0	0	0	0	0	0	0
Poaceae	C4	<i>Schizachyrium spp.</i>	SCHIZspp	0	0	0	0	0	0	0	0	0	0	0	0	0	0	0	0	0	0	0	0
Poaceae	C4	<i>Setaria incrassata</i>	SETARincra	0	0	0	0	0	0	0	0	0	0	0	0	0	0	0	0	0	0	0	0
Poaceae	C4	<i>Setaria plicatilis</i>	SETARplic	0	0	4	0	0	0	0	0	0	0	0	0	0	0	0	0	0	0	0	0
Poaceae	C4	<i>Setaria poiretiana</i>	SETApoir	0	0	1	0	0	0	0	0	0	0	0	0	0	0	0	0	0	0	0	0

Family	Photosynthetic pathway	Species	Codes	Hair bases	Hair	Stomata/Hair	Scutiform/prickles	Parallelepiped elongate verrucate	Parallelepiped facetate	Parallelepiped elongate indet.	Parallelepiped blocky psilate round heads	Parallelepiped blocky psilate square heads	Parallelepiped thin psilate	Parallelepiped elongate thin rugulate	Fibres sensu lato	Tabular crenate	Tabular dendriform	Tabular elongate	Tabular facetate	Tabular lanceolate	Tabular oblong	Tabular scrobiculate	Tabular sinuate	Tabular trapezoid
				HB	HR	STHR	SCPR	PAELV	PARF	PPEI	PBPR	PBPSQ	PTP	PELTS	FBL	TBCR	TADE	TABELG	TABFAC	TABLAN	TABOBL	TABSCR	TABSI	TABTRP
Poaceae	C4	<i>Eragrostis pilosa</i>	ERAGRpil	0	0	0	3	0	0	0	0	0	0	0	0	0	0	0	0	0	0	0	0	0
Poaceae	C4	<i>Eragrostis racemosa</i>	ERAGROrac	0	0	19	0	0	0	0	0	0	0	0	0	28	0	0	0	0	0	0	0	0
Poaceae	C4	<i>Eragrostis superba</i>	ERAGRsup	0	0	38	21	0	0	0	0	0	0	0	0	0	0	0	0	0	0	0	1	0
Poaceae	C4	<i>Harpachne shimperi</i>	HARPshimp	0	0	0	15	0	0	0	0	0	0	0	0	30	0	0	0	0	0	0	0	0
Poaceae	C4	<i>Hyparrhenia hirta</i>	HYPARhir	0	0	11	1	0	0	0	0	0	0	0	0	6	6	0	0	0	0	1	1	0
Poaceae	C4	<i>Hyparrhenia drageana</i>	HYPARdrag	0	0	0	0	0	0	0	0	0	0	0	0	0	0	0	0	0	0	0	0	0
Poaceae	C4	<i>Melinis ambigua</i>	MELambi	0	0	38	4	0	0	0	0	0	0	0	0	2	1	0	0	0	0	0	0	0
Poaceae	C4	<i>Melinis minutiflora</i>	MELminut	0	0	15	0	0	0	0	0	0	0	0	0	2	0	0	0	0	0	0	0	0
Poaceae	C4	<i>Melinis repens</i>	MELrep	0	0	0	0	0	0	0	0	0	0	0	0	3	0	0	0	0	0	0	0	0
Poaceae	C4	<i>Oplismenus compositus</i>	OPLIScomp	0	0	54	0	0	0	0	0	0	0	0	0	3	0	0	0	0	0	0	0	0
Poaceae	C4	<i>Oplismenus hirtellus</i>	OPLIShirt	0	0	0	0	0	0	0	0	0	0	0	0	2	0	0	0	0	0	0	0	0
Poaceae	C4	<i>Panicum eickii</i>	PANICEcki	0	0	0	20	0	0	0	0	0	0	0	0	0	0	0	0	0	0	0	0	0
Poaceae	C4	<i>Panicum maximum</i>	PANImax	0	0	0	0	0	0	0	0	0	0	0	0	0	0	0	0	0	0	0	0	0
Poaceae	C4	<i>Pennisetum polystachion</i>	PENNpol	0	0	11	0	0	0	0	0	0	0	0	0	1	0	0	0	0	0	0	1	0
Poaceae	C4	<i>Ischaemum rugosum</i>	ISCHARug	0	0	95	13	0	0	0	0	0	0	0	0	0	0	0	0	0	0	0	4	0
Poaceae	C4	<i>Pennisetum purpureum</i>	PENNpurp	0	0	12	1	0	0	0	0	0	0	0	0	0	0	0	0	0	0	0	0	0
Poaceae	C3	<i>Phragmites australis</i>	PHRAGaus	0	0	0	0	0	0	0	0	0	0	0	0	1	0	0	0	0	0	0	0	0
Poaceae	C3	<i>Phragmites mauritanus</i>	PHRAGmau	0	0	38	0	0	0	0	0	0	0	0	0	0	0	4	0	0	0	0	0	0
Poaceae	C4	<i>Schizachyrium brevifolium</i>	SCHIZbrevi	0	0	10	6	0	0	0	0	0	0	0	0	41	0	0	0	0	0	0	0	0
Poaceae	C4	<i>Schizachyrium jeffreysii</i>	SCHIZjeff	0	0	62	0	0	0	0	0	0	0	0	0	0	0	0	0	0	0	0	0	0
Poaceae	C4	<i>Schizachyrium spp.</i>	SCHIZspp	0	0	0	1	0	0	0	0	0	0	0	0	0	0	0	0	0	0	0	0	0
Poaceae	C4	<i>Setaria incrassata</i>	SETARincra	0	0	0	0	0	0	0	0	0	0	0	0	1	0	0	0	0	0	0	0	0
Poaceae	C4	<i>Setaria plicatilis</i>	SETARplic	0	0	0	3	0	0	0	0	0	0	0	0	4	0	0	0	0	0	0	0	0
Poaceae	C4	<i>Setaria poiretiana</i>	SETApoir	0	0	0	0	0	0	0	0	0	0	0	0	13	0	0	0	0	0	0	0	0

Family	Photosynthetic pathway	Species	Codes	Tabular trapezoid	Trapeziform crenate	Irregular verrucate	Irregular Echnates	Irregular forms	Cystoliths	Indeterminables	Total Sum
				TABTRP	TRAPCRE	IRVE	IRRECH	IRRFOR	CYT	INDT	TOT
Poaceae	C4	<i>Eragrostis pilosa</i>	ERAGRpil	0	0	0	0	0	0	0	0
Poaceae	C4	<i>Eragrostis racemosa</i>	ERAGRrac	0	0	0	0	0	0	0	0
Poaceae	C4	<i>Eragrostis superba</i>	ERAGRsup	0	0	0	0	0	0	0	0
Poaceae	C4	<i>Harpachne shimperi</i>	HARPshimp	0	0	0	0	0	0	0	0
Poaceae	C4	<i>Hyparrhenia hirta</i>	HYPARhir	0	0	0	0	0	0	0	0
Poaceae	C4	<i>Hyparrhenia drageana</i>	HYPARdrag	0	0	0	0	0	0	0	0
Poaceae	C4	<i>Melinis ambigua</i>	MELambi	0	0	0	0	0	0	0	0
Poaceae	C4	<i>Melinis minuteflora</i>	MELminut	0	0	0	0	0	0	0	0
Poaceae	C4	<i>Melinis repens</i>	MELrep	0	0	0	0	0	0	0	0
Poaceae	C4	<i>Oplismenus compositus</i>	OPLIScomp	0	0	0	0	0	0	0	0
Poaceae	C4	<i>Oplismenus hirtellus</i>	OPLISHirt	0	0	0	0	0	0	0	0
Poaceae	C4	<i>Panicum eickii</i>	PANICEcki	0	0	0	0	0	0	0	0
Poaceae	C4	<i>Panicum maximum</i>	PANImax	0	0	0	0	0	0	0	0
Poaceae	C4	<i>Pennisetum polystachion</i>	PENNpol	0	0	0	0	0	0	0	0
Poaceae	C4	<i>Ischaemum rugosum</i>	ISCHARug	0	0	0	0	0	0	0	0
Poaceae	C4	<i>Pennisetum purpureum</i>	PENNpurp	0	0	0	0	0	0	0	0
Poaceae	C3	<i>Phragmites australis</i>	PHRAGGaus	0	0	0	0	0	0	0	0
Poaceae	C3	<i>Phragmites mauritianus</i>	PHRAGmau	0	0	0	0	0	0	0	0
Poaceae	C4	<i>Schizachyrium brevifolium</i>	SCHIZbrevi	0	0	0	0	0	0	0	0
Poaceae	C4	<i>Schizachyrium jeffreysii</i>	SCHIZjeff	0	0	0	0	0	0	0	0
Poaceae	C4	<i>Schizachyrium spp.</i>	SCHIZspp	0	0	0	0	0	0	0	0
Poaceae	C4	<i>Setaria incrassata</i>	SETARincra	0	0	0	0	0	0	0	0
Poaceae	C4	<i>Setaria plicatilis</i>	SETARplic	0	0	0	0	0	0	0	0
Poaceae	C4	<i>Setaria poiretiana</i>	SETApoir	0	0	0	0	0	0	0	0

Family	Photosynthetic pathway	Species	Codes	Bilobate concave outer margin long shank	Bilobate concave outer margin short shank	Bilobate convex outer margin long shank	Bilobate convex outer margin short shank	Bilobate flattened outer margin long shank	Bilobate flattened outer margin short shank	Bilobate nodular	Bilobate notched/flared outer margin long shank	Bilobate notched/flared outer margin short shank	Polylobate	Quadrilobate/crosses	Rondel	Saddle	Saddle long	Saddle ovate	Saddle plateau	Saddle squat	Tower flat	Tower horned
			Codes	BCOMLS	BCOMSS	BCXMLS	BCXMSS	BFOMLS	BFOMSS	BN	BNFMLS	BNFMSS	PLY	QCR	ROND	SAD	SADL	SADP	SADO	SADS	TWF	TWHN
Poaceae	C4	<i>Sporobulus africanus</i>	SPOROafri	0	0	0	0	0	0	0	66	85	11	37	0	0	0	15	0	0	18	21
Poaceae	C4	<i>Sporobulus consimilis</i>	SPOROcons	0	0	0	0	0	0	0	0	0	0	0	0	0	0	0	0	0	25	171
Poaceae	C4	<i>Themeda triadra</i>	THEMtria	49	94	21	39	10	8	0	2	0	2	14	0	0	0	0	0	0	0	0
Poaceae	C4	<i>Themeda villosa</i>	THEMvill	40	124	7	9	4	4	0	0	0	0	12	0	0	0	0	0	0	37	9
Acanthaceae	C3	<i>Barleria sp</i>	BARLsp	0	0	0	0	0	0	0	0	0	0	0	0	0	0	5	0	0	0	0
Acanthaceae	C3	<i>Acanthus eminence</i>	ACANTHemin	0	0	0	0	0	0	0	0	0	0	0	0	1	0	0	0	0	0	0
Anarcadiaceae	C3	<i>Rhus natalensis</i>	RHUnat	0	0	0	0	0	0	0	0	0	0	0	0	0	0	0	0	0	0	0
Asteraceae	C3	<i>Vernonia brachaetous</i>	VERNbrac	0	0	0	0	0	1	0	0	0	0	0	0	0	0	0	0	0	0	0
Capparaceae	C3	<i>Cleome sp</i>	CLEOMsp	0	0	0	2	0	0	0	0	0	0	0	0	0	0	0	0	0	0	0
Leguminosae-Mimosoideae	C3	<i>Acacia sp1</i>	ACACsp	0	0	0	0	0	0	0	0	0	0	0	0	0	0	0	0	0	0	0
Leguminosae-Papilionoideae	C3	<i>Indigofera sp.</i>	INDIGsp	0	0	0	0	0	0	0	0	0	0	0	0	0	0	0	0	0	0	0
Leguminosae-Papilionoideae	C3	<i>Crotalaria sp</i>	CROTSP	0	0	0	0	0	0	0	0	0	0	0	0	0	0	0	0	0	0	0
Malvaceae	C3	<i>Abutilon sp.</i>	ABUTSP	0	0	0	0	0	0	0	0	0	0	0	0	0	0	0	0	0	0	0
Moraceae	C3	<i>Ficus natalensis</i>	FICnat	0	0	0	8	0	0	0	0	0	0	0	0	0	0	0	0	0	0	0
Rubiaceae	C3	<i>Tarenna graveolens</i>	TARENgraveol	0	0	0	0	0	0	0	0	0	0	0	0	0	3	0	0	0	0	0
Rubiaceae	C3	<i>Rubus sp.</i>	RUBsp	0	0	0	0	0	0	0	0	0	0	0	0	0	0	0	0	0	0	0
Tiliaceae	C3	<i>Grewia fallax</i>	GREWfallx	0	0	0	0	0	0	0	0	0	0	0	0	0	0	0	0	0	0	0

Family	Photosynthetic pathway	Species	Codes	Tower horned	Tower wide	Epidermal short cells (Rondels)	Epidermal Short cells (Saddles)	Epidermal Long cells (Bilobate)	Bulliform	Parallepiped Blocky	Blocky facetate	Conical	Cylindroid verrucate	Cylindroid Clavate/wavy	Cylindroid Psilate bulbous	Cylindroid psilate	Cylindroid rugulate	Cylindroid clavate	Platelet Psilate	Platelets rugulate	Platelets verrucate	Scleireids	Tracheids
				TWHN	TWW	EPROND	EPISAD	EPIBI	BLL	PB	BF	CN	CV	CCW	CPB	CP	CSC	CYC	PLPS	PLSC	PLVE	SCLD	TRCD
Poaceae	C4	<i>Sporobulus africanus</i>	SPOROafri	21	0	0	0	0	1	0	0	0	0	0	0	0	0	0	0	0	0	0	0
Poaceae	C4	<i>Sporobulus consimilis</i>	SPOROcons	171	28	0	0	0	0	0	0	0	1	0	0	0	0	0	0	0	0	0	0
Poaceae	C4	<i>Themeda triadra</i>	THEMtria	0	0	0	0	0	2	0	0	0	0	0	0	0	0	0	0	0	0	0	0
Poaceae	C4	<i>Themeda villosa</i>	THEMvill	9	0	0	0	0	15	0	0	0	4	0	0	0	0	0	0	0	0	0	0
Acanthaceae	C3	<i>Barleria sp</i>	BARLsp	0	0	0	0	0	11	0	0	0	0	0	0	4	8	0	20	92	0	0	3
Acanthaceae	C3	<i>Acanthus eminence</i>	ACANTHemin	0	0	0	0	0	5	0	0	0	1	3	0	10	8	0	32	0	11	0	11
Anarcadiaceae	C3	<i>Rhus natalensis</i>	RHUnat	0	0	0	0	0	0	0	0	0	0	0	7	2	0	1	4	0	0	8	0
Asteraceae	C3	<i>Vernonia brachaetusa</i>	VERNbrac	0	0	0	0	0	5	0	7	0	4	0	0	0	3	1	1	0	15	0	14
Capparaceae	C3	<i>Cleome sp</i>	CLEOMsp	0	0	0	0	0	0	0	0	0	0	0	0	0	0	0	7	11	0	1	11
Leguminosae-Mimosoideae	C3	<i>Acacia sp1</i>	ACACsp	0	0	0	0	0	0	0	0	0	0	0	0	0	0	0	0	0	0	0	0
Leguminosae-Papilionoideae	C3	<i>Indigofera sp.</i>	INDIGsp	0	0	0	0	0	0	0	0	0	0	0	0	0	0	0	0	0	0	9	6
Leguminosae-Papilionoideae	C3	<i>Crotalaria sp</i>	CROTSP	0	0	0	0	0	0	0	0	0	0	0	0	0	0	0	0	3	0	0	0
Malvaceae	C3	<i>Abutilon sp.</i>	ABUTSP	0	0	0	0	0	8	0	0	0	0	0	0	11	0	0	0	0	0	0	0
Moraceae	C3	<i>Ficus natalensis</i>	FICnat	0	0	0	0	0	0	0	0	0	0	0	7	0	0	3	1	0	0	4	0
Rubiaceae	C3	<i>Tarenna graveolens</i>	TARENgraveol	0	0	0	0	0	1	0	0	0	0	0	0	4	0	1	20	11	0	0	0
Rubiaceae	C3	<i>Rubus sp.</i>	RUBsp	0	0	0	0	0	2	0	0	0	0	0	0	0	0	0	1	3	0	0	0
Tiliaceae	C3	<i>Grewia fallax</i>	GREWfallx	0	0	0	0	0	0	0	0	0	0	0	0	0	3	0	4	12	0	0	0

Family	Photosynthetic pathway	Species	Codes	Tracheids	Mesophyl	Silica skeletons sensu lato	Silica skeleton long cells psilate	Silica skeleton long cells psilate	Silica skeleton long cell verrucate	Silica skeleton with globulars/ellipsoids cells	Silica skeleton wt polyhedral cells	Silica skeleton jigsaw puzzle	Silica skeleton cylindroid cells sinous	Epidermal crenate	Epidermal jig-saw	Epidermal polygonal	Globular echinate irregular ridged	Psilate Bulbous	Globular folded	Honey comb elongate Psilate	Honey comb assemblage	Honeycomb elongates	Honey comb globular	globular echnate
				TRCD	MSPY	SSSL	SSCP	SSLCP	SSLCV	SSSEC	SSPC	SSJS	SSCCS	EPCR	EPJG	EPYP	GLEC	PSB	GB	HYEP	HYAS	HYEL	HYSP	SPEC
Poaceae	C4	<i>Sporobulus africanus</i>	SPOROafri	0	0	0	0	0	0	0	0	0	0	0	0	0	0	0	0	0	0	0	0	0
Poaceae	C4	<i>Sporobulus consimilis</i>	SPOROcons	0	0	0	0	0	0	0	0	0	0	0	0	0	0	0	0	0	0	0	0	0
Poaceae	C4	<i>Themeda triadra</i>	THEMtria	0	0	0	0	0	0	0	0	0	0	0	0	0	0	0	0	0	0	0	0	0
Poaceae	C4	<i>Themeda villosa</i>	THEMvill	0	0	0	0	0	0	0	0	0	0	0	0	0	0	0	0	0	0	0	0	0
Acanthaceae	C3	<i>Barleria sp</i>	BARLsp	3	0	6	0	0	0	0	0	0	0	0	0	0	0	0	0	0	3	0	0	1
Acanthaceae	C3	<i>Acanthus eminence</i>	ACANTHemin	11	4	1	0	8	3	0	0	2	0	0	0	0	0	2	0	14	0	0	0	11
Anarcadiaceae	C3	<i>Rhus natalensis</i>	RHUnat	0	0	8	0	0	0	13	8	0	4	0	0	0	0	28	0	0	3	0	12	6
Asteraceae	C3	<i>Vernonia brachaetuis</i>	VERNbrac	14	0	7	0	1	0	0	0	0	0	0	0	0	0	0	0	0	0	0	0	0
Capparaceae	C3	<i>Cleome sp</i>	CLEOMsp	11	0	1	0	0	0	0	0	0	0	0	0	0	0	0	0	0	0	0	0	0
Leguminosae-Mimosoideae	C3	<i>Acacia sp1</i>	ACACsp	0	0	0	0	0	0	0	0	0	0	0	0	0	0	0	0	0	0	0	0	0
Leguminosae-Papilionoideae	C3	<i>Indigofera sp.</i>	INDIGsp	6	0	10	0	0	0	0	3	0	4	0	0	0	0	0	0	0	0	0	3	1
Leguminosae-Papilionoideae	C3	<i>Crotalaria sp</i>	CROTSP	0	0	0	0	0	0	0	0	0	0	0	0	0	0	0	0	0	0	0	0	0
Malvaceae	C3	<i>Abutilon sp.</i>	ABUTSP	0	0	0	0	0	0	0	0	0	0	0	0	0	0	0	0	0	0	0	0	0
Moraceae	C3	<i>Ficus natalensis</i>	FICnat	0	0	0	18	0	0	24	1	0	0	0	0	0	0	3	0	0	11	20	6	0
Rubiaceae	C3	<i>Tarenna graveolens</i>	TARENgraveol	0	0	5	0	0	0	0	0	0	0	0	0	0	0	0	0	0	0	0	0	1
Rubiaceae	C3	<i>Rubus sp.</i>	RUBsp	0	0	0	0	0	0	0	0	0	0	0	0	0	0	0	0	0	0	0	0	0
Tiliaceae	C3	<i>Grewia fallax</i>	GREWfallx	0	0	16	11	0	0	0	0	0	0	0	0	0	0	0	0	0	0	0	0	0

Family	Photosynthetic pathway	Species	Codes	globular ednate	globular verrucate	globular psilate	globular Colpate	globular rugulate	Ovate	Ellipsoid verrucate	Ellipsoid rugulate	Ellipsoid polylobate	Ellipsoid Psilate	Discoid Psilate	Discoid rugulate	Long cell wavy/polylobate	Long cell Psilate	long cell sinuate	Long cell dendritic	Long cell verrucate	Papillae	Achene	Hair bases
				SPEC	SPVE	SPPS	SPCOL	SPHSC	Ovate	ELLVE	EESC	ELLPOL	ELLPS	DSCPSI	DICSC	LCWPL	LCPS	LCSI	LCDC	LCVE	PAPL	ECHN	HB
Poaceae	C4	<i>Sporobulus africanus</i>	SPOROafri	0	0	0	0	0	0	0	0	0	0	0	0	0	0	0	0	0	0	0	0
Poaceae	C4	<i>Sporobulus consimilis</i>	SPOROcons	0	0	0	0	0	0	0	0	0	0	0	0	0	0	0	0	0	0	0	0
Poaceae	C4	<i>Themeda triadra</i>	THEMtria	0	0	0	0	0	0	0	0	0	0	0	0	0	0	0	0	0	0	0	0
Poaceae	C4	<i>Themeda villosa</i>	THEMvill	0	0	0	0	0	0	0	0	0	0	0	0	0	0	0	0	0	0	0	0
Acanthaceae	C3	<i>Barleria sp</i>	BARLsp	1	21	16	0	0	0	0	9	0	7	1	10	0	1	0	0	0	0	0	0
Acanthaceae	C3	<i>Acanthus eminence</i>	ACANTHemin	11	18	42	0	12	0	0	9	0	9	4	0	5	9	6	0	18	0	0	0
Anarcadiaceae	C3	<i>Rhus natalensis</i>	RHUnat	6	0	203	5	7	0	9	0	0	11	0	0	0	4	9	4	0	0	0	0
Asteraceae	C3	<i>Vernonia brachaetis</i>	VERNbrac	0	3	0	0	3	0	0	0	0	0	0	0	0	0	0	0	0	0	0	0
Capparaceae	C3	<i>Cleome sp</i>	CLEOMsp	0	0	3	0	3	0	1	5	0	7	0	0	0	0	0	0	0	0	0	0
Leguminosae-Mimosoideae	C3	<i>Acacia sp1</i>	ACACsp	0	0	0	0	0	0	2	0	0	0	0	0	0	0	0	0	0	0	0	0
Leguminosae-Papilionoideae	C3	<i>Indigofera sp.</i>	INDIGsp	1	0	14	0	82	0	0	13	1	0	0	0	0	1	0	0	1	0	0	1
Leguminosae-Papilionoideae	C3	<i>Crotalaria sp</i>	CROTSP	0	0	0	0	0	0	0	0	0	3	0	0	0	0	0	0	0	0	0	0
Malvaceae	C3	<i>Abutilon sp.</i>	ABUTSP	0	0	0	0	0	0	0	0	0	0	0	0	0	0	0	0	0	0	0	0
Moraceae	C3	<i>Ficus natalensis</i>	FICnat	0	3	22	2	0	0	0	1	0	6	2	0	0	1	0	0	57	0	0	7
Rubiaceae	C3	<i>Tarenna graveolens</i>	TARENGraveol	1	3	6	1	9	0	0	13	0	4	0	0	0	4	0	0	0	0	0	0
Rubiaceae	C3	<i>Rubus sp.</i>	RUBsp	0	0	0	0	0	0	0	0	0	0	0	2	0	0	0	0	0	0	0	0
Tiliaceae	C3	<i>Grewia fallax</i>	GREWfallx	0	0	0	0	0	0	0	0	0	0	0	0	0	0	0	0	0	0	0	0

Family	Photosynthetic pathway	Species	Codes	Hair bases	Hair	Stomata/Hair	Scutiform/prickles	Parallelepiped elongate verrucate	Parallelepiped facetate	Parallelepiped elongate indet.	Parallelepiped blocky psilate round heads	Parallelepiped blocky psilate square heads	Parallelepiped thin psilate	Parallelepiped elongate thirn rugulate	Fibres sensu lato	Tabular crenate	Tabular dendriform	Tabular elongate	Tabular facetate	Tabular lanceolate	Tabular oblong	Tabular scrobiculate	Tabular sinuate	Tabular trapezoid
				HB	HR	STHR	SCPR	PAELV	PARF	PPEI	PBPR	PBPSQ	PTP	PELTS	FBL	TBCR	TADE	TABELG	TABFAC	TABLAN	TABOBL	TABSCR	TABSI	TABTRP
Poaceae	C4	<i>Sporobulus africanus</i>	SPOROafri	0	0	12	0	0	0	0	0	0	0	0	0	11	0	0	0	0	0	0	0	0
Poaceae	C4	<i>Sporobulus consimilis</i>	SPOROcons	0	0	0	0	0	0	0	0	2	0	0	0	0	0	12	0	0	0	0	0	0
Poaceae	C4	<i>Themeda triadra</i>	THEMtria	0	0	0	4	0	0	0	0	0	0	0	0	18	0	0	0	0	0	0	0	0
Poaceae	C4	<i>Themeda villosa</i>	THEMvill	0	0	12	6	0	0	0	0	0	0	0	4	0	0	0	0	0	0	0	0	0
Acanthaceae	C3	<i>Barleria sp</i>	BARLsp	0	2	0	5	0	0	4	0	6	0	2	0	0	0	0	0	0	0	0	0	0
Acanthaceae	C3	<i>Acanthus eminence</i>	ACANTHemin	0	2	0	11	0	3	38	0	14	9	6	9	0	0	0	0	0	0	0	0	0
Anarcadiaceae	C3	<i>Rhus natalensis</i>	RHUnat	0	0	6	1	0	0	0	0	2	0	0	5	0	0	0	0	0	0	0	0	0
Asteraceae	C3	<i>Vernonia brachaetis</i>	VERNbrac	0	0	0	0	0	0	0	3	8	0	0	5	0	0	0	0	0	0	0	0	0
Capparaceae	C3	<i>Cleome sp</i>	CLEOMsp	0	1	0	3	0	0	25	0	3	2	0	0	0	0	0	0	0	0	0	0	0
Leguminosae-Mimosoideae	C3	<i>Acacia sp1</i>	ACACsp	0	0	0	0	0	0	0	0	0	0	0	0	0	0	0	0	0	0	0	0	0
Leguminosae-Papilionoideae	C3	<i>Indigofera sp.</i>	INDIGsp	1	25	0	0	0	0	0	0	0	0	0	0	0	0	0	0	0	0	0	0	0
Leguminosae-Papilionoideae	C3	<i>Crotalaria sp</i>	CROTSP	0	0	0	3	0	0	0	0	6	0	6	0	0	0	0	0	0	0	0	0	0
Malvaceae	C3	<i>Abutilon sp.</i>	ABUTSP	0	0	0	0	0	0	0	0	0	0	0	0	0	0	0	0	0	0	0	0	0
Moraceae	C3	<i>Ficus natalensis</i>	FICnat	7	0	5	1	1	0	0	0	0	0	0	156	0	0	0	0	0	0	0	0	0
Rubiaceae	C3	<i>Tarenna graveolens</i>	TARENGraveol	0	1	0	7	0	0	0	0	0	1	0	0	0	0	0	0	0	0	0	0	0
Rubiaceae	C3	<i>Rubus sp.</i>	RUBsp	0	0	0	0	0	0	0	0	0	0	0	0	0	0	0	0	0	0	0	0	0
Tiliaceae	C3	<i>Grewia fallax</i>	GREWFallx	0	0	0	0	0	0	0	0	0	0	0	16	0	0	0	0	0	0	0	0	0

Family	Photosynthetic pathway	Species	Codes	Tabular trapezoid	Trapeziform crenate	Irregular verrucate	Irregular Echnates	Irregular forms	Cystoliths	Indeterminables	Total Sum
				TABTRP	TRAPCRE	IRRVE	IRRECH	IRRFOR	CYT	INDT	TOT
Poaceae	C4	<i>Sporobulus africanus</i>	SPOROafri	0	0	0	0	0	0	0	0
Poaceae	C4	<i>Sporobulus consimilis</i>	SPOROcons	0	0	0	0	0	0	0	0
Poaceae	C4	<i>Themeda triadra</i>	THEMtria	0	0	0	0	0	0	0	0
Poaceae	C4	<i>Themeda villosa</i>	THEMvill	0	0	0	0	0	0	0	0
Acanthaceae	C3	<i>Barleria sp</i>	BARLsp	0	0	0	0	69	0	0	69
Acanthaceae	C3	<i>Acanthus eminence</i>	ACANTHemin	0	0	0	0	60	0	28	88
Anarcadiaceae	C3	<i>Rhus natalensis</i>	RHUnat	0	0	0	0	15	0	3	18
Asteraceae	C3	<i>Vernonia brachaetus</i>	VERNbrac	0	0	0	0	20	0	19	39
Capparaceae	C3	<i>Cleome sp</i>	CLEOMsp	0	0	15	0	0	0	49	64
Leguminosae-Mimosoideae	C3	<i>Acacia sp1</i>	ACACsp	0	0	0	0	0	0	0	0
Leguminosae-Papilionoideae	C3	<i>Indigofera sp.</i>	INDIGsp	0	0	0	0	0	0	10	10
Leguminosae-Papilionoideae	C3	<i>Crotalaria sp</i>	CROTSP	0	0	17	0	0	0	11	28
Malvaceae	C3	<i>Abutilon sp.</i>	ABUTSP	0	0	0	0	0	0	0	0
Moraceae	C3	<i>Ficus natalensis</i>	FICnat	0	0	0	0	14	0	5	19
Rubiaceae	C3	<i>Tarenna graveolens</i>	TARENgraveol	0	0	0	0	24	0	26	50
Rubiaceae	C3	<i>Rubus sp.</i>	RUBsp	0	0	0	0	1	0	5	6
Tiliaceae	C3	<i>Grewia fallax</i>	GREWfallx	0	0	0	0	0	0	0	0

Appendix III. Raw phytolith data counted in ODP core samples

Spheroid echinate	9	1	19		12	16	26	16	2	27	18	14	24	4	11	21	8	19	17	26	11	135	50	111	104	6	25	2	43	88		9	5	25			
Spheroid echinate (Palm)		1	2		8	1	11	5		9	1	3										30	16	20					12	3							
Spheroid rugulate	1	2	5		1	5	3									8		32	16	34		1	13										2		7		
Spheroid scalloped												5																									
Total diagnostic woody phytoliths	48	90	172	39	82	44	111	136	192	267	382	182	329	266	387	188	215	339	307	381	644	242	323	329	303	36	127	37	452	358	156	166	106	186			
Spheroid psilate	7	10	21	4	6	4	12	8	24	19	24	16	13	37	38	23	48	41	30	38	24	50	38	46	93	10	37	2	22	62	84	58	22	40			
Cone-shaped			1																																		
Crenate Clavate										1																											
Cylindroid crenate								5	1																												
Cylindroid dendriform										1																											
Cylindroid echinate					7	7	12																														
Cylindroid scabrate														8																							
Cylindroid sinuate		2				2	4																														
Ellipsoid echinate		1	1	2								8																									
Ellipsoid psilate		4	14				3	5	2	7		16	21	6	3	4	15	6	21	12	6				3		4	20	9	6	13	1	21				
Ellipsoid scabrate	6	3	3	2	5		8	7	6	15	4	8	5		6		8		6	7	10	13				7		7	5				6				
Ellipsoid verrucate																																					
Epidermal long cells							2	3		3	6	4	11	7	64		23	10	5	14	23		10	3	8					7	1	7	1	12			
Facetate							6				12	5	11		9				6											2							
Fusiform																																					
Hair cell							2								5		7									1											
Honeycomb assemblages																						2															
Honeycombs elongate					1																																
Honeycombs spheroid							5							6																							
Irregular psilate			1				7	6			6		4		35		2	4	3							4											
Irregular scabrate													16																								
Irregular verrucate											3	2			9																						
Mesophyl																																					
Parallelipiped crenate				1	2																																
Parallelipiped echinate	2				18	3	4																														
Parallelipiped granulate				1																																	
Parallelipiped psilate			1																																		
Parallelipiped scabrate							3																														
Parallelipiped thin wavy	2																																				
Parallelipiped wavy			1	6	2																																
Polyhedrals		13	52	3	11	5	8	1	4					36			21	22	17	2	14	3				2			20		4	1					
Prickle		5	4	8	7		1	1	2		9	3		7			3	5	6	2										6	4	5	14		5		
Scutiform	3	27	17	9	4	4	7	7	1	3	9	8	7	10	5		30	10	10	6	11	17	7		14	8		3	3	7	14	14	9	8			
Starlets			2	2									9		3																						
Stomatal cells							1																														
Indeter	12	8	9	6	16	2		28	13	14	31	11	12		43	3	11	4	27	20	3			17	8			8	2	3	15	4		3			
Non-diagnostic woody and herbs	20	66	117	38	63	25	67	43	50	35	91	50	95	101	210	32	141	121	77	89	97	86	71	49	132	32	51	9	80	94	114	107	39	86			
Total assemblage per sample	318	242	598	419	452	367	492	533	319	439	614	332	518	498	694	323	952	548	590	531	758	443	486	632	662	86	243	57	580	556	327	372	308	584			

245320	246142	249834	250087	250521	250955	258963	261310	264034	266730	269619	272179	274843	277401	279963	282479	285126	287797	290531	293154	295105	297564	300268	302610	305199	308810	311660	314092	316860	319497	322009	325927	328168	330865	334408	340195	343510	347285	350268	353118	355976	358728	361842	364746		
164	165	166	167	168	169	170	171	172	173	174	175	176	177	178	179	180	181	182	183	184	185	186	187	188	189	190	191	192	193	194	195	196	197	198	199	200	201	202	203	204	205	206	207		
0	0	0	0	1	0	0	0	1	7	0	0	1	0	0	0	3	0	0	0	0	0	2	2	5	5	0	0	0	0	0	4	16	3	1	0	0	0	0	3	17	3	4			
1	8	1	2	4	2	11	21	3	19	7	6	1	1	6	1	2	1	3	4	5	8	7	2	1	8	7	1	9	19	6	15	8	3	6	19	3	7	10	3	8	11	3	5	2	1
2	0	0	36	0	0	81	112	50	204	89	115	183	46	90	68	120	3	8	14	6	33	59	0	16	1	0	0	0	1	45	101	7	0	3	2	24	1	43	32	254	51	40			
90	85	3	90	80	13	1	4	7	2					1	2					1	1	3	1	1	1				1	6	6							3	8	3	3				
186	151	1	73	28	17	8	6	6	8											1	5	5	1	2				1	28	11				1	1	2	5	7	40	20	26				
65	40	1	32	46	8	6	15	2	9	32	26	5		1	3				1	1	1	5	4					2	7	1	13	6			12	5	9	26	122	17	8	50			

Appendix IV: Raw phytolith assemblage count for Koobi Fora Basin

Morphotypes	Modern samples				Late Holocene samples			Mid-Holocene samples (4.2-1.34kyr)								
	SS1	SS2	SS3	SS4	FwjJ5-RK-3	FwjJ5-RK-2	FwjJ5-RK-1	FwjJ25-RK-3	FwjJ25-RK-2	FwjJ25-RK-1	GajJ4-RK-1	GajJ4-RK-2	GajJ4-RK-3	GajJ4-RK-4	GajJ4-RK-5	
Bilobate convex long	0	0	0	0	0	0	0	0	0	0	0	0	0	0	0	
Saddle Plateau	0	2	0	0	0	0	0	0	0	2	1	2	0	0	0	
Saddle squat	0	0	0	0	0	0	0	0	0	0	0	0	0	0	0	
Saddle collapse	0	0	0	0	0	1	0	0	0	0	1	0	0	0	0	
Saddles	7	6	1	1	1	0	0	0	1	0	3	1	0	0	0	
Bilobate flattened short	3	7	0	0	0	0	0	0	0	1	3	0	0	4	1	
Crosses	0	0	0	0	3	0	0	0	0	1	3	0	0	5	0	
Bilobate panicoid	0	6	0	0	0	0	0	0	0	0	0	0	0	0	0	
Bilobate convex short	2	5	1	0	8	1	6	2	0	0	1	0	0	0	0	
Bilobate concave short	0	0	0	0	0	0	1	0	0	0	0	0	0	0	0	
Tower horned	0	0	0	0	0	0	0	0	0	1	0	0	0	0	0	
Polylobate	0	5	0	0	0	0	1	0	0	0	0	0	0	1	0	
Tower wide	0	1	0	0	0	0	0	2	0	0	0	0	0	0	0	
Saddle long	0	1	0	0	11	0	1	0	0	0	0	0	0	0	0	
Tower long	0	0	0	0	0	0	0	1	0	0	0	0	0	0	0	
Bilobate flattened long	0	0	0	0	0	0	0	0	0	0	0	1	0	0	0	
Tower tall	0	0	0	0	1	0	0	0	0	0	0	0	0	0	0	
Poaceae pollen	0	0	0	0	0	0	0	0	7	0	0	0	0	0	0	
Epidermal GSSC	0	9	0	0	0	0	0	0	0	0	0	0	0	0	0	
Rondels	53	8	1	0	0	4	3	1	0	0	15	6	9	10	12	
Bulliforms	16	10	0	0	6	1	11	3	0	0	7	0	0	6	4	
Bilobate indet	0	0	0	0	0	0	0	0	0	0	0	0	0	0	0	
Globular granulate	0	2	0	0	55	4	5	41	0	7	28	25	3	25	85	
Tracheids	13	170	5	0	5	140	77	7	0	15	150	18	4	9	46	
Sclereids	1	0	0	0	2	1	12	0	2	0	22	14	1	0	43	
Globular echinate	0	3	5	0	0	0	8	0	0	1	0	4	0	1	11	
Globular verrucate	0	3	0	0	0	0	0	0	0	0	1	2	0	0	15	
Facetate	0	0	0	0	0	0	0	0	0	0	0	0	0	0	0	

Morphotypes	Early-Mid-Holocene transition			Early Holocene samples (ca.9.6-6kyr)						Early Pliocene samples (ca. 1.525Ma to 1.51Ma)						
	Fxj27-RK-3	Fxj27-RK-2	Fxj27-RK-1	Fxj108-6	Fxj108-5	Fxj108-4	Fxj108-3	Fxj108-2	Fxj108-1	1A-Du-ET-11-02-Area 1A	AV-ET-11-1-Area 1A	AV-ET-11-1-Area 1A	AV-ET-11-1-Area 1A	AV-ET-11-1-Area 1A	AV-ET-11-1-Area 1A	
Bilobate convex long	0	0	0	0	0	1	0	0	0	0	0	0	0	0	0	0
Saddle Plateau	7	2	0	1	0	0	0	0	2	0	0	0	0	0	0	0
Saddle squat	0	3	0	0	0	1	0	0	0	0	0	0	0	0	0	0
Saddle collapse	0	0	0	0	0	0	0	0	0	0	0	0	1	1	0	0
Saddles	12	3	1	0	1	9	1	0	1	0	2	2	0	1	0	0
Bilobate flattened short	2	2	2	0	1	4	0	0	0	0	3	2	1	0	0	0
Crosses	0	0	2	0	0	0	0	0	0	0	0	0	0	0	0	0
Bilobate panicoid	16	0	0	0	0	0	0	0	0	0	0	0	0	0	0	0
Bilobate convex short	11	2	1	0	1	0	2	1	3	3	0	0	0	1	0	0
Bilobate concave short	3	0	0	0	0	0	0	0	0	0	0	0	0	0	0	0
Tower horned	0	0	0	0	0	0	0	1	1	0	0	0	0	0	0	0
Polylobate	1	0	0	0	0	1	0	0	0	0	0	0	0	0	0	0
Tower wide	0	0	0	0	0	0	0	0	0	0	0	0	0	0	0	0
Saddle long	2	2	0	0	1	0	0	0	0	0	5	0	1	0	0	0
Tower long	0	0	0	0	0	0	0	0	0	0	0	0	0	0	0	0
Bilobate flattened long	2	0	0	0	0	2	0	0	0	0	0	0	0	0	0	0
Tower tall	0	0	0	0	0	0	0	0	0	0	0	0	0	0	0	0
Poaceae pollen	0	1	0	0	0	0	0	0	0	0	0	0	0	0	0	0
Epidermal GSSC	0	0	0	0	0	0	0	0	0	0	0	1	0	0	0	0
Rondels	13	16	8	4	2	16	5	2	8	14	21	0	6	8	2	2
Bulliforms	20	2	5	0	14	0	2	0	0	0	3	1	2	6	2	2
Bilobate indet	0	0	0	0	0	0	0	0	0	0	0	0	0	0	0	0
Globular granulate	12	7	7	46	8	3	29	0	2	20	137	5	3	3	16	16
Tracheids	130	30	145	17	51	19	60	0	6	8	5	14	43	38	12	12
Sclereids	9	9	6	0	2	1	6	0	0	5	20	0	4	4	4	4
Globular echinate	10	6	2	0	0	0	11	0	0	0	6	2	3	1	2	2
Globular verrucate	0	0	0	0	0	0	0	0	0	0	5	0	6	0	0	0
Facetate	0	0	0	0	0	0	0	0	0	0	0	0	0	0	0	0

Morphotypes	Early Pliocene samples (ca. 1.525Ma to 1.51Ma)					
	1A-Du-ET-11-02-Area 1A	1A-Du-ET-11-02-Area 1A	1A-Du-ET-11-02-Area 1A	1A-Du-ET-11-02-Area 1A	14A-8A-GS-2-Area 8A	14A-8A-GS-5-Area 8A
Bilobate convex long	0	0	0	0	0	0
Saddle Plateau	0	1	1	0	0	0
Saddle squat	0	0	0	0	0	0
Saddle collapse	0	0	0	1	0	0
Saddles	0	0	1	0	0	0
Bilobate flattened short	0	0	0	0	1	0
Crosses	0	0	2	0	0	0
Bilobate panicoid	0	0	1	0	1	0
Bilobate convex short	0	0	0	0	3	0
Bilobate concave short	0	0	0	0	0	0
Tower horned	0	0	0	0	0	0
Polylobate	0	0	0	0	0	0
Tower wide	0	0	0	0	0	0
Saddle long	0	0	0	0	0	0
Tower long	0	0	0	0	0	0
Bilobate flattened long	0	0	0	0	0	0
Tower tall	0	0	0	0	0	0
Poaceae pollen	0	0	0	0	0	0
Epidermal GSSC	0	0	0	0	0	0
Rondels	0	4	1	1	1	6
Bulliforms	0	1	9	5	0	0
Bilobate indet	0	0	0	0	1	0
Globular granulate	5	270	29	0	108	0
Tracheids	1	13	127	12	12	1
Sclereids	3	0	13	1	6	1
Globular echinate	0	9	8	0	17	1
Globular verrucate	1	1	4	0	31	0
Facetate	0	0	0	0	3	0

Morphotypes	Modern samples				Late Holocene samples			Mid-Holocene samples (4.2-1.34kyr)								
	SS1	SS2	SS3	SS4	Fwj5-RK-3	Fwj5-RK-2	Fwj5-RK-1	Fwj25-RK-3	Fwj25-RK-2	Fwj25-RK-1	Gaj4-RK-1	Gaj4-RK-2	Gaj4-RK-3	Gaj4-RK-4	Gaj4-RK-5	
Irregular verrucate	0	0	0	0	0	0	0	0	0	0	0	0	0	0	0	
Palm echinate	0	15	0	0	0	0	0	0	0	0	0	0	0	0	0	
Scutiform	0	1	0	0	2	1	0	1	0	0	4	0	0	0	0	
Ellipsoid scabrate	0	0	0	0	0	0	0	1	0	0	0	0	0	0	0	
Globular psilate	0	1	1	0	2	1	3	0	0	0	0	1	4	3	11	
Prickle	5	0	0	0	1	0	0	0	0	0	0	0	0	0	0	
Ellipsoid psilate	10	5	0	0	1	0	0	0	0	0	1	0	0	3	0	
Stomatal cells	0	0	0	0	0	0	0	0	0	0	0	0	0	0	0	
Polygonal	0	2	0	0	0	0	0	0	0	0	0	0	0	0	0	
Irregular psilate	8	0	0	0	0	0	0	0	0	0	0	0	6	20	16	
Ellipsoid echinate	0	0	0	0	0	0	0	0	0	0	0	0	0	2	0	
Longcell appendages	0	0	0	0	0	5	3	0	0	0	0	0	0	0	0	
Hair cells	0	0	0	0	0	0	0	0	0	0	2	0	0	1	0	
Irregular scabrate	0	0	0	0	0	0	0	0	0	0	0	4	0	0	5	
Honey assemblages	0	0	0	0	0	0	0	0	0	0	0	0	0	0	0	
Sedge/Achene	0	5	0	0	4	0	1	1	0	0	1	0	0	1	0	
Cyperaceae	0	0	0	0	0	0	0	0	32	0	0	0	0	0	0	
Typhaceae	0	0	0	0	0	0	0	0	33	0	0	0	0	0	0	
Indeterminables	0	0	0	0	12	0	0	4	0	0	0	0	0	0	0	
Agavaceae	0	0	0	0	0	0	0	0	8	0	0	0	0	0	0	
Hyphaene	0	0	0	0	0	0	0	0	7	0	0	0	0	0	0	
Acanthaceae	0	0	0	0	0	0	0	0	1	0	0	0	0	0	0	
Capparaceae	0	0	0	0	0	0	0	0	1	0	0	0	0	0	0	
Fossil pollen	0	0	0	0	0	0	0	0	0	0	3	0	0	0	2	
Spicules	0	3	0	0	0	0	8	0	0	4	0	0	0	0	0	
Diatoms	0	11	0	0	0	1	3	0	0	0	2	0	0	0	0	
Palynomorphs	0	0	0	2	0	0	0	0	0	0	0	0	0	0	0	
Total assemblage	118	281	14	3	114	160	143	64	92	32	248	78	27	91	251	

Morphotypes	Early-Mid-Holocene transition			Early Holocene samples (ca.9.6-6kyr)						Early Pliocene samples (ca. 1.525Ma to 1.51Ma)					
	Fxj27-RK-3	Fxj27-RK-2	Fxj27-RK-1	Fxj108-6	Fxj108-5	Fxj108-4	Fxj108-3	Fxj108-2	Fxj108-1	1A-Du-ET-11-02-Area 1A	AV-ET-11-1-Area 1A	AV-ET-11-1-Area 1A	AV-ET-11-1-Area 1A	AV-ET-11-1-Area 1A	AV-ET-11-1-Area 1A
Irregular verrucate	0	0	0	0	0	0	0	0	0	0	0	0	0	0	0
Palm echinate	5	0	0	0	0	0	0	0	0	0	0	0	0	1	0
Scutiform	2	1	0	0	0	0	0	0	0	0	0	1	0	0	0
Ellipsoid scabrate	0	0	0	3	0	0	1	0	1	0	0	0	0	0	0
Globular psilate	2	1	1	1	1	0	5	1	0	0	3	0	0	5	0
Prickle	12	1	0	0	0	0	0	0	0	0	0	0	0	0	0
Ellipsoid psilate	3	2	0	0	0	0	0	0	2	0	2	0	0	0	0
Stomatal cells	0	0	0	0	0	0	0	0	1	0	0	0	0	0	0
Polygonal	0	0	0	0	0	0	0	0	0	0	0	0	0	0	0
Irregular psilate	0	0	0	0	0	0	0	0	0	5	11	0	0	0	0
Ellipsoid echinate	0	0	0	0	0	0	0	0	0	0	0	0	0	0	0
Longcell appendages	0	1	0	0	1	0	0	0	0	0	1	0	3	0	0
Hair cells	0	2	0	0	0	0	0	0	0	0	0	0	1	0	0
Irregular scabrate	0	0	0	0	0	0	8	0	0	0	25	0	0	0	0
Honey assemblages	0	0	2	0	0	0	0	0	0	0	0	0	0	0	0
Sedge/Achene	2	1	1	0	3	0	0	0	0	0	0	0	7	6	0
Cyperaceae	0	0	0	0	0	0	0	0	0	0	0	0	0	0	0
Typhaceae	0	0	0	0	0	0	0	0	0	0	0	0	0	0	0
Indeterminables	0	4	0	8	6	7	0	0	15	0	0	0	0	5	3
Agavaceae	0	0	0	0	0	0	0	0	0	0	0	0	0	0	0
Hyphaene	0	0	0	0	0	0	0	0	0	0	0	0	0	0	0
Acanthaceae	0	0	0	0	0	0	0	0	0	0	0	0	0	0	0
Capparaceae	0	0	0	0	0	0	0	0	0	0	0	0	0	0	0
Fossil pollen	0	0	0	0	0	1	2	0	0	0	0	0	0	0	0
Spicules	0	0	7	0	0	0	0	0	0	0	0	0	3	3	1
Diatoms	8	0	1	0	3	0	0	0	0	2	0	0	1	21	0
Palynomorphs	0	0	0	0	5	2	0	0	0	0	0	0	0	0	0
Total assemblage	284	98	191	80	100	67	132	5	42	57	249	28	85	104	42

Morphotypes	Early Pliocene samples (ca. 1.525Ma to 1.51Ma)					
	1A-Du-ET-11-02-Area 1A	1A-Du-ET-11-02-Area 1A	1A-Du-ET-11-02-Area 1A	1A-Du-ET-11-02-Area 1A	14A-8A-GS-2-Area 8A	14A-8A-GS-5-Area 8A
Irregular verrucate	0	0	1	0	35	0
Palm echinate	0	0	0	0	0	0
Scutiform	0	0	0	0	0	0
Ellipsoid scabrate	0	1	0	0	0	0
Globular psilate	1	0	6	0	1	0
Prickle	0	0	0	0	0	0
Ellipsoid psilate	1	0	2	0	0	0
Stomatal cells	0	0	0	0	0	0
Polygonal	0	0	0	0	0	0
Irregular psilate	0	0	0	0	0	0
Ellipsoid echinate	0	0	0	0	0	0
Longcell appendages	0	0	9	0	5	0
Hair cells	0	0	0	0	0	0
Irregular scabrate	0	0	0	0	7	0
Honey assemblages	0	0	1	0	0	0
Sedge/Achene	1	0	4	0	0	0
Cyperaceae	0	0	0	0	0	0
Typhaceae	0	0	0	0	0	0
Indeterminables	0	1	16	3	0	0
Agavaceae	0	0	0	0	0	0
Hyphaene	0	0	0	0	0	0
Acanthaceae	0	0	0	0	0	0
Capparaceae	0	0	0	0	0	0
Fossil pollen	0	0	0	0	3	0
Spicules	0	0	0	0	0	0
Diatoms	0	0	0	3	0	0
Palynomorphs	0	5	16	124	0	0

